Exploration of Novel Sapphyrin Isomer through Design, its Coordination Chemistry and Naphthobipyrrole-Derived BODIPYs as NIR Emitting Dyes

A Thesis submitted for the Degree
of DOCTOR OF PHILOSOPHY

प्रतिष्ठित संस्थान
INSTITUTION OF EMINENCE
राष्ट्रीय अपेक्षाएँ, वैश्विक मानक
National Needs, Global Standards

By

Sipra Sucharita Sahoo
School of Chemistry
University of
Hyderabad
Hyderabad-500 046
India

July 2022

Dedicated to

Mamu

Contents

Part B

Chapter 3: Introduction

Chapter 4: Functionalization of Napthobipyrrole Derived BODIPY

Chapter 5: Bis(napthobipyrrolyl)methene derived helical BODIPY

Chapter 6: Conclusion

Appendix

DECLARATION

I hereby declare that the matter embodied in the thesis entitled **"Exploration of Novel Sapphyrin Isomer through Design, its Coordination Chemistry and Naphthobipyrrole-Derived BODIPYs as NIR Emitting Dyes"** is the result of investigations carried out by me in the School of Chemistry, University of Hyderabad, Hyderabad, India under the supervision of **Prof. Pradeepta K. Panda** and it has not been submitted elsewhere for the award of any degree or diploma or membership, etc. This work is free from plagiarism. I hereby agree that my thesis can be deposited in Shodhganga/INFLIBNET.

In keeping with the general practice of reporting scientific investigations, due acknowledgements have been made wherever the work described is based on the findings of other investigators. Any omission or error that might have unintentionally crept in, is sincerely regretted.

Sipra Sucharita Sahoo.

Date: July 2022

Sipra Sucharita Sahoo

UNIVERSITY OF HYDERABAD
Central University (P.O.), Hyderabad-500046, INDIA

Pradeepta K. Panda
Professor
School of Chemistry

Tel: 91-40-23134818 (Office)
Fax: 91-40-23012460
E-mail: pkpsc@uohyd.ernet.in
pradeepta.panda@uohyd.ac.in

Certificate

This is to certify that the work described in this thesis entitled **"Exploration of Novel Sapphyrin Isomer through Design, its Coordination Chemistry and Naphthobipyrrole-Derived BODIPYs as NIR Emitting Dyes"** has been carried out by Ms. Sipra Sucharita Sahoo, holding the Reg. No. 15CHPH26 under my supervision, for partial fulfilment for the award of Doctor of Philosophy in Chemistry and the same has not been submitted elsewhere for any degree, which is a plagiarism free thesis.

Part of thesis have been:

Published in following journals

1. Sahoo, S. S; Sahoo, S.; Panda, P. K. *Dalton Trans.*, **2022**, *51*, 6526.

Presented in the following conferences

1. International Conference on 'RECENT ADVANCES IN MATERIALS CHEMISTRY' (RAMC 2017), 24-26th February 2017, Utkal University, Bhubaneswar, Odisha.
2. "Recent Advances in bis and tetra-Pyrrolic Molecular Materials" virtual meeting held on 24-26th August, 2020 organized by Central University of Kerala, Kerala.
3. National Seminar on "RECENT ADVANCES IN MATERIALS CHEMISTRY" virtual meeting held on 8-9th March, 2021 organized by Utkal University, Bhubaneswar, Odisha.

4. Chemfest-2021 (Chemistry beyond challenges), 19-20th February 2021, an annual in-house symposium, School of Chemistry, University of Hyderabad, Hyderabad.

5. ICPP 11 (International Conference on Porphyrins and Phthalocyanines), virtual meeting held from 28th June-3rd July 2021.

Further the student has passed the following courses towards fulfilment of course work requirement for the Ph.D. degree.

Name of the course	Credits	Pass/Fail
1) CY-801 Research proposal	3	Pass
2) CY-802 Chemistry Pedagogy (CY-405 Inorganic Chemistry Lab: Qualitative and Quantitative analysis)	3	Pass
3) CY-805 Instrumental Methods A	3	Pass
4) CY-806 Instrumental Methods B	3	Pass
5) CY-501 Spectroscopic Methods for Structure Elucidation	3	Pass

Ashwini Mangle
Dean
School of Chemistry

Dean
SCHOOL OF CHEMISTRY
University of Hyderabad
Hyderabad-500 046

06/07/2022
Prof. Pradeepta K. Panda
(Thesis Supervisor)

Pradeepta K. Panda
Professor
School of Chemistry
University of Hyderabad
Hyderabad - 500 046.

PREFACE

The thesis entitled **"Exploration of Novel Sapphyrin Isomer through Design, its Coordination Chemistry and Naphthobipyrrole-Derived BODIPYs as NIR Emitting Dyes"** is divided into two parts. Part A consists of two chapters and part B consists of three chapters followed by the final chapter about thesis conclusion. At the end the appendix provides information about the synthetic routes followed for the literature reported compounds along with the details of materials and methods employed during the analysis. Part A deals with design and synthesis of novel sapphyrin isomer, its complexation and their detailed structural and photophysical studies. Part B is about synthesis of different near infrared (NIR) absorbing and emitting BODIPY dyes and exploring their structural and electronic properties. All new molecules have been characterized with standard spectroscopic techniques. Structural analysis by SCXRD and photophysical studies have been done for final molecules. **Chapter 1** provides an insight into the literature overview of porphyrin and its structural isomers, contracted porphyrins along with existing structural isomers, expanded porphyrins and their existing structural isomers. **Chapter 2** describes about the design and synthesis of a novel core-modified isomer of sapphyrin. Further, we have explored its coordination chemistry with both anions and transition metal ions. Optimized structural attributes from DFT analysis of both the molecules have been included in the chapter to understand the stability of tautomers, site of protonation and mode of binding to metal ion**.** **Chapter 3** discusses about different BODIPY dyes, its optical properties owing to the structural modifications. It also discusses some reports of applications of BODIPY dyes in different fields. **Chapter 4** documents functionalization of bis(naphthobipyrrolyl)BODIPY at terminal α-positions with different functional groups like formyl, nitrile, nitro, bromo to tune their photophysical properties along with their photostability. **Chapter 5** describes the synthesis and photophysical study of hydrochloride salt of hexapyrrolic oligomer derived from naphthobipyrrole along with its BODIPY analogue.

July 2022 ***Sipra Sucharita Sahoo***

Acknowledgement

Whatever a person achieves, there is an underlying effort from different people, which makes the path little smoother, little better. Acknowledging them all after reaching the destination is a first and must to do responsibility. This dissertation would be incomplete without expressing gratitude to people whose presence has either personally or professionally made this achievable.

First and foremost, I would like to offer my gratitude to the almighty for endowing me with strength and patience to complete this long journey. Faith on him kept me cross all ups and downs in the path.

Words cannot express my gratitude to my supervisor, Professor Pradeepta K. Panda, without whose support and guidance this journey would not have been possible the way, it is today. His constant encouragement never let my negative thoughts overtake my enthusiasm to complete my job. His support and motivation not only helped to go through the toughest times of the journey but shaped my mind not to give up on my job when I face a failure rather explore many other paths which may take me to the destination.

I would like to thank the former and present Dean, School of Chemistry, for their constant effort to make department better place to carry out our woks smoothly. I would like to thank my doctoral committee members Prof. K. Muralidharan and Prof. Tushar Jana for their support at times I needed. I am also thankful individually to all the faculty members of the school for their kind help and cooperation at various stages of my stay in the campus.

I would take this opportunity to thank a few people who took a little extra effort, beyond their professional commitments, to make my otherwise difficult task of data collection a little easier. I am thankful to Mr. Durgesh Kumar S. and Mr. G. Mahender, for their patience and efforts to allow me to make the best use of the available NMR facility. I am also grateful to Mr. Mahesh Rathod, for all his help in recording SCXRD, Ms. Asia Parvez and Dr. Manasi Dalai are deeply acknowledged for their continuous help in availing HRMS facilities. I am also thankful to Dr. Bhaskar and Mr. B. Anandam for all their cooperation. I would like to thank all other non-teaching staff for their assistance at various occasion.

Special gratitude to all my seniors is must to mention in this part of my thesis. I would like to thank Dr. Narendra Nath Pati for his encouragement, guidance which shaped my professional and personal growth throughout this long journey. I am very much thankful

to Dr. B. Sathish for his guidance to deal with problems I faced at various part of my dissertation work. I would like to thank Mr. J. Nagamaiah for not only helping me professionally but also being a senior cum friend to make the hard times little lighter. I am greatly thankful to Dr. Nanda Kishore, Dr. Rahul Soman, Dr. T. Vikranth, Dr. Anup Rana, Dr. Brijesh Chandra, Dr. P. Obaiah, Dr. Chandrashekhar, Dr. Sudhakar for providing all types of guidance and assistance I needed at various times. I am very much thankful to Jyotsna Bania and Ishfaq Ah. Bhat for showing belief in me and encouraging me at times when I feel it is not possible. I am thankful to my juniors Shanmugapriya, Jiji, Mahendra, Narmada, Raghuvaran for willing to help whatever way they can. I am thankful to project students Vijaya, Arnab, Chitrak, Preeti, Soumya with whom I have spent less but good times in lab.

I am very luck to have beautiful friendship with a few beautiful persons in this campus. I cann't express my gratitude in words for my friendship with Ms. Sameeta, Mrs. Mou and Dr. Tanmay. But I will definitely thank Ms. Sameeta for being my personal and professional support system, Mrs. Mou for constantly encouraging and believing me when there is lack of confidence, burden of regrets and Dr. Tanmay for anytime any help. This long journey with a roller-coaster ride was not so painful for support of you people. I am very much thankful to Dr. Arijit Saha for being an elder brother and providing guidance and help whenever I needed. I am also thankful Dr. Ankit for being a friend to laugh with to make time little lighter. I am thankful to my friend Mr. Subhashis for being my support at all times I break down, at all time I think to backout.

I am thankful to Mr. Sumanta for his help in singlet-state lifetime measurement and Mr Jay Krushna for his valuable times to help me to carry out some of my theoretical works. I am thankful to Ms Prachi for her suggestions to understand many theoretical problems I faced during dissertation time. My pleasant times with some of friends and juniors in HCU such as Sautrick, Suman, Gorachand, Mamina, Monika, Arosmita, Subham, Pradeepta, Satya, Uma, Sarita, Priya, Baikuntha, Chiranjit, Biswa, Raju bhai and Majhi bhai are unforgettable. You people have made life little more colourful in HCU.

Finally, I would express my gratitude deep from my heart to my parents, my brothers and sisters and to my whole family. Your belief in me has always pushed me to give my best to achieve what I dreamt. I cann't express in words how much I owe you all.

Sipra Sucharita Sahoo

List of abbreviations

acac	acetylacetonate
CMSD	Centre for Modelling, Simulation & Design
CT	Charge transfer
d	doublet
DCE	1,2-Dichloroethane
DCM	Dichloromethane
DMF	N,N-Dimethylformamide
DMSO	Dimethylsulfoxide
DFT	Density functional theory
g	Grams
h	Hour(s)
HOMA	Harmonic Oscillator Model of Aromaticity
HOMO	Highest occupied molecular orbital
HRMS	High resolution-mass spectrometry
ICT	Internal charge transfer
IR	Infrared
ISC	Intersystem crossing
LUMO	Lowest unoccupied molecular orbital
m	Multiplet
mg	milligram
min	minute(s)
mL	millilitre
Mb	myoglobin
MO	Molecular orbitals
NIR	Near Infra-red
NLO	Nonlinear Optical
nm	Nanometer
NMR	Nuclear Magnetic Resonance
o	ortho
OAc	acetate

p	para
PDT	Photodynamic therapy
PET	Photo electron transfer
$TBAPF_6$	Tetrabutyl ammonium hexafluoro phosphate
THF	Tetrahydrofuran
TLC	Thin layer chromatography
TMS	Trimethyl silane
UV-Vis	Ultraviolet-visible
SCXRD	Single crystal X-Ray diffraction

Part A

Chapter 1

Introduction

1.1. History of Porphyrin

Today's earth, with a great biodiversity would have not been possible without existence of oxygen. Going back to billions of years, the evolution of photosynthetic cyanobacteria switched the fate of earth's atmosphere from reduced to oxidized one and then evolution continued to result in a great diversity of flora and fauna. Haemoglobin, an iron containing metalloprotein is responsible for oxygen transport in the body of almost all higher vertebrates. After years of research, Hoppe-Seyler observed structural similarity between chlorophyll derived porphyrin i.e. phylloporphyrin and hematin and also both show red fluorescence.[1] It was observed then that many vital functions of life like photosynthesis (chlorophyll), oxygen transport (haemoglobin), oxygen storage (myoglobin), electron transport (cytochromes b and c), O_2 activation and utilisation (cytochrome oxidase), hydrocarbon oxidation (cytochrome P_{450}) and also anti-pernicious anaemia factor (vit. B_{12}) are carried out by same family of molecule i.e., a metal ion coordinated to an organic ligand, where the organic part is a tetrapyrrolic macrocycle (**Figure 1.1**). These observations gave the title 'pigment of life' to these tetrapyrrolic molecule.[2] Battersby and MacDonald shown that protohaem and chlorophyll are biosynthesized from a common parent unit i.e., uroporphyrinogen-III. Structure of porphyrin was first proposed by Küster in 1912 but was not accepted by scientific community.[1] Later Fischer synthesised chlorohemin which proved the structure of porphyrin that was similar to the one proposed by Küster.[3] This bagged him Nobel prize in 1930. Thus began the renaissance of porphyrin synthesis.

Porphyrin is an 18π conjugated molecule having four pyrrole units connected to each other by four methine bridges. Its extensive arrangement of delocalised π-electrons owing to its equalisation of bonds results in its fascinating aromaticity. Much of the research interest on porphyrin hinge on its photophysical properties. Porphyrin exhibits an intense colour which could be decoded by molecular orbital theory proposed by M. Gouterman.[4] Absorption spectrum of porphyrin is comprised of two regions. One around 400 nm is called B-band (Soret band) region and another is around 500-600 nm is called Q band region. Former one being an allowed transition (S_0-S_2) shows a highly intense peak for a freebase porphyrin while Q band being partially allowed transition (S_0-S_1) consists of four weak bands. For a metalloporphyrin, Soret band is not much disturbed while Q bands merge to give more intense two bands due to higher symmetry.

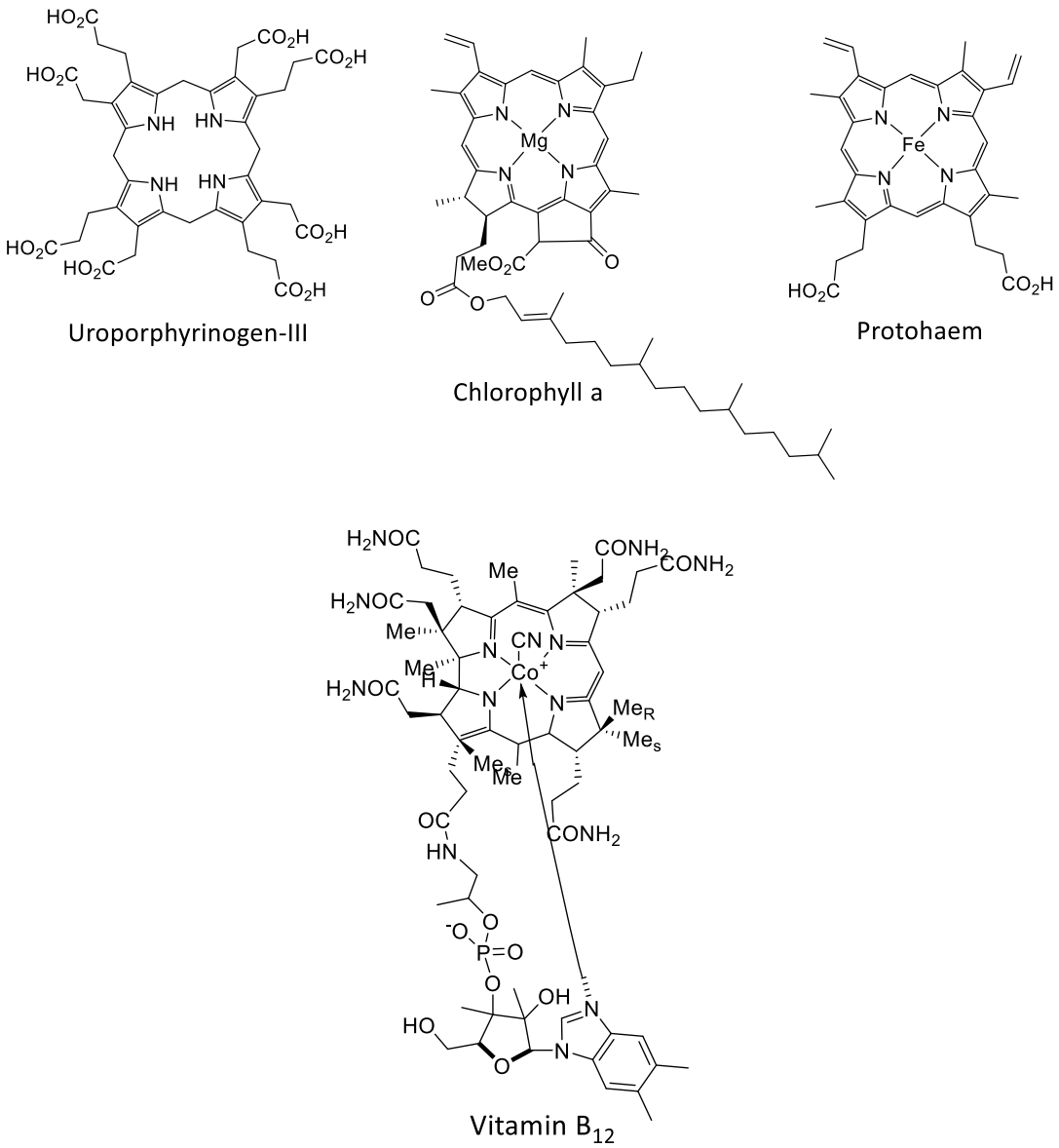

Figure 1.1: Examples of few naturally occurring tetrapyrroles.

Another fascinating property of porphyrin is its coordination to metal ions. Being a very versatile ligand, nearly all metals has been inserted to the pocket of porphyrin.[5] Metal ion is chelated to the tetradentate dianionic porphyrin ligand with covalent and dative bonds. Owing to its interesting photophysical and coordination properties, innumerable articles have been published showing its application in sensing,[6] opto-electronics,[7] dye sensitised solar cells,[8] catalysis,[9] photodynamic therapy.[10] A new direction of research on the macrocycle lead to many structural variants including constitutional isomers, N-confused and core modified derivatives (**Figure 1.2**). Further, contracted and expanded analogues emerged as other new areas with wide application potentials enriching the fundamental understanding of their chemistry (**Figure 1.2**).[11]

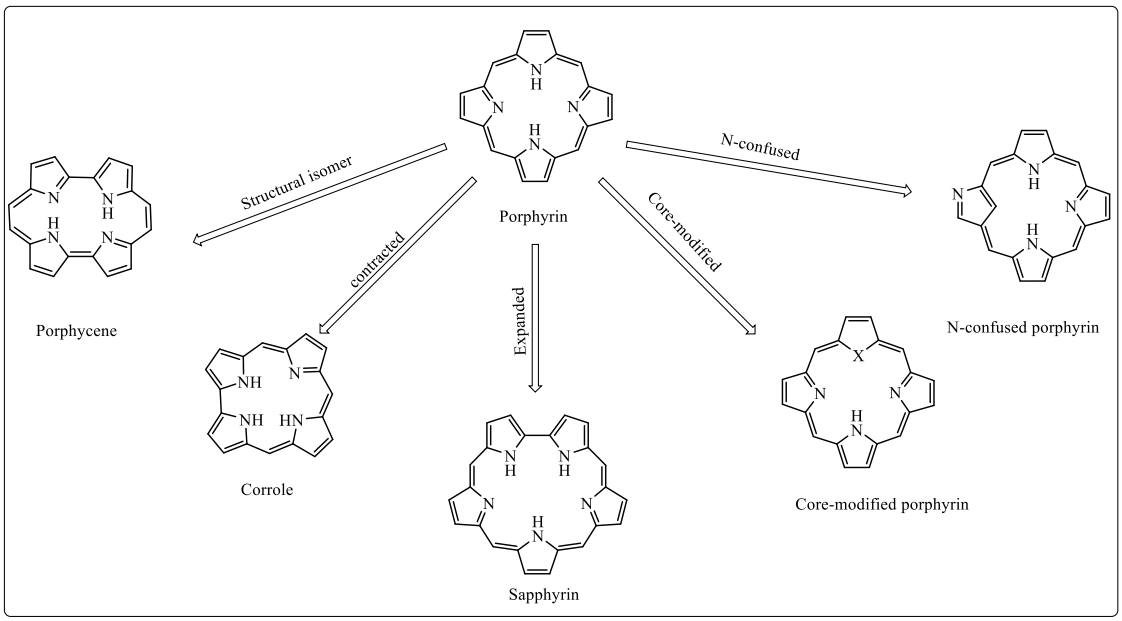

Figure 1.2: Structure of porphyrin and few representative modified porphyrinoids.

1.2. Nomenclature

In Fischer type nomenclature, all pyrrolic *β* positions are numbered from 1-8 and the bridging *meso* carbons are named as *α, β, γ, δ* positions. IUPAC has assigned a conventional strategy for nomenclature of porphyrins. According to this approach all the carbon atoms are allotted with numbers from 1-20 and internal nitrogen atoms are numbered from 21-24 as shown in **figure 1.3**.

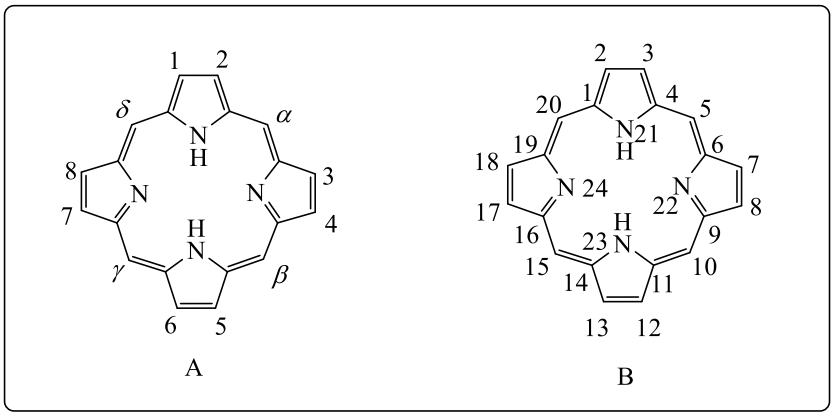

Figure 1.3: A. Fischer; B. IUPAC nomenclatures of porphin.

Along with the above-mentioned nomenclature conventions, many trivial names are attributed to different porphyrinoids like sapphyrin for pentapyrrolic macrocycle having a bipyrrole unit due to its deep blue colour like ‘sapphire’ in its solid state, hexaphyrin having six heterocycles in the macrocycle, or bronzaphryin for its bronze colour in solution. In

addition, Franck's systematic nomenclature is popular for naming any macrocycle.[12] In this type of nomenclature, porphyrin is named as [18]porphyrin(1.1.1.1). First number in the bracket represents the no of π-electrons in conjugation. The bracketed numbers in the right side represents the no of bridging carbons between heterocycles which starts from highest numbers of atoms and then runs in a unique direction (**Figure 1.4**). Similarly, we can name porphycene as [18]porphyrin(2.0.2.0), expanded porphyrin viz. sapphyrin as [22]pentaphyrin(1.1.1.1.0), hexaphyrin as [26]hexaphyrin(1.1.1.1.1.1).

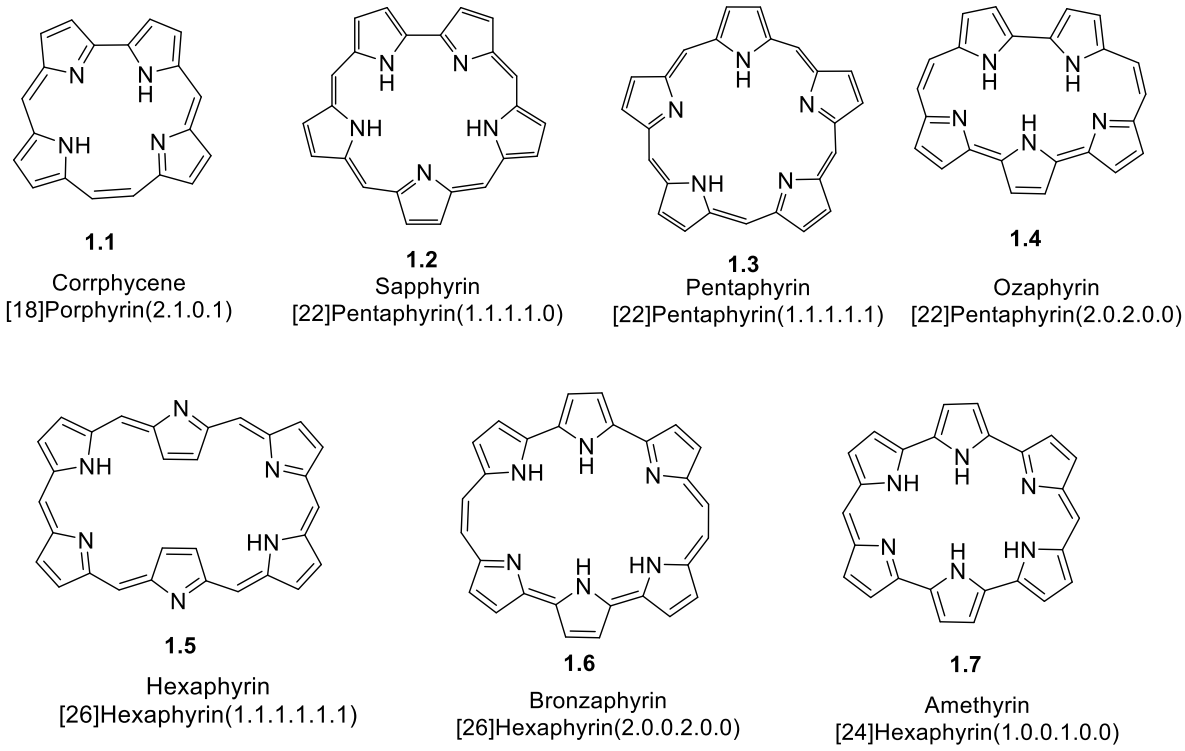

Figure 1.4: Some porphyrinoid's trivial names along with names according to Franck's convention.

1.3. Isomers of porphyrin

As porphyrins hold an important position in nature for survival and synthetic porphyrins play important roles in many applications, it was anticipated that its isomers could also show very interesting properties. Isomers of porphyrin will be having same $C_{20}H_{14}N_4$ molecular formula with different configurations by reshuffling of *meso* carbons. First and most stable structural isomer of porphyrin i.e. porphycene is first reported by Vogel in 1986.[13] Theoretically there are seven possible isomers with in-core nitrogens as shown in **figure 1.5**.[14] Except porphycene, three other isomers of porphyrins were synthesised and isolated so far i.e. corrphycene (**1.1**), hemiporphycene (**1.9**) and isoporphycene (**1.10**).[15]-[17] Another isomer of

porphyrin, which can be visualised as one of the pyrrolic NH is flipping out of the core and named as N-confused porphyrin (**1.11**) or mutant porphyrin was reported in 1994, independently by Furuta group and Latos-Grażyński's group.[18] All these macrocycles maintain an 18π- conjugation pathway making them Hückel aromatic.

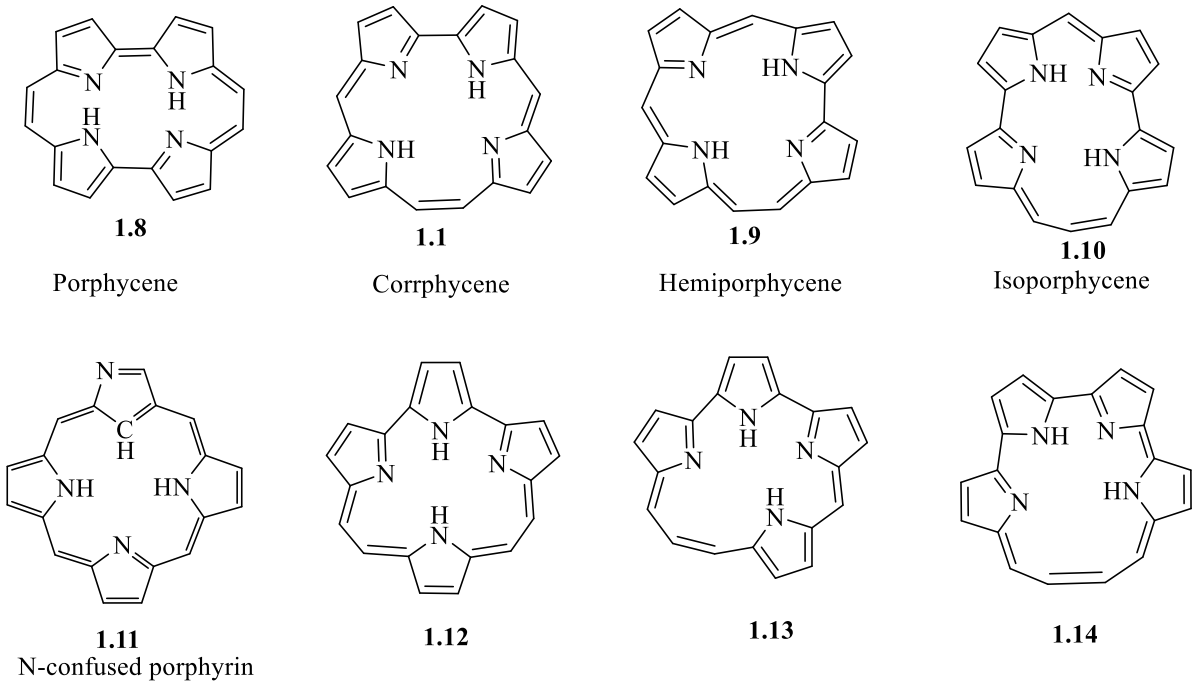

Figure 1.5: All possible constitutional isomers of porphyrin.

While parent porphyrin possesses D_{2h} and D_{4h} point group for freebase and metalated one, respectively, there is a reduction in symmetry for porphycene freebase to C_{2h} and D_{2h} for metal complexes. Freebase corrphycene possesses a planar structure and *cis* form of corrphycene (two NHs on bipyrrole) belongs to C_{2v} point group. Freebase hemiporphycene also has a planar structure but it possesses C_s point group whereas its metal complexes being saddle shaped also possess same C_s point group.[19] From a temperature dependent NMR study, *trans* form of freebase octaethylisoporphycene is seen to have C_{2v}, C_s or C_2 molecular symmetry depending on whether the ring has planar, concave or twisted structure representing the rapid NH tautomerism.[20]

Absorption spectra of porphyrin and its isomers are qualitatively similar to some extend i.e., an intense Soret band around 400 nm and a group of low energy Q-bands around 500-700 nm range but there are substantial differences in their pattern, intensity ratio and shape. Absorption spectrum of porphycene have a split Soret band and three lower energy Q-bands. Parent porphycene has a blue shifted Soret band and red shifted Q-bands and also the ratio of

Q bands to Soret band is more compared to the case of porphin. Further, the S_0-S_1 transition energy can be tuned with substituent effects. Fluorescence is usually weak for porphycene due to more intersystem crossing to triplet state. Singlet oxygen quantum yield is more in porphycene (0.3 for parent porphycene). These properties along with its stability towards photooxidation are fascinating for its application in many fields, particularly in photodynamic therapy.[21] Corrphycene has quiet similar absorption with that of porphyrin. If we compare octaethylporphyrin (OEP) and octethylcorrphycene (OECn) we can see, the Soret band and Q-bands of corrphycene are little red shifted (**Figure 1.6**).[22] Both Soret and Q bands for octaethylhemiporphycene (OEHPc) are red shifted, Q bands being less red shifted compared to shift of OEPc to OEP. Compared to porphyrin and corrphycene, intensity of Q bands to Soret band is more in case of hemiporphycene but the ratio will be less compared to porphycene. Soret band of octaethylisoporphycene most red shifted compared to any other isomers and Q-bands shift somewhat similar to that of porphycene.

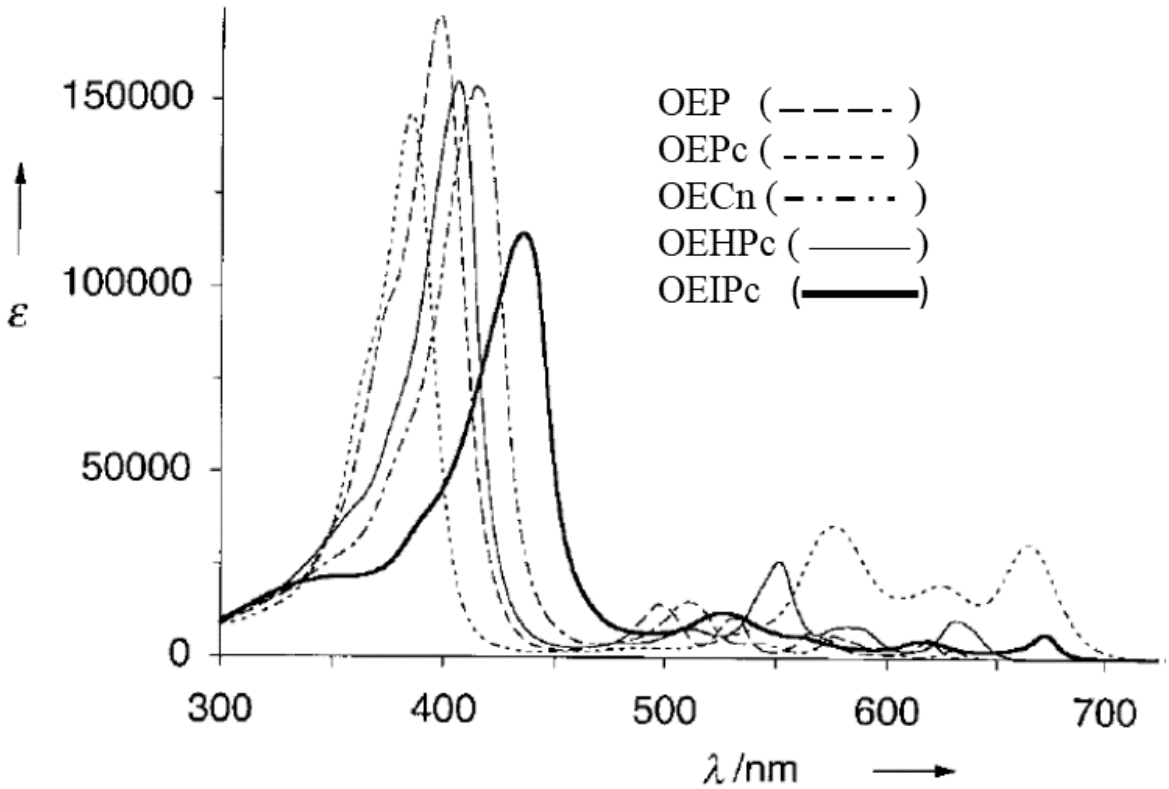

Figure 1.6: UV-vis spectra of porphyrin, porphycene, hemiporphycene, corrphyecene, isoporphycene with octaethyl-substitution.[20]

DFT calculations anticipate porphycene to be most stable isomer having 1.5 kcal/mol lesser energy than porphyrin followed by hemiporphycene, corrphycene and isoporphycene. Others have very high energy to be stable. Theoretically all the isomers are predicted to have a

planar structure except **1.14.**[23] Structural analysis of all the synthesised isomers proved above prediction to be true and all those are planar and aromatic. Due to rectangular size of core as well as smaller N_4 core of porphycene compared to porphyrin, there exists a strong N-H···N intramolecular H-bonding, which make it a demanding model to study for cooperative hydrogen transfer mechanism. Energy calculations with B_3LYP/TZ_2P show that the N-H tautomerization is more facile in porphycene than porphyrin. For example, the *trans-cis* tautomerization in porphycene has a barrier of 4.9 kcal/mol than that for porphyrin (16.2 kcal/mol). Similarly, those for the *cis-trans* tautomerization in porphycene is 2.4 kcal/mol vs 8.3 kcal/mol in porphyrin.[24] This clearly indicates in both cases the *trans*-tautomers are most stable. The above discussed properties of porphycene make it a weaker cheland compared to porphyrin. Shape and size of N_4 core contributes to the affinity of the isomers towards metal complexation. Porphyrin has a square type core, in turn, porphycene has a rectangular one, corrphycene has trapezoidal one and hemiporphycene has an irregular core shape. But all of them have shown complexation with many metal ions.[22,25] They all possess conformational flexibility to adhere to the metal ion coordination sphere. Corrphycene having a distorted trapezoid shape anticipated to have a less affinity for complexation but on contrary it has already encompassed a lot of metals from the periodic table.[25] Hemiporphycene are different due to its metal centred chirality due to dissymmetric nature of the ligand.

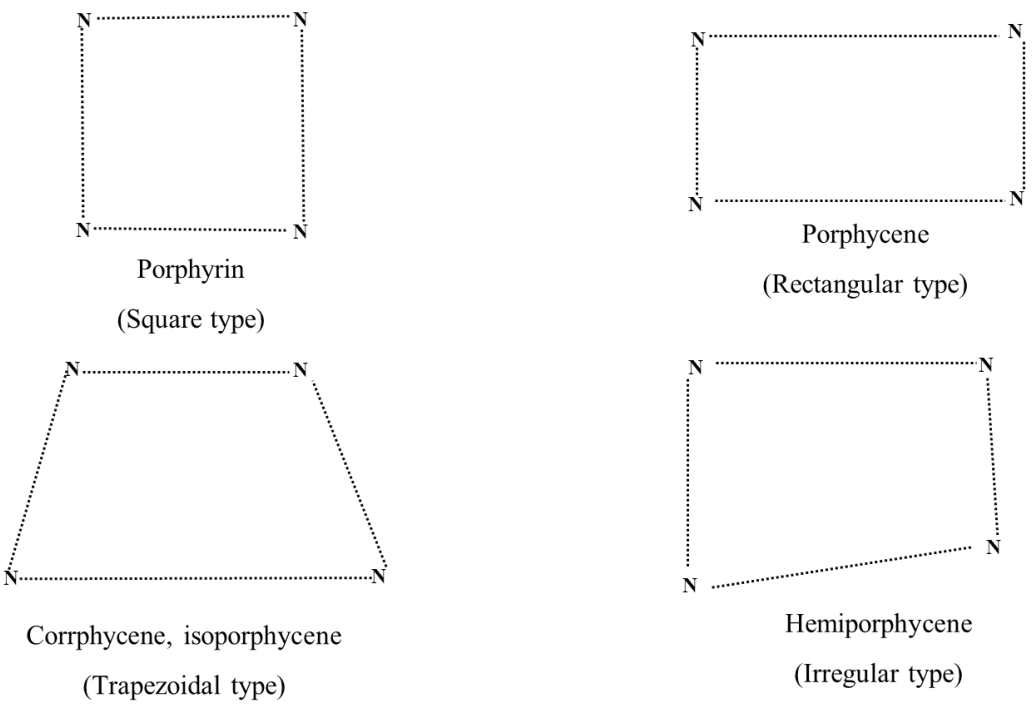

Figure 1.7: N_4 core shape of porphyrin, porphycene, corrphycene, hemiporphycene and isoporphycene.[25]

1.4. Contracted porphyrins

Contracted congeners have a smaller number of heterocycles or *meso*-methine moieties compared to porphyrin. Corroles are first contracted porphyrin to be reported. It was discovered serendipitously by Johnson and Kay while working for getting corrin ring for vit B_{12}.[26] The macrocycle is having 18π- conjugation like porphyrin but unlike porphyrin it lacks one *meso*-methine unit, instead has a bipyrrole link. Further removal of another *meso* carbon from corrole will ensue the formation of norcorrole, which is a 16-π antiaromatic system. Experimentally the molecule was realised by Martin Bröring in 2008.[27] Gram-scale synthesis of Ni-norcorrole is carried out successfully by Kobayashi and Shinokubo et al. in 2012.[28] Another important member of contracted porphyrin is a tripyrrolic 14π aromatic system i.e. subporphyrin. It was introduced by Osuka and coworkers in 2006.[29] All the subporphyrin derivatives reported have a dome shaped structure and are not stable without boron complexation. But just by inserting one more *meso*-sp^2 carbon to the skeletal structure, it enhances the stability and brings a drastic change in structure and properties. It will result in [14]triphyrin (2.1.1), which is planar and also free of metal reported in 2008 by Shen and Yamada.[30]

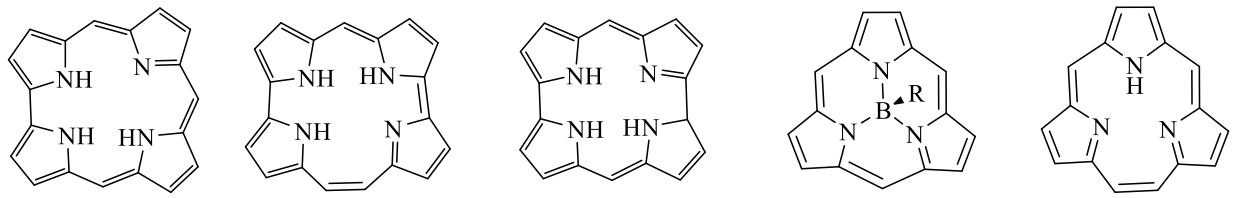

1.15 Corrole | **1.16** Isocorrole | **1.17** Norcorrole | **1.18** Subporphyrin | **1.19** Triphyrin(2.1.1)

Figure 1.6. Contracted porphyrins.

1.4.1. Isomerism in contracted porphyrins

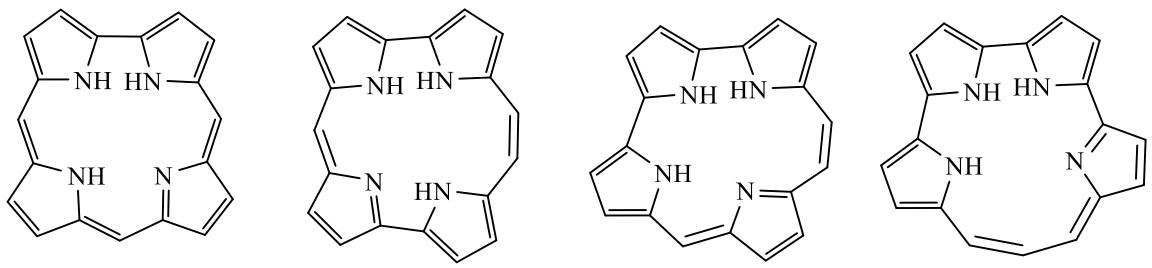

1.15 Corrole [18]porphyrin(1.1.1.0) | **1.16** Isocorrole [18]porphyrin(2.0.1.0) | **1.20** [18]porphyrin(2.1.0.0) | **1.21** [18]porphyrin(3.0.0.0)

Figure 1.7: Corrole and its possible structural isomers.

As corrole has been the most studied contracted porphyrin it is an obvious thought to consider for possible isomeric structures. One less *meso* carbon in corrole reduces it's number of possible isomers to three which has been represented in **figure 1.7**. Theoretically, isocorrole comes out to be the most stable isomer of corrole having 3.5-4 kcal/mol higher energy relative to corrole (calculated by PM3 and BLYP/6-31G**//3-21G).[31] Isocorrole is the only isomer of corrole synthesized till date. Properties of both the isomers will be discussed briefly here.

Though corrole was discovered serendipitously, rational synthetic approaches from appropriate precursors were reported after that. But synthesis of precursors was lengthy and yields were low. So, despite of having intriguing properties it was underdeveloped. The momentous discovery which came in 1999 i.e., one-pot synthesis of corrole brought an avalanche of research and publications in this field. Both Robert Paolesse and Zeev Gross independently reported easy and single step synthesis of corrole from commercially available reagents i.e., pyrrole and aldehyde.[32]

If one *meso* sp^2 carbon of porphyrin, is replaced the skeletal structure turns out to be that of corrole and is considered to be contracted porphyrin. Following similar analogy, isocorrole would be called contracted porphycene. Though corrole is having an almost planar structure, isocorrole is slightly more deformed from planarity.[31,33] In *meso*-formyl tetraethyltetrabromoisocorrole, distortion is due to steric crowding of two amine type NHs in the dipyrromethene end resulting in a twisting of both pyrrole by 23° in the opposite direction to each other from mean plane of macrocycle.[33] In crystal structure of *meso*-free octaethylisocorrole, two NHs are localised on the two pyrroles of ethylene side and one pyrrole is tilted by 18° from mean plane. ^{1}H NMR spectrum of a freebase octaalkylcorrole shows a broad signal at -3.48 ppm for three NHs[26b] but for isocorrole one NH comes at 6.18 while other two NHs comes at -1.2 ppm. Downfield shift of one NH is due to strong hydrogen bonding while in the other side hydrogen bonding is disrupted due to ruffling in the structure. UV-vis absorption spectrum of freebase isocorrole is almost similar to that for corrole but slightly hypsochromically shifted. Soret band of octethylisocorrole is observed at 384 nm compared to 396 nm for octaethylcorrole. Also, Q band intensity is more for isocorrole in comparison with corrole as it is shown in in **figure 1.8**.[31]

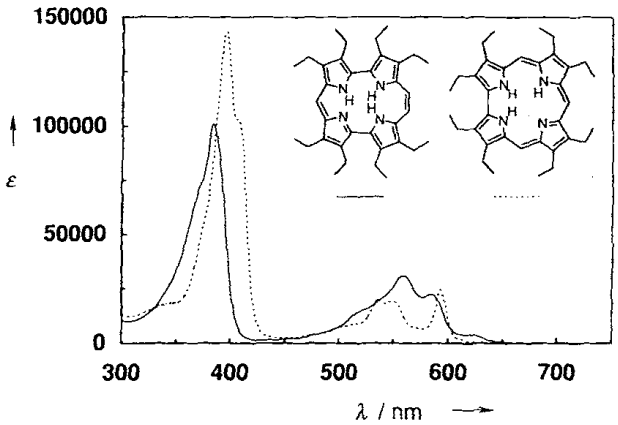

Figure 1.8: UV-vis spectra of octaethylisocorrole and octethylcorrole in CH_2Cl_2.[31]

1.5. Expanded porphyrin

Sessler defined expanded porphyrinoids in their review in 2003 as "macrocycles that contain pyrrole, furan, thiophene, or other heterocyclic subunits linked together either directly or through one or more spacer atoms in such a manner that the internal ring pathway contains a minimum of 17 atoms".[34] First expanded porphyrin to be observed was a pentapyrrolic macrocycle discussed by Woodward in the aromaticity conference in 1966.[35] It was a serendipitous observation in the chase for the synthesis of vitamin B_{12}. He named it as sapphyrin for its intense blue colour like sapphire in solid state. The observation of expected higher analogue of porphyrin along with the curiosity for larger aromatic annulenes and also a larger core for metal coordination fascinated researchers to go for rational synthesis and isolation of the macrocycle. First report of sapphyrin came in 1972 as its core-modified analogue.[36a] Though it was started with Woodward in 1960s,[35,36b] but boosting came with the discovery of improved synthesis of sapphyrin by Sessler in 1990 and also, he demonstrated its application in anion binding and PDT.[37,38]

Subsequently, anion binding by expanded porphyrin became an intriguing research topic.[37] In this field many pioneer discoveries have been documented by Sessler's group. Sapphyrin, cyclo[8]pyrroles have played major roles as anion receptors. Among these, sapphyrin is most studied expanded porphyrin for this purpose. Sapphyrin has a 25% larger core size and more basic than porphyrin. Many sapphyrins continue to exist in monoprotonated form in higher pH also.[39] Early on, sapphyrin **1.22** has shown versatile anion binding properties towards halides, phosphate and azide with a selective affinity for fluoride ion (K_a of ca. 2.8×10^5 M^{-1} in methanol solution) in its mono or diprotonated form.[37],[39] Sapphyrin with two hydroxypropyl substituent in its β-position (**1.23**) is explored for deaggregation-based

fluorescence sensor. It exhibits substrate dependent deaggregation upon addition of inorganic phosphate resulting in phosphate-sapphyrin complex. It leads to an increase in fluorescence intensity.[40] Cyclo[8]pyrrole, which was first reported by Sessler in 2002 has a large, N-H rich core. It exhibits a good binding capacity towards many oxoanions like sulphate, phosphate, pertechnetate. From XRD structure of sulphate-complex, it was revealed to be a planar structure and sulphate ion sitting in the core binds to the macrocycle with hydrogen bonding.[41] After this discovery cyclo[8]pyrrole is fine-tuned for selective binding for anions like pertechnetate, perrhenate etc.[42]

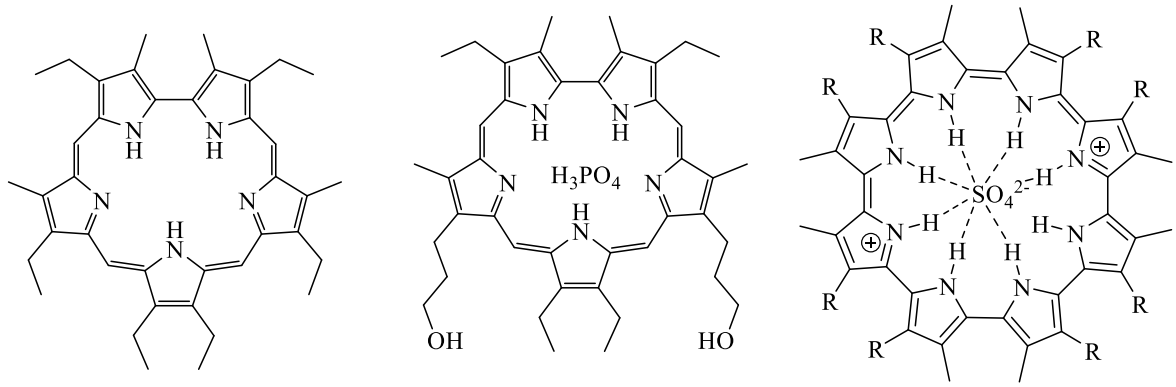

Figure 1.9: Examples of some expanded porphyrins showing anion binding.

An important feature of expanded porphyrin is its large and flexible π-conjugated pathway which is responsible for its strong aromaticity, intense colour and fluorescence in NIR region and also, large two-photon absorption cross section.[43] Structural constraints to get aromatised, peripheral substitution, hydrogen bonding are main factors which contribute significantly for various conformations of expanded porphyrin. [26]Hexaphyrin(1.1.1.1.1.1) has been a widely used model molecule to study conformational flexibility. There are examples of the said macrocycle with different *meso* substitutions to exist in different conformations like rectangular, dumbbell, figure-eight and even triangular.[44] Though most of the *meso*-aryl substituted hexaphyrins prefer rectangular conformation with two central but opposite pyrroles inverted, dumbbell shaped molecules also exist quite often. Dumbbell-shaped [26]hexaphyrins will have four intramolecular hydrogen bonding while rectangular one will have only two. But, in dumbbell comformations, steric congestion of inward-facing *meso* aryl groups is a main factor for destabilisation. If 5 and 20 positions don't have bulky *meso*-aryl groups the structure would be dumbbell shaped with perfect planarity and effective hydrogen bonding as seen in case of 5,20-*meso*-thien-3-yl-10,15,25,30-*meso*-pentafluorophenyl substituted [26]hexaphyrin.[44c]

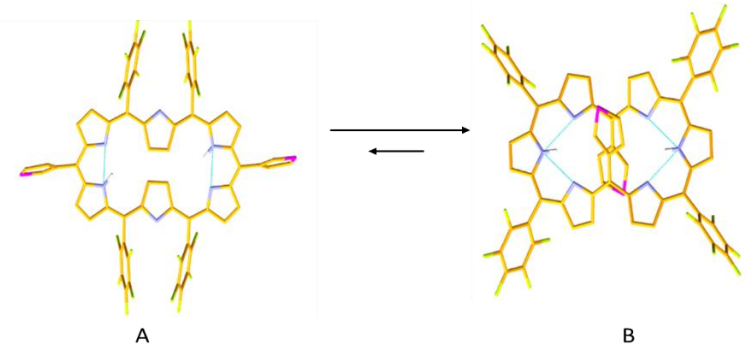

Figure 1.10: Interconversion of conformation due to less bulky thienyl group in *meso* positions.[44c]

In the year 1994, Sessler gave a new area to porphyrin scientists to work upon i.e. supramolecular chirality. He reported synthesis of largest expanded porphyrin, *β*-alkyl [40]decaphyrin(1.0.1.0.0.1.0.1.0.0), also named as turcasarin, which showed a twist in the general loop structure of macrocycles instead of an open circular conformation resulting in conformational chirality.[45] The complex proton NMR spectrum invoked the thought of existing enantiomeric pair, though a stereogenic centre was absent. From crystal structure of the tetraprotonated macrocycle, a C_2 symmetric but a twisted 'figure-eight' structure was obtained which confirmed the presence of two opposite directional twist resulting in a pair of enantiomers.

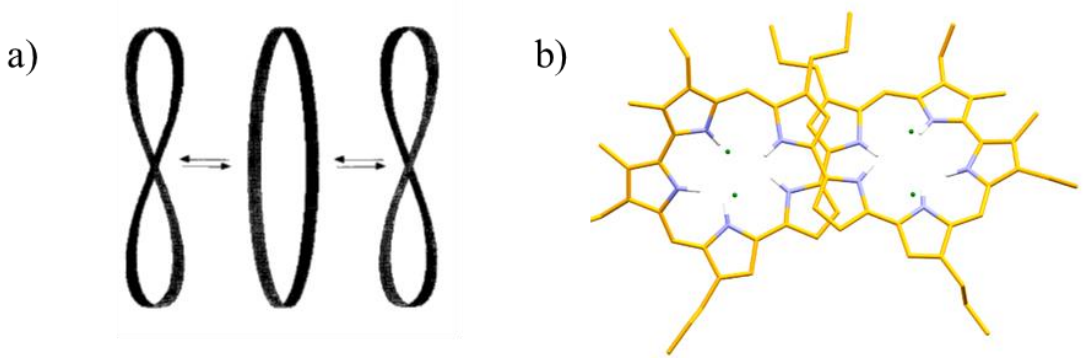

Figure 1.11: a) Schematic representation showing interconversion from loop to figure-eight and **b)** crystal structure of tetraprotonated form of turcasarin.[45]

Aromaticity, which can be considered as a measure of stability of conjugated cyclic structure is an important area of research in chemistry. In 1931, Hückel reported his theory of (4n+2)π system to determine aromatic character of conjugated cyclic structure.[46] According to this theory annulenes with (4n+2)π conjugation is said to be aromatic while annulenes with 4nπ conjugation are antiaromatic. As porphyrins exhibit a strong aromatic character with 18π-

conjugation, research on expanded porphyrin initially was expected to have an intriguing aromatic property due to its higher π-conjugated system and flexible structure. Heilbronner proposed new concept of Möbious-aromaticity which was completely opposite to Hückel theory.[47] Here a 4nπ conjugated molecule can be aromatic if it is having half-twisted Möbious strip topology. The concept was put on theoretical base. But, realising the existance was really difficult because a twist in a cyclic molecule would create a lots of strain in the ring and also the overlap of *p*-orbitals, thus delocalisation would be disturbed. So putting a twist and complete π-conjugation into a single ring was a challenging task. Almost after four decades, in 2003, the dream came true when Herges group reported first example of a cyclic hydrocarbon with mobious aromaticity.[48] Soon after this, in 2007, Latos-Grażyński reported an expanded porphyrin (di-*p*-benzi[28]hexaphyrin) with far stronger ring current and Möbius-aromaticity.[49a] Subsequently, many expanded porphyrins with Möbius aromaticity were reported. While Hückel theory and Möbius theory determines aromaticity of planar and distorted or half twisted cyclic molecules respectively, molecules with another conformation like doubly twisted figure of eight structure remained back. Molecules with figure of eight structure are weekly aromatic if they have (4n+2)π conjugation and weakly antiaromatic if they have 4nπ conjugation like Huckel aromaticity for planar molecules.

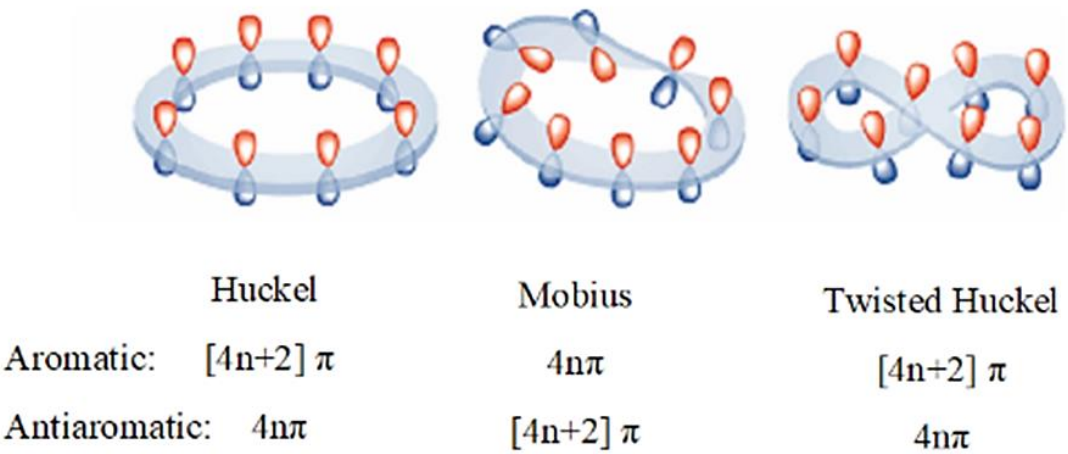

Figure 1.12: Hückel and Möbius topology and aromaticity.[49]

Apart from many theoretical caculations for degree of aromaticity, like nuclear independent chemical shift (NICS), bond length alteration (BLA), harmonic oscillator model of aromaticity (HOMA) or anisotropy of induced current density (AICD), there are some intrinsic properties of porphyrinoids like ^{1}H NMR or photophysical properties to determine their aromatic nature experimentally. For an aromatic porphyrinoid, inner NHs and outer *β*-protons exhibits an

upfield shift and downfield shift respectively in ^{1}H NMR scale due to its ring current. On contrary, an antiaromatic porphyrinoid shows a reverse character in the spectrum. This holds true for both Hückel and Möbius system. Analysing photophysical properties can also make out the difference between an aromatic and antiaromatic molecule. An aromatic expanded porphyrin has sharp Soret band and distinct Q-bands in visible and NIR regions, respectively. The absorption spectral pattern attributes to the fact that aromatic expanded porphyrins have a larger HOMO-LUMO gap compared to the antiaromatic one and also, the HOMO pairs, HOMO and HOMO-1 are almost degenerate. But the degeneracy is broken for antiaromatic

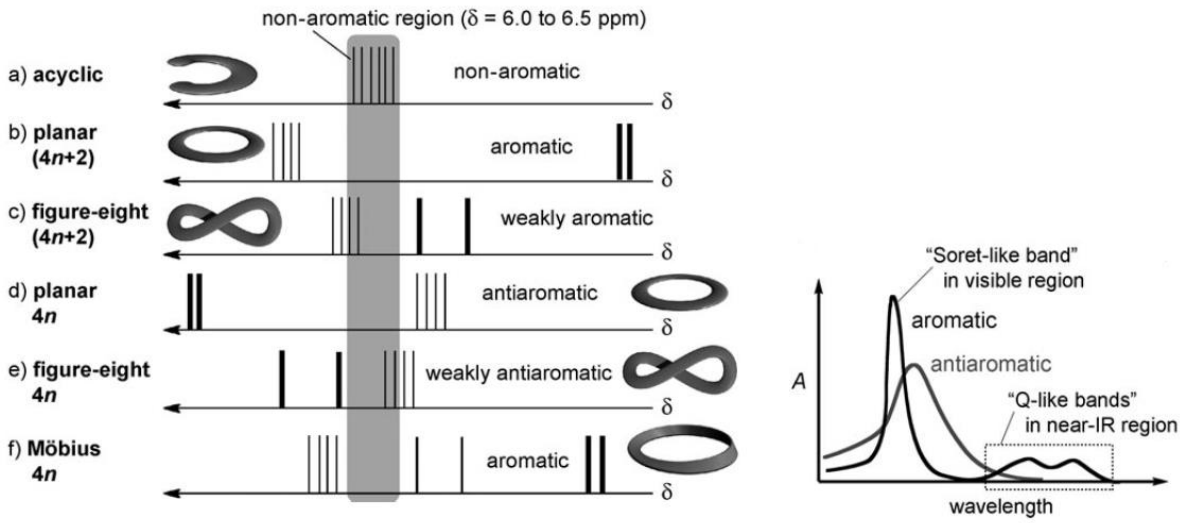

Figure 1.13: (Left) ^{1}H NMR spectra of (a) acyclic compound; (b)-(f) porphyrins. (Right) Absorption spectra of aromatic and antiaromatic expanded porphyrin.[42]

compounds resulting in narrow HOMO-LUMO gap and many transition energies.[43, 51] Thus, broad and diffuse absorption bands in visible region and a very weak absorption (due to forbidden g-g transition from HOMO-LUMO) in NIR region are characteristics of antiaromatic compound. In contrast to the aromatic species, antiaromatic compounds have a very short excited state lifetime and do not exhibit fluorescence due to presence of lowest excited optically dark states enhancing nonradiative decay channels.[52] Aromaticity of expanded porphyrins can be regulated by external stimulus like temperature, solvent polarity, protonation and deprotonation.[49a, 53]

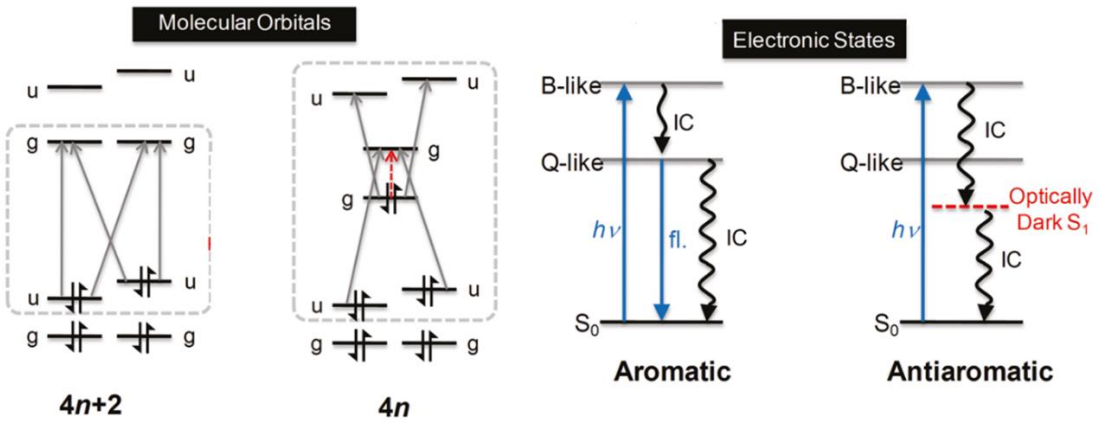

Figure 1.14: Schematic diagram of molecular orbital and electronic states of Hückel aromatic and antiaromatic compounds.[52]

Expanded porphyrins have been observed to act as very flexible ligands to adopt the coordination sphere of variety of metal ions and can form monometallic or multimetallic complex. Due to presence of more numbers of pyrrole atoms they can undergo multiple imin-amine conversion which helps to stabilise different oxidation states of metal ion. Number of metal complexes of expanded porphyrins have been reported in the literature and has shown unique mode of binding. They can show gable T-shaped binding, rectangular mode of binding, or Mobius twisted-type coordination.[54] Larger expanded porphyrins where structural characterization has been difficult due to many flexible conformations, metal complexation becomes a good method of restricting the conformation and help in structural characterization.[55]

1.5.1. Structural isomerism in expanded porphyrin

Like the case of porphyrin and contracted porphyrin, isomerism has also been explored in expanded porphyrin but the reports are very few compared to porphyrin. Along with structural isomerism, stereoisomerism also exists in expanded porphyrin. Discussing stereoisomerism in detail here is out of scope. So only structural isomerism is discussed here. With four *meso* carbons and five heterocycles, many structural isomers of sapphyrin are possible. But neither experimental work, nor theoretical studies has been carried out for all the possible structures. Only isolated isomers of sapphyrin are [22]pentaphyrin(2.0.2.0.0) with trivial name ozaphyrin as its core modified analogue, [22]pentaphyrin(2.1.0.0.1) as all-aza analogue. Smaragdyrin has one structural isomer namely isosmaragdyrin. Though lots of hexapyrrolic macrocycles has been studied structural isomerism exists only for few. Only

rubyrin has three isomers i.e. isorubyrin and bronzaphyrin and [26]hexaphyrin(1.1.1.0.1.0). We will discuss about all the above said structural isomers in this section.

1.5.1.1. Sapphyrin and isomers

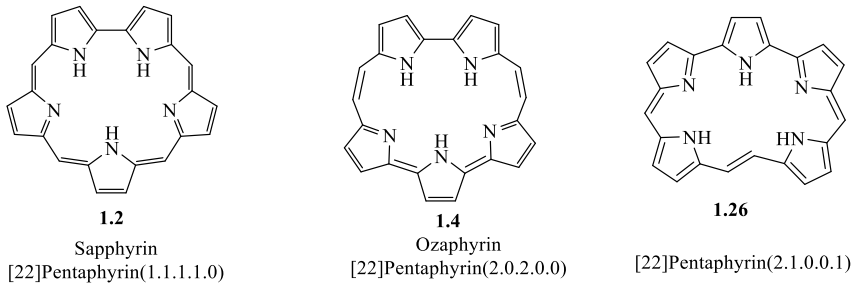

Figure 1.15. Structural representation of sapphyrin and its isomers.

Sapphyrin is the first and most widely studied pentapyrrolic macrocycle. The aromatic macrocycle contains five pyrroles with four *meso* methine bridges and a bipyrrolic link. After early reports of Woodward and Johnson, Sessler and coworkers brought a major breakthrough in 1990 by improving the synthetic procedures for the precursors involved in MacDonald [3+2] condensation i.e. diformyl bipyrrole and tripyrromethane diacid.[37a,b] First *meso*-aryl substituted sapphyrin was reported by Latos-Grażyński and co-workers in 1995.[56] All-aza *meso*-aryl substituted sapphyrin was a minor product in Rothemund type condensation of pyrrole and benzaldehyde in presence of $BF_3.OEt_2$ (**Scheme 1.1**) and isolated 1% yield. In this work, he observed an inversion of the pyrrole ring opposite to the bipyrrole unit from ^{1}H-NMR. Also, he found that the inverted pyrrole is flipping by 180° on protonation, resulting all the pyrrole NHs inside the core of the macrocycle.

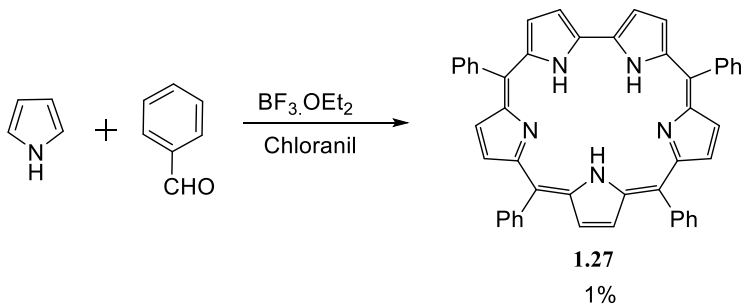

Scheme 1.1: Synthesis of *meso*-aryl sapphyrin by Latos-Grażyński group.[56]

In 1998, Chandrashekar and coworkers reported an improved synthetic method, where they carried out the reaction with 5-phenyldipyrromethane as only precursor in Lindsey type condensation reaction (**scheme1.2**).[57] They isolated *meso*-aryl substituted sapphyrin with 3-

11% yield along with porphyrin and rubyrin. They also observed the inversion of pyrrole opposite to bipyrrole unit in sapphyrin, which on protonation flipped by 180°, consistent with observation of Latos-Grażyński.

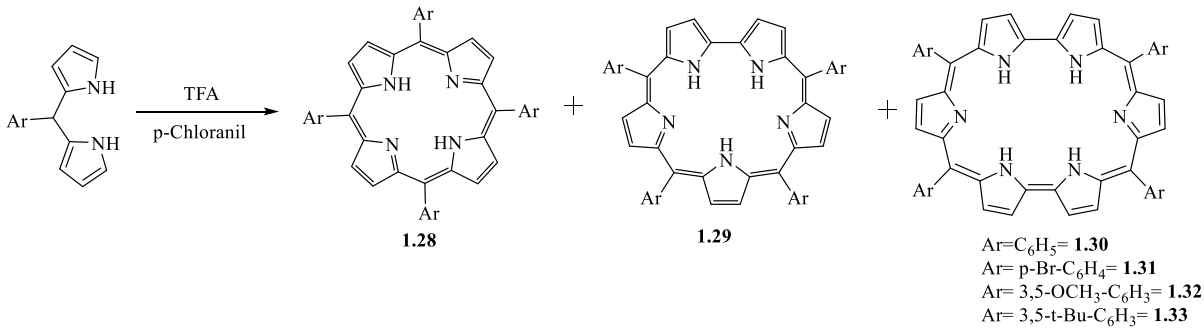

Scheme 1.2: Synthesis of *meso*-aryl sapphyrin by Chandrashekar's group.[57]

Sessler's group reported an efficient method for *meso*-diaryl sapphyrin by condensing 5,5′-diformyl bipyrrole, pyrrole and benzaldehyde catalysed by $BF_3.CH_3OH$ followed by oxidation with o-chloranil or DDQ.[58] They obtained crystal structure for the diprotonated species and found it to be planar.

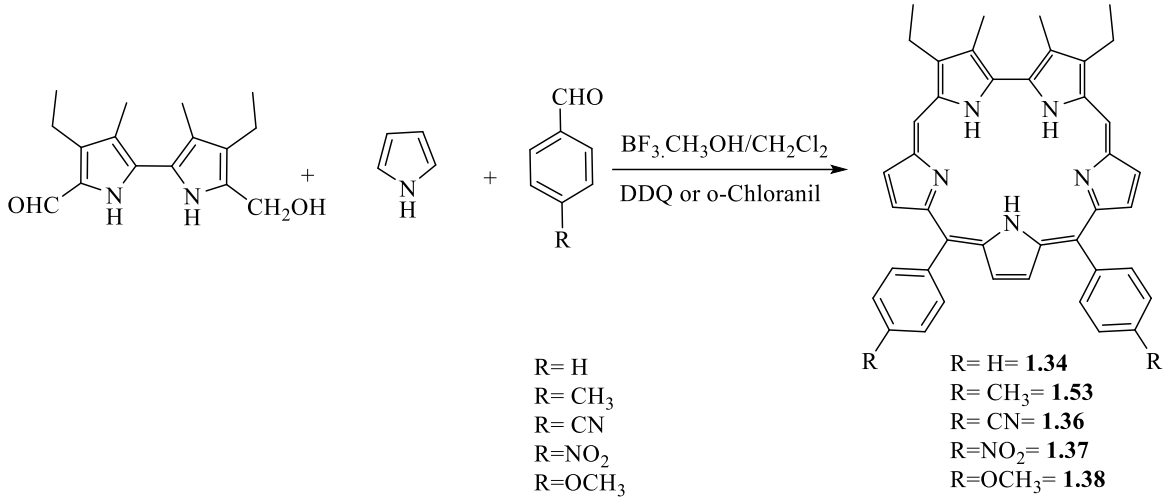

Scheme 1.3. Synthesis of *meso*-diaryl sapphyrin.[58]

Unlike porphyrins, sapphyrins show bright green colour in solution. Freebase sapphyrins exhibit a Soret band at *ca.* 450 nm, approximately 50 nm bathochromically shifted from that of porphyrins and three weak Q-bands at 620-670 nm.[37a,b],[56] *Meso*-phenyl substituted sapphyrins show a similar but red shifted absorption bands relative to *meso* unsubstituted *β*-alkyl sapphyrins. For example, *meso*-tetraphenylsapphyrin, **1.27** displays a split Soret band at 493 and 518 nm followed by four Q-type bands at 640, 697,710 and 790 nm.[56] On protonation, the dicationic sapphyrins show slightly red or blue shifted Soret band

depending upon the acid used and red shifted Q-bands and also molar extinction coefficients are increased drastically for all the absorption bands.[59] As its Q-bands absorbs within 'physiological optical window' or 'therapeutic window' where absorption of light by common physiological chromophores is low, it can be a promising candidate for PDT. Various water-soluble saphhyrins were demonstrated to be biologically active to be good PDT agents by Sessler's group.[60] They showed absorption at 675 nm in aqueous medium and good singlet oxygen quantum yield. A few water-soluble core-modified sapphyrins are seen to be suitable candidate for drug uptake into human erythrocytes and also the retention time was faster than that of photofrin.[61]

Larger core size of sapphyrin (5.5 Å inner N-N diameter) relative to porphyrin (4.4 Å) and a greater number of chelating atoms provide intriguing properties to study its unique metal coordination. At first it was expected this will stabilise many larger metals like lanthanides and actinides mostly which cannot be accommodated in the core of porphyrins and also it may stabilise many unusual oxidation states of metals. But afterwards, it was realised to be not so practical. The coordination chemistry of sapphyrin was started by Woodward with many 1st row transition metals among which only Zn (II) and Co (II) complexes could be isolated.[36b] Both the complexes are tetra ligated in case of all aza sapphyrin but, for mono-oxa or mono-thia sapphyrin, Co(II) was bound to the macrocycle without deprotonation.[62] When sapphyrin was treated with second or third row transition metal salts like $HgCl_2$, $CdCl_2$, $PdCl_2$, $RhCl_3$, $IrCl_3$, and $RuCl_3$, $PdCl_2(CH_3CN)_2$, the resulting complexes were decomposed. When sapphyrin was treated with carbonyls of iridium and rhodium i.e. $[RhCl(CO)_2]_2$ and $[IrCl(CO)_2Py]$ it resulted in monometallic complexes for less equivalents of salts and bimetallic complexes for excess equivalents of salts.[63] Only actinide metal ion to be incorporated into all-aza sapphyrin core till date is uranyl ion which was demonstrated to be nonaromatic due to disruption of its aromaticity.[64]

Sapphyrin being an aromatic and basic macrocycle with two imine nitrogen, easily undergo protonation to give monoprotonated or diprotonated species and hence a hydrogen-bond donor. This property of sapphyrin along with larger inner core has provided an excellent platform to study the coordination chemistry of anions. Anion binding property of sapphyrin has been mentioned briefly in the previous section. Sapphyrins has not only served as anion receptors but also, they have shown good performance as translocators across membrane.[65] The first anion recognition with expanded porphyrin started serendipitously while trying to get a crystal structure of the diprotonated macrocycle by counter-ion exchange reaction with Cl^- or

PF_6^-.[37b] Though fluoride ion is trapped inside the core of sapphyrin by N-H···F hydrogen bonds in $[H_5Sap.F^-]^+$, but, chloride ion being bigger in size stabilises itself above and below the plane of the macrocycle in a symmetrical manner in dihydrochloride salt.[37c] In case of monooxa and monoselena sapphyrin, the chloride ion binding is same like all-aza system but it is different for dioxasapphyrin. It has only one chloride ion above the plane of the macrocycle.[66] From the X-ray crystal structure of bis(trifluoroacetic acid)-complexed sapphyrin it was confirmed that one TFA ion was bound above the macrocycle with three hydrogen bondings while second one lies below the plane with two hydrogen bondings.[66] Sapphyrin has been studied for many other anion binding like benzoic acid[67] or phosphate ions[37d] and also DNA binding.[68]

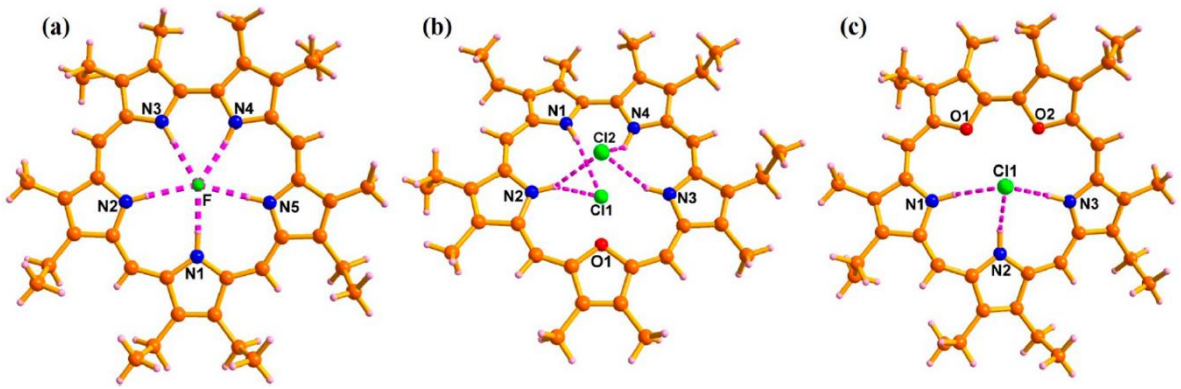

Figure 1.16: Crystal structure of a. $[H_5SapF^-]PF_6^-$; b. $[H_4OxasapCl^-_2]^-$; c. Mono chloride salt of dioxasapphyrin.[38]

While sapphyrin remains as most studied expanded porphyrin, its isomeric analogue, ozaphyrin, [22]pentaphyrin(2.0.0.2.0) are scarcely studied molecules. [22]pentaphyrin(2.0.0.2.0) is the first isomer to be isolated as monooxa analogue.[69] This has an emerald green colour in solution phase like sapphyrin. Ibers named it as 'Ozaphyrin' after name of the Emerald city of Oz. McMurry coupling of dipyrrolylfuran dialdehyde and bipyrrole dialdehyde resulted in the formation of first ozaphyrin, **1.39**. Soon after this tetrapropylmonothiaozaphyrin was also reported by following same procedure with appropriate precursers.[70] But all-aza ozaphyrin couldn't be synthesised yet. Both oxa and thiaozaphyrin are aromatic in nature like sapphyrin. Both the derivatives show similar ^{1}H NMR spectral features with internal NH at -2.16 and -2.72 ppm for oxa and thia derivatives, respectively. Whereas ^{1}H NMR spectrum of 3,7,18,22-tetraethyl-2,8,17,23-tetramethy1-27-thiasapphyrin has its internal NH protons at -3.34.[70] **1.39** has a split Soret band at 414 and 430 nm and three Q bands between 640 and 750 nm and thiaozaphyrin has a red shifted Soret band at 425 nm with a shoulder at 467 nm and four Q-bands between 650-750 nm.

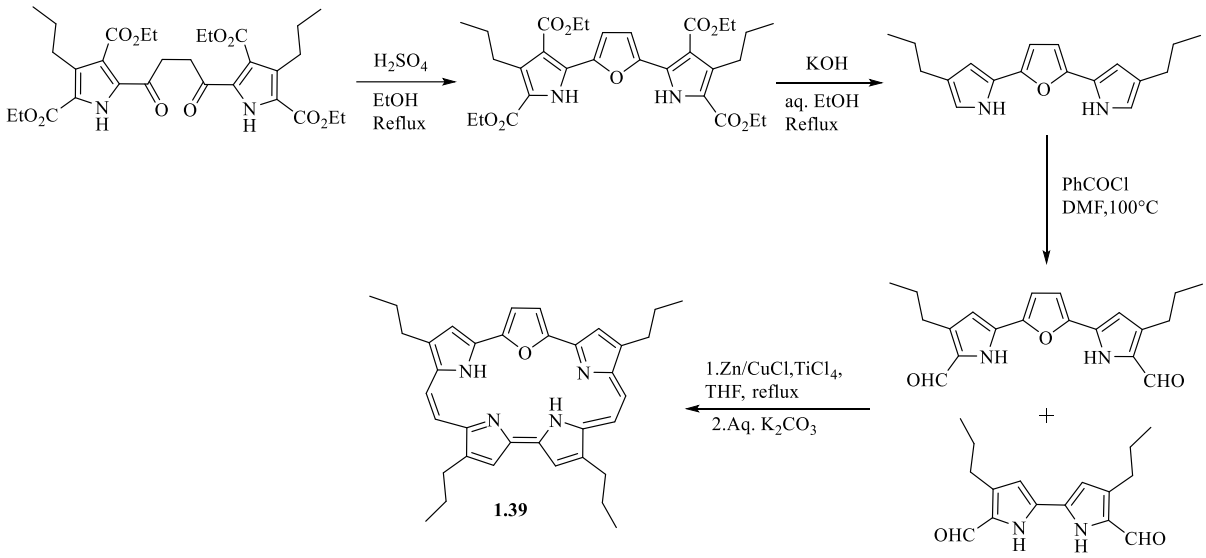

Scheme 1.4: Synthesis of monooxaozaphyrin.[69]

Intensity ratio of Q bands to Soret band in sapphyrin varies from 1-10%, whereas for ozaphyrin it varies from 30-50% like in porphycene. Ozaphyrin is a planar pentapyrrolic macrocycle. It exhibits a flat but unsymmetrical and irregular shaped core as compared to the symmetrical cavity of sapphyrin. The core size of ozaphyrin is~5.0 Å which is bigger compared to porphyrin and porphycene but comparable to that of sapphyrin.

All aza isomer of sapphyrin joined the macrocycle community in 1995 when Sessler reported the synthesis of [22]pentaphyrin(2.1.0.0.1) in 1995.[71] They carried out HCl catalyzed condensation of terpyrrole and diformyl alkyne-stretched bipyrrole to get [22]dehydropentaphyrin(2.1.0.0.1), **1.40**, which on hydrogenation gave the novel sapphyrin isomer **1.41**.

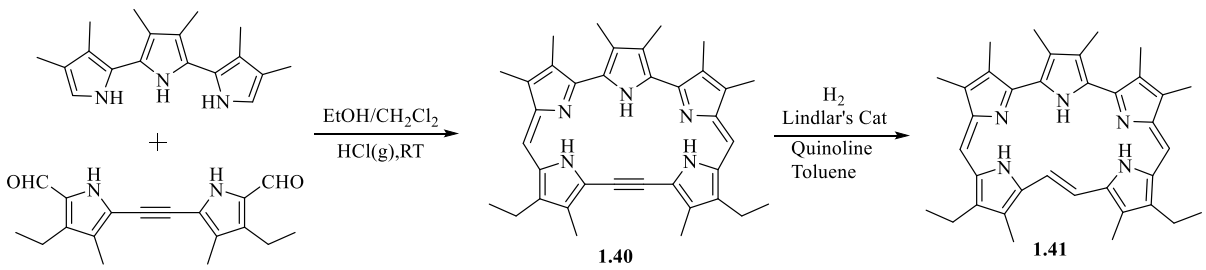

Scheme 1.5: Synthesis of [22]pentaphyrin(2.1.0.0.1).[71]

Both **1.40** and **1.41** are 22π Hückel aromatic systems like sapphyrin. Compound **1.40** also has same number of *meso* carbons and pyrroles like sapphyrin but it has an alkyne bridge instead of alkene. But it has properties similar to that of sapphyrin. For instance, it has green colour in solution and blue colour in solid state like sapphyrin. Its dihydrochloride salt exhibits

a more intense Soret band than that of freebase like sapphyrin. Also, it has two less intense Q bands. Its freebase has a broader and less intense absorption band. In crystal structure, the alkyne bridge is prominently seen which is in contrast to stretched porphycene and platyrin where alkyne unit remains as cumulene like moiety.[68] Freebase of **1.40** displays a red shifted Soret band at 476 nm compared to sapphyrin, and shows three Q- bands between 600-700 nm. Similar to **1.40,** protonated form of **1.41** has more intense Soret band along with two Q-bands. It has a *trans*-alkene bridge with one alkene proton in shielded and another in deshielded region in NMR scale. Dihydrochloride salt of **1.41** has a planar structure as seen from crystal structure.

1.5.1.2. Smaragdyrin and isomer

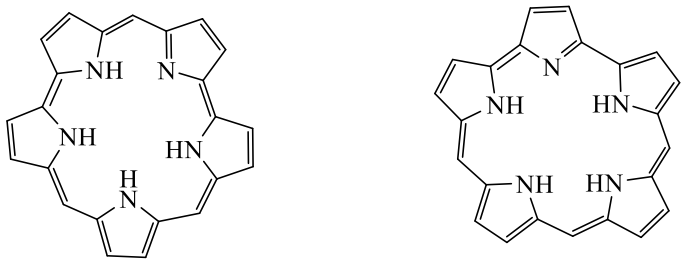

1.42
Smaragdyrin
[22]Pentaphyrin(1.1.0.1.0)

1.43
Isosmaragdyrin
[22]Pentaphyrin(1.1.1.0.0)

Figure 1.17: Structures of smaragdyrin and isosmaragdyrin.

Woodward while discussing his experience with sapphyrin in the aromaticity conference, also discussed about the probable existence of another pentapyrrolic macrocycle having one *meso* carbon less than that of sapphyrin.[34] But, its practical existence was realised by Johnson and Grigg during their attempt to synthesize sapphyrin. They called it as norsapphyrin.[36] Their approach for synthesising the macrocycle has been shown in the **scheme 1.6**. They could isolate dioxanorsapphyrin and obtain its UV-visible absorption and mass spectra but attempt to isolate all-aza analogue (reaction mixture exhibited expected absorption spectrum) didn't give success and resulted in decomposition. Woodward named the macrocycle as smaragdyrin as it exhibits bright emerald green colour (from Greek word *smaragdos* meaning emerald).[72] Chandrashekar's group had brought an improved synthetic procedure for *meso*-aryl core-modified smaragdyrin by avoiding the use of bipyrrolic precurser which are inherently less stable and making use of easily available precursors i.e. tripyrranes and dipyrromethanes (**Scheme 1.7**).[73] Here, direct pyrrole-pyrrole bond is formed in final step by oxidative coupling. They were able to get crystal structure for freebase oxasmaragdyrin and observed a nonplanar structure of the macrocycle and mentioned that the nonplanarity might

have arisen from the strain created in the whole molecule due to the introduction of an additional pyrrole ring, direct pyrrole-pyrrole interactions, and the steric repulsion between imino hydrogen atoms. Following the [3+2] oxidative coupling strategy many different *meso*-substituted smaragdyrin were synthesised and characterised.[74]

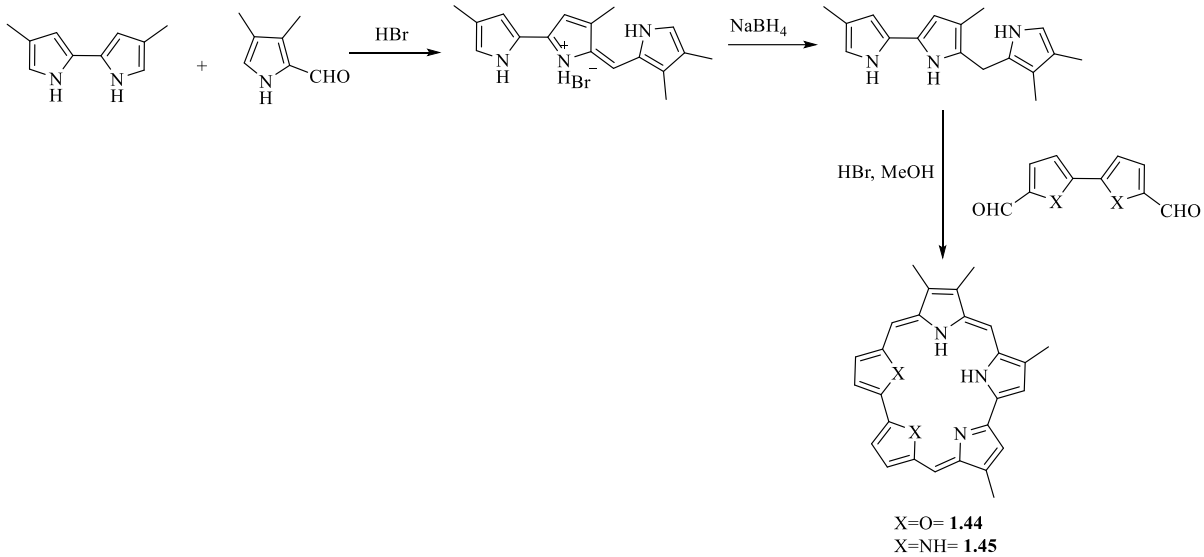

Scheme 1.6: First synthesis of dioxasmaragdyrin.[36]

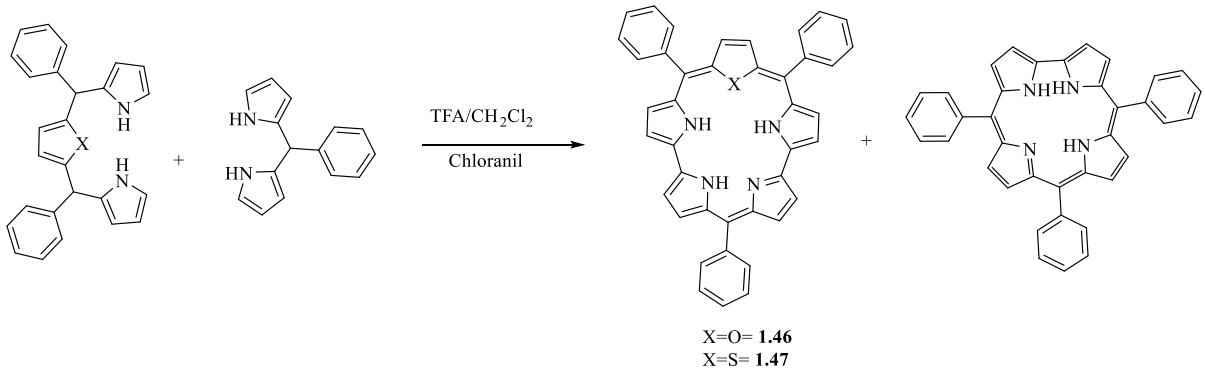

Scheme 1.7: Synthesis of 25-Oxasmaragdyrin.[73]

Meso-aryl 25-oxasmaragdyrin **1.46** exhibits a Soret band at 443 nm and four Q-bands between 500-700 nm. As expected, increasing conjugation at *meso* results in red shift of the absorption bands.

Chandrashekar's group has introduced rhodium and nickel complexes of **1.46** and **1.47** with carbonyl salt of rhodium, $[RhCl(CO)_2]_2$ and $NiCl_2$, respectively. He revealed that Rh(I) binds to the macrocycles in μ^2-fashion with one amino and one imino nitrogen of DPM unit forming an out of plane square-planar complex. But Ni(II) is coordinated to all four nitrogen of 25-oxasmaragdyrin and the ligand is oxidised to give a π-cation radical which was confirmed

from EPR and broad ^{1}H NMR signals.[75] As 25-oxasmaragdyrin has a dipyrromethene unit as part of the molecule, it could be explored for BF_2-complexation. Ravikanth's group has used this structural property and introduced one BF_2 unit into the macrocycle to get complex **1.48**.[76] **1.48** shows a strong absorption band at 702 nm, which is three times more intense than absorption band of freebase in the same region. Also, fluorescence band of BF_2-complex is bathochromically shifted and the quantum yield is two times more relative to that of freebase. They prepared $B(OR)_2$-complexes and $B(OH)_2$-complex from **1.48**. Compound **1.49** behaves as a selective sensor for F^- ion among anions like F^-, Cl^-, Br^-, I^-, HSO_4^-, ClO_4^-. F^- ion binds to the molecule by means of H-bonding with -OH and -NH protons. Phosphorous complex of 25-oxasmaragdyrin was also synthesised by treating the macrocycle with $POCl_3$ in presence of triethylamine in toluene.[77]

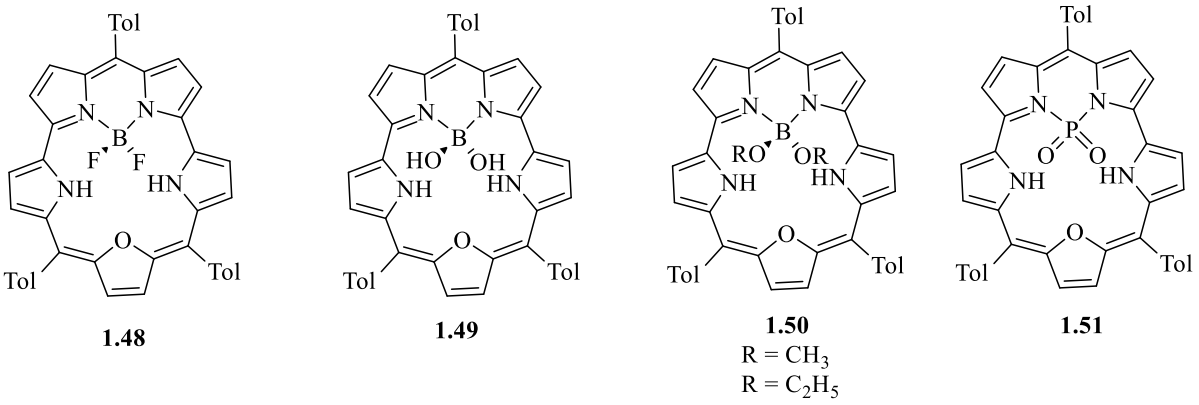

Figure 1.17: Boron and phosphorous complexes of smaragdyrin.[76,77]

All-aza smaragdyrin has four NHs inside the core if we consider a 22π-conjugation (aromatic system) but, it will have two amino type protons for its 20π congener. Though aromatic system, **1.42A,** feels a coulombic repulsion between the inner core NH protons making it less stable. On contrary, intramolecular hydrogen bonding interaction in **1.42B** will stabilise it despite of its antiaromatic behaviour.[78]

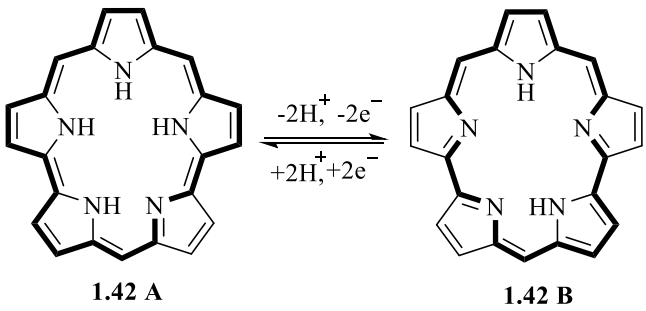

Figure 1.18: Aromatic switching between 22π and 20π smaragdyrin.[78]

Recently, Osuka and coworkers could synthesise all-aza smaragdyrin and also demonstrated the aromatic switching between its 22π and 20π systems. They synthesised BF_2-complex of 22π-smaragdyrin **1.52** via S_NAr mechanism, which was treated with methane sulphonic acid and then triethylamine to remove the BF_2 unit. This will be resulting in 20π-smaragdyrin **1.53**. The latter upon reduction in glove box gives 22π freebase smaragdyrin, **1.54** which is not so stable and immediately oxidises to the 20π-congener.[78]

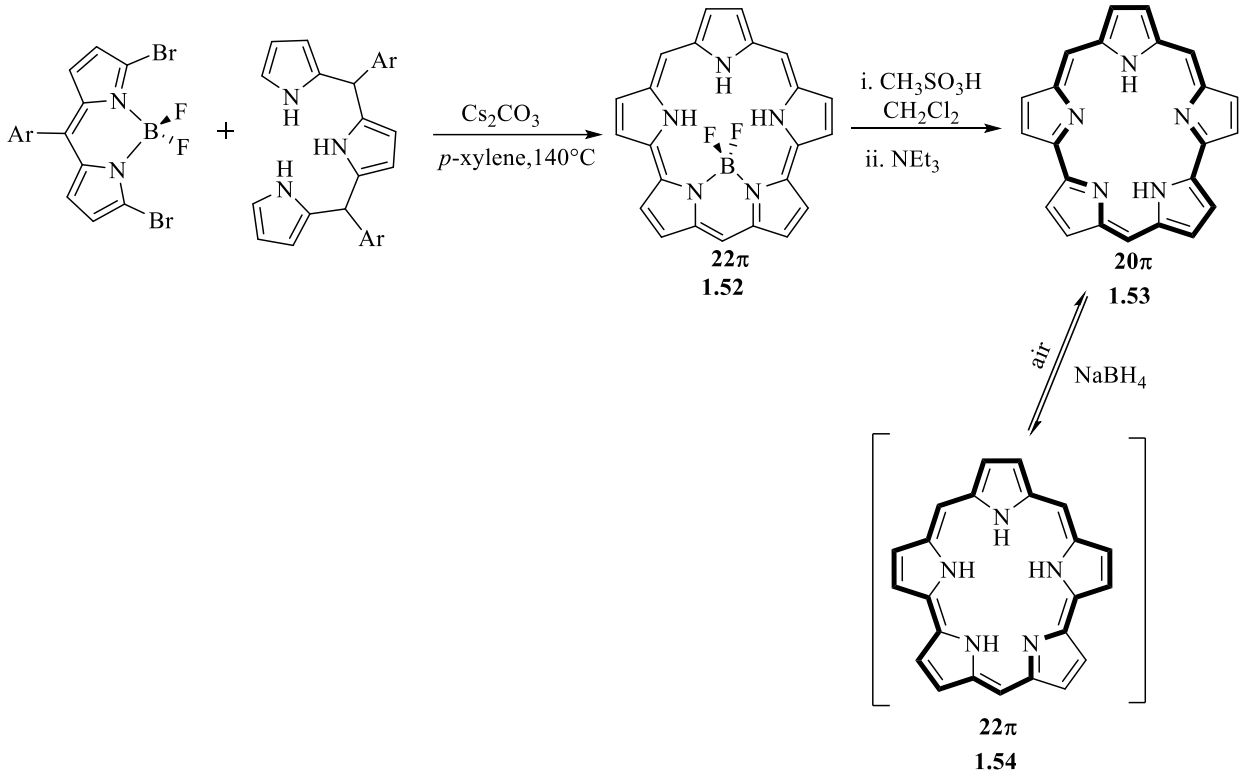

Scheme 1.8: Synthesis of 20π- conjugated freebase all-aza smaragdyrin.[78]

Almost after two decades of synthesis of dioxasmaragdyrin, and a failure to synthesize all-aza smaragdyrin, Sessler's group reported successful isolation of all-aza isomer of smaragdyrin, namely isosmaragdyrin (**1.55**) along with its monooxa analogue (**1.56**) by acid catalysed condensation of terpyrrole and bisformyl dipyrromethane (**Scheme 1.9**).[79] Though both the macrocycles are very much stable and can be stored for months in freeze, monooxa analogue **1.56** is more stable than the all-aza **1.55**. NMR spectra and UV-vis absorption spectra showed the aromatic nature of both the macrocycles. Soret band of **1.55** and **1.54** appears around similar wavelength (~455 nm), but Q bands pattern and position both are different from that of all-aza smaragdyrin **1.54**. Two Q bands of **1.55** lies between 650–700 nm whereas smaragdyrin exhibits a greater number of Q bands which spreads over 600–900 nm region.[78]

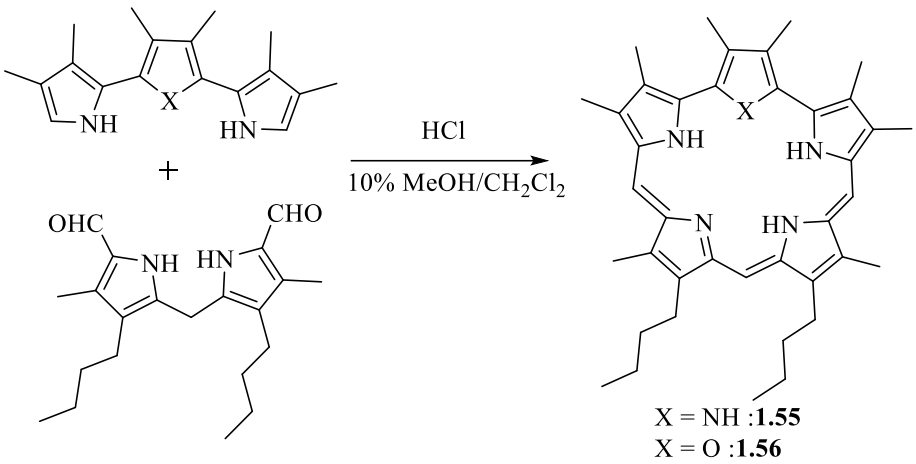

Scheme 1.9: Synthesis of isosmaragdyrin.

1.5.1.3. Rubyrin and isomers

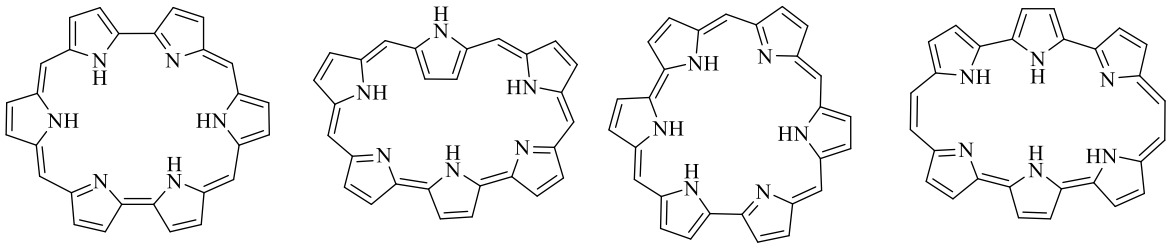

1.57 Rubyrin [26]Hexaphyrin(1.1.0.1.1.0)

1.58 Isorubyrin [26]Hexaphyrin(1.1.1.1.0.0)

1.59 [26]Hexaphyrin(1.1.1.0.1.0)

1.6 Bronzaphyrin [26]Hexaphyrin(2.0.0.2.0.0)

Figure 1.19: Structural representation of rubyrin and its isomers.

The decade of 1990 has seen synthesis of maximum numbers of new macrocycles in porphyrin chemistry. In 1991, Sessler reported first synthesis of a hexapyrrolic macrocycle, **1.57**.[80] He named this as rubyrin due to bright red colour of its diprotonated form. It is a 26π aromatic molecule having six pyrrole and four *meso* carbons. Then after, isorubyrin[81] and bronzaphyrin[67] were discovered which can be considered as structural isomer of parent rubyrin having same four *meso* carbons and six heterocycles.

1.5.1.3.1. Synthesis

Diprotonated form of 4,8,13,18,23,27- hexaethyl-3,9,14,17,22,28-hexamethylrubyrin, **1.60** was synthesised by condensing the diacid of tetrapyrrolic precursor and diformyl bipyrrole as shown in **scheme 1.10**. With all possible efforts they could not obtain freebase or metalated rubyrin.[80] In 1998, Chandrashekar's group successfully synthesised all-aza rubyrin in its freebase form as a minor product in attempt to get sapphyrin from 5-phenyl-dipyrromethane with 1 eq. of TFA as catalyst.[56a] But they could only obtain mass and UV-Vis absorption

spectra. Further characterisation was not done. Chandrashekar and coworkers reported synthesis and characterisation of a few derivatives of core modified rubyrin by TFA catalysed oxidative coupling of *meso*-phenyltripyrranes with one heterocycle other than pyrrole.[82]

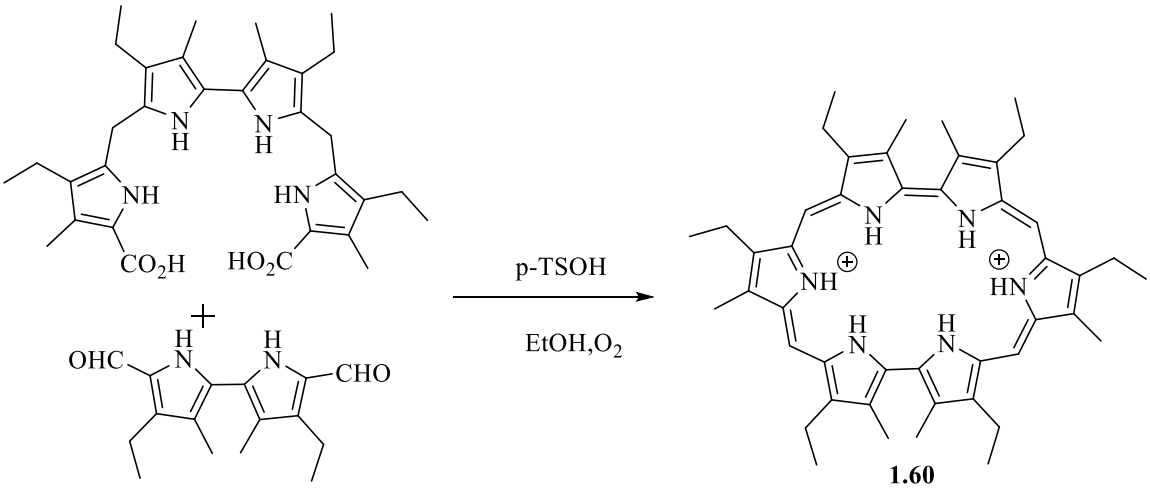

Scheme 1.10: Synthesis of diprotonated rubyrin.[80]

Using Chandrashekar's procedure, Osuka and coworkers attempted synthesis of expanded porphyrin. They carried out oxidative coupling of *meso*-pentafluorophenyl substituited tripyrrane using TFA as catalyst. They were able to get 5,10,19,24-tetrakis(pentafluorophenyl)-[26]hexaphyrin(1.1.0.1.1.0), **1.61** as a stable violet solid along with 5,10,19,24,33,38-hexakis(pentafluorophenyl)-[38]nonaphyrin(1.1.0.1.1.0.1.1.0), **1.62** as minor product.[83]

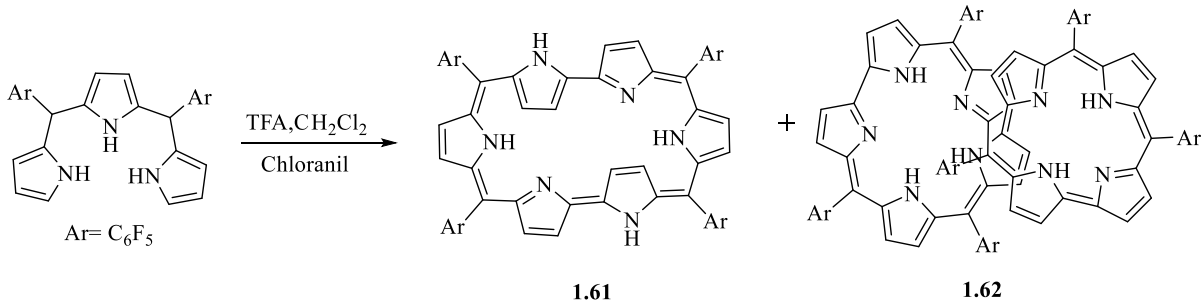

Scheme 1.11: Synthesis of freebase all-aza rubyrin and nonaphyrin.[83]

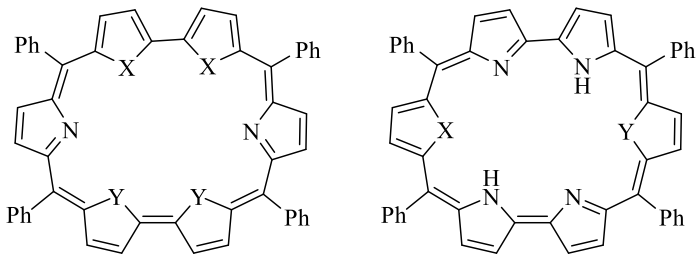

X	Y	
S	S:	**1.63**
S	O:	**1.64**
O	O:	**1.65**
S	Se:	**1.66**
Se	Se:	**1.67**

X	Y	
S	S:	**1.68**
O	O:	**1.69**
S	O:	**1.70**
Se	Se:	**1.71**
Te	Te:	**1.72**

Figure 1.20: Examples of isolated core-modified rubyrins.[82]

[26]Hexaphyrin(2.0.0.2.0.0), having four *meso* carbons and six heterocycles is an isomer of rubyrin. Johnson and Ibers reported first synthesis of the core-modified macrocycle with four pyrroles and 2 thiophene.[84] They carried out McMurry coupling of precursor dialdehyde to get the target macrocycle **1.73**. Due to its bronze colour in chloroform, they coined the name bronzaphyrin.[70]

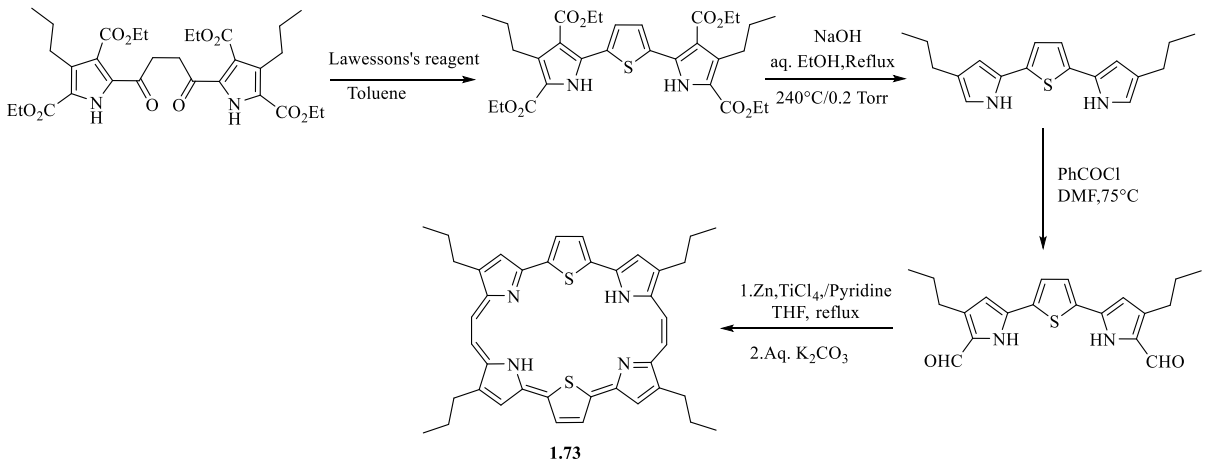

Scheme 1.12: Synthesis of tetrapropylbronzaphyrin.[84]

Though bronzaphyrin was synthesised first in 1992, first structural characterisation *via* XRD reported in 2018 by Kishore and Panda.[85] Analogous to core-modified rubyrin, bronzaphyrin **1.74** shows a rectangular conformation with inversion of both the thiophene rings and with a dihedral angle of 22° from the plane of macrocycle. The conformation stays alike in solution state also which was verified by ^{1}H NMR analysis. On protonation, thiophene rings maintains the inversion. This inversion of thiophene rings was attributed to the steric repulsion between its β-CH protons and inner ethyl substituents of pyrroles of terpyrrole moiety.

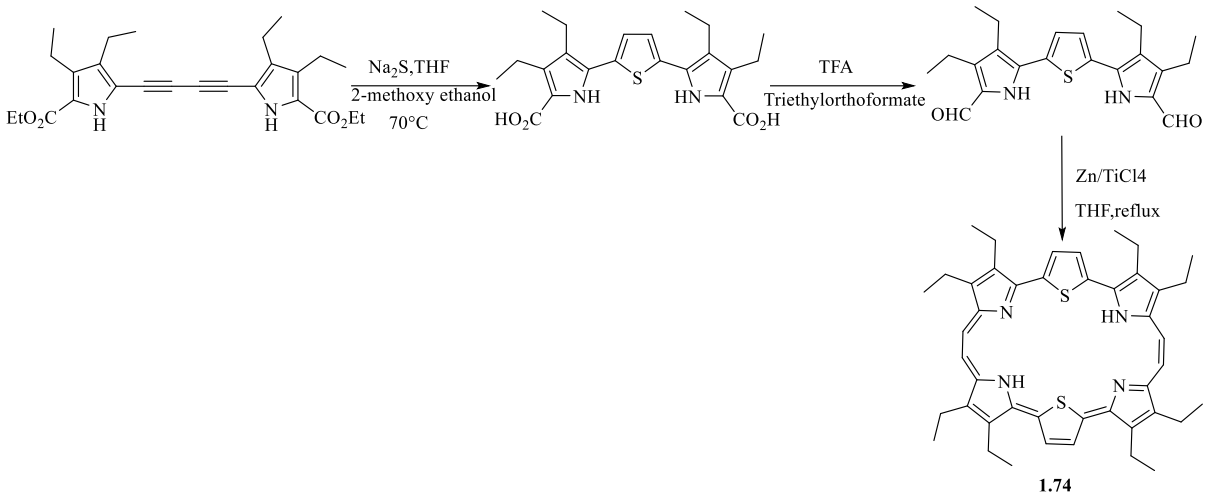

Scheme 1.13: Synthesis of octaehtyldithiabronzaphyrin by Panda and coworkers.[85]

Keeping in view the conformational flexibility, interesting coordinating behaviour and many other interesting properties shown by hexaphyrins, Sessler's group came up with another new hexaphyrin which is an isomer of rubyrin, [26]hexaphyrin(1.1.1.1.0.0) also named as isorubyrin.[81] **1.75** was synthesised using acid mediated condensation of a *meso*-substituted tripyrromethane and terpyrrole dialdehyde as shown in **scheme 1.14**. Unfortunately, despite being structurally well characterised and showing good stability this isomer also remained neglected and unexplored further.

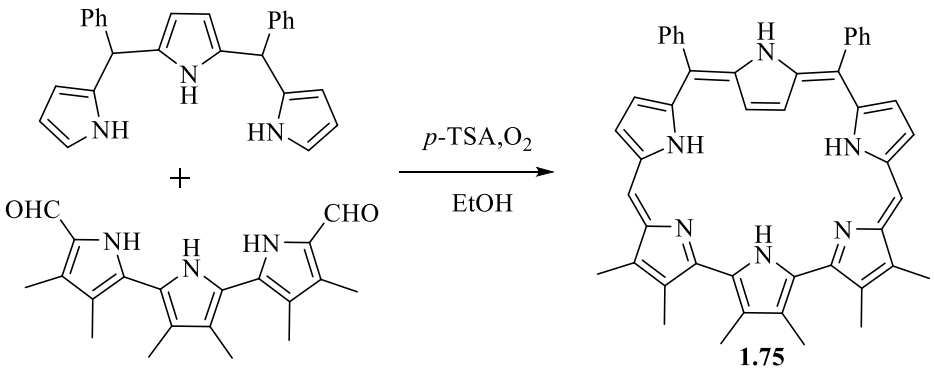

Scheme 1.14: Synthesis of all-aza [26]hexaphyrin(1.1.1.1.0.0).[81]

Chandrshekar's group carried out [3+3] acid catalysed condensation of tripyyrane containing one thiophene or selenophene with terthiophene diol and obtained **1.76** and **1.77**. But, only by changing mesityl group in the terthiophene to anisole results in [3+3+3+3] condensation product along with [3+3] condensation product.[86]

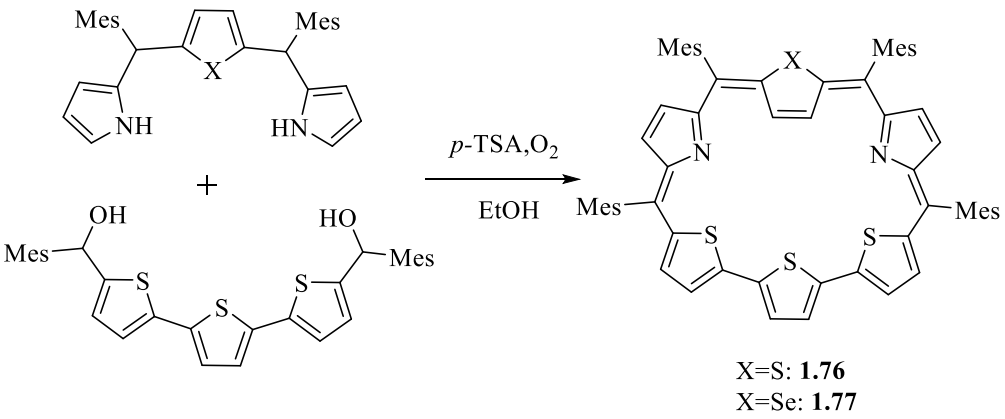

Scheme 1.15: Synthesis of core-modified [26]hexaphyrin(1.1.1.1.0.0).

Another structural variant of rubyrin was sythesised by Pushpan et al. in 2001, which was a core modified analogue namely, [26]hexaphyrin(1.1.1.0.1.0). Synthetic approach for the new macrocycle was acid catalysed oxidative coupling of hetero tetrapyrrane and hetero tripyrrane. The mentioned macrocycle was actually a minor product in addition to heptaphyrin. They could isolate four core modified derivatives (**Scheme 1.16**).[87]

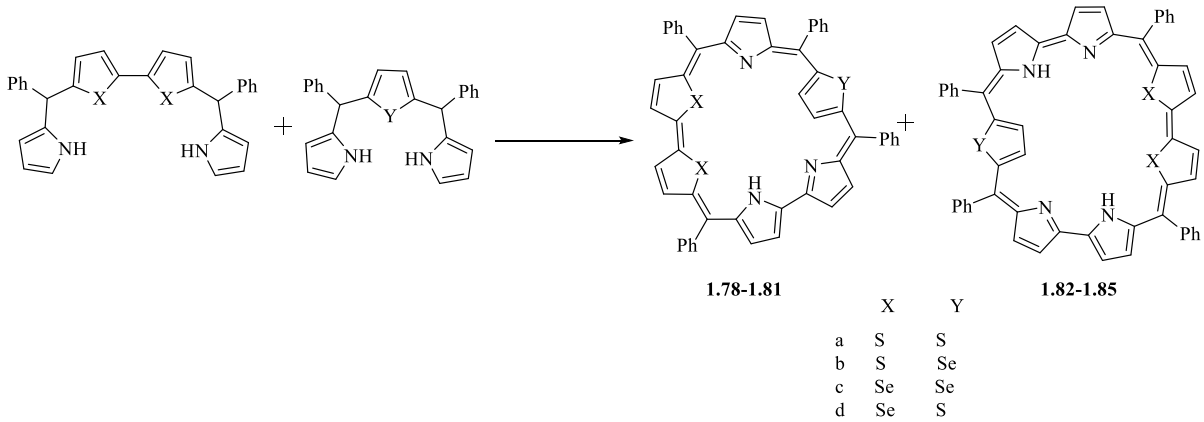

Scheme 1.16: Synthesis of [26]hexaphyrin(1.1.1.0.1.0).[87]

1.5.1.3.2. Structure and Electronic Properties

First rubyrin to be structurally characterised was a Cl^- salt of diprotonated all-azarubyrin **1.60**, where it showed almost planar conformation.[80] **1.61.2TFA** retained the inverted character like parent molecule but both the pyrroles flipped by 180° in case of **1.61.2HCl** to give similar structure like that of **1.60**. Both core-modified rubyrins **1.70** and **1.71** exhibit a rectangular conformation with both the thiophene and selenophene rings are inverted and out of molecular plane and also all the thiophene and selenophene takes position along the longer side of rectangle. [82b]

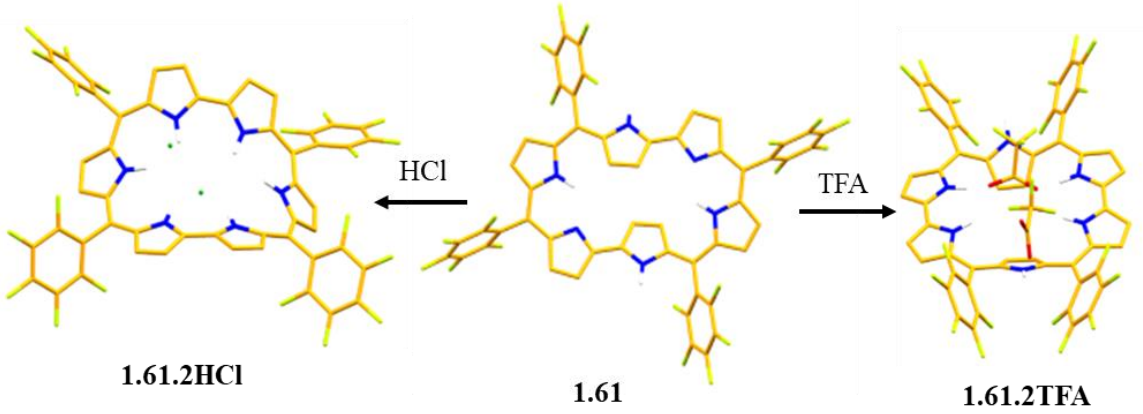

Figure 1.21: Conformation control of all-aza rubyrin by protonation with different acids.[83]

On the contrary, [26]hexaphyrin(1.1.1.1.0.0) **1.75** having all *β*-alkyl substituted pyrroles in the terpyrrole unit and *meso*-phenyl substitution in tripyrrane unit exhibits selective inversion of only one middle pyrrole ring in the tripyrrane side, which may be due to the arising steric repulsion of *β*-methyl substitutions if it is inverted.[81] Also, the macrocycle doesn't exhibit a complete planar structure due to which there is a reduced aromatic character. The heteroanalogue **1.76.TFA** shows inversion of the thiophene ring opposite to the terthiophene moiety.[86] From ^{1}H NMR spectra, with upfield *β*-CH protons, **1.78-1.81** depicts the inversion of the thiophene or selenophene ring opposite to bithiophene and biselenophene.[87]

Freebase form of all-aza rubyrin, **1.61** exhibits a sharp Soret band at 537 nm and three weak, broad Q bands between 800-919 nm. Upon protonation with TFA, Soret band with almost double intensity gets red shifted to 555 nm, but on changing the acid to HCl, it displays an unusual blue shift to 518 nm, which is also similar to the HCl salt of **1.60** with Soret band at 505 nm. This behaviour is attributed to the conformation change upon protonation with HCl unlike TFA (**Figure 1.21**). Core-modified rubyrins display Q bands in a broad range between 600-1000 nm. UV-Vis absorbance of bronzaphyrins with two ethene bridges, displays a pattern like that of porphycene. They show broad and split Soret bands between 450-550 nm with intensity comparable to that of porphyrin and Q-bands intensity almost 50% intensity ratio to Soret band and also shows drastic *β*-substituent effect. Upon protonation, Soret band shows an enhancement in intensity with a red shift and slight blue shifted Q-bands. **1.75** displays split Soret band at 502 and 531 nm and a single broad Q band with 30% intensity. Like other expanded porphyrin, this also shows a red shift and enhancement in Soret peak but unlike parent molecule, it shows two Q bands. Changing the terpyrrole moiety to terthiophene moiety in **1.76**, gives a single Soret at 527 nm and there is an enhancement in the intensity. Similarly,

macrocycle **1.77** exhibits Soret band at 530 nm but it has five Q bands between 600-1000 nm. Upon protonation, there is red shift of Soret peak to 563 nm and number of Q bands reduces to three and the last Q band is blue shifted.

1.6. Scope of the present work

The limited works on isomerism in expanded porphyrin encouraged us to think and explore more isomers of expanded porphyrin and study their structural, photophysical, aromatic and specifically coordination property. We have synthesised and characterised new pentapyrrolic macrocycles which will be discussed in detail in coming chapter.

1.7. References

1. Warren, M. J.; Smith, A. G. *Tetrapyrroles: Birth, Life and Death* **2009**, 5.
2. Battersby, A. R.; Fookes, C. J. R.; Matcham, G. W. J.; McDonald, E. Biosynthesis of the Pigments of Life: Formation of the Macrocycle. *Nature* **1980**, *285*, 17.
3. Fischer, H.; Zeile, K. Synthese des Hämatoporphyrins, Protoporphyrins und Hämins. *Justus Liebigs Ann. Chem.* **1929**, *468*, 98.
4. Gouterman, M. Spectra of Porphyrin. *J. Mol. Spectrosc.* **1961**, *6*, 138.
5. Biesaga, M.; Pyrzynska, K.; and Trojanowicz, M., Porphyrins in analytical chemistry. A review. *Talanta*, **2009**, *51*, 209.
6. [a] Paolesse, R.; Nardis, S.; Monti, D.; Stefanelli, M.; Natale, C. D. Porphyrinoids for chemical sensor application. *Chem. Rev.* **2017**, *117*, 2517. [b] Rana, A.; Panda, P.K.; Fluorescent turn-off-based sensing of nitrated explosives using porphyrin and their zinc derivatives. *RSC Adv.*, **2012,** *2*, 12164.
7. Ambroise, A.; Wagner, R. W.; Rao, P.D.; Riggs, J. A.; Hascoat, P.; Diers, J. R.; Seth, J.; Lammi, R. K.; Bocian, D. F.; Holten, D.; Lindsey, J. S. Design and synthesis of porphyrin-based optoelectronic gates. *Chem. Mater.*, **2001,** *13*, 1023.
8. Mathew, S.; Yella, A.; Gao, P.; Humphry-Baker, R.; Curchod, B. F. E.; Ashari-Astani, N.; Tavernelli, I.; Rothlisberger, U.; Nazeeruddin, M. K.; Grätzel, M. Dye-sensitized solar cells with 13% efficiency achieved through the molecular engineering of porphyrin sensitizers. *Nat. Chem.* **2014,** *6*, 242.
9. Fleischer, E. B.; Krishnamurthy, M. Reduction of acetylene and nitrogen by a cobalt-porphyrin system. *J. Am. Chem. Soc.* **1972**, *94*, 1382.
10. Pushpan, S. K.; Venkatraman, S.; Anand, V. G.; Sankar, J.; Parmeswaram, D.; Ganesan, S.; Chandrashekar, T.K.; Porphyrins in photodynamic therapy - a search for ideal photosensitizers. *Current Medicinal chemistry. Anti-cancer Agents*., **2002**, 2,187.
11. Sessler, J. L.; Weghorn, S. J.; Expanded, Contracted & Isomeric Porphyrins. *Tetrahedron Org. Chem.*, **1997**, *15*.
12. Gosmann, M.; Franck, B. Synthesis of a Fourfold Enlarged Porphyrin with an Extremely Large, Diamagnetic Ring-Current Effect. *Angew. Chem., Int. Ed. Engl*., **1986**, *25*, 1100
13. Vogel, E.; Kocher, M.; Schmickler, H.; Lex, J. Porphycene—a Novel Porphin Isomer. *Angew. Chem., Int. Ed. Engl.*, **1986**, *25*, 257.
14. Waluk, J.; Michl, J.; The perimeter model and magnetic circular dichroism of porphyrin analogues, *J. Org. Chem.*, **1991**, *56*, 2729.

15. Sessler, J. L.; Brucker, E. A.; Weghorn, S. J.; Kisters, M.; Schiifer, M.; Lex, J.; Vogel, E. Corrphycene: A New Porphyrin Isomer. *Angew. Chem., Int. Ed. Engl.,* **1994,** *33, 2308*
16. Callot, H. J.; Rohrer, A.; Tschamber, T.; Metz, B. A novel porphyrin isomer: hemiporphycene. Formation and single-crystal x-ray diffraction structure determination of a hemiporphycene nickel complex. *New J. Chem*., **1995**, *19*, 155.
17. Vogel, E.; Bröring, M.; Erben, C.; Demuth, R.; Lex, J.; Nendel, M.; Houk, K. N. Palladium complexes of the new porphyrin isomers (Z)- and (E)-isoporphycene-Pd^{II}-induced cyclization of tetrapyrrolealdehydes. *Angew. Chem., Int. Ed. Engl*., **1997**, *36,* 353.
18. [a] Furuta, H.; Asano, T.; Ogawa, T. "N-Confused Porphyrin": A New Isomer of Tetraphenylporphyrin. *J. Am. Chem. Soc.* **1994**, *116*, 767. [b] Chmielewski, P. J.; Latos-Grażyński, L.; Rachlewicz, K.; Glowiak, T. Tetra-p-tolylporphyrin with an Inverted Pyrrole Ring: A Novel Isomer of Porphyrin. *Angew., Chem. Int. Ed. Eng.,* **1994**, *33,* 779.
19. Waluk, J. Structure, spectroscopy, photophysics, and tautomerism of free-base porphycenes and other porphyrin isomers. *Handb. Porphyrin Sci.,* **2010**, *7*, 359.
20. Vogel, E.; Scholz, P.; Demuth, R.; Erben, C.; Bröring, M.; Schmickler, H.; Lex, J.; Hohlneicher, G.; Bremm, D.; Wu, Y.-D. Isoporphycene: the fourth constitutional isomer of porphyrin with an N_4 core-occurrence of E/Z isomerism. *Angew. Chem., Int. Ed.,* **1999**, *38*, 2919.
21. Stockert, J.; Cañete, M.; Juarranz, A.; Villanueva, A.; Horobin, R.; Borrell, J.; Teixido, J.; Nonell, S. Porphycenes: Facts and Prospects in Photodynamic Therapy of Cancer. *Curr. Med. Chem.,* **2007**, *14*, 997.
22. Fowler, C. J.; Sessler, J. L.; Lynch, V. M.; Waluk, J.; Gebauer, A.; Lex, J.; Heger, A.; Zuniga-y-Rivero, F. and Vogel E. Metal Complexes of Porphycene, Corrphycene, and Hemiporphycene: Stability and Coordination Chemistry. *Chem. Eur. J.,* **2002**, *8*, 3485.
23. Wu, Y. D.; Chan, K. W. K.; Yip, C. P.; Vogel, E.; Plattner, D. A.; Houk, K. N. Porphyrin Isomers: Geometry, Tautomerism, Geometrical Isomerism, and Stability. *J. Org. Chem.,* **1997**, *62*, 9240.
24. Kozlowski, P. M.; Zgierski, M. Z.; Baker, J. *J. Chem. Phys.,* **1998**, *109*, 5905.
25. Vogel, E. Novel porphyrinoid macrocycle and their metal complexes. *J. Heterocyclic Chem.,* **1996,** 33, 1461.
26. [a] Johnson, A. W.; Kay, I. T. The Pentadehydrocorrin (Corrole) Ring System. *Proc. Chem. Soc. London,* **1964**, 89. [b] Johnson, A. W.; Kay, I. T. Corroles. Part I. Synthesis. *J. Chem. Soc.,***1965**, 1620.

27. Bröring, M.; Köhler, S.; Kleeberg. C. Norcorrole: Observation of the Smallest Porphyrin Variant with a N_4 Core. *Angew. Chem., Int. Ed.*, **2008**, *47*, 5658.
28. Ito, T.; Hayashi, Y.; Shimizu, S.; Shin, J.-Y.; Kobayashi, N.; Shinokubo. H. Gram-Scale Synthesis of Nickel (II) Norcorrole: The Smallest Antiaromatic Porphyrinoid. *Angew.Chem., Int. Ed.*, **2012**, *51*, 8542.
29. Inokuma, Y.; Kwon, J. H.; Ahn, T. K.; Yoo, M.-C.; Kim, D.; Osuka, A. Tribenzosubporphines: Synthesis and Characterization. *Angew. Chem., Int. Ed.*, **2006**, *45*, 961.
30. Xue, Z.-L.; Shen, Z.; Mack, J.; Kuzuhara, D.; Yamada, H.; Okujima, T.; Ono, N.; You, X.-Z.; Kobayashi, N. A Facile One-Pot Synthesis of *meso*-Aryl-Substituted [14]Triphyrin(2.1.1). *J. Am. Chem. Soc.*, **2008,** *130*, 16478.
31. Vogel, E.; Binsack, B.; Hellwig, Y.; Erben, C.; Heger, A.; Lex, J.; and Wu, Y.-D. Contracted Porphyrins: Octaethylisocorrole. *Angew. Chem. Int. Ed. Engl.* **1997**, *36*, 2612.
32. [a] Gross, Z.; Galili, N.; Saltsman, I. The First Direct Synthesis of Corroles from Pyrrole. *Angew. Chem., Int. Ed.*, **1999**, *38*, 1427. [b] Paolesse, R.; Jaquinod, L.; Nurco, D.J.; Mini, S.; Sagone, F.; Boschi, T.; Smith, K.M. 5,10,15-Triphenylcorrole: a product from a modified Rothemund reaction. *Chem. Commun.*, **1999**, 1307.
33. Will, S.; Rahbar, A.; Schmickler, H.; Lex, J.; Vogel, E. Isocorroles: Novel Tetrapyrrolic Macrocycles. *Angew. Chem., Int. Ed. Engl.*, **1990**, *29*, 1390.
34. Sessler, J. L.; Seidel, D. Synthetic Expanded Porphyrin Chemistry. *Angew. Chem., Int. Ed.*, **2003**, *42*, 5134.
35. Woodward, R. B. *Aromaticity: An International Symposium Sheffield, 1966*; Special Publication no. 21; The Chemical Society: London, **1966**.
36. [a] Broadhurst, M. J.; Grigg, R.; Johnson, A. W. The synthesis of 22 π-Electron Macrocycles: Sapphyrins and Related Compounds. *J. Chem. Soc., Perkin Trans. 1*, **1972,** *1*, 2111. [b] Bauer, V. J.; Clive, D. L. J.; Dolphin, D.; Paine, J. B., III; Harris, F. L.; King, M. M.; Loder, J.; Wang, S. W. C.; Woodward, R. B. Sapphyrins: Novel Aromatic Pentapyrrolic Macrocycles. *J. Am. Chem. Soc.*, **1983**, *105*, 6429.
37. [a] Sessler, J. L.; Cyr, M. J.; Lynch, V.; McGhee, E.; Ibers, J. A. Synthetic and structural studies of sapphyrin, a 22-.pi.-electron pentapyrrolic "expanded porphyrin". *J. Am. Chem. Soc.*, **1990**, *112*, 2810. [b] Sessler, J. L.; Cyr, M. J.; Burrell, A. K. Sapphyrins: New Life for an Old “Expanded Porphyrin. *Synlett*, **1991**, *1991*, 127. [c] Judy, M. L.; Matthews, J. L.; Newman, J. T.; Skiles, H.; Boriack, R.; Cyr, M.; Maiya, B. G.; Sessler J. L.; In vitro photodynamic inactivation of Herpes simplex virus with sapphyrins: 22π-elctron porphyrin

like macrocycles. *Photochem. Photobiol.,* **1991,** *53,*101. [d] Shionoya, M.; Furuta, H.; Lynch, V.; Harriman, A.; Sessler, J. L. Diprotonated Sapphyrin: A Fluoride Selective Halide Anion Receptor. *J. Am. Chem. Soc*., **1992**, *114,* 5714.

38. Chatterjee, T.; Srinivasan, A.; Ravikanth, M.; Chandrashekar, T. K. Smaragdyrin and sapphyrin Analogues. *Chem. Rev.,* **2017**, *117,* 3329.
39. Král, V.; Furuta, H.; Shreder, K.; Lynch, V.; Sessler, J. L. Protonated Sapphyrins. Highly Effective Phosphate Receptors. *J. Am. Chem.Soc*., **1996**, *118,* 1595.
40. Král, V.; Andrievsky, A.; Sessler, J. L. A Covalently Linked Sapphyrin Dimer. A New Receptor for Dicarboxylate Anions. *J. Am. Chem. Soc*., **1995**, *117,* 2953.
41. Seidel, D.; Lynch, V.; Sessler, J. L. Cyclo[8]pyrrole: A Simple-to-Make Expanded Porphyrin with No *Meso* Bridges. *Angew. Chem., Int. Ed.,* **2002**, *41*, 1422.
42. [a] Eller, L. R.; Stępien, M.; Fowler, C. J.; Lee, J. T.; Sessler, J. L.; Moyer, B. A. Octamethyl-octaundecylcyclo[8]pyrrole: A Promising Sulfate Anion Extractant. *J. Am. Chem. Soc.,* **2007**, *129,* 11020. Correction: *J. Am. Chem. Soc.* **2007**, *129,* 14523. [b] Kataev, E. A.; Pantos, P.; Karnas, E.; Kolesnikov, G. V.; Tananaev, I. G.; Lynch, V. M.; Sessler, J. L. Perrhenate and pertechnetate anion recognition properties of cyclo [8] pyrrole. *Supramol. Chem.,* **2015**, *27,* 346.
43. Saito, S.; Osuka, A. Expanded porphyrin: Intriguing Structures, Elctronic Properties, and Reactivities. *Angew. Chem. Int. Ed.,* **2011**, *50,* 4342.
44. [a] Shimizu, S.; Aratani, N.; Osuka, A. meso-Trifluoromethyl-Substituted Expanded Porphyrins. *Chem. Eur. J.,* **2006**, *12,* 4909. [b] Xie, Y.-S.; Yamaguchi, K.; Toganoh, M.; Uno, H.; Suzuki, M.; Mori, S.; Saito, S.; Osuka, A.; Furuta, H. Triply N-Confused Hexaphyrins: Near-Infrared Luminescent Dyes witha Triangular Shape. *Angew. Chem., Int. Ed.* **2009**, *48,* 5496. [c] Suzuki, M.; Osuka, A. Conformational Control of [26]Hexaphyrins(1.1.1.1.1.1) by meso-Thienyl Substituents. *Chem. Eur. J.,* **2007**, *13,* 196.
45. Sessler, J. L.; Weghorn, S. J.; Hisaeda, Y.; Lynch, V. Turcasarin, the Largest Expanded Porphyrin to Date. *Chem. Eur. J.,* **1995**, *1,* 56.
46. Hückel, E. Zur Quantentheorie der Doppelbindung. *Eur. Phys. J. A,* **1931**, *70,* 204.
47. Heilbronner, E. Hückel Molecular Orbitals of Möbius-Type Conformations of Annulenes. *Tetrahedron Lett.,* **1964**, *5,* 1923.
48. Ajami, D.; Oeckler, O.; Simon, A.; Herges, R. Synthesis of a Möbius aromatic hydrocarbon. *Nature,* **2003**, *426,* 819.
49. [a] Stępień, M.; Latos-Grażyński, L.; Sprutta, N.; Chwalisz, P.; Szterenberg, L. Expanded Porphyrin with a Split Personality: A Hückel-Möbius Aromaticity Switch. *Angew. Chem.,*

Int. Ed,. **2007**, *46*, 7869. [b] Stępień, M.; Szyszko, B.; Latos-Grażyński, L. Three-Level Topology Switching in a Molecular Möbius Band. *J. Am. Chem. Soc*., **2010**, *132*, 3140.

50. Sylvetsky, N.; Banerjee, A.; Alonso, M.; Martin, J. M. L. Performance of Localized Coupled Cluster Methods in a Moderately Strong Correlation Regime: Hückel−Möbius Interconversions in Expanded Porphyrins. *J. Chem. Theory comput.*, **2020**, *16*, 3641.
51. Sung, Y. M.; Oh, J.; Cha, W.-Y.; Kim, W.; Lim, J. M.; Yoon, M.-C.; Kim, D. Control and Switching of Aromaticity in Various All-Aza-Expanded Porphyrins: Spectroscopic and Theoretical Analyses. *Chem. Rev.*, **2017**, *117*, 2257.
52. Cho, S.; Yoon, Z. S.; Kim, K. S.; Yoon, M. C.; Cho, D. G.; Sessler, J. L.; Kim, D. Defining Spectroscopic Features of Heteroannulenic Antiaromatic Porphyrinoids. *J. Phys. Chem. Lett.*, **2010**, *1*, 895.
53. Cha, W.-Y.; Soya, T.; Tanaka, T.; Mori, H.; Hong, Y.; Lee, S.; Park, K. H.; Osuka, A.; Kim, D. Multifaceted [36]octaphyrin (1.1.1.1.1.1.1.1): deprotonation-induced switching among nonaromatic, Möbius aromatic, and Hückel antiaromatic species. *Chem. Commun.*, **2016**, *52*, 6076.
54. [a] Saito, S.; Furukawa, K.; Osuka, A. T-Shaped Three-Coordinate Copper (II) Heptaphyrin Complexes. *Angew. Chem. Int. Ed.*, **2009**, *48*, 8086. [b] Mori, S.; Shimizu, S.; Taniguchi, R.; Osuka, A. Group 10 Metal Complexes of meso-Aryl-Substituted [26]Hexaphyrins with a Metal-Carbon Bond. *Inorg. Chem.*, **2005**, *44*, 4127. [c] Mori, S.; Kim, K. S.; Yoon, Z. S.; Noh, S. B.; Kim, D.; Osuka, A. Peripheral Fabrications of a Bis-Gold(III) Complex of [26]-Hexaphyrin(1.1.1.1.1.1) and Aromatic versus Antiaromatic Effect on Two-Photon Absorption Cross Section. *J. Am. Chem. Soc.* **2007**, *129*,11344.
55. [a] Tanaka, Y.; Mori, H.; Koide, T.; Yorimitsu, H.; Aratani, N.; Osuka, A. Rearrangements of a [36]Octaphyrin Triggered by Nickel(II) Metalation: Metamorphosis to a Directly meso-β-Linked Diporphyrin. *Angew. Chem. Int. Ed.*, **2011**, *50*, 11460. [b] Soya, T.; Naoda, K.; Osuka, A. Ni(II) Metalations of [40]- and [42]Nonaphyrins(1.1.1.1.1.1.1.1.1): The Largest Doubly Twisted Hückel Antiaromatic Molecule. *Chem. - Asian J.*, **2015**, *10*, 231.
56. Chmielewski, P. J.; Latos-Grażyński, L.; Rachlewicz, K. 5,10,15,20-Tetraphenylsapphyrin-Idenfication of a Pentapyrrolic Expanded Porphyrin in the Rothemund Synthesis. *Chem. - Eur. J.*, **1995**, *1*, 68.
57. [a] Narayanan, S. J.; Sridevi, B; Chandrashekar, T. K; Vij, A.; Roy, R. Sapphyrin Supramolecules through C–H·····S and C–H·····Se Hydrogen Bonds–First Structural Characterization of meso-Arylsapphyrins Bearing Heteroatoms. *Angew. Chem. Int. Ed*., **1998,** *37*, 3394. [b] Narayanan, S. J.; Sridevi, B.; Srinivasan, A.; Chandrashekar, T. K.;

Roy, R. One step Synthesis of Sapphyrin and N-confused Porphyrin using Dipyrromethane. *Tetrahedron Lett.*, **1998**, *39*, 7389.

58. Sessler, J. L.; Lisowski, J.; Boudreaux, K. A.; Lynch, V.; Barry, J.; Kodadek, T. J. Synthesis and Characterization of Diaryl Sapphyrins Prepared under Lindsey-Type Conditions. *J. Org. Chem.*, **1995**, *60*, 5975.
59. Sessler, J. L.; Weghorn, S. J.; Expanded, Contracted & Isomeric Porphyrins,**1997**, *15*,270.
60. Král, V.; Davis, J.; Andrievsky, A.; Kralová, J.; Synytsya, A.; Poucková, P.; Sessler, J. L. Synthesis and Biolocalization of Water-Soluble Sapphyrins. *J. Med. Chem.*, **2002**, *45*, 1073.
61. Parmeswaran, D.; Pushpan, S. K.; Srinivasan, A.; Kumar, M. R.; Chandrashekar, T. K.; Ganesan, S. In Vitro and In Vivo Investigations on the Photodynamic Activity of Core-Modified Expanded Porphyrin− Ammonium Salt of 5,10,15,20-tetrakis-(*meso*-p-sulfonato phenyl)-25,27,29-trithia Sapphyrin. *Photochem. Photobiol*., **2003**, *78*, 487.
62. Sessler, J. L.; Burrell, A. H.; Lisowski, J.; Gebauer, A.; Cyr, M. J.; Lynch, V. Cobalt(II) and Rhodium(I) Complexes of Thia- and Oxasapphyrins. *Bull. Soc. Chem. Fr.*, **1996**, *133*, 725.
63. Burrell, A. K.; Sessler, J. L.; Cyr, M. J.; McGhee, E.; Ibers, J. A. Metal Carbonyl Complexes of Sapphyrins. *Angew. Chem., Int. Ed. Engl.*, **1991**, *30*, 91.
64. Burrell, A. K.; Cyr, M. J.; Lynch, V.; Sessler, J. L. Nucleophilic Attach at the *meso* position of a Uranyl Sapphyrin Complex. *J. Chem. Soc., Chem. Commun.*, **1991**, 1710.
65. Sessler, J. L.; Ford, D. A.; Cyr, M. J.; Furuta, H. Enhanced Transport of Fluoride Anion Effected using Protonated Sapphyrin as a Carrier. *J. Chem. Soc., Chem. Commun.*, **1991**, 1733.
66. Sessler, J. L.; Hoehner, M. C.; Gebauer, A.; Andrievsky, A.; Lynch, V. Synthesis and Characterization of All-Alkyl-Substituted Mono-, Di-, and Trioxosapphyrins. *J. Org. Chem.*, **1997**, *62*, 9251.
67. Sessler, J. L.; Andrievsky, A.; Král, V.; Lynch, V. Chiral Recognition of Dicarboxylate Anions by Sapphyrin-Based Receptors. *J. Am. Chem. Soc.*, **1997**, *119*, 9385.
68. Král, V.; Lang, K.; Králová, J.; Dvořák, M.; Martásek, P.; Chin, A. O.; Andrievsky, A.; Lynch, V.; Sessler, J. L. Polyhydroxylated Sapphyrins: Multisite Non-Metallic Catalysts for Activated Phosphodiester Hydrolysis. *J. Am. Chem. Soc.*, **2006**, *128*, 432.
69. Miller, D. C.; Johnson, M. R.; Becker, J. J.; Ibers, J. A. Synthesis and Characterization of the New 22-π Aromatic Furan-Containing Macrocycle, “Ozaphyrin”. *J. Heterocycl. Chem.*, **1993**, *30*, 1485.

70. Miller, D. C.; Johnson, M. R.; Ibers, J. A. Synthesis and Characterization of New "Expanded" Thiophene- and Furan-Containing Macrocycles. *J. Org. Chem.*, **1994**, *59*, 2877.
71. Weghorn, S. J.; Lynch, V.; Sessler, J. L. [22]Dehydropentaphyrin-(2.1.0.0.1) and [22]Pentaphyrin-(2.1.0.0.1): Novel Sapphyrin Analogues. *Tetrahedron Letters*, **1995**, *36*, 4713.
72. King, M. M. Ph.D. Dissertation, Harvard University, Cambridge, MA, **1970**.
73. Narayanan, S. J.; Sridevi, B.; Chandrashekar, T. K.; Englich, U.; Ruhlandt-Senge, K. Core-Modified Smaragdyrins: First Examples of Stable *Meso*-Substituted Expanded Corrole. *Org. Lett.*, **1999**, *1*, 587.
74. [a] Venkatraman, S.; Kumar, R.; Sankar, J.; Chandrashekar, T. K.; Sendhil, K.; Vijayan, C.; Kelling, A.; Senge, M. O. Oxasmaragdyrin-Ferrocene and Oxacorrole-Ferrocene Conjugates: Synthesis, structure, and Nonlinear Optical Properties. *Chem. - Eur. J.*, **2004**, *10*, 1423. [b] Misra, R.; Kumar, R.; Chandrashekar, T. K.; Suresh, C. H.; Nag, A.; Goswami, D. 22π SmaragdyrinMolecular Conjugates with Aromatic Phenylacetylenes and Ferrocenes: Syntheses, Electrochemical, and Photonic Properties. *J. Am. Chem. Soc.*, **2006**, *128*, 16083. [c] Gokulnath, S.; Prabhuraja, V.; Sankar, J.; Chandrashekar, T. K. Smaragdyrin-Azobenzene Conjugates: Syntheses, Structure, and Spectral and Electrochemical Properties. *Eur. J. Org. Chem.*, **2007**, *2007*, 191.
75. Sridevi, B.; Narayanan, S. J.; Rao, R.; Chandrashekar, T. K.; Englich, U.; Ruhlandt-Senge, K. Meso-Aryl Smaragdyrin: Novel Anion and Metal Receptors. *Inorg. Chem.*, **2000**, *39*, 3669.
76. Rao, M. R.; Ravikanth, M. Boron Complexes of Oxasmaragdyrin, a Core-Modified Expanded Porphyrin. *J. Org. Chem.*, **2011**, *76*, 3582.
77. Kalita, H.; Lee, W.-Z.; Ravikanth, M. Phosphorus Complexes of meso-Triaryl-25-Oxasmaragdyrins. *Inorg. Chem.*, **2014**, *53*, 9431.
78. Xie, D.; Liu, Y.; Rao, Y.; Kim, G.; Zhou, M.; Yu, D.; Xu, L.; Yin, B.; Liu, S.; Tanaka, T.; Aratani, N.; Osuka, A.; Liu, Q.; Kim, D; Song, J. *meso*-Triaryl-Substituted Smaragdyrins: Facile Aromaticity Switching. *J. Am. Chem. Soc.*, **2018**, *140*, 16553.
79. Sessler, J. L.; Davis, J. M.; Lynch, V. Synthesis and Characterization of a Stable Smaragdyrin Isomer. *J. Org. Chem.*, **1998**, *63*, 7062.
80. Sessler, J. L.; Morishima, T.; Lynch, V. Rubyrin: A New Hexapyrrolic Expanded Porphyrin. *Angew. Chem. Int. Ed. Engl.*, **1991**, *30*, 977.

81. Sessler, J. L.; Seidel, D.; Bucher, C.; Lynch, V. [26]Hexaphyrin(1.1.1.1.0.0): an all-aza isomer of rubyrin with an inverted pyrrole subunit. *Chem. Commun.*, **2000**, 1473.
82. [a] Srinivasan, A.; Reddy, V.M.; Narayanan, S. J.; Sridevi, B.; Pushpan, S. K.; Ravikumar, M.; Chandrashekar, T. K. Tetrathia- and Tetraoxarubyrins: Aromatic, Core-Modified, Expanded Porphyrins. *Angew. Chem. Int. Ed. Engl*., **1997**, *36*, 2598. [b] Narayanan, S. J.; Sridevi, B; Chandrashekar, T. K; Vij, A.; Roy, R. Novel Core-Modified Expanded Porphyrins with *meso*-Aryl Substituents: Synthesis, Spectral and Structural Characterization. *J. Am. Chem. Soc*., **1999**, *121*, 9053. [c] Srinivasan, A.; Pushpan, S. K.; Ravikumar, M.; Chandrashekar, T. K.; Roy, R. Novel Heteroatom Containing Rubyrins *Tetrahedron* **1999**, *55*, 6671. [d] Narayanan, S. J.; Srinivasan, A.; Sridevi, B.; Chandrashekar, T. K.; Senge, M. O.; Sugiura, K.; Sakata, Y.; *Eur. J. Org. Chem*., **2000,** 2357.
83. Shimizu, S.; Taniguchi, R.; Osuka, A. meso-Aryl-Substituted [26]Hexaphyrin(1.1.0.1.1.0) and [38]Nonaphyrin(1.1.0.1.1.0.1.1.0) from Oxidative Coupling of a Tripyrrane. *Angew. Chem. Int. Ed*., **2005**, *44*, 2225.
84. Johnson, M. R.; Miller, D. C.; Bush, K.; Becker, J. J.; Ibers, J. A. Synthesis and Characterization of a New 26π-Aromatic Thiophene-Containing Macrocyclic Ligand. *J. Org. Chem.*, **1992**, *57*, 4414.
85. Kishore, M. V. N.; Panda, P. K. Revisiting the intense NIR active bronzaphyrin, a 26-π aromatic expanded porphyrin: synthesis and structural analysis. *Chem. Commun.*, **2018**, *54*, 13135.
86. Kumar, R.; Misra, R.; Chandrashekar, T. K. Effect of Meso-Aryl Substituents on the Synthesis of Core-Modified Expanded Porphyrins. *Org. Lett.*, **2006**, *8*, 4847.
87. Pushpan, S. K.; Anand, V. R. G.; Venkatraman, S.; Srinivasan, A.; Gupta A. K.; and Chandrashekar, T. K. Characterization of a new meso-aryl rubyrin isomer: [26]hexaphyrin (1.1.1.0.1.0) with an inverted heterocyclic ring. *Tetrahedron Lett.*, **2001**, *42*, 3391.

Chapter 2

Monothia [22]pentaphyrin(2.0.1.1.0): A core modified isomer of Sapphyrin

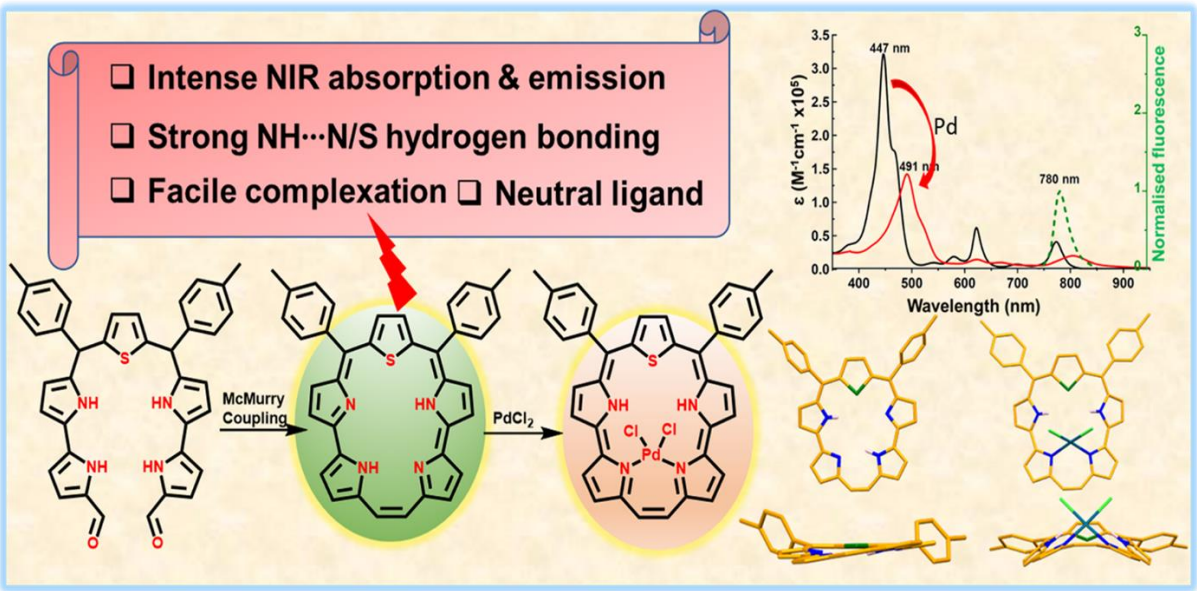

2.1. Introduction

It is the curiosity which leads the research from nature to science and then necessity from science to technology. Tetrapyrrolic unit 'porphyrin' being referred as 'pigment of life' has only seen development of its structure, property from fundamental science to ongoing research for applications.[1] It has been modified in many possible ways to get the best out of it to satisfy our scientific curiosity. One such modification is expansion of the core of porphyrin. Sapphyrin is the first expanded porphyrin to be discovered serendipitously by Woodward in 1966.[2] Though it was a slow initial take up, but never exhausted after 1990s. Reports showing easier access to building blocks, anion binding, applications in PDT have given new paths to research on sapphyrin.[3] Different synthetic procedures for all-aza sapphyrin has been discussed briefly in chapter 1. We will be discussing more about core-modified sapphyrin in the following section of the chapter.

2.1.1. Core-modified sapphyrin

Core-modified sapphyrins have one or more pyrroles substituted with other heterocycles like thiophene, furan, selenophene or tellurophene etc. Core-modification in macrocycles leads to increase in core-size, alter electronic structure as a result of which optical, electrochemical properties changes. Johnson reported first synthesis of sapphyrin in 1972 as its core-modified analogue.[4] Dioxasapphyrin, **2.1** was synthesised by [3+2] MacDonald-type condensation of tripyrromethane diacid with diformyl bifuran.

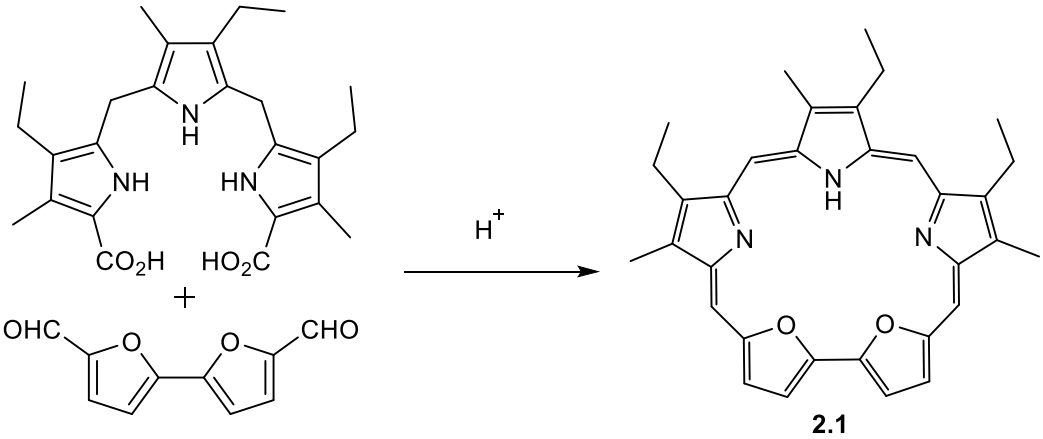

Scheme 2.1: Synthesis of dioxasapphyrin.[4]

A series of monothia, monoselena, monooxa, dioxa and trioxa sapphyrin has been synthesized by Sessler and coworkers by [3+2] MacDonald-type condensation of appropriate precursors with *p*-TSA as catalyst followed by oxidation.[5]

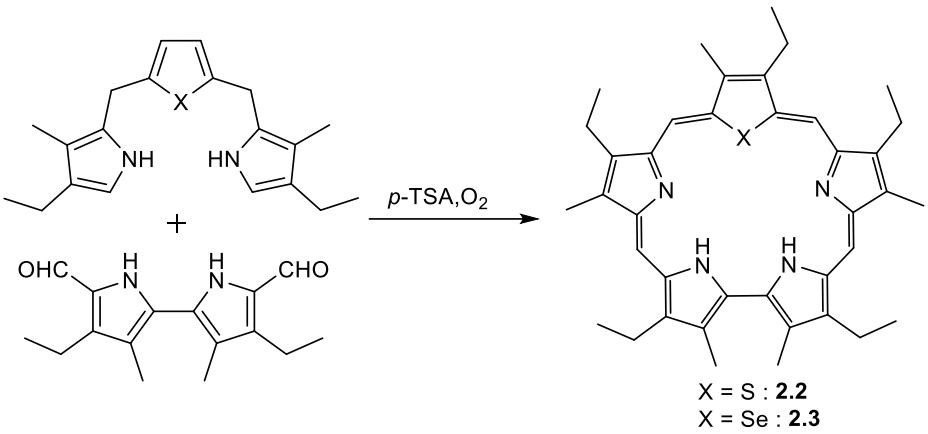

Scheme 2.2: Synthesis of different monothia and monoselena sapphyrin.[5a]

Chandrashekar and co-workers have synthesised *meso*-aryl core modified sapphyrin by TFA catalyzed condensation of bithiophene diol or biselenophene diol with tripyrromethane.[6] Structural analysis shows they have similar conformation as *meso*-aryl all-aza isomer i.e., the heterocycle opposite to bithiophene or biselenophene is inverted.

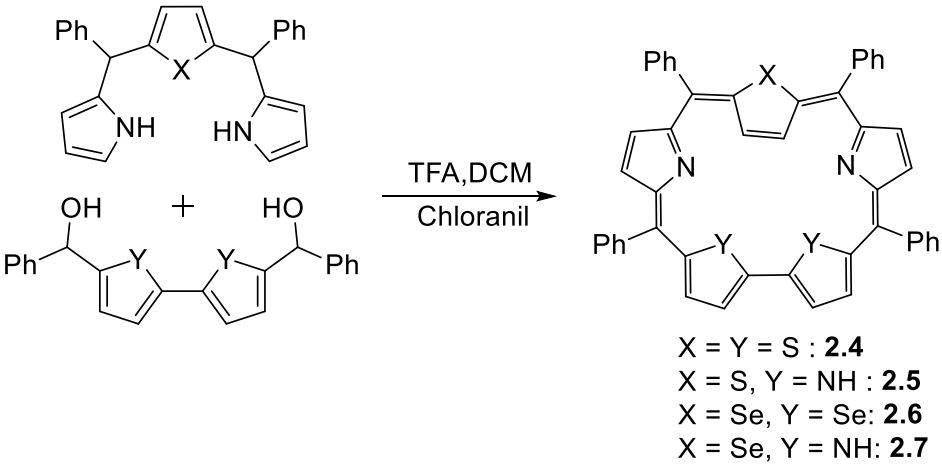

Scheme 2.3: Synthesis of *meso*-aryl core-modified sapphyrins.[6]

Acid-mediated oxidative coupling of modified tripyrromethane leads to a different series of core-modified sapphyrin along with core-modified rubyrin and porphyrin.[7] The product distribution depends on the nature and concentration of the catalyst used. With a low concentration of TFA, core-modified rubyrin was the exclusive product but with a high concentration of acid, core-modified porphyrin and sapphyrin also formed. With a low concentration of acid, only self-coupling of tripyrromethane takes place resulting in rubyrin formation exclusively. But with higher concentration, scrambling of tripyrromethane takes place resulting in the formation of sapphyrin and porphyrin.

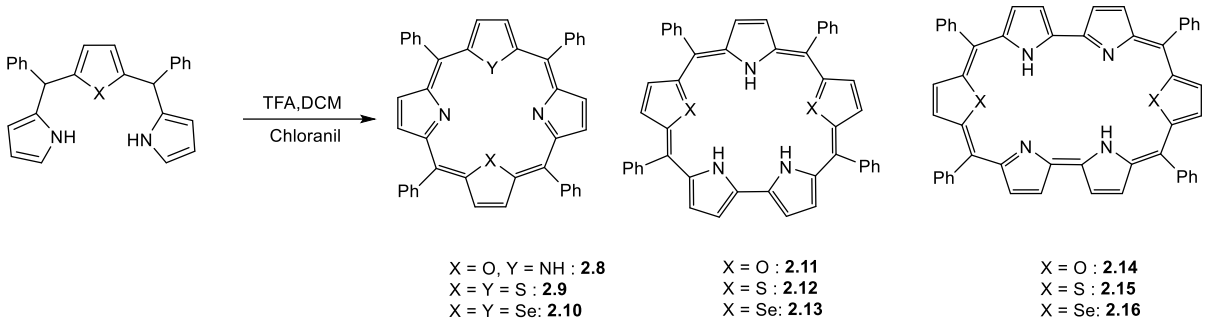

Scheme 2.4: Synthesis of core-modified sapphyrin acid mediated oxidative coupling.[7]

Ditellurasapphyrin was also prepared by condensation of telluratripyrromethane with 2,5-bis(phenylhydroxy)methyltellurophene.[8] Though ditelluraporphyrin was the primary product in the reaction, ditellurasapphyrin was also formed and characterized fully.

The structure of *meso*-aryl sapphyrin depends on the nature and position of heterocycles.[7] The presence of heterocycle with smaller atoms like nitrogen or oxygen adjacent to bipyrrole unit makes the heterocycle opposite to bipyrrole flip inside out like seen in all-aza sapphyrin or **2.4-2.7**. If bigger heterocycles (with S, Se, or Te) are present adjacent to bipyrrole unit, ring flipping is avoided and we get a planar structure like observed in the case of **2.11-2.13**. Ring flipping does not depend on the heterocycle present in the bipyrrole unit. Unlike *meso*-aryl all-aza sapphyrin, which undergoes ring flipping upon protonation to get all in-core nitrogen structure, core-modified sapphyrins (**2.4-2.7**) retain the inverted structure after protonation also. From all spectroscopic properties, it is observed that inverted sapphyrins have reduced aromaticity than the planar sapphyrins which holds for both all aza and core-modified analogs.

Typically, electronic spectra of sapphyrins have one sharp and intense Soret band around 435-470 nm and 2-5 weak Q bands around 600-750 nm. It is seen that thia analogs have a red-shifted while oxa analogues have blue-shifted Soret bands than all-aza analogues.[9]

2.1.2. Anion binding

The core size of sapphyrin being larger than porphyrin has been explored vividly for molecular recognition. With the first discovery of fluoride binding in 1990 by Sessler and co-workers,[3] a number of studies on anion binding,[5,10] nucleotide binding[11] or DNA binding[12] has been reported thereafter. Though diprotonated all-aza sapphyrin accommodates fluoride ion inside the core, other anions being larger arrange themselves below or above the plane of sapphyrin. Covalently bound sapphyrin dimer has been studied to bind effectively with carboxylate ions where arylated carboxylates bind more strongly due to π-π interaction, C-

H···*N* or C-H···π interaction.[13] They are seen to act as effective transporters across membranes also. Sessler and co-workers also showed that sapphyrin can bind to nucleotide bases and act as a carrier.[11] It shows efficient transportation of monophosphate derivative (shows anti-HSV activity) in U-tube type, AqI−CH_2Cl_2−AqII, model membrane system at a pH of 3.5.

2.1.3. Coordination chemistry

Due to the larger core size and more no. of nitrogens in sapphyrin, it was expected to show rich coordination chemistry. In the early stage, Woodward and Dolphin tried metalation with 3d-metal ions like Ni^{2+}, Fe^{2+}, Cd^{2+}, Mn^{2+}, Co^{2+}, and Zn^{2+} with their acetate salt.[14] Though electronic spectra showed complexation of metals with a bathochromic shift of Soret band from freebase, structural elucidation couldn't be done. In 1991, Sessler and co-workers revealed the first structural confirmation of Ir and Rh complex of sapphyrin.[15] Sapphyrin **1.19** on treatment with 1eq of [{$RhCl(CO)_2$}$_2$] or [$IrCl(CO)_2$(Py)] gives monometallic $Rh(CO)_2$Sap **2.17** or $Ir(CO)_2$Sap **2.18**, which on further treatment with excess metal carbonyl complexes gives bimetallic complexes **2.19** and **2.20**. The bimetallic complex could also be achieved by treating freebase with excess metal carbonyl. If mono Rh or Ir complexes were treated further with Ir or Rh carbonyls then it resulted in heterobimetallic complexes **2.21**. Metals were arranged above and below the sapphyrin plane. The bis-Rh(I) complex of monothiasapphyrin and bis-Ir(I) complex of monoselenasapphyrin has also been synthesized by treating monothia and monoselenasapphyrin with respective metal carbonyl salts.[5a,16]

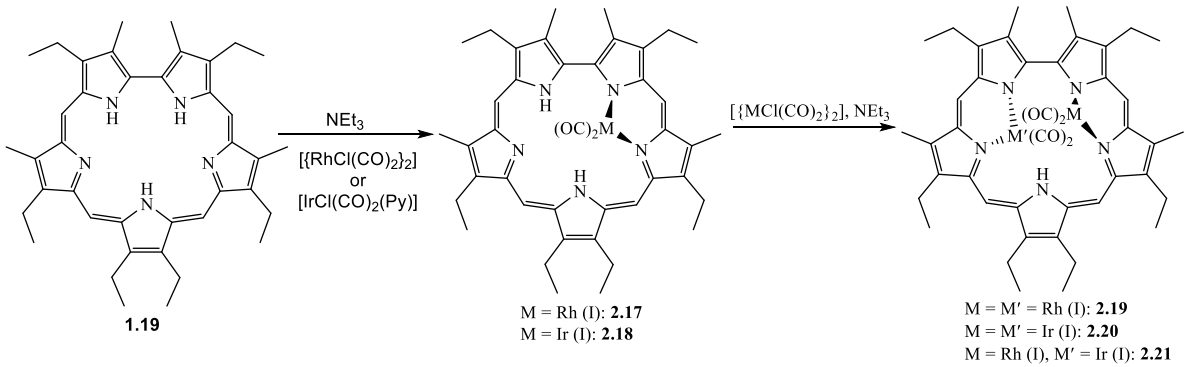

Scheme 2.5: Synthesis of Rh(I) and Ir(I) complex of sapphyrin.

Uranyl complex of all-aza sapphyrin has been synthesized by Sessler and co-workers in 1991 where sapphyrin undergoes nucleophilic addition of a methoxide group at *meso*- position after complexation (**Scheme 2.6**).[17] This resulted in the loss of aromaticity and also disruption of planar structure to a severely distorted structure. Attack of methoxide was a crucial step to stabilize the complex without which it was decomposed. However, monooxasapphyrin being a

dianionic ligand could stabilize uranyl ion without disrupting the macrocycle skeleton.[18] The complex showed a saddle-shaped conformation (**Figure 2.1**).

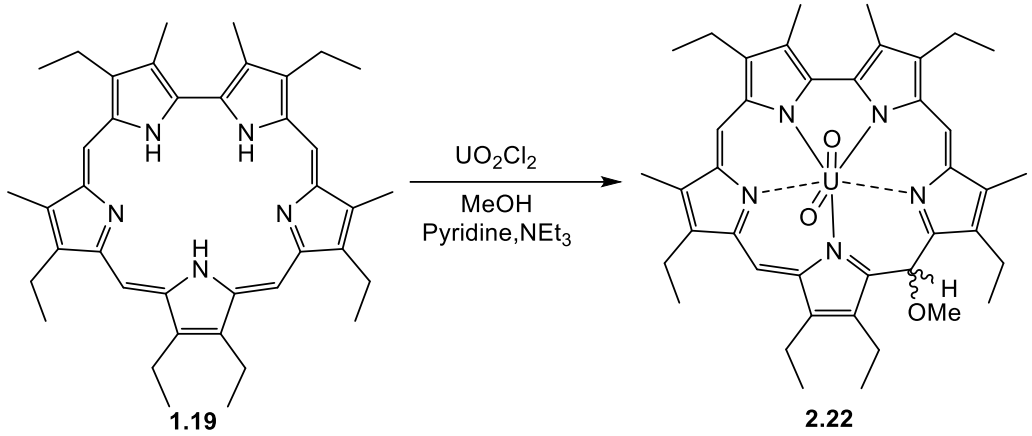

Scheme 2.6: Synthesis of uranyl complex of all-aza sapphyrin with a nucleophilic attack at *meso*-position.[17]

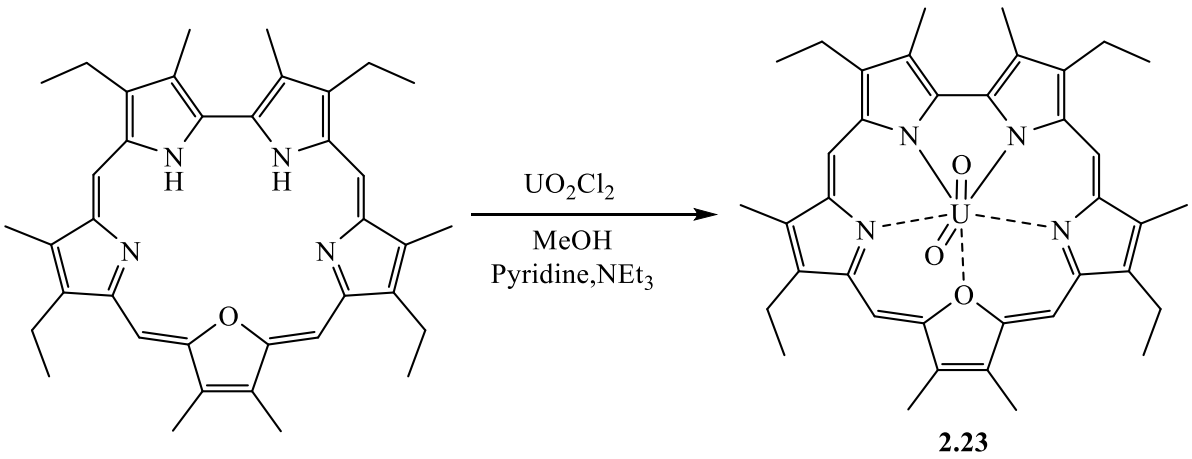

Scheme 2.7: Synthesis of uranyl complex of oxa sapphyrin with a nucleophilic attack at *meso*-position.[18]

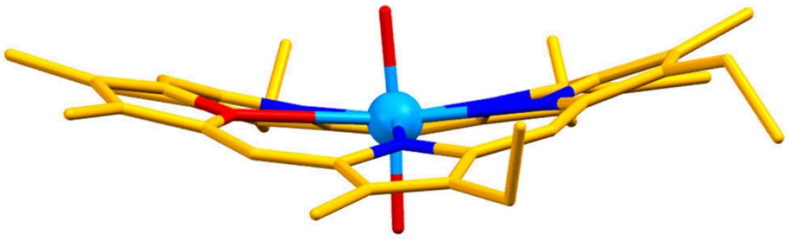

Figure 2.1: Structure of uranyl complex of oxa sapphyrin.[18]

These all complexes discussed above are *β*-substituted and *meso*-unsubstituted sapphyrin complexes. As *meso*-substituted sapphyrin showed inversion of heterocycle opposite to

bipyrrolic unit, it would be interesting to see if the inversion is retained or flipped in the metal complexes. Gross and co-workers first revealed about Rh(I) complex of *meso*-aryl sapphyrin, **2.25** where spectral characterisation indicates retention of inversion in the metal complex also.[19]

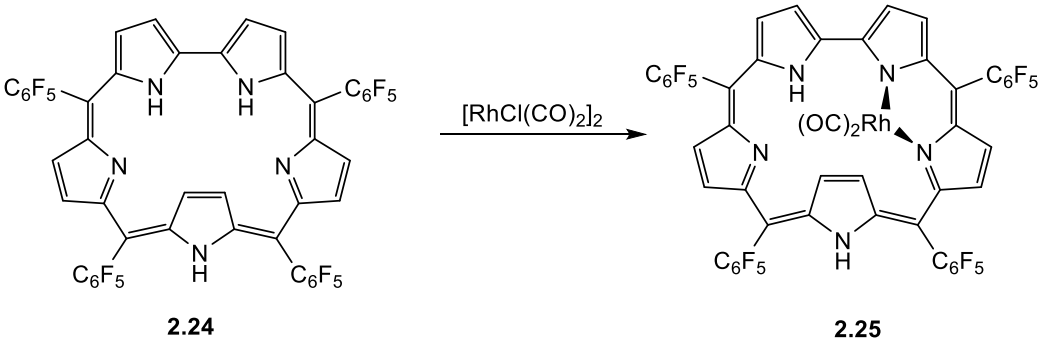

Scheme 2.8: Synthesis of Rh(I) complex of *meso*-aryl all-aza sapphyrin.[19]

Recently, Gross and co-workers have shown Re(I) metalation of *meso*-substituted sapphyrin showed inverted or planar structure depending on the *meso* substituents. In **2.26**, Re is hexacoordinated.[20] One water molecule was coordinated to Re(I) along with other three CO as co-ligands. Water molecule was seen to have hydrogen bonding with all pyrrole NHs keeping all the pyrroles with in-core nitrogen. But, with *meso*-CF_3 substitution in **2.27**, Re was pentacoordinated. One pyrrole remained inverted in the structure, and showed a presence of hydrogen bonding between CF_3 and inverted pyrrole NH.

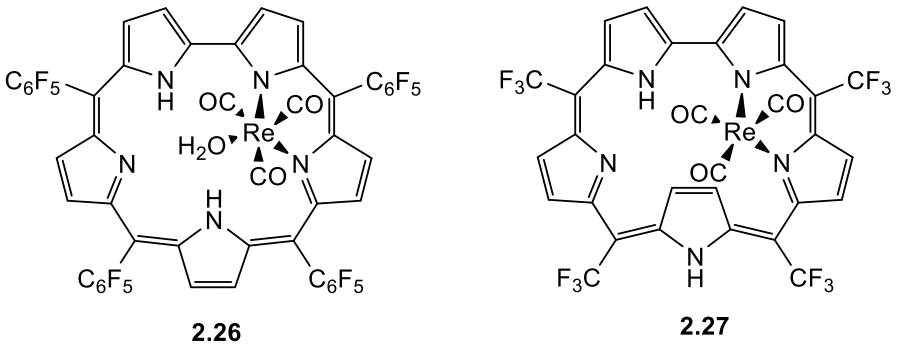

Figure 2.2: Examples of Re(I) complexes of *meso*-substituted sapphyrin.[20]

After many fruitless attempts of Pd complexation of sapphyrin with PdX_2 (X = Cl, I, CN and acetate), Gross and co-workers succeeded finally with $[PdCl(allyl)]_2$ as a metal source.[21] They finally obtained mono and di Pd complexes of sapphyrin in which one Pd was coordinated to two nitrogens of sapphyrin dipyrromethene unit and other coordinating sites were occupied by

π-allyl group as co-ligand. Though it was a *meso*-aryl substituted sapphyrin, pyrrole was not inverted in the di-Pd complex but it was inverted in the mono-Pd complex.

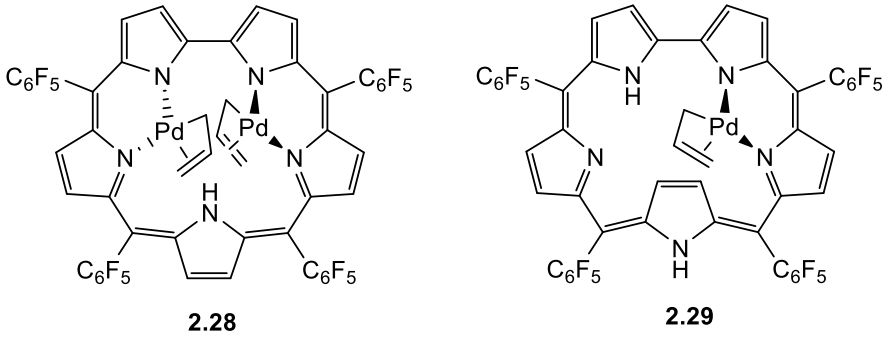

Figure 2.3: Structure of mono and di-Pd complexes of *meso*-aryl sapphyrin.[21]

2.2. Research Goal

Keeping the above perspectives in view, we plan a core-modified structural isomer of sapphyrin which will have an ethene bond in the skeleton. The introduction of the ethene bridge is expected to bring changes in structural and electronic properties. Intensification of Q bands like porphycene is expected in the absorption spectrum. Core modification with a thiophene ring is expected to increase core size as well as it may shift the absorption spectrum to the NIR region. Also, the core-modification strategy gives easier access to building blocks. The introduction of *meso*-aryl groups may reduce aggregation and enhance solubility. Exploration of the coordination chemistry of the target molecule is expected to be interesting.

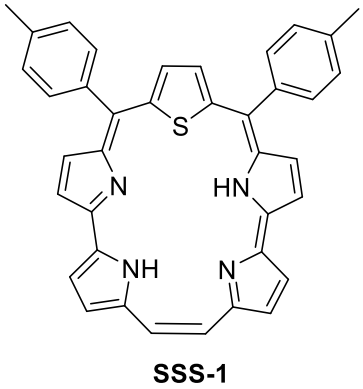

Figure 2.4: Designed structural isomer of sapphyrin.

2.3. Result and discussion

2.3.1. Synthesis

After Vogel reported McMurry coupling of formyl group for porphycene,[22] it has been a well-established method to introduce ethene bond to the skeleton of macrocycles. As seen in the synthesis of corrphycene,[23] intramolecular McMurry coupling of tetrapyrrole dialdehyde results in the formation of desired corrphycene molecule, we also envisioned a similar strategy for the synthesis of **SSS-1** i.e. McMurry coupling of open-chain thiapentapyrrane dialdehyde. This strategy minimizes the formation of other by-products which could have made the isolation difficult.

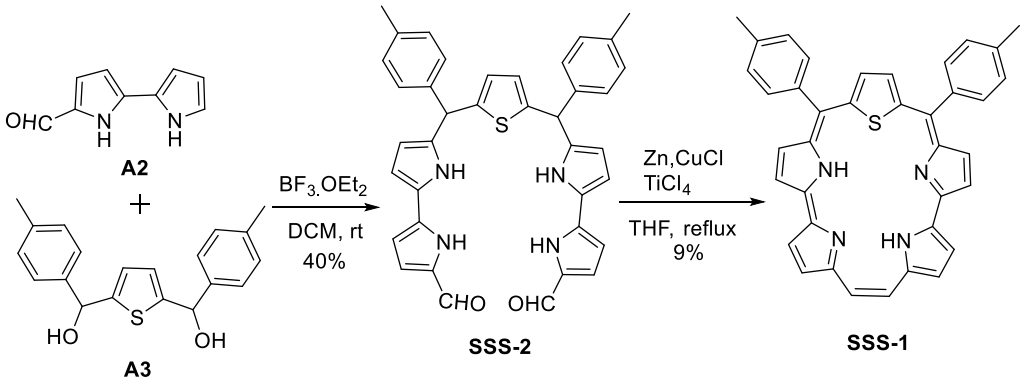

Scheme 2.9: Synthesis of **SSS-1**.

Required precursor thiapentapyrrane dialdehyde, **SSS-2** was synthesized by acid-mediated condensation of bipyrrole monoaldehyde, **A2** and thiophene-2,5-diylbis(*p*-tolylmethanol), **A3** with 40% yield. Then intramolecular reductive McMurry coupling of the thiapentapyrrane dialdehyde, **SSS-2** in reflux condition followed by open-air oxidation resulted in the formation of desired macrocycle **SSS-1** with 9% yield. In the hope of increasing the yield further, we tried another synthetic route. We tried Lewis acid-mediated oxidative C-C coupling of thiatripyrromethane and dipyrroethene with $BF_3.OEt_2$ as catalyst. But we could not obtain our target molecule through this reaction. **SSS-1** and its precursor, **SSS-2** have been characterized fully by standard spectroscopic analysis like ^{1}H NMR, ^{13}C NMR, IR spectroscopy, UV-Vis-NIR spectroscopy, and HRMS analysis. **SSS-1** has also been confirmed with SCXRD analysis.

2.3.2. Characterization

^{1}H NMR spectrum of **SSS-1** manifested a set of *meso*-protons, four sets of pyrrole *β*-protons and one set of thiophene *β*-protons in deshielded region from 10.48 ppm to 9.42 ppm. Presence

of all the β-protons in downfield region indicates that none of the heterocycles are inverted unlike in the case of *meso*-aryl sapphyrin.[6] Both the NH protons should show upfield shift and appear in negative region in the ^{1}H NMR spectrum due to the ring current effect. But we could not detect any of the NH peaks in the spectrum, which may be attributed to the faster tautomerization. This prompted us to go for a low temperature ^{1}H NMR experiment. Upon lowering the temperature to -30 °C, NH peak appeared at 5.4 ppm as a single broad peak in $CDCl_3$. But it was not possible to resolve both the NH peaks by further lowering the temperature. Here downfield shift of NH peaks is noteworthy and can be attributed to the presence of strong NH···N hydrogen bonding due to the presence of acene moiety like porphycene. This was not observed in thia or oxa ozaphyrin, which is also a structural isomer of sapphyrin having two ethylene bonds.[24] They exhibit NH peaks in the negative region like sapphyrin.

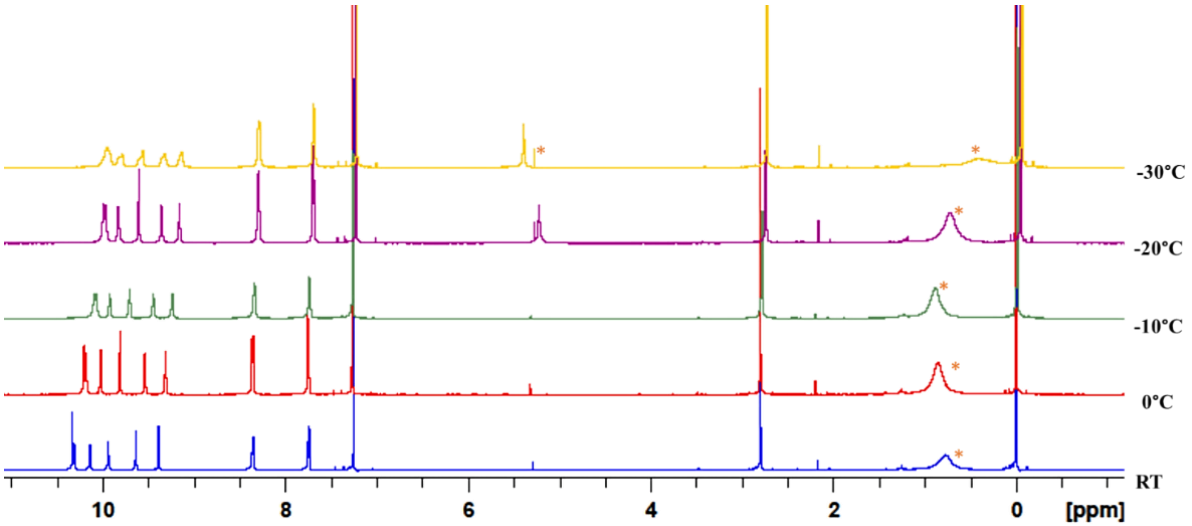

Figure 2.5: Variable temperature ^{1}H NMR spectra of **SSS-1** in $CDCl_3$. Solvent residual peak (*).

Though only one NH is experiencing strong NH···N hydrogen bonding, failure to resolve the NH peaks at -70 °C is intriguing. However, protonation of the macrocycle would arrest the tautomeric process. ^{1}H NMR titration of **SSS-1** with TFA demonstrated clear separation of both non-equivalent NH peaks. Interestingly, the titration experiment showed sequential formation of both monoprotonated and diprotonated species. With addition of 8 eq of TFA, monoprotonation took place and one NH peak became upfield shifted (-0.96 ppm) and another resonated in the downfield region (4.56 ppm). This type of trend is not observed in porphycene. Due to the unsymmetrical nature of the core owing to which stronger NH···N hydrogen bonding

was retained and monoprotonation took place on the other available imine nitrogen. Upon addition of excess TFA, diprotonation took place and there was an interruption of hydrogen bonding as a result of which all the NHs shifted to the upfield region and were observed at -0.50 and -0.91 ppm.

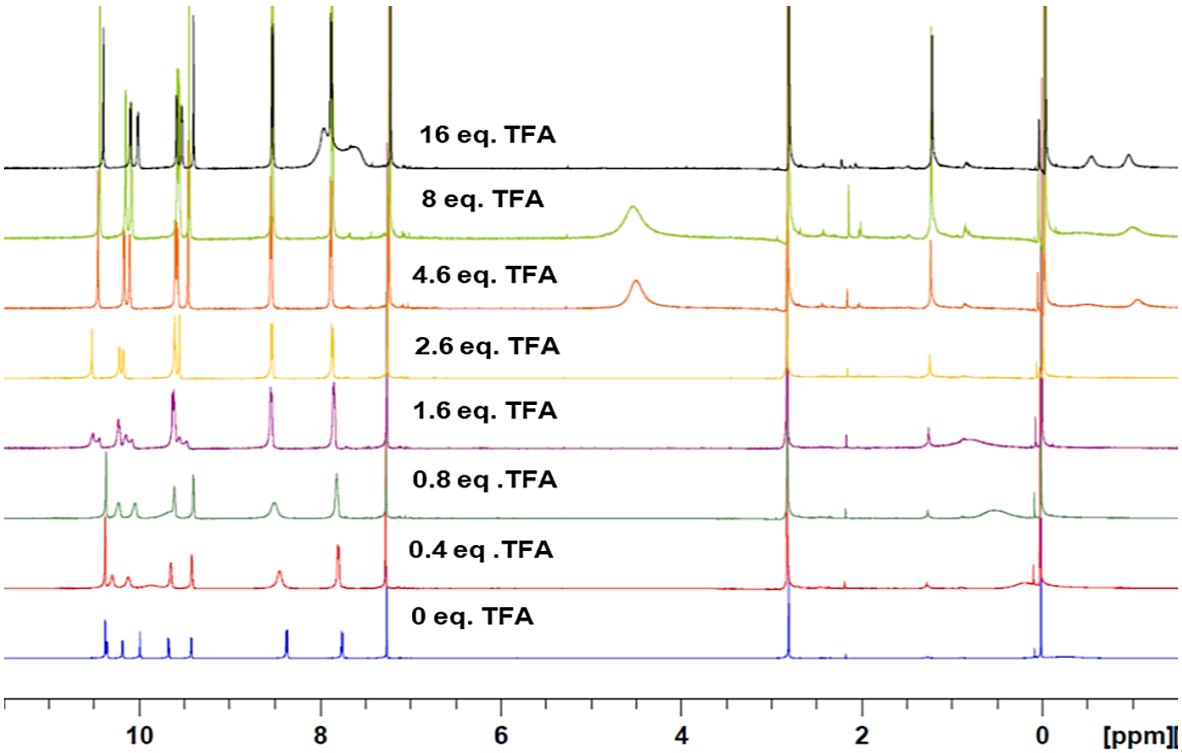

Figure 2.6: ^{1}H NMR spectra of compound **SSS-1** in $CDCl_3$ titrated with TFA.

2.3.2.1 Optical Properties

The absorption spectrum of **SSS-1** exhibits a sharp and intense Soret band (447 nm) accompanied by a shoulder on the longer wavelength side (467 nm). Along with this several lower energy Q bands are present with the lowest energy Q-band at λ_{max} 773 nm, which is bathochromically shifted relative to monothiasapphyrin (691 nm) and monothiaozaphyrin (755 nm).[24] The molar absorptivity of the Soret band is quite high in comparison to all other analogues. In contrast to sapphyrin, **SSS-1** exhibits two intense Q bands in the lower energy region. The absorption coefficient of the lowest energy Q band is approximately 20% of that of the Soret band, which is almost double that in the case of corrphycene (~10%) which also has an ethene bond in the structure.[23] As **SSS-1** shows structural and behavioral similarity with both sapphyrin and porphycene, we named this *sapphycene*. Further, freebase **SSS-1** exhibits weak near infrared (NIR) emission at 780 nm, indicating its potential utility in NIR diagnostics (**Figure 2.7**).

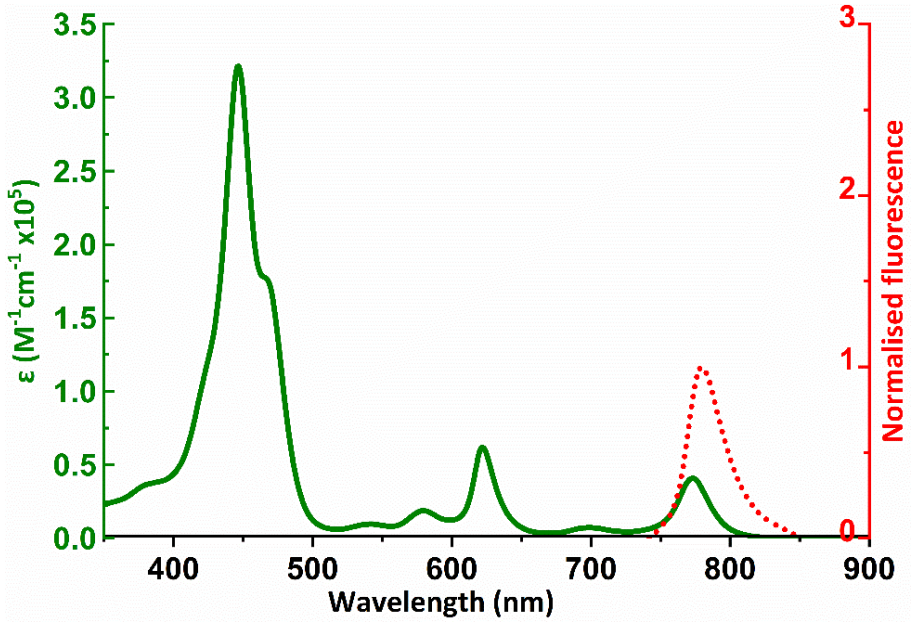

Figure 2.7: UV-Vis-NIR absorption spectrum of **SSS-1** along with normalised emission spectrum in $CHCl_3$ (λ_{exc} = 640 nm).

UV-Vis-NIR spectral changes have been observed upon protonation with different acids. Protonation causes enhancement in molar extinction coefficient. Bathochromic shift in the Soret band and hypsochromic shift in Q bands along with a change in Q-band pattern were observed for TFA, HCl, HF and perchloric acids. Titration with TFA, showed distinct monoprotonation and diprotonation species spectra. As such the freebase **SSS-1** is found harder to protonate. Upon addition of relatively less equivalent TFA, monoprotonation took place and the Soret band shifted to 465 nm. But, **SSS-1** required quite an excess of TFA for diprotonation, possibly owing to strong intermolecular hydrogen bonding owing to an increase in TFA concentration.[25] Observation of stepwise protonation of **SSS-1** with TFA in NMR and UV-Vis-NIR spectra intrigued us to check for the site of monoprotonation. We carried out a theoretical calculation for the stability of both the possible monoprotonated species, which showed less energy for the structure having monoprotonation at pyrrole nitrogen adjacent to thiophene (**Table 2.2**). Anion binding of **SSS-1.2TFA** with TBACl didn't show any significant spectral change. Whereas, a gradual blue shift in the Soret band was observed on addition of TBAF solution to **SSS-1.2TFA** indicating fluoride binding. However, upon addition of excess TBAF (15 equivalent), it regenerated the freebase **SSS-1** absorption spectrum (**Figure 2.8d**).

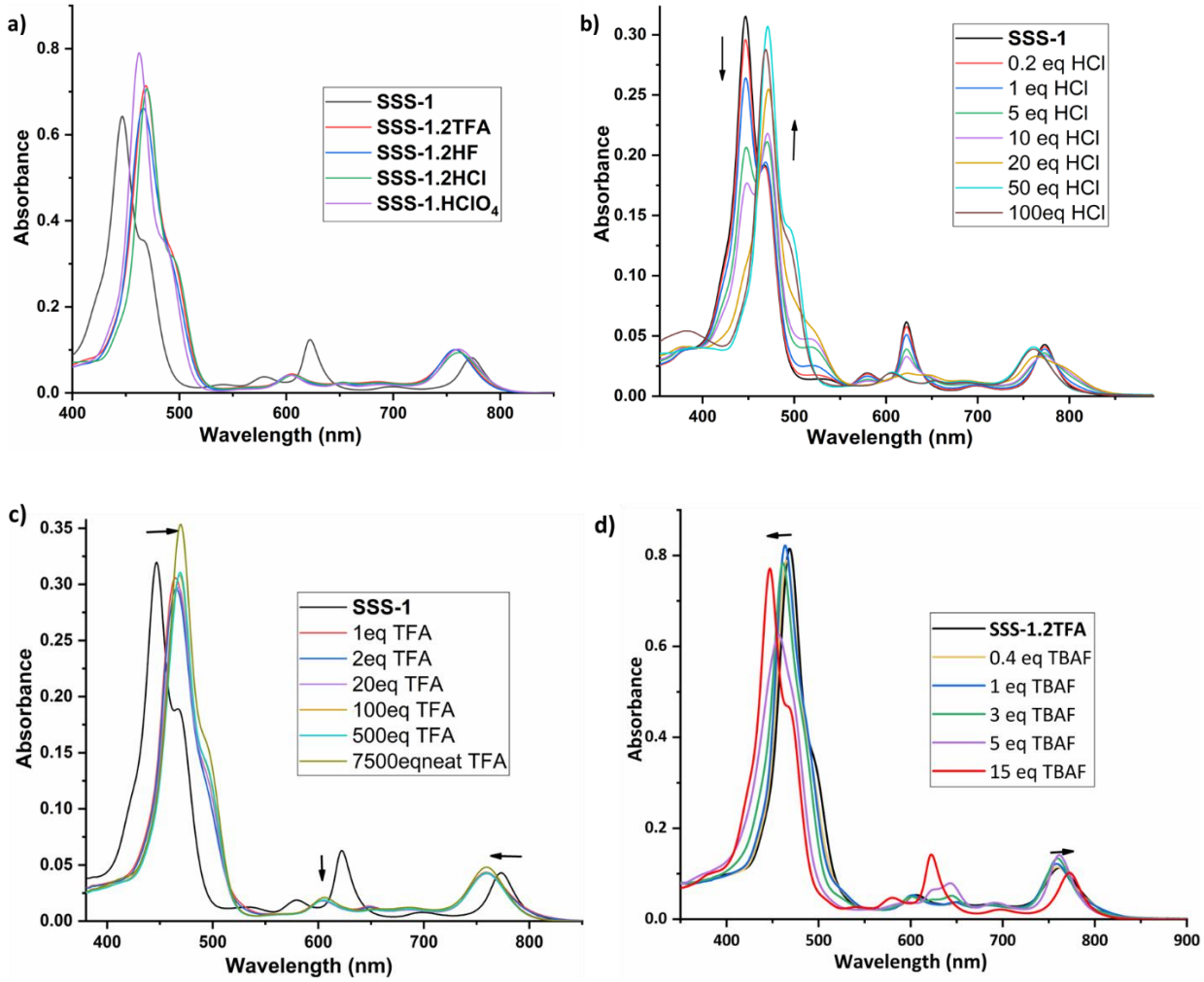

Figure 2.8: UV-Vis-NIR absorption of **SSS-1** (a) with excess of different acids; (b) Titration with HCl; (c) Titration with TFA; (d) Titration of TBAF with **SSS-1.2TFA** in $CHCl_3$.

2.3.2.2. Structural analysis of SSS-1

A diffraction grade crystal was obtained from slow evaporation of chloroform solution of **SSS-1**. SCXRD analysis elucidates the solid state structure, which confirms inward disposition of all the heteroatoms in freebase **SSS-1** unequivocally. It exhibits a slight nonplanar structure with maximum mean plane deviations occurring at the C_{β}-positions of the dipyrroethene pyrroles. Positive deviations of 0.210 and 0.269 Å were observed for C6 and C7, respectively from the mean sapphycene plane (excluding tolyl substituents), whereas, C12 and C13 manifests negative deviations of 0.183 and 0.218 Å, respectively. Rapid tautomerization made the assignment of the amino protons to two particular nitrogens difficult. These were fixed at *trans*-pyrrolic nitrogens (N1 and N3), which provided the lowest reliability factor (R-factor). **SSS-1** exhibits a trapezoidal N4 core with a core size (N2-N4 distance) of 4.899(4) Å, which is relatable to that of monooxaozaphyrin (4.929(6) Å).[26] Further analysis revealed that N-N

bipyrrolic distances are slightly different (N1-N2: 3.008(4) Å and N3-N4: 3.071(4) Å). This could be attributed to N1-H1′···S1 intramolecular hydrogen bonding (N1-S1: 2.910(3) Å), in addition to the corresponding N3-H3′···N2 hydrogen bond (N3-N2: 3.094(4) Å), possibly making the *trans*-NH tautomer to be the most stable conformation. The presence of the additional strong N-H···S hydrogen bonding probably facilitated the rate of proton transfer in the solution state, thus complying with fluxional behaviour observed in ^{1}H NMR spectrum under ambient conditions. Further, the packing diagram revealed π-π stacking with an interplanar distance of 3.445 Å, where the core is aligned in a staggered manner with thiophene rings aligned in opposite directions to each other.

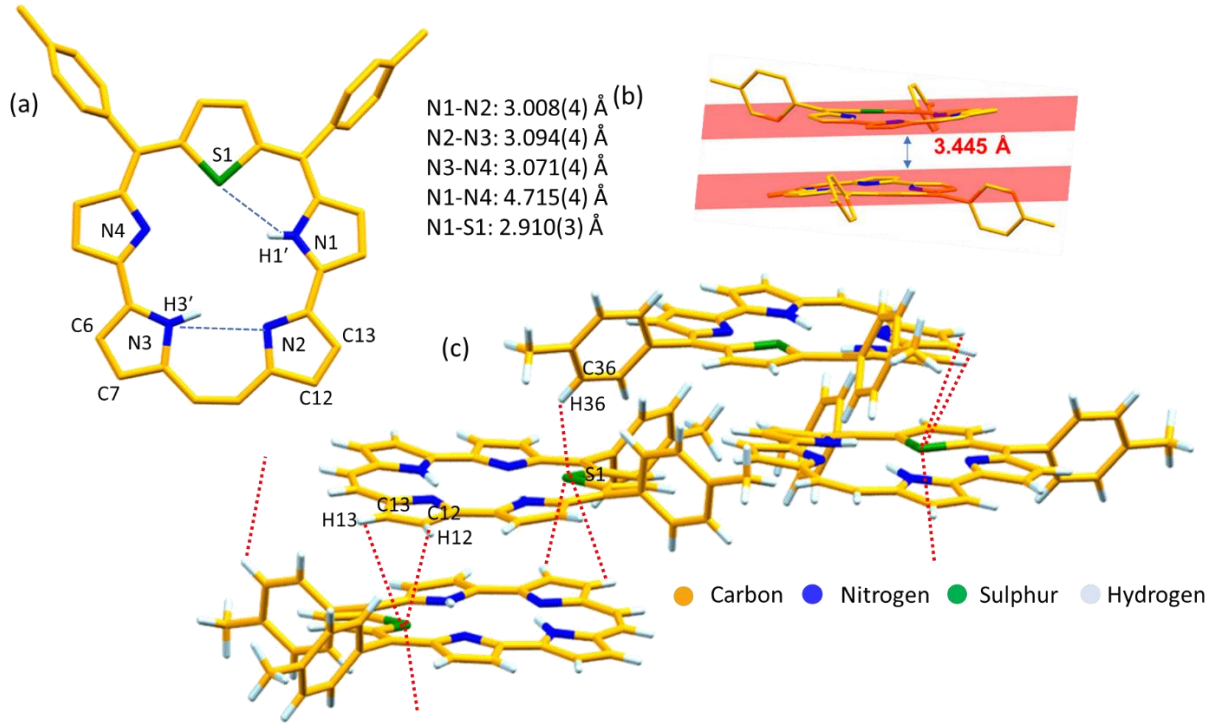

Figure 2.9: Molecular structure of **SSS-1** (a) front view; (b) side view with interplanar distance; (c) intermolecular interactions.

2.3.2.3. Theoretical calculation

To check the relative stability of all the isomers of sapphyrin, we carried out optimization of unsubstituted all-aza isomers using B3LYP/6-31G+(d,p).[27] It revealed that [22]pentaphyrin(2.1.0.0.1) is the most stable isomer followed by sapphycene. On the other hand, ozaphyrin has the highest energy followed by sapphyrin.

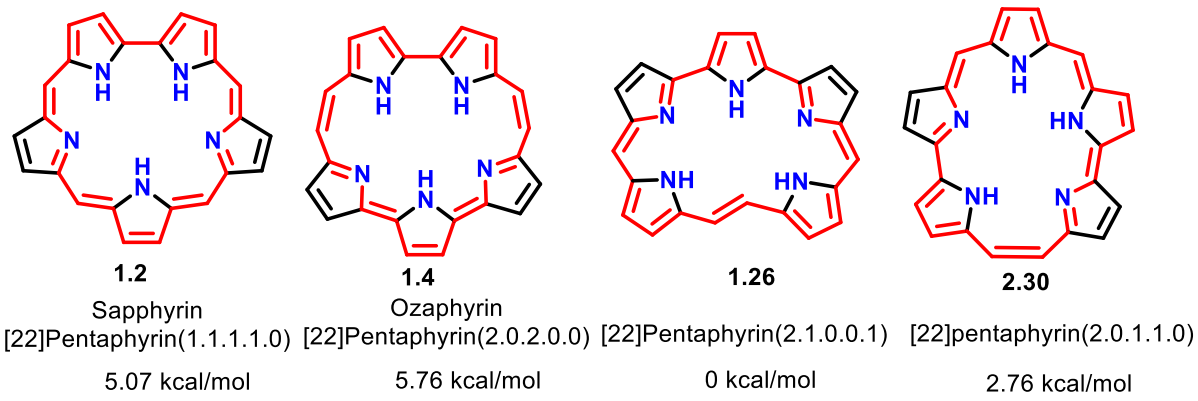

Figure 2.10: Relative energies of all-aza sapphyrin and its realised isomers calculated using DFT/B3LYP/6-31G+(d,p).

To understand the relative stability of all possible tautomers which was observed in the solid and solution state, optimization and ground state energies were calculated in the gas phase and $CHCl_3$. Study showed in both the cases *trans*-NH tautomer be the most stable form, surprisingly, followed by tautomer with *cis* NH in the dipyrroethene (*cis*-3), and one of the bipyrrole (*cis*-2), whereas the tautomer having NH on the two internal pyrrolic units (*cis*-1) was the least stable one (**Table 2.1**). The latter can be ascribed to the greater distortion in the macrocycle, where the thiophene ring and the two pyrrole moieties having NHs are on the opposite sides of the molecular plane. To understand further the existing intramolecular hydrogen bonding, we performed a natural bond orbital (NBO) analysis on the optimized sapphycene (*trans*-tautomer).[28] We encountered a strong interaction between sulphur lone pair and σ^* of N1-H1 and also between lone pair of N2 and σ^* of N3-H3 having stabilization energy of 5.99 and 4.00 kcalmol^{-1}, respectively. This supports the presence of intramolecular N-H···S and N-H···N hydrogen bonding complying with the solid-state structural analysis.

Table 2.1: Optimized structure and properties of different tautomers of **SSS-1** (tolyl groups are removed for clarity).

Front view	Side views	Optimized energy difference in gas phase (kcal/mol)	HOMO-LUMO gap (kcal/mol)	Optimized energy difference in $CHCl_3$ (kcal/mol)
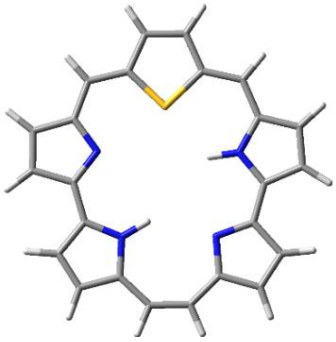 ***trans***	 	0	48.66	0
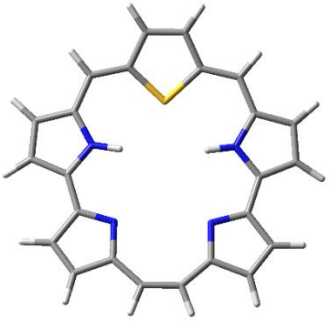 ***cis1***	 	12.9	48.20	10.37
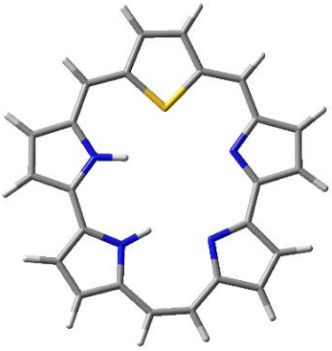 ***cis2***	 	6.68	48.20	5.07
				

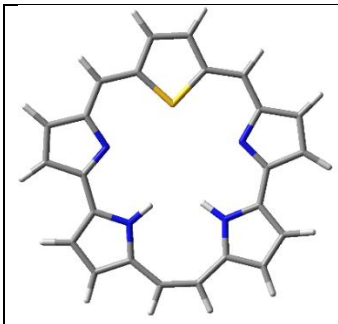 ***cis3***	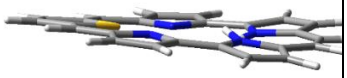	4.15	50.73	3.22

Table 2.2: Relative energies of optimized geometries of different modes of mono-protonation of **SSS-1** in chloroform (tolyl groups are removed for clarity).

Front View	Side Views	Relative energies(kcal/mol)
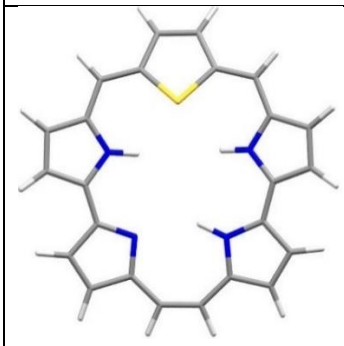 **SSS-1.Ha**	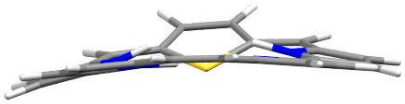 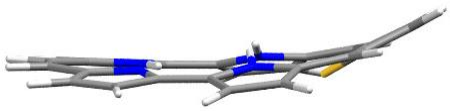	0
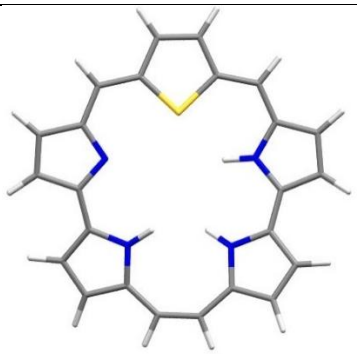 **SSS-1-Hb**	 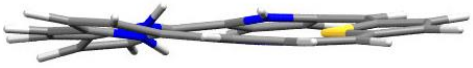	4.76

2.3.3. Complexation of sapphycene SSS-1

Interesting structural features of **SSS-1** fascinated us to explore its coordination chemistry with transition metals. The preliminary observations indicated fascinating results. For example, our initial attempts with 3d-transition metal ions like Ni^{2+}, Cu^{2+} and Zn^{2+} using their respective acetate salts indicated Cu and Zn exhibit easy and facile complexation upon addition of metal salts at room temperature. Unfortunately, we could not characterize them properly so far due to the labile nature of these complexes. Only UV-Vis-NIR absorption spectra (**Figure 2.11a**) indicated the formation of these complexes as HRMS data only provided mass corresponding to the freebase **SSS-1**. Unexpectedly, freebase **SSS-1** decomposed during complexation with nickel(II) acetate under reflux condition. However, metalation with $PdCl_2$ showed a facile and stable complexation with quantitative yield. This has been well characterized with all standard spectroscopic characterizations.

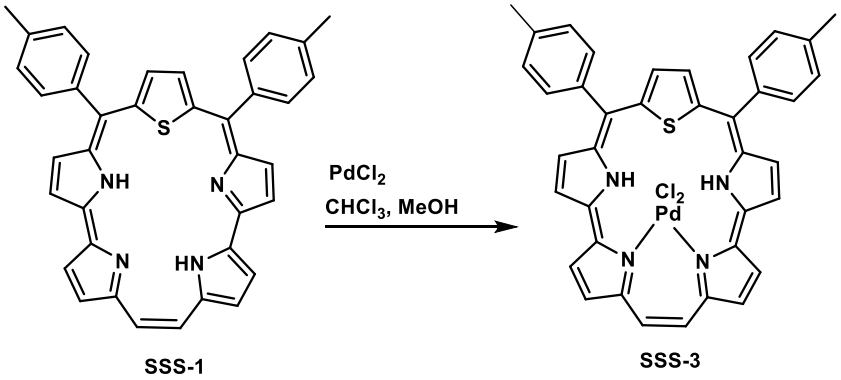

Scheme 2.10: Synthesis of Pd(II) complex of sapphycene.

2.3.3.1. Charcterization of Pd(II) complex

Metal complex **SSS-3** exhibits a red shifted Soret band with less absorption coefficient value compared to freebase **SSS-1**. Soret band of **SSS-3** appears at 491 nm with three broad Q-type bands at 623, 667 and 804 nm. However the HRMS data didn't match to regular tetra-coordinated complexation. ^{1}H NMR data showed downfield shift of thiophene and *meso*-protons compared to **SSS-1**, whereas, β-protons showed little upfield shift. Two protons appeared in the negative region at -1.56 ppm, which disappeared in hydrogen-deuterium exchange experiment with deuterium oxide, confirming the presence of two NH protons inside the core.

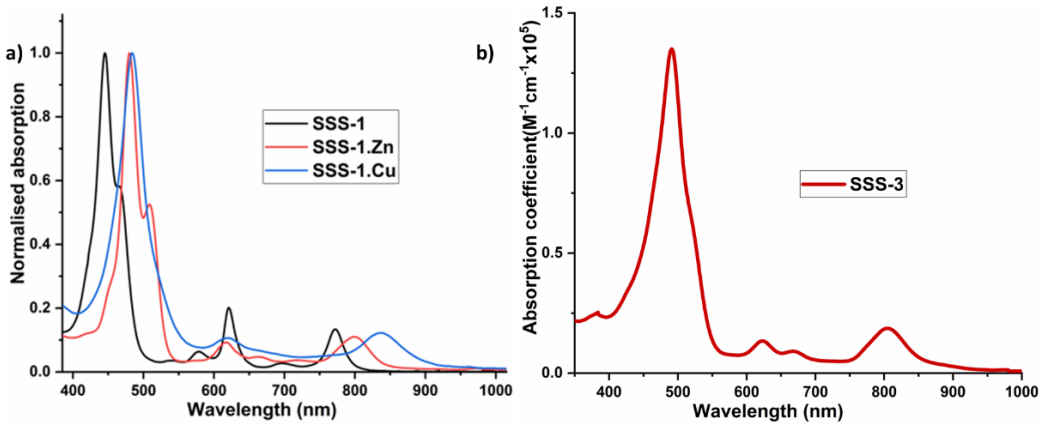

Figure 2.11: Absorption spectra of a) sapphycene, Zn(II) and Cu(II) complex; b) Pd(II) complex recorded in $CHCl_3$.

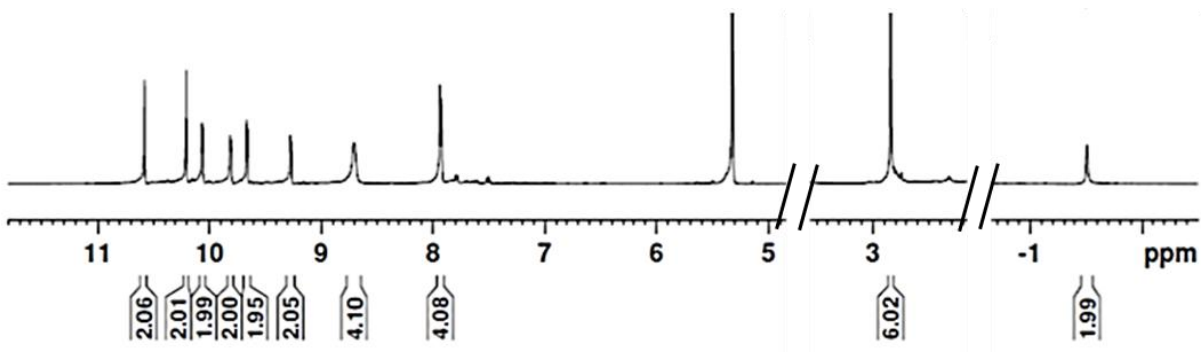

Figure 2.12: Selected region of ^{1}H NMR spectrum of **SSS-3** in $CDCl_3$.

2.3.3.2. Structural elucidation of SSS-3

The solid state structure of **SSS-3** established from crystals obtained by slow evaporation of $CDCl_3$ solution, revealed a unique coordination mode where the sapphycene is behaving as a neutral bidentate ligand. Both NHs were present on pyrroles adjacent to thiophene and sapphycene chelates through dipyrroethene side with two imine type nitrogens. The other two coordination sites were occupied with two Cl^- ions, which mentains the charge neutrality. Pd being on the top of the macrocycle distorted the macrocyclic plane to a greater extent. It adopts a saddle distorted shape. This kind of seven membered metallacycle has been observed in smaller macrocycles like triphyrin and porphycene but hardly observed in expanded systems.[29,30] Palladium sits 1.065 Å above the mean plane (of the four *meso*-carbons) with Pd-N2 distance 2.027 Å. While nitrogens (N2) coordinated to palladium were less distorted from the mean plane, the non-coordinated nitrogens (N1) were relatively more distorted with dihedral angles between mean plane of *meso*-carbons and those of pyrrole A and pyrrole B 36.87° and 22.94°, respectively. Further, the dihedral angle between pyrroles coordinating to

palladium is 134.2°, which is more than that in case of Pd-triphyrin complex (116.2°). In-core pyrrolic NHs experienced hydrogen bonding with thiophene-S (S-N: 2.863 Å) as well as with the chloride ligands on their side (Cl-N: 3.152(4) Å). The N1-N2 distance (3.125(5) Å) across the bipyrrole was elongated in the metallo-derivative compared to that in case of freebase **SSS-1**. This type of elongation is a typical attribute observed in case of porphycenes upon complexation due to interruption of N-H···N hydrogen bonding.[31] Further, molecular packing diagram of the complex showed the solid-state structure was stabilized by intermolecular Cl···H-C (*meso* of another complex) hydrogen bonding (Cl1-C17: 3.487(3) Å). In addition, a solvent dichloromethane molecule also interacts with sulphur (S1···H20A-C20) of one molecule and palladium of another molecule (Pd···H20B-C20) to further stablise the crystal packing.

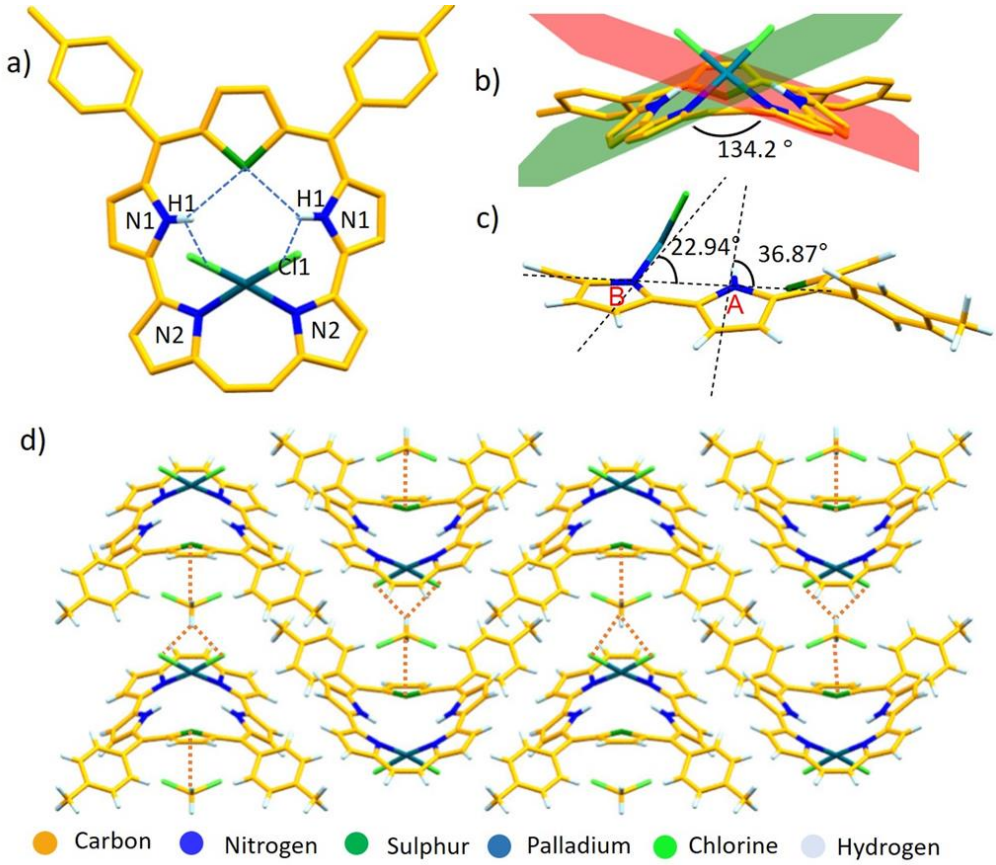

Figure 2.13: Crystal structure elucidation of SSS-3 (hydrogen omitted for clarity): a) front view; b) Side view showing dihedral angle of bipyrroles; c) side view showing pyrrole distortion in bipyrrole; d) packing along b axis.

2.3.3.3. Theoretical calculations of Pd(II) complex

To check the stable binding mode of Pd to the sapphycene core, we calculated ground state energy for two possible modes of binding where one structure binds through bipyrrole nitrogen and other through dipyrroethene nitrogens. This would form a six and seven membered metallacycles, respectively. Relative energies revealed that seven membered metallacycle is more stable structure and most suitable mode of binding.

Table 2.3: Relative energies of conformations having different mode of binding of Pd to **SSS-1** (tolyl groups are removed for clarity).

Front View	Side Views	Relative energies (kcal/mol)
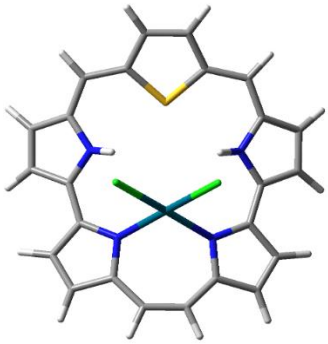	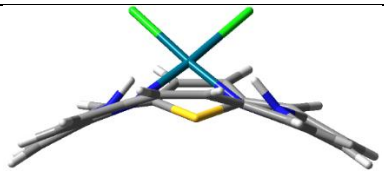 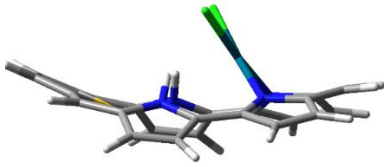	0
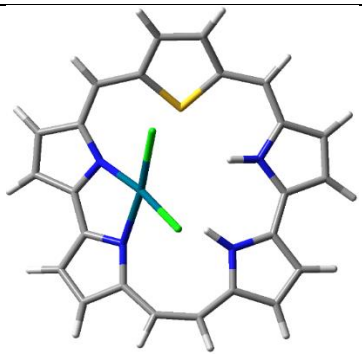	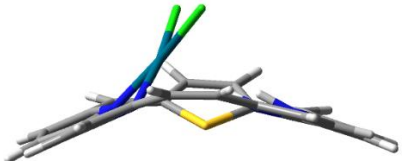 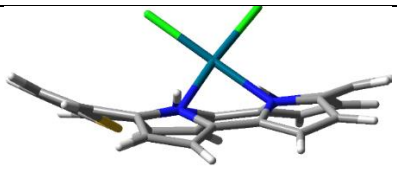	9.68

Frontier orbital diagram of both sapphycene freebase, **SSS-1** and Pd(II)-complex, **SSS-3** showed a reduction of HOMO-LUMO gap upon complexation. Reduction of HOMO-LUMO gap was also reflected in theoretical absorption spectra and in experimental spectra.

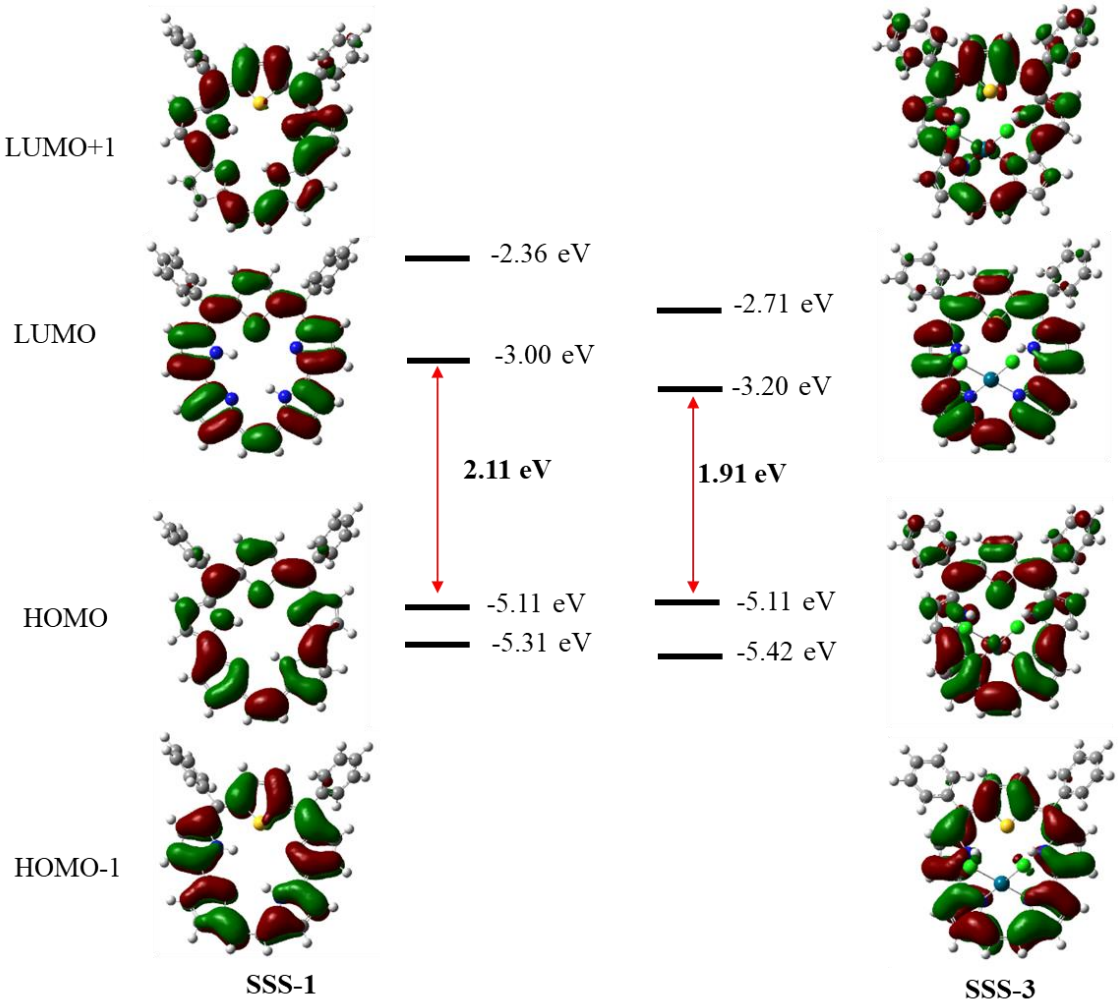

Figure 2.14: Frontier orbital diagrams of sapphycene and its Pd(II) complex.

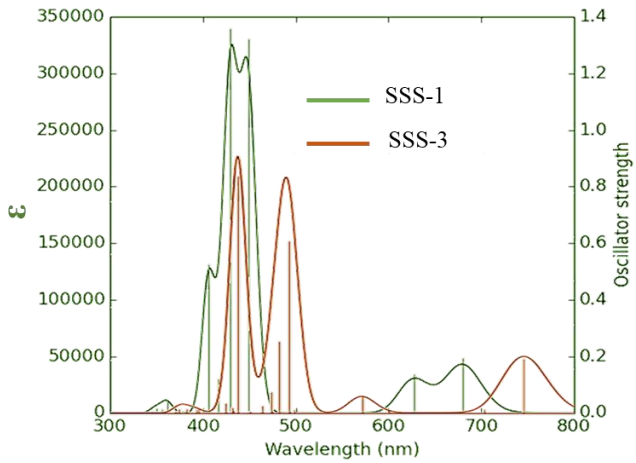

Figure 2.15: Calculated absorption spectra of **SSS-1** and **SSS-3**.

Table 2.4: Calculated electronic transitions of **SSS-1** in chloroform.

Sl. No	Wavelength (nm)	Oscillator strength	Electronic transitions
1	406	0.528	H-3 → LUMO (81%), H-1 → L+1 (11%)
2	429	1.360	H-1 → L+1 (68%), HOMO → LUMO (15%)
3	448	1.324	HOMO → L+1 (67%), H-1 → LUMO (26%)
4	627	0.138	H-1 → LUMO (57%), HOMO → L+1 (21%)
5	679	0.196	HOMO → LUMO (63%), H-1 → LUMO (15%), H-1 → L+1 (15%)

Table 2.5: Calculated electronic transitions of **SSS-3** in chloroform.

Sl. No	Wavelength (nm)	Oscillator strength	Electronic transitions
1	441	1.078	H-1 → L+1 (44%), H-1 → L+2 (37%)
2	484	0.326	H-1 → L+1 (32%), H-1 → L+2 (57%)
3	494	0.782	H-1 → LUMO (26%), HOMO → L+1 (40%), HOMO → L+2 (20%)
4	740	0.246	HOMO → LUMO (82%)

Further, nucleus-independent chemical shift (NICS(0) and NICS$(1)_{zz}$) values and harmonic oscillator model of aromaticity (HOMA) indices were calculated using optimized geometries of **SSS-1** and **SSS-3**.[32] Both NICS(0) and NICS$(1)_{zz}$ for **SSS-3** (-10.1 and -11.9, respectively) revealed a reduction of aromaticity owing to complexation compared to those of freebase **SSS-1** (-13.6 and -12.7, respectively) and was further supported by HOMA indices of **SSS-1** (0.738) and **SSS-3** (0.669), which can be attributed to its large deformation.

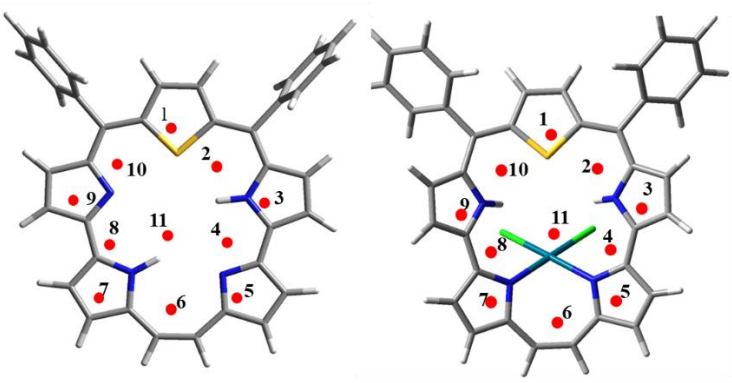

Positions	NICS(0) for SSS-1	NICS(0) for SSS-3
1	-20.4	-19.2
2	-22.7	-22.2
3	-13.5	-13.9
4	-29.6	-29.1
5	-2.9	-7.2
6	-21.5	-20.5
7	-14.7	-7.2
8	-29.7	-29.1
9	-0.8	-13.9
10	-21.9	-22.2
11	-13.6	-10.1

Figure 2.16: NICS values for **SSS-1** and **SSS-3** at different geometrical centers.

Table 2.6: Aromaticity indices of **SSS-1** and **SSS-3**.

Compounds	NICS(0)	$NICS_{zz}(1)$	HOMA
SSS-1	-13.6	-12.7	0.738
SSS-3	-10.1	-11.9	0.669

2.4. Conclusion

A rational synthesis of novel core-modified sapphyrin isomer, **SSS-1** has been carried out successfully. This exhibited NIR absorption and emission. This also showed anion binding in diprotonated state like sapphyrin. Q bands of UV-Vis-NIR absorption spectrum showed intense Q bands like porphycene. Also, like porphycene, NH resonated in downfield region in ^{1}H NMR spectrum and appeared at 5.4 ppm due strong intramolecular NH···N and NH···S hydrogen bonding. As this showed attributes of both sapphyrin and porphycene, it was named as sapphycene. The macrocycle displayed an unusual coordination ability, where it undergoes large out-of-plane distortion in order to complex with $PdCl_2$ as a neutral bidentate ligand.

2.5. Experimental

Synthesis of 5',5'''-(thiophene-2,5-diylbis(p-tolylmethylene))bis((1H,1'H-[2,2'-bipyrrole]-5-carbaldehyde), SSS-2:

2,5-Bis(4-tolylhydroxymethyl)thiophene (**A3**) (200 mg, 0.62 mmol) and [2,2'-bipyrrole]-5-carboxaldehyde (**A2**) (247 mg, 1.54 mmol) were taken in an oven dried 500 mL two necked RB and dissolved in CH_2Cl_2 (300 mL). The solution was bubbled with N_2 for 20 min and then $BF_3.OEt_2$ (60 µL) was added to it. The mixture was stirred at room temperature in dark under N_2 atmosphere for 6 h. Then the reaction mixture was washed with water and organic layer, and was dried over anhydrous Na_2SO_4. Then concentrated under reduced pressure. The resulting solid was purified by column chromatography with 20% ethyl acetate:hexane mixture to obtain **SSS-2** as bright yellow coloured solid. Yield: 40%; Decomposed >180 °C before melting.

^{1}H NMR (500 MHz, DMSO-D_6) δ in ppm: 11.89 (s, 2H), 11.06 (s, 2H), 9.31 (s, 2H), 7.18 (d, J = 8.28 Hz, 4H), 7.14 (d, J = 8.13 Hz, 4H), 6.99 (dd, *J* = 2.27 Hz, 2H), 6.62 (s, 2H), 6.60 (t, *J* = 2.84 Hz, 2H), 6.51 (dd, *J* = 2.24 Hz, 2H), 5.82 (t, *J* = 2.66 Hz, 2H), 5.58 (s, 2H), 2.51 (s, 6H); ^{13}C NMR (125 MHz, DMSO-D_6) δ in ppm: 177.7, 146.4, 140.4, 136.4, 136.2, 134.7, 132.3, 129.5, 128.5, 125.4, 123.7, 109.0, 108.2, 106.9, 45.3, 21.1; HRMS(ESI+): m/z calculated for $C_{38}H_{32}N_4SO_2$ ($M+H^+$): 609.2323; found: 609.2325; IR (ν in cm^{-1}): 3259, 3212, 1599, 1544, 1509.

Synthesis of sapphycene SSS-1:

A low-valent titanium reagent was prepared in situ by adding $TiCl_4$ (0.36 mL,3.28 mmol) to a solution of activated Zn (426 mg, 6.56 mmol), CuCl (64.98 mg, 0.656 mmol) and THF in a three-necked RB at 0 °C and then heating to reflux for 3 h. To this slurry, THF solution of compound **SSS-2** (100 mg, 0.164 mmol**)** was added dropwise for 1 h under reflux condition. After completion of addition, the reaction mixture was kept for refluxing for additional 2 h and then slowly brought to room temperature. Then it was cooled to 0 °C and hydrolysed with aqueous K_2CO_3 solution. It was kept for open air oxidation overnight and then the rection mixture was filtered using celite. The filtrate was washed with water and the organic layer was dried over anhydrous Na_2SO_4 and concentrated under reduced pressure. The crude reaction mixture was purified by silica gel column chromatography with 80:20 of hexane-ethyl acetate mixture as eluent to obtain **SSS-1** as blue colour solid. Yield: 9%. M.P: >300 °C.

^{1}H NMR (500 MHz, $CDCl_3$) δ in ppm: 10.38 (s, 2H), 10.36 (d, *J* = 4.17 Hz, 2H), 10.19 (d, *J* = 4.61 Hz, 2H), 9.99 (s, 2H), 9.68 (d, *J* = 4.17 Hz, 2H), 9.43 (d, *J* = 4.59 Hz, 2H), 8.37 (d, *J* = 7.74 Hz, 4H), 7.76 (d, *J* = 7.53 Hz, 4H), 2.81 (s, 6H); ^{13}C NMR (125 MHz, $CDCl_3$) δ in ppm: 144.6, 143.4, 141.0, 138.8, 138.1, 134.3, 134.3, 132.5, 132.4, 129.3, 128.4, 128.4, 127.8, 126.7, 126.2, 112.9, 21.6; UV-vis-NIR in $CHCl_3$ (λ_{max} nm, log ε): 447 (5.50), 467 (5.24), 542 (3.98), 579 (4.27), 622 (4.79), 699 (3.86), 773 (4.61); HRMS (ESI+): m/z calculated for $C_{38}H_{28}N_4S$ ($M+H^+$): 573.2113; found:573.2100; IR (ν in cm^{-1}): 2920, 2581, 1597, 1510.

Synthesis of palladium(II)-sapphycene SSS-3:

Thiasapphycene **SSS-1** (2 mg) was taken in a two-necked RB in N_2 atmosphere and dissolved in 5 mL chloroform and methanol (1 mL) was added to it and then $PdCl_2$ (25 mg) was added to the above solution and kept for stirring at rt. Reaction was monitored using TLC and absorption spectroscopy. After 10-15 min all the starting material was consumed and it was concentrated under reduced pressure. Then the crude product was purified by silicagel column chromatography to yield **SSS-3** as brown colour solid. Yield: quantitative.

^{1}H NMR (500 MHz, CD_2Cl_2) δ in ppm: 10.58 (s, 2H), 10.21 (s, 2H), 10.06 (d, *J* = 4.46 Hz, 2H), 9.81 (d, 2H, *J* = 4.47 Hz), 9.66 (d, *J* = 4.44 Hz, 2H), 9.27 (d, *J* = 4.57 Hz, 2H), 8.71 (bs, 4H), 7.94 (d, *J* = 7.66 Hz, 4H), 2.84 (s, 6H); ^{13}C NMR (125 MHz, CD_2Cl_2) δ in ppm: 149.7, 142.2, 140.2, 138.3, 138.0, 137.1, 136.3, 134.8, 132.4, 129.7, 129.6, 129.4, 126.7, 124.2, 115.5, 21.4; UV-vis-NIR in $CHCl_3$ (λ_{max} nm, log ε): 491 (5.13), 623 (4.12), 667 (3.96), 804 (4.27); HRMS (ESI+): m/z calculated for $C_{38}H_{28}ClN_4PdS$ ($M-Cl^-$): 713.0757, found: 713.0754; IR (ν in cm^{-1}): 2959, 2918, 2851,1588.

2.6 References

1. Battersby, A. R.; Fookes, C. J. R.; Matcham, G. W. J.; McDonald, E. Biosynthesis of the Pigments of Life: Formation of the Macrocycle. *Nature*, **1980**, *285*, 17.

2. Woodward, R. B. *Aromaticity: An International Symposium Sheffield, 1966*; Special Publication no. 21; The Chemical Society: London, **1966**.

3. [a] Sessler, J. L.; Cyr, M. J.; Lynch, V.; McGhee, E.; Ibers, J. A. Synthetic and structural studies of sapphyrin, a 22-pi-electron pentapyrrolic "expanded porphyrin". *J. Am. Chem. Soc.*, **1990**, *112*, 2810. [b] Sessler, J. L.; Cyr, M. J.; Burrell, A. K. Sapphyrins: New Life for an Old "Expanded Porphyrin. *Synlett*, **1991**, *1991*, 127. [c] Judy, M. L.; Matthews, J. L.; Newman, J. T.; Skiles, H.; Boriack, R.; Cyr, M.; Maiya, B. G.; Sessler J. L.; In vitro photodynamic inactivation of Herpes simplex virus with sapphyrins: 22π-elctron porphyrin like macrocycles. *Photochem. Photobiol.*, **1991,** *53*, 101. [d] Shionoya, M.; Furuta, H.; Lynch, V.; Harriman, A.; Sessler, J. L. Diprotonated Sapphyrin: A Fluoride Selective Halide Anion Receptor. *J. Am. Chem. Soc.*, **1992**, *114*, 5714.

4. Broadhurst, M. J.; Grigg, R.; Johnson, A. W. The synthesis of 22 π-Electron Macrocycles: Sapphyrins and Related Compounds. *J. Chem. Soc., Perkin Trans. 1*, **1972,** *1*, 2111.

5. [a] Lisowski, J.; Sessler, J. L.; Lynch, V. Synthesis and X-ray Structure of Selenasapphyrin. *Inorg. Chem.*, **1995**, *34*, 3567. [b] Sessler, J. L.; Hoehner, M. C.; Gebauer, A.; Andrievsky, A.; Lynch, V. Synthesis and Characterization of All-Alkyl-Substituted Mono-, Di-, and Trioxosapphyrins. *J. Org. Chem.*, **1997**, *62*, 9251.

6. [a] Srinivasan, A.; Pushpan, S. K.; Ravi Kumar, M.; Mahajan, S.; Chandrashekar, T. K.; Roy, R.; Ramamurthy, P. *meso*-Aryl sapphyrins with heteroatoms; synthesis, characterization, spectral and electrochemical properties. *J. Chem. Soc., Perkin Trans. 2*, **1999**, 961. [b] Srinivasan, A.; Anand, V. G.; Narayanan, S. J.; Pushpan, S. K.; Kumar, M. R.; Chandrashekar, T. K.; Sugiura, K.-i.; Sakata, Y. Structural Characterization of *meso*-Aryl Sapphyrins. *J. Org. Chem.*, **1999**, *64*, 8693.

7. [a] Narayanan, S. J.; Sridevi, B.; Chandrashekar, T. K.; Vij, A.; Roy, R. Novel Core-Modified Expanded Porphyrins with *meso*-Aryl Substituents: Synthesis, Spectral and Structural Characterization. *J. Am. Chem. Soc.*, **1999**, *121*, 9053. [b] Narayanan, S. J.; Sridevi, B.; Chandrashekar, T. K.; Vij, A.; Roy, R. Sapphyrin Supramolecules through C-

H⋯S and C-H⋯Se Hydrogen Bonds − First Structural Characterization of *meso*-Aryl Sapphyrins bearing Heteroatoms. *Angew. Chem., Int. Ed.*, **1998**, *37*, 3394.

8. Sathyamoorthy, B.; Axelrod, A.; Farwell, V.; Bennett, S. M.; Calitree, B. D.; Benedict, J. B.; Sukumaran, D. K.; Detty, M. R. Novel 21,23-Ditelluraporphyrins and the First 26,28-Ditellurasapphyrin and 30,33-Ditellurarubyrin. *Organometallics*, **2010**, *29*, 3431.

9. Shin, K.; Lim, C.; Choi, C.; Kim, Y.; Lee, C.-H. Synthesis and X-ray Crystal Structure of 27-Oxa-25,29-Dithiasapphyrin: Bithiophene- Containing Sapphyrin Have an Inverted Structure. *Chem. Lett.*, **1999**, *28*, 1331.

10. [a] Sessler, J. L.; Ford, D. A.; Cyr, M. J.; Furuta, H. Enhanced Transport of Fluoride Anion Effected using Protonated Sapphyrin as a Carrier. *J. Chem. Soc., Chem. Commun.* **1991**, 1733. [b] Sessler, J. L.; Andrievsky, A.; Gale, P. A.; Lynch, V. Anion Binding: Self-Assembly of Polypyrrolic Macrocycles. *Angew. Chem., Int. Ed. Engl.* **1996**, *35*, 2782. [c] Král, V.; Furuta, H.; Shreder, K.; Lynch, V.; Sessler, J. L. Protonated Sapphyrins. Highly Effective Phosphate Receptors. *J. Am. Chem. Soc.*, **1996**, *118*, 1595.

11. [a] Furuta, H.; Cyr, M. J.; Sessler, J. L. Phosphate Anion Binding: Enhanced Transport of Nucleotide Monophosphates Using a Sapphyrin Carrier. *J. Am. Chem. Soc.*, **1991**, *113*, 6677. [b] Král, V.; Sessler, J. L.; Furuta, H. Synthetic Sapphyrin-Cytosine Conjugates: Carriers for Selective Nucleotide Transport at Neutral pH. *J. Am. Chem. Soc.* **1992**, *114*, 8704.

12. [a] Iverson, B. L.; Shreder, K.; Král, V.; Sessler, J. L. Phosphate Recognition by Sapphyrin. A New Approach to DNA Binding. *J. Am. Chem. Soc.*, **1993**, *115*, 11022. [b] Iverson, B. L.; Shreder, K.; Morishima, T.; Rosingana, M.; Sessler, J. L. Syntheses of a Sapphyrin-EDTA Conjugate and Preliminary Cleavage Results Using a Supercoiled Plasmid DNA Assay. *J. Org. Chem.*, **1995**, *60*, 6616.

13. [a] Král, V.; Andrievsky, A.; Sessler, J. L. A Covalently Linked Sapphyrin Dimer. A New Receptor for Dicarboxylate Anions. *J. Am. Chem. Soc.*, **1995**, *117*, 2953. [b] Sessler, J. L.; Andrievsky, A.; Král, V.; Lynch, V. Chiral Recognition of Dicarboxylate Anions by Sapphyrin-Based Receptors. *J. Am. Chem. Soc.*, **1997**, *119*, 9385.

14. Bauer, V. J.; Clive, D. L. J.; Dolphin, D.; Paine, J. B., III; Harris, F. L.; King, M. M.; Loder, J.; Wang, S. W. C.; Woodward, R. B. Sapphyrins: Novel Aromatic Pentapyrrolic Macrocycles. *J. Am. Chem. Soc.*, **1983**, *105*, 6429.

15. Burrell, A. K.; Sessler, J. L.; Cyr, M. J.; McGhee, E.; Ibers, J. A. Metal Carbonyl Complexes of Sapphyrins. *Angew. Chem., Int. Ed. Engl.*, **1991**, *30*, 91.

16. Sessler, J. L.; Burrell, A. H.; Lisowski, J.; Gebauer, A.; Cyr, M. J.; Lynch, V. Cobalt(II) and Rhodium(I) Complexes of Thia- and Oxasapphyrins. *Bull. Soc. Chem. Fr.*, **1996**, *133*, 725.

17. Burrell, A. K.; Cyr, M. J.; Lynch, V.; Sessler, J. L. Nucleophilic Attack at the *meso* position of a Uranyl Sapphyrin Complex. *J. Chem. Soc., Chem. Commun.* **1991**, 1710.

18. Sessler, J. L.; Gebauer, A.; Hoehner, M. C.; Lynch, V. Synthesis and characterization of an oxasapphyrin-uranyl complex. *Chem. Commun.*, **1998**, 1835.

19. Simkhovich, L.; Rosenberg, S.; Gross, Z. Facile synthesis of a novel sapphyrin and its rhodium(I) complex. *Tetrahedron Lett.*, **2001**, *42*, 4929.

20. Yadav, P.; Fridman, N.; Mizrahiab, A.; Gross, Z. Rhenium(I) Sapphyrins: Remarkable Difference Between the C_6F_5 and CF_3-substituted Derivatives. *Chem. Commun.*, **2020**, *56*, 980.

21. Chen, Q.-C.; Fridman, N.; Diskin-Posner, Y.; Gross, Z. Palladium Complexes of Corroles and Sapphyrins. *Chem. Eur. J.*, **2020**, *26*, 9481.

22. Vogel, E.; Köcher, M.; Schmickler, H.; Lex, J. Porphycene, a new type of porphine isomer. *Angew. Chem., Int. Ed. Engl*. **1986**, *25*, 257.

23. Sessler, J. L.; Brucker, E. A.; Weghorn, S. J.; Kisters, M.; Schaefer, M.; Lex, J.; Vogel, E. Corrphycene: a new porphyrin isomer. *Angew. Chem., Int. Ed. Engl.*, **1994**, *33*, 2308.

24. [a] Sessler, J. L.; Cyr, M. J.; Burrell, A. K. Sapphyrins and heterosapphyrins. *Tetrahedron*, **1992**, *48*, 9661. [b] Miller, D. C.; Johnson, M. R.; Ibers, J. A. Synthesis and Characterization of New "Expanded" Thiophene- and Furan-Containing Macrocycles. *J. Org. Chem.*, **1994**, *59*, 2877.

25. Kishore, M. V. N.; Panda, P. K. Revisiting the intense NIR active bronzaphyrin, a 26-π aromatic expanded porphyrin: synthesis and structural analysis. *Chem. Commun.*, **2018**, *54*, 13135.

26. Miller, D. C.; Johnson, M. R.; Becker, J. J.; Ibers, J. A. Synthesis and characterization of the new 22-π aromatic furan-containing macrocycle, "ozaphyrin". *J. Heterocycl. Chem.*, **1993**, *30*, 1485.

27. Frisch, M. J.; Trucks, G. W.; Schlegel *et al.*, H. B. Gaussian09, Revision C.01, (Gaussian, Inc., Wallingford CT, **2010**).

28. H. S. Biswal, S. Wategaonkar, Nature of the N-H· · · S Hydrogen Bond. *J. Phys. Chem. A*, **2009**, *113*, 12763.

29. [a] Xue, Z. L.; Kuzuhara, D.; Ikeda, S.; Okujima, T.; Mori, S.; Uno, H.; Yamada, H. Synthesis and characterization of new platinum (II) and platinum (IV) triphyrin complexes. *Inorg. Chem.* **2013**, *52*, 1688. [b] Xue, Z. L.; Wang, Y.; Mack, J.; Fang, Y.; Ou, Z.; Zhu, W.; Kadish, K. M. Synthesis and Characterization of Palladium(II) Complexes of meso-Substituted [14]Tribenzotriphyrin(2.1.1). *Inorg. Chem.*, **2015**, *54*, 11852.

30. Sarma, T.; Kumar, B. S.; Panda, P. K. β,β′-Bipyrrole Fusion-Driven cis-Bimetallic Complexation in Isomeric Porphyrin. *Angew. Chem. Int. Ed.*, **2015**, *54*, 14835.

31. Fowler, C. J.; Sessler, J. L.; Lynch, V. M.; Waluk, J.; Gebauer, A.; Lex, J.; Heger, A.; Zuniga-y-Rivero, F.; Vogel, E. Metal complexes of porphycene, corrphycene, and hemiporphycene: stability and coordination chemistry. *Chem. Eur. J.*, **2002**, *8*, 3485.

32. [a] Von, P.; Schleyer, R.; Maerker, C.; Dransfeld, A.; Jiao, H.; van Eikema Hommes, N. J. R.; Nucleus-Independent Chemical Shifts: A Simple and Efficient Aromaticity Probe *J. Am. Chem. Soc.*, **1996**,*118*, 6317. [b] Krygowski, T. M.; Cryański, M. Separation of the energetic and geometric contributions to the aromaticity of π-electron carbocyclics. *Tetrahedron* **1996**, *52*, 1713. [c] Krygowski, T. M.; Cryański, M. Separation of the energetic and geometric contributions to the aromaticity. Part IV. A general model for the π-electron systems. *Tetrahedron*, **1996**, *52*, 10255.

2.7. Spectra

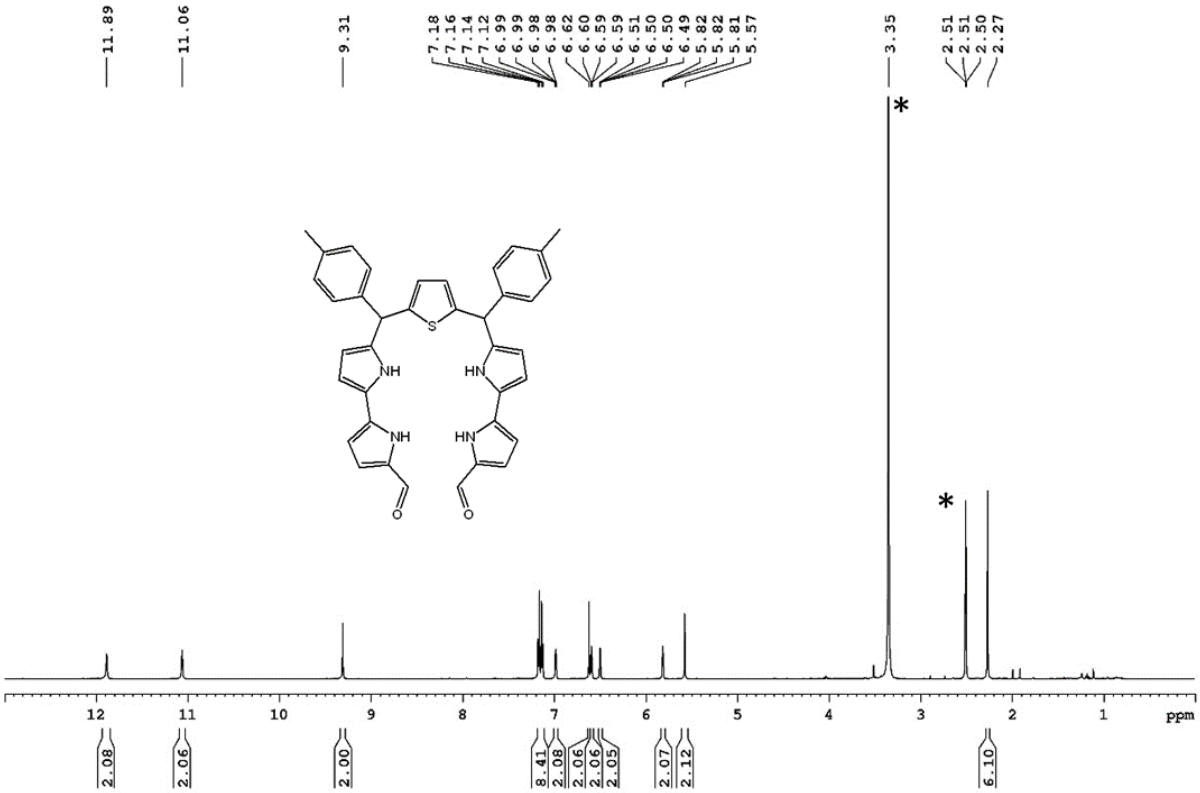

Figure 2.17: ^{1}H NMR spectrum of **SSS-2** in DMSO-d_6 (*water and residual protons of solvent).

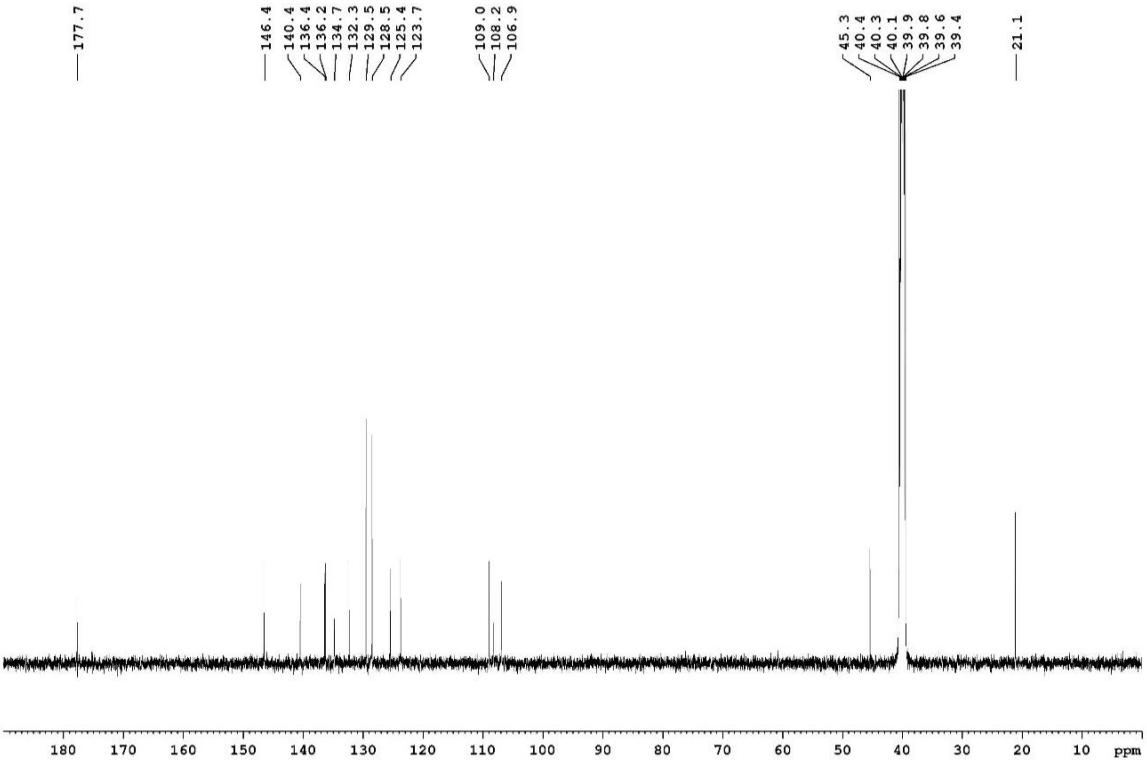

Figure 2.18: ^{13}C NMR spectrum of **SSS-2** in DMSO-d_6.

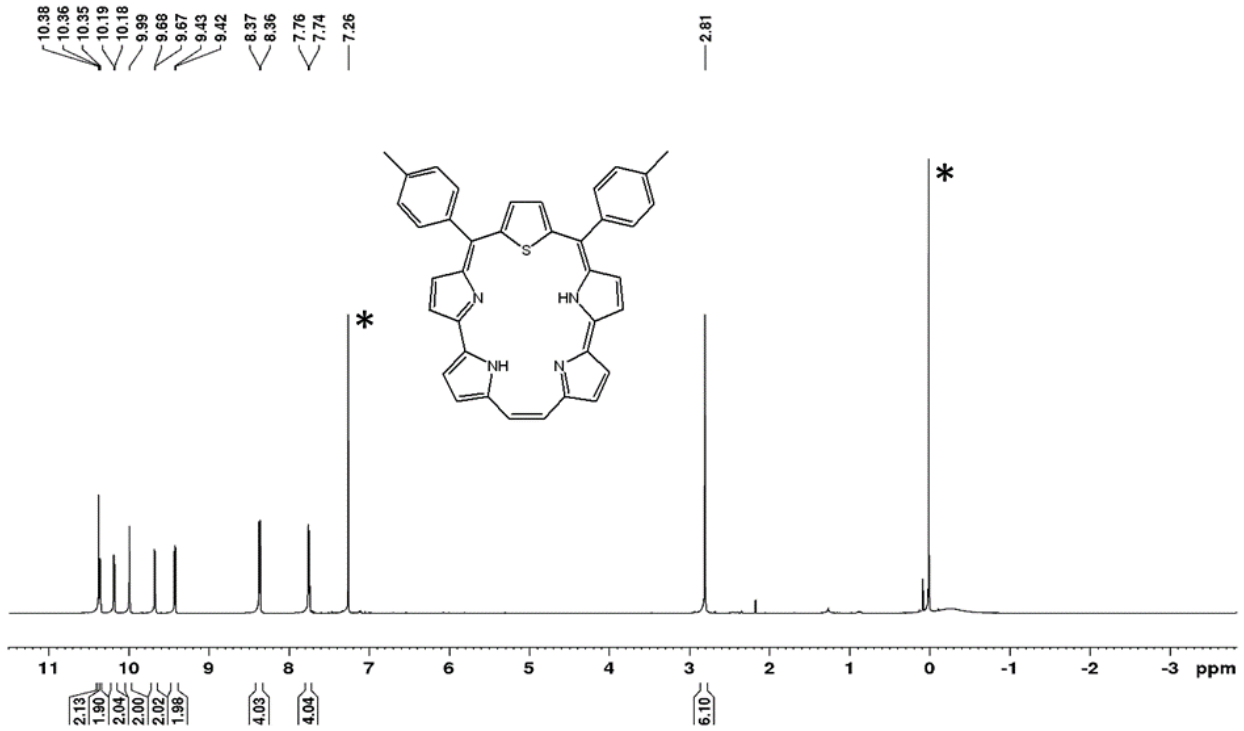

Figure 2.19: ^{1}H NMR spectrum of compound **SSS-1** in $CDCl_3$ (* water and residual protons of solvent).

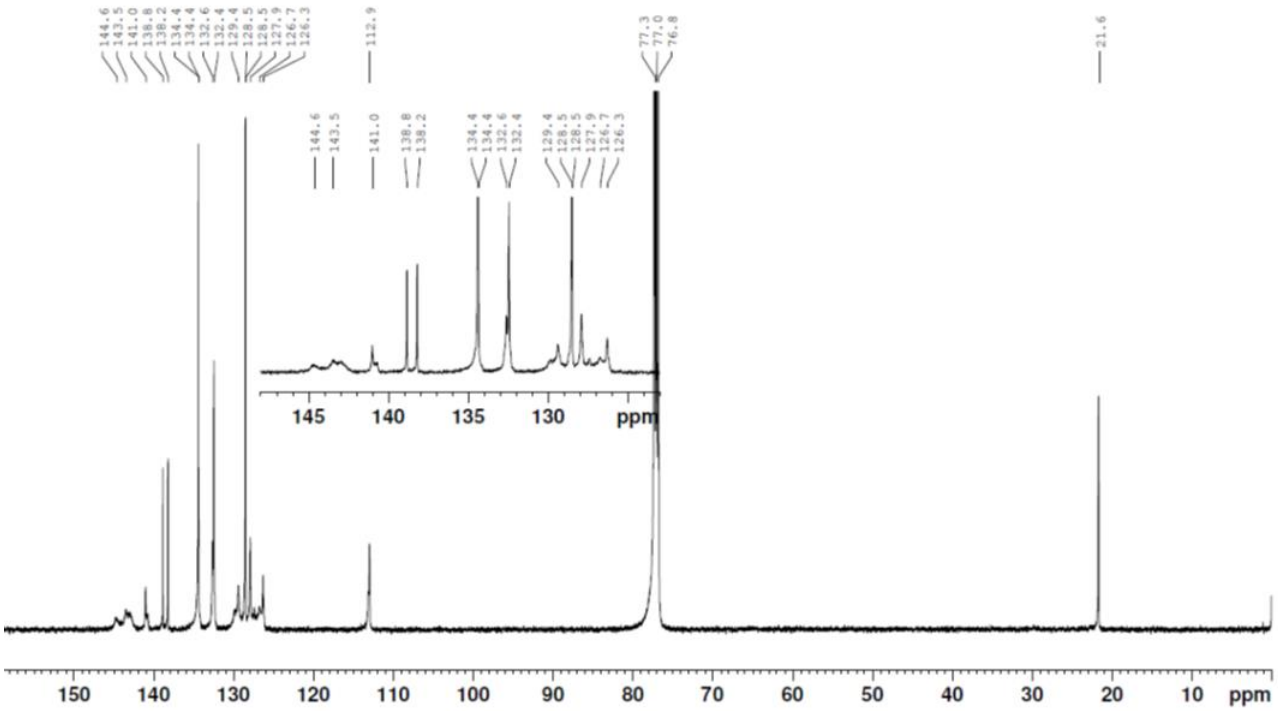

Figure 2.20: ^{13}C NMR spectrum of **SSS-1** in $CDCl_3$.

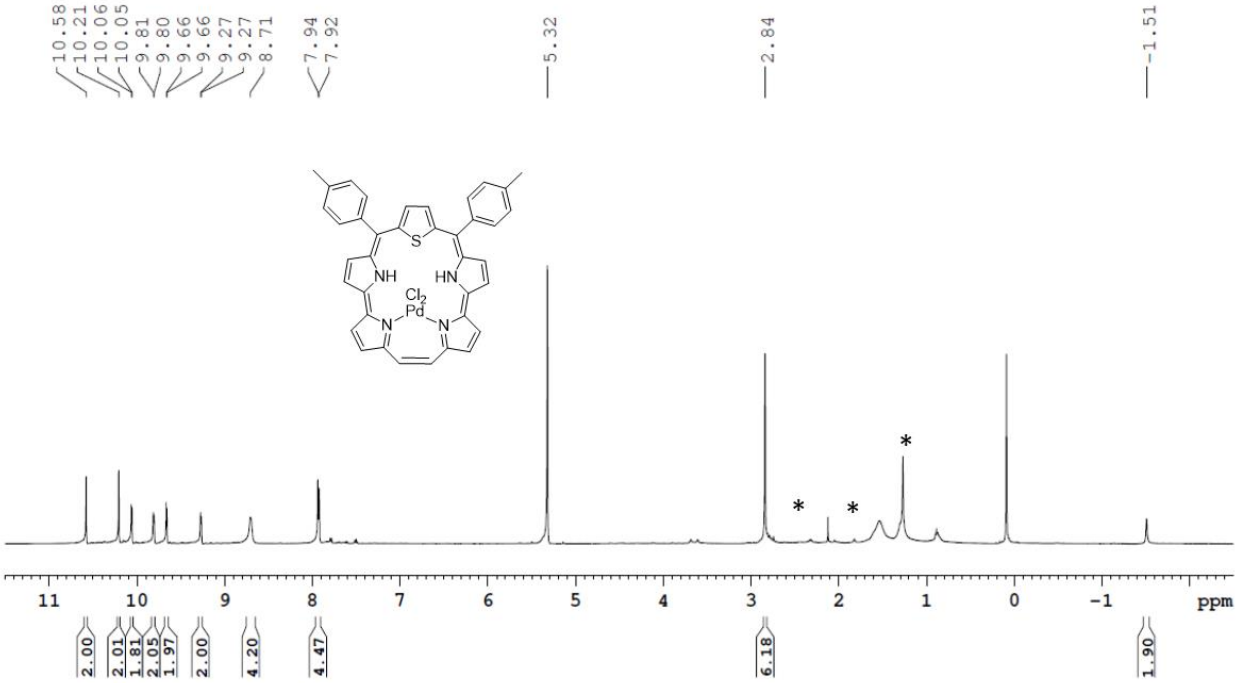

Figure 2.21: ^{1}H NMR spectrum of **SSS-3** in CD_2Cl_2 (* water and residual protons of solvent and impurities due to less solubility of sample).

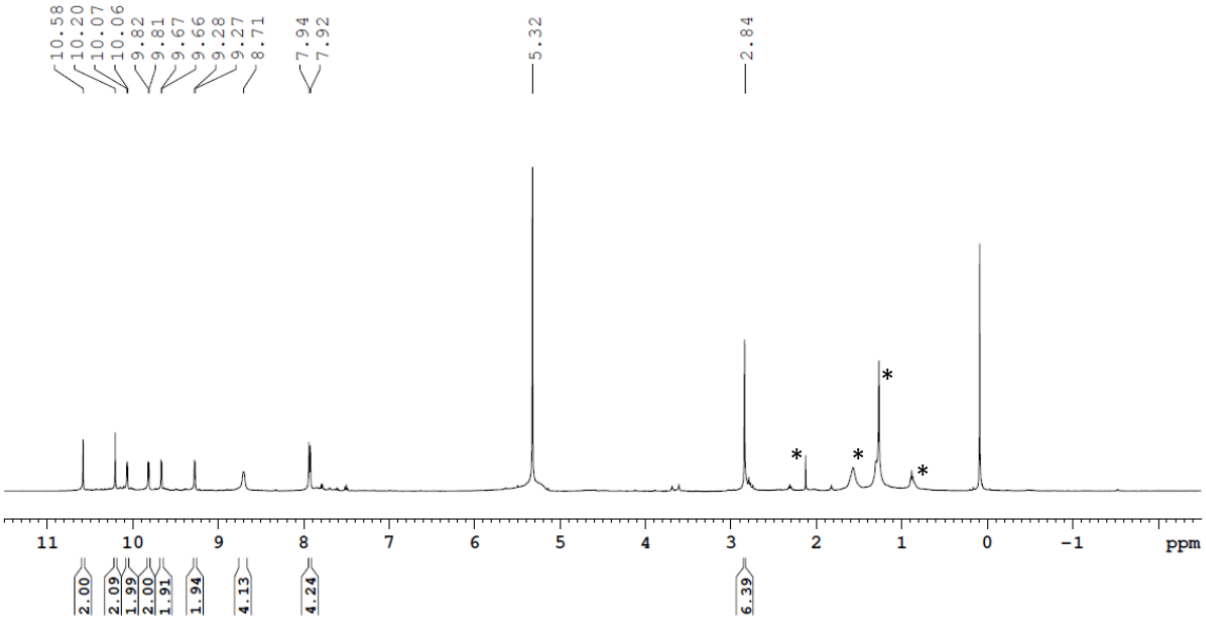

Figure 2.22: D_2O exchange ^{1}H NMR spectrum of **SSS-3** in CD_2Cl_2 (* water and residual protons of solvent and impurities due to less solubility of sample).

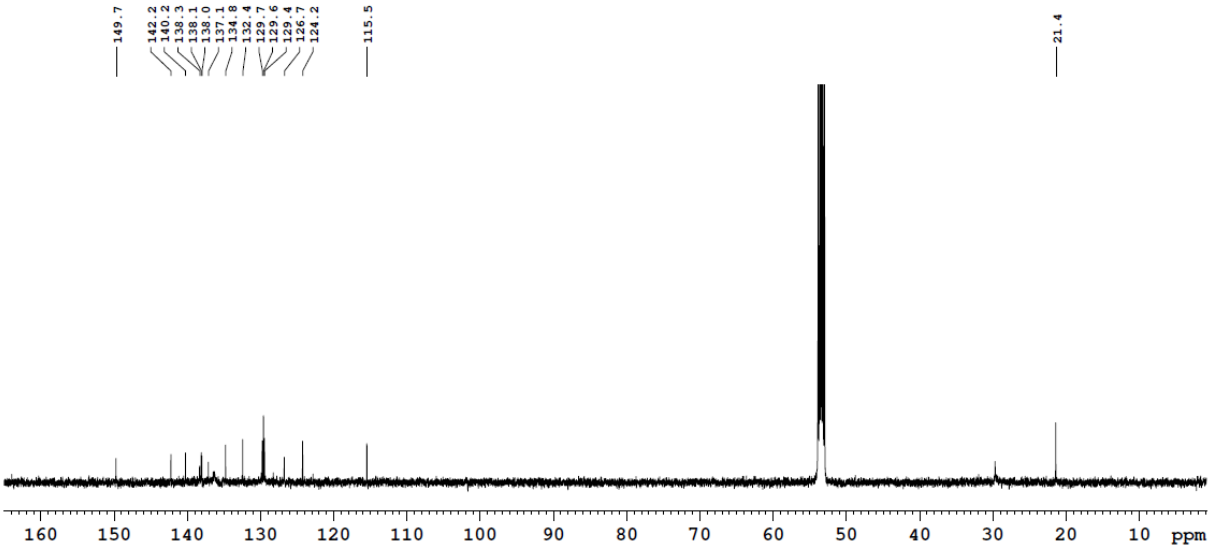

Figure 2.23: ^{13}C NMR spectrum of **SSS-3** in CD_2Cl_2.

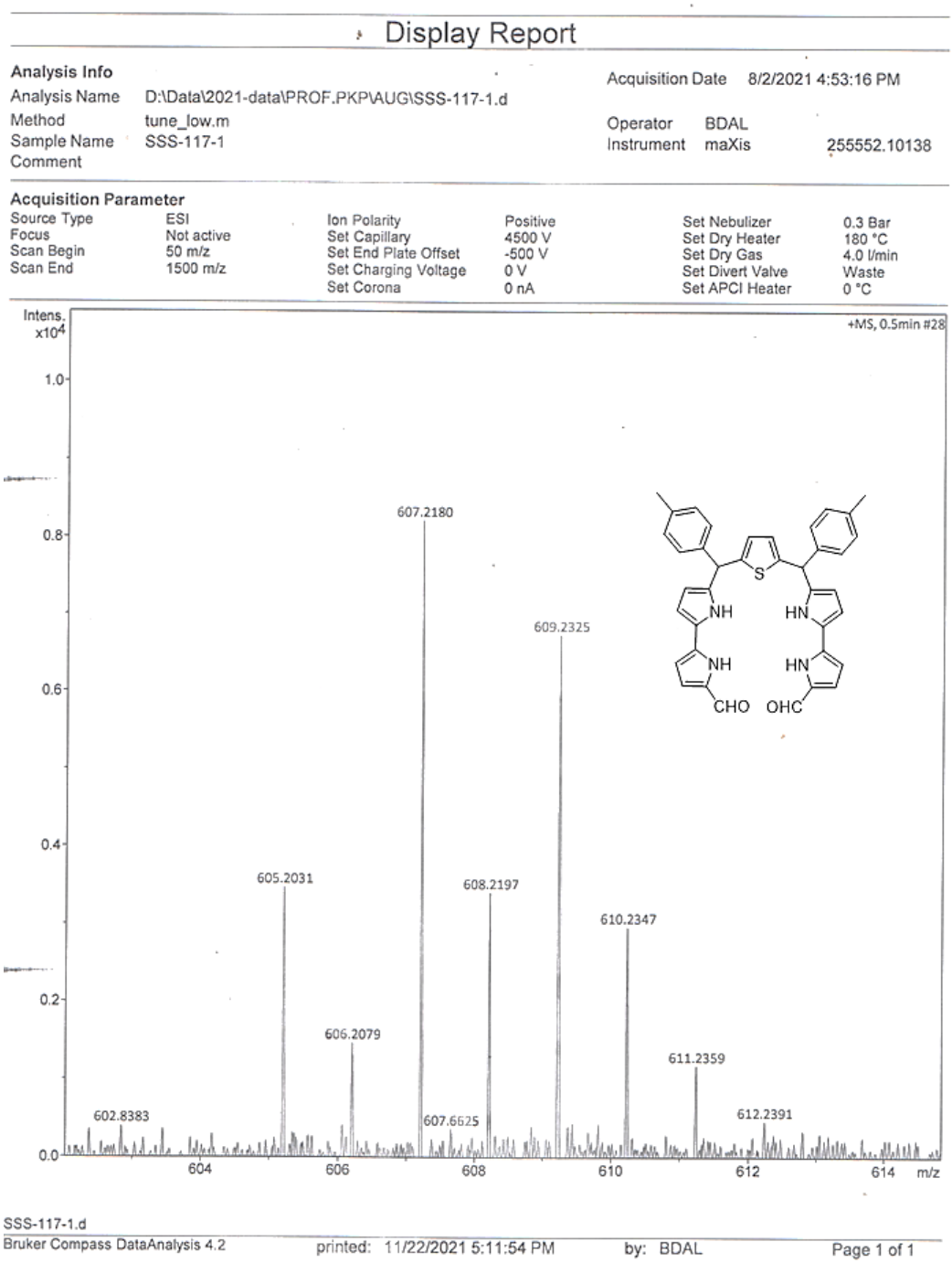

Figure 2.24: HRMS data of **SSS-2**: m/z calculated for $C_{38}H_{32}N_4SO_2$ ($M+H^+$): 609.2323; found: 609.2325.

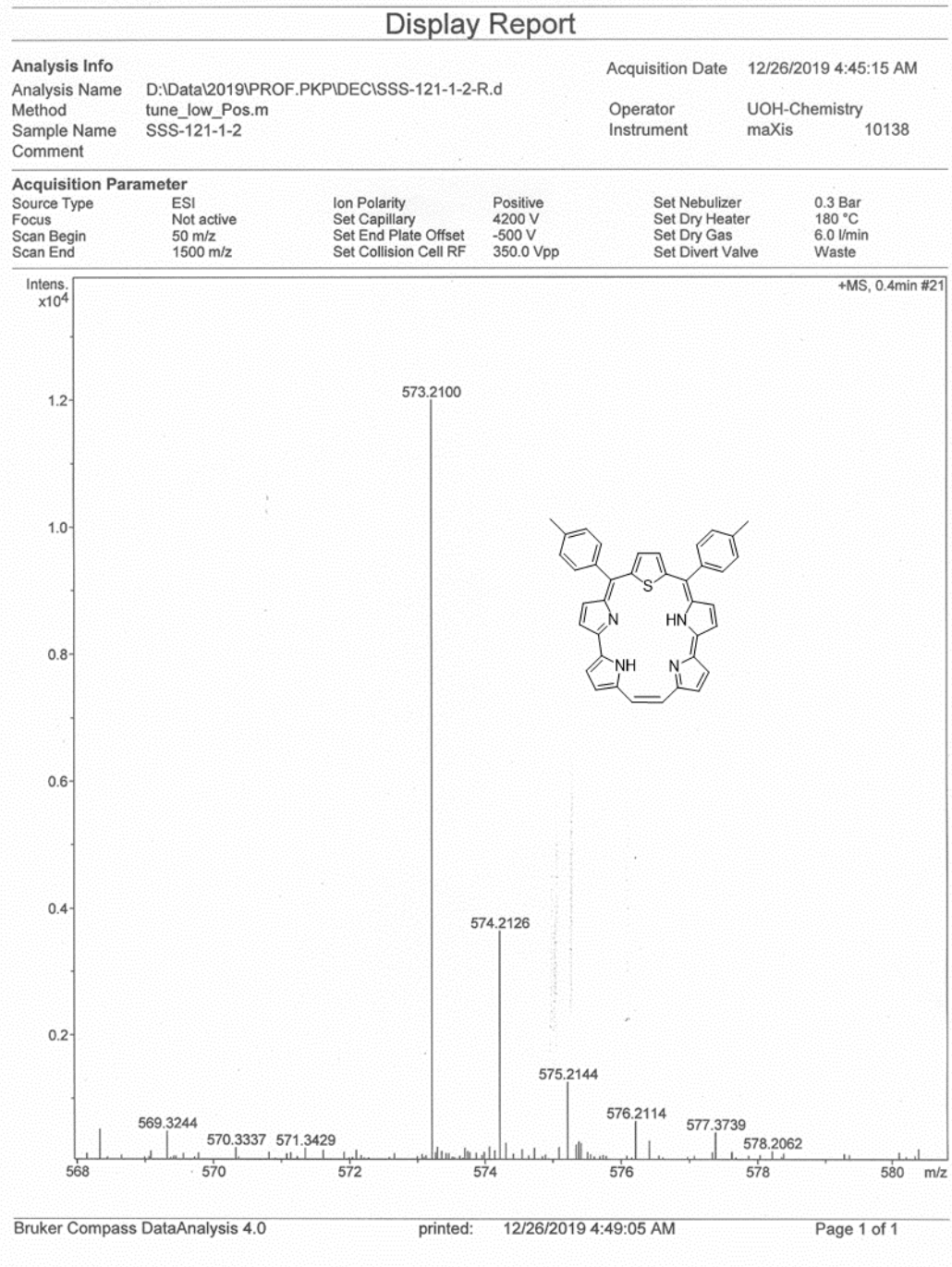

Figure 2.25: HRMS data of **SSS-1**. Calculated m/z $C_{38}H_{28}N_4S$ ($M+H^+$): 573.2113; found: 573.2100.

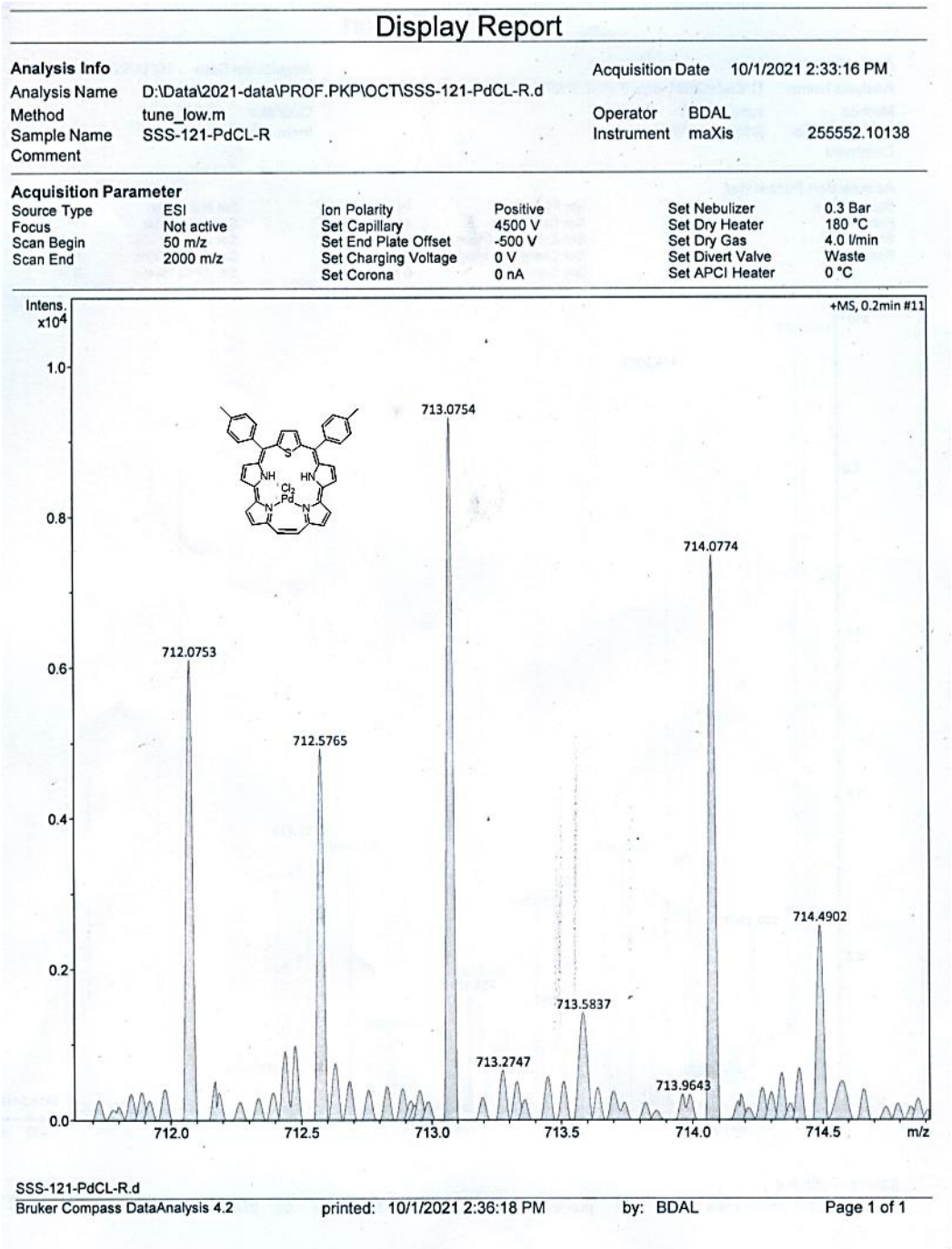

Figure 2.26: HRMS data of **SSS-3**: m/z calculated for $C_{38}H_{28}ClN_4PdS$ (M-Cl$^-$): 713.0757; found: 713.0754.

Table 2.7: Crystal data and structure refinement parameters for sapphycene **SSS-1.**

Empirical formula	$C_{38}H_{28}N_4S$
Formula weight	572.2
Temperature	109(2) K
Wavelength	0.71073 Å
Crystal system, space group	Monoclinic, I 2/a
Unit cell dimensions	alpha = 90 deg. a = 12.4940(3) Å

	beta = 91.562(2) deg. b = 22.0708(8) Å gamma = 90 deg. c = 20.4806(8) Å
Volume	5645.5(3) $Å^{-3}$
Z, Calculated density	8, 1.348 Mg/m^3
Absorption coefficient	0.151 mm^{-1}
F(000)	3150
Crystal size	0.14 x 0.12 x 0.08 mm
Theta range for data collection	1.874 to 27.038 deg.
Limiting indices	$-15 \leq h \leq 15$, $-27 \leq k \leq 27$, $-24 \leq l \leq 26$
Reflections collected / unique	25264 / 5829 [R(int) = 0.1338]
Completeness to theta = 25.242	98.7 %
Refinement method	Full-matrix least-squares on F^2
Data / restraints / parameters	5829 / 0 / 398
Goodness-of-fit on F^2	1.000
Final R indices [I>2sigma(I)]	R1 = 0.0762, wR2 = 0.1887
R indices (all data)	R1 = 0.1437, wR2 = 0.2464
Extinction coefficient	n/a
Largest diff. peak and hole	0.697 and -0.808 e.$Å^{-3}$

Table 2.8: Crystal data and structure refinement data for Pd(II)sapphycene **SSS-3.**

Empirical formula	$C_{39}H_{30}Cl_4N_4PdS$
Formula weight	834.93
Temperature	293(2) K
Wavelength	0.71073 Å
Crystal system, space group	Monoclinic, P 21/m
Unit cell dimensions	alpha = 90 deg. a = 7.9019(2) Å beta = 102.071(3) deg. b = 22.3765(6) Å gamma = 90 deg. c = 9.7921(4) Å
Volume	1693.13(9) $Å^3$
Z, Calculated density	2, 1.638 mg/m^3
Absorption coefficient	0.963 mm^{-1}
F(000)	844
Crystal size	0.200 x 0.150 x 0.100 mm
Theta range for data collection	2.313 to 25.026 deg.
Limiting indices	$-9 \leq h \leq 9$, $-26 \leq k \leq 26$, $-11 \leq l \leq 11$
Reflections collected / unique	10880 / 3009 [R(int) = 0.0686]
Completeness to theta = 25.026	97.6 %
Refinement method	Full-matrix least-squares on F^2
Data / restraints / parameters	3009 / 0 / 227
Goodness-of-fit on F^2	1.081
Final R indices [I>2sigma(I)]	R1 = 0.0432, wR2 = 0.1044
R indices (all data)	R1 = 0.0548, wR2 = 0.1124
Extinction coefficient	n/a
Largest diff. peak and hole	1.0158 and -1.000 e. $Å^{-3}$

Part B

Chapter 3

Introduction

3.1. Background

"Near-infrared materials are defined as the substances that interact with NIR light (750-2500 nm), such as absorption and reflection, and emit NIR light under external stimulation such as photoexcitation, electric field, and chemical reaction."[1] Research on dyes active in NIR region is on constant demand due to exigencies for fluorescence imaging, photoacoustic imaging, photosensitizers in medical application, sensing, advanced optoelectronics, solar cells etc. Deep tissue fluorescence imaging having more advantage over other tomographic imaging suffers some technical limitations for more development. For a better *in vivo* imaging high signal to noise ratio is necessary. This problem can be solved by two ways; i) developing better instrumentation for imaging (confocal microscopy, two- and multi-photon microscopy, light-sheet microscopy, adaptive optical microscopy, optical coherence tomography and fluorescence-mediated tomography) and ii) designing new fluorophores with better quantum yield, spectral properties, photostability, and biocompatibility.[2] Due to abundance of fluorophores emitting in visible range, existing technologies relies on those and suffers from more scattering, autofluorescence by biological tissues hindering the clarity of imaging. Major advantages of NIR fluorophores for bioimaging on other fluorophores are a) deeper tissue penetration of NIR photons compared to visible light, b) low light absorption and scattering by biological tissues, c) significant reduction of autofluorescence of biomolecules leading to low background noise hence better signal to noise ratio.[3] NIR dyes which can be tuned to have more ISC (intersystem crossing) are studied for photosensitization in photodynamic therapy.[4] Though there are plenty of examples for NIR absorbing dyes, active research is still going on for NIR emissive compounds mainly due to advanced bioimaging technology. Therefore, molecules which absorbs or emits in the biological window (700-1500 nm) are significant for medical application.

Desirable properties of a biologically active NIR dye includes intense absorption and emission with high molar extinction coefficient and fluorescence quantum yield. Dye should have good photostability and brightness. Most importantly, it should have good water solubility. But, most of the organic dyes have extended π-conjugation which reduces its water solubility and increase aggregation. Aggregation affects its photophysical properties and it becomes difficult to control absorption and emission properties. Among many of the studied NIR emissive dyes, squaraine dyes, cyanine dyes and BODIPY dyes are widely explored classes of NIR dyes.

3.1.1. Squaraine Dyes

Squaraine dyes are represented by an electron deficient four membered ring having a zwitter-ionic structure which is resonance stabilized. It was first reported by Treibs and Jacob in 1965.[5] They have donor-acceptor-donor (D-A-D) type general skeletal structure. These types of dyes have an inherent low HOMO-LUMO energy gap and show intense visible or NIR absorption. They show good photostability and high quantum yield.[6] They have easy and direct synthesis.[7] Most of the squaraine dye synthesis starts from the building block, squaric acid. Symmetrical squaraines have same substituents in the 1st and 3rd position of squaric acid moiety whereas unsymmetrical ones have different substituents on these positions. Photophysical properties of squaraines can be tuned by changing substituents attached to the central squaric acid moiety. For instance, symmetrical or unsymmetrical groups, by extending π-conjugation, or inserting S, Se to the backbone of conjugated chain, etc.[8] Absorption maxima of majority of squaraines comes around 600-700 nm and emission maxima comes around 650-750 nm. Variation of donor group can alter absorption maxima and can extend upto 900 nm.

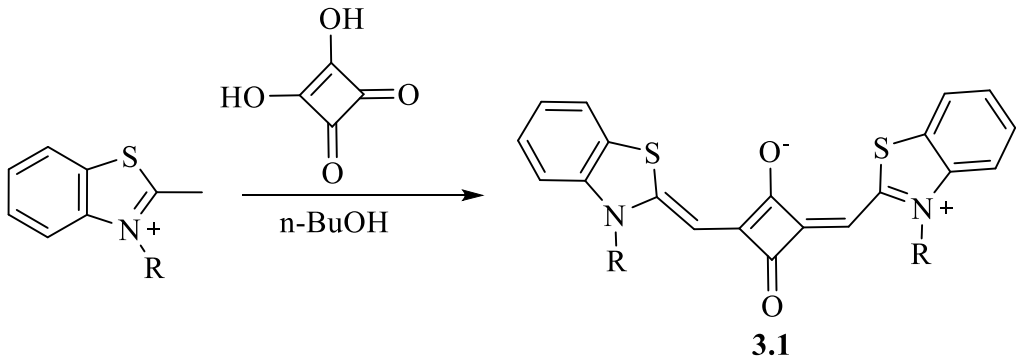

Scheme 3.1: General synthetic pathway for symmetrical squaraine dyes.

Limitations associated with squaraine dyes incudes toxicity, solubility, aggregation leading to fluorescence quenching. Due to electron deficient nature of the central core, these dyes are susceptible to nucleophilic substitution reactions which limits its potential for *in vivo* application. Many efforts have been put to protect the dye from nucleophilic attack which includes encapsulation of dye with micelles[9] or liposomes[10] or rotaxenes.[11] Introducing charged sulfonate groups has shown enhanced water solubility and biocompatibility.[12] Squaraine dyes have shown potential application as photosensitizer for PDT, as a promising candidate for bioimaging and photothermal therapy.[13]

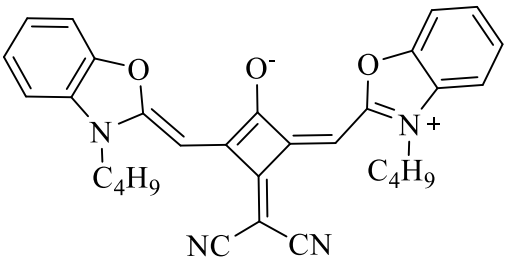

3.2
$\lambda_{abs/emi}$=626 nm/646 nm
φ_f=0.91

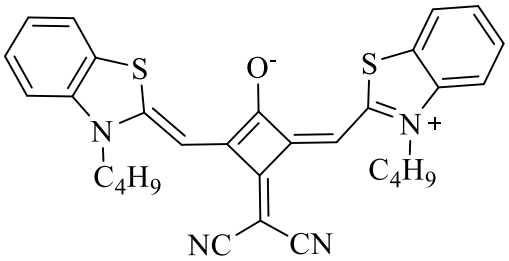

3.3
$\lambda_{abs/emi}$=701 nm/720 nm
φ_f=0.79

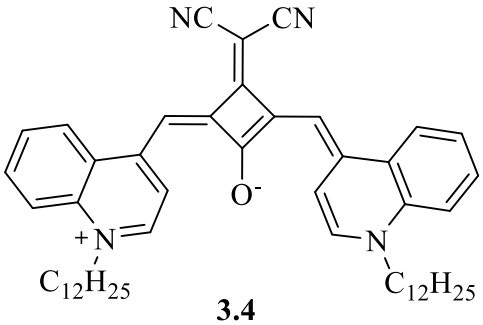

3.4
$\lambda_{abs/emi}$=870 nm/890 nm
φ_f=0.1

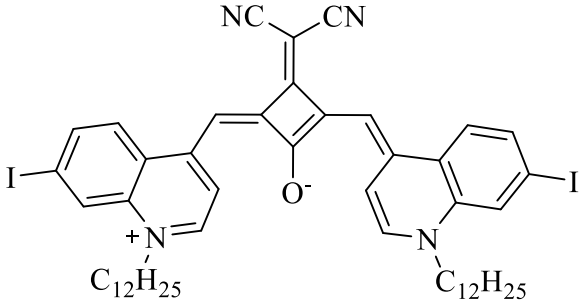

3.5
$\lambda_{abs/emi}$=900 nm/920 nm
φ_f=0.17

Figure 3.1: Examples of some squaraine dyes which absorbs or emits in NIR region.

3.1.2. Cyanine dyes

Cyanine dyes are well known dyes from centuries due to their photosensitivity and have shown potential applications in fluorescence imaging. Cyanine dyes are represented by two nitrogen centres separated by conjugated carbon chains as shown in **Figure 3.2**. Nitrogen centres may be heterocyclic or non-cyclic group. Due to extensive π-conjugation these dyes absorb and emits in the broad range of UV-Vis-NIR spectrum. Addition of each vinyl group creates a ~100 nm red shift in absorption spectrum.[14] Cyanine dyes are named according to the number of methine bridges between two nitrogen centres. For example, if one methine group is present it is called monomethine cyanine. Accordingly, with 2, 3 or 5 are called as di-, tri- or pentamethine cyanine dyes. Charles Hanson Greville Williams first synthesized cyanine dye namely 'quinoline blue' in 1856, which is a monomethine cyanine dye.[15] Cyanine dyes have served as potential photosensitizers for photography. Majority of monomethine cyanine dyes are used as fluorescent labels for macromolecules or DNA because

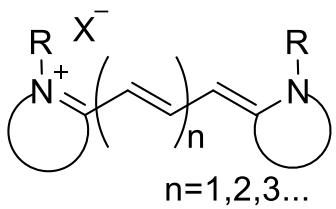

Figure 3.2: Representation of skeletal structure of cyanine dye.

of their enhanced emissive nature after attachment with the target biomolecules.[16] Though cyanine dyes have shown wide range of photophysical properties, aggregation, low quantum yield due to flexible nature and low photostability limits its use for many of the recent application.[17] Heptamethine dye, indocyanine green (ICG) is the only dye (absorption and emission above 700 nm) approved for use in human.[18] Polyanionic IRdye 800CW (CW800), Alexa Fluor-647 are commercially available dyes, which has been used for development of many fluorescent molecular probes that are under clinical trial.

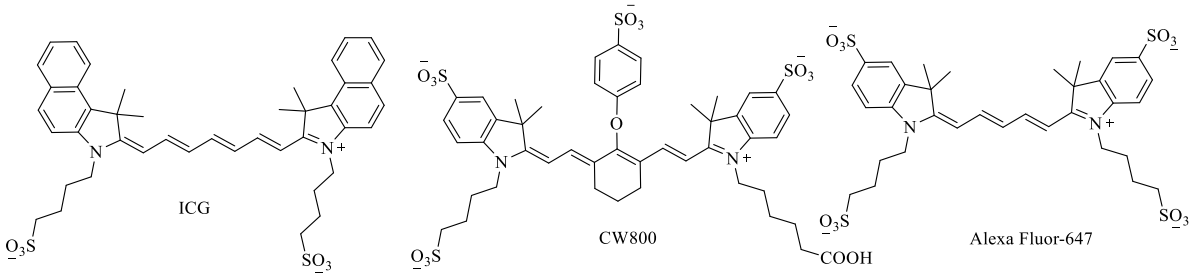

Figure 3.3: Examples of some commercially available cyanine dye.

3.1.3. Boron dipyrromethene dyes (BODIPY)

4,4-Difluoro-4-bora-3a,4a-diaza-*s*-indacene commonly called as BODIPY are small organic molecule having intense and sharp UV-Vis absorption along with sharp emission. These dyes were first reported by Treibs and Kreuzer in 1968.[19] Periphery of the BODIPY can be structurally modified to tune its electronic properties. These dyes are unique class of fluorophores in terms of their properties like high extinction coefficient, high quantum yield, excellent photostability, low sensitivity towards polarity or pH of the medium. They have been used in a number of applications like laser dyes, photovoltaic devices, protein labelling, bio imaging, chemical sensors.[20]

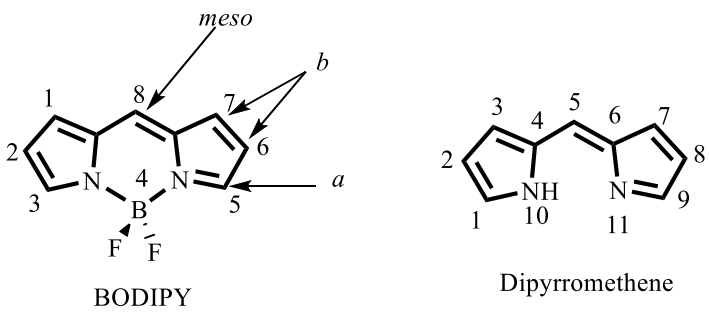

Figure 3.4: IUPAC numbering of BODIPY and dipyrromethene.

IUPAC numbering of BODIPY is not same as that for the dipyrromethene and it is shown in the **Figure 3.4.** General synthetic method includes acid mediated condensation of pyrrole and aldehyde to give dipyrromethane, which on oxidation and subsequent treatment with $BF_3.OEt_2$ yields BODIPY.

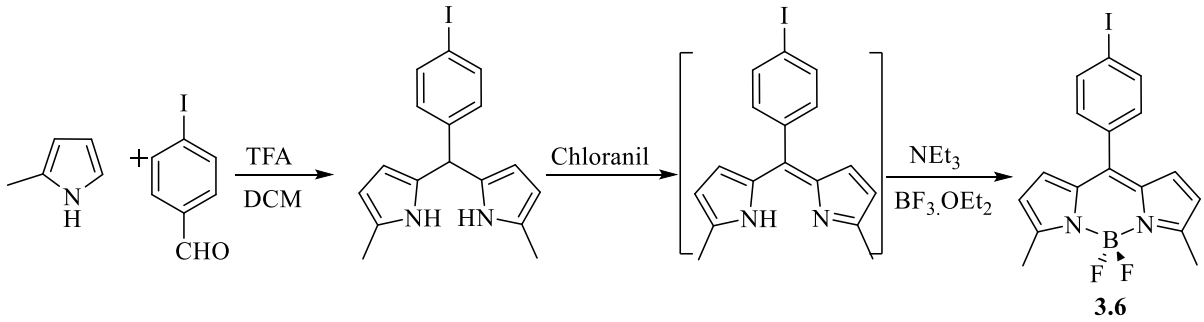

Scheme 3.2: Synthesis of BODIPY by acid mediated condensation of pyrrole and aldehyde.[21]

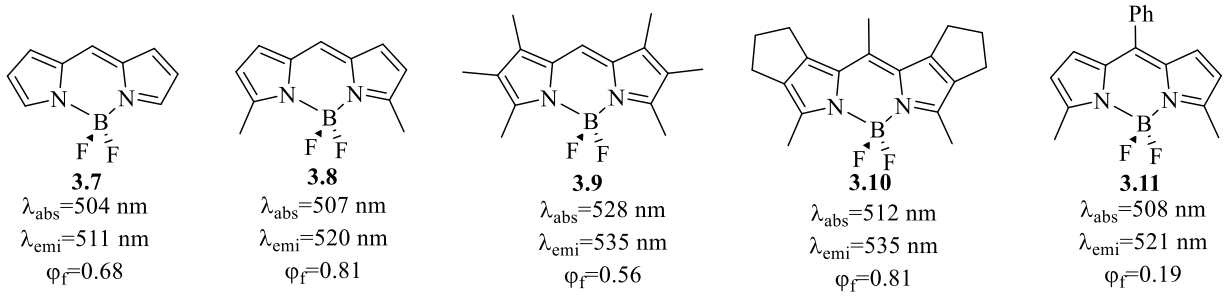

Figure 3.5: Unsubstituted BODIPY and some of its alkyl substituted derivatives.[22]

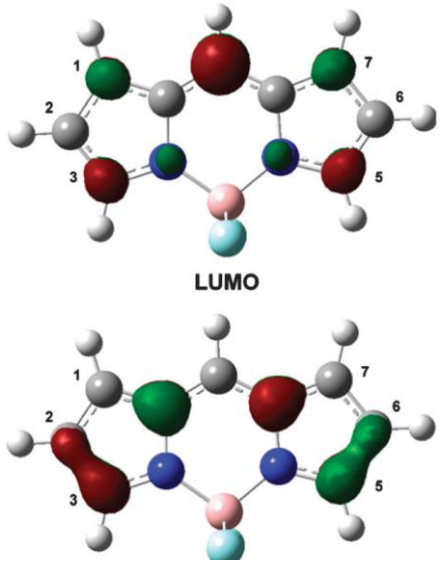

Figure 3.6: Nodal patterns of the HOMO and LUMO of an unsubstituted BODIPY model compound at an isosurface of 0.07 a.u.[23]

Fine-tuning of electronic properties can be done by different structural modifications like alkyl substitution on the periphery (*α*, *β* or *meso*) shifts the absorption and emission slightly towards longer wavelength. *Meso*-phenyl substitution has no significant effect on the absorption and emission spectra owing to its perpendicular orientation with respect to the BODIPY plane resulting in weak conjugation. As can be seen from the **figure 3.6**, HOMO coefficient on 3,5-positions on the unsubstituted BODIPY is more, thus substituent effect on 3,5-positions have proved to be efficient strategy to tune optical properties.[23] So extension of conjugation on these positions causes positive mesomeric effect, which can destabilize HOMO and reduces HOMO-

LUMO gap.[24] However, most of these BODIPY dyes absorb and emit below 600 nm. They exhibit low stokes shift. Other approaches for shifting the main absorption band towards NIR region includes: i) introduction of push-pull effect by different *α, β* substitutions; ii) replacing *meso* carbon by N to get aza-BODIPY; iii) Fusion at periphery to get extended conjugation.

3.1.3.1. Push-pull effect

Substitution of EDG on 3,5- positions and EWG at 8- position is expected to be an efficient strategy to affect both HOMO and LUMO of the BODIPY and reduce HOMO-LUMO gap. This will create a push-pull effect on the fluorophore and can change spectroscopic properties. We can see the impact of push-pull substituents by comparing **3.12** and **3.13**.[25] Presence of EDG on 3,5-phenyl and EWG on 8-phenyl creates addition D-π spacer-A system and brings a bathochromic shift of 25 and 27 nm in absorption and emission spectra, respectively. Same trend is observed for **3.14** and **3.15**.

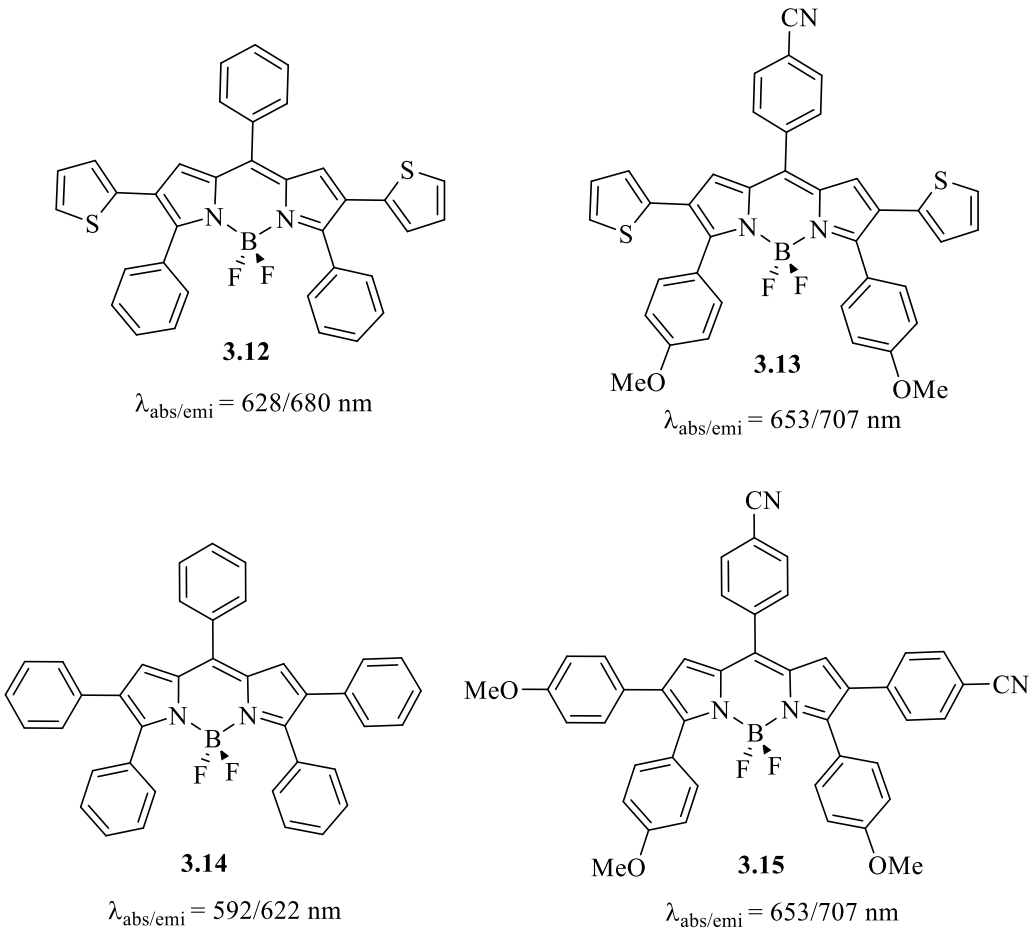

Figure 3.7: Examples showing difference in optical properties due to push-pull effect.[25]

3.1.3.2. Aza-BODIPY

First aza-BODIPY was synthesised by O'Shea in 2002 as a tetraaryl substituted analogue which showed a bathochromic shift in absorption and emission relative to BODIPY analogue.[26] However replacing nitrogen in *meso* position causes a significant reduction in fluorescence quantum yield as well as decrease in its photostability.[27]

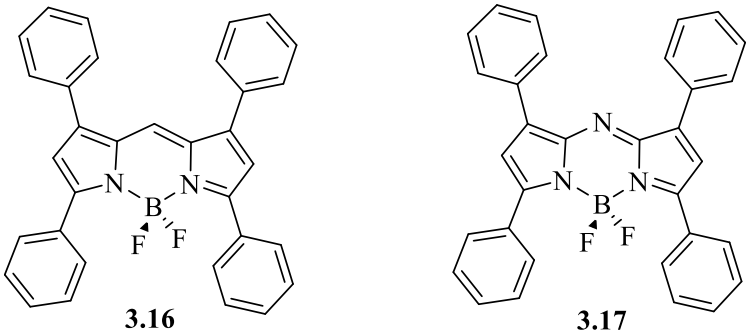

3.16 $\lambda_{abs/emi}$ = 570/603 nm

3.17 $\lambda_{abs/emi}$ = 650/672 nm

Figure 3.8: Examples showing difference between BODIPYs having *meso*- C/N.

UV-Vis absorption maxima of tetraaryl aza-BODIPY largely depend on aryl substituents. Presence of EDG at 5- position of aryl group results in a large bathochromic shift. Presence of OMe and NMe_2 on 5-phenyl group as in **3.18** and **3.19** causes a 38 and 149 nm bathochromic

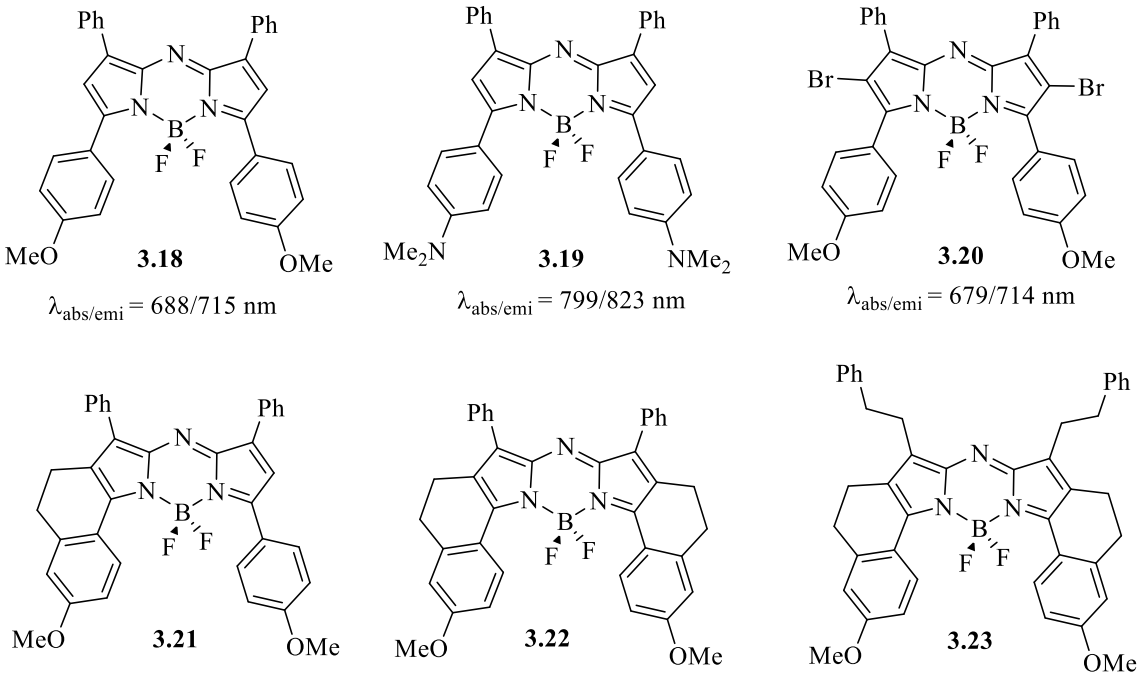

3.18 $\lambda_{abs/emi}$ = 688/715 nm

3.19 $\lambda_{abs/emi}$ = 799/823 nm

3.20 $\lambda_{abs/emi}$ = 679/714 nm

3.21 $\lambda_{abs/emi}$ = 708/732 nm

3.22 $\lambda_{abs/emi}$ = 740/752 nm

3.23 $\lambda_{abs/emi}$ = 721/732 nm

Figure 3.9: Examples of aza-BODIPY.[23]

shift in absorption spectra, respectively.[28] However, introduction of heavy atoms like Br group (**3.20**) directly to the core diminishes the fluorescence quantum yield and increases ISC due to internal heavy atom effect. This increases triplet state lifetime and it can act as singlet oxygen producer. Rigidifying the methoxy phenyl group on 3,5- positions induces a dramatic effect by giving 52 and 37 nm bathochromic shift in the absorption and emission spectra. Also, absorption coefficient increases drastically.[29]

3.1.3.3. Annulation of periphery

Fusing aromatic rings to periphery of the BODIPY has been a promising research topic to get NIR active BODIPY dyes. There are three possible ways for annulation of the BODIPY i.e., fusion at *a*, *b* or *zigzag* positions. However due to low reactivity of 1 and 7- position very less no of reports have been there in literature. From the **figure 3.10**, where HOMO-LUMO gap has been shown for fusion at [*a*] and [*b*] bonds, it is clear that reduction of HOMO-LUMO gap more in case of [*b*]-fusion.[30]

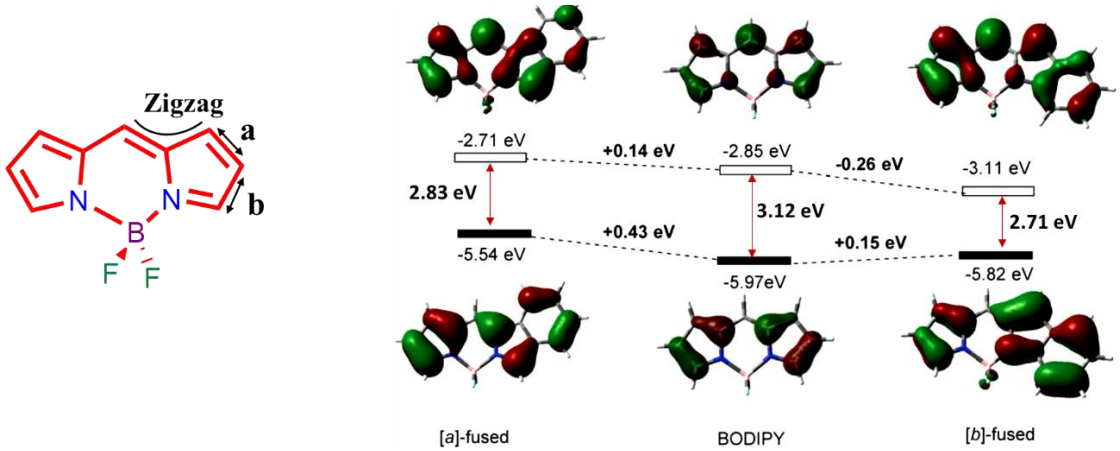

Figure 3.10: Frontier orbital diagram of unsubstituted BODIPY and changes after [*a*], [*b*]-fusion.

Though theoretical calculation shows fusion at [*a*] bond is less efficient strategy for reducing HOMO-LUMO gap, still there are some reports about exploring annulation of aromatic rings like benzene, naphthalene or phenananthrene groups to pyrrole in BODIPY.[31] Synthesis of fused BODIPYs require multiple steps for synthesis. Many of the [*a*] fused BODIPYs exhibit good absorption coefficient and red shifted absorption spectra relative to non-fused systems due to extended π-conjugation. They exhibit good fluorescence quantum yields.

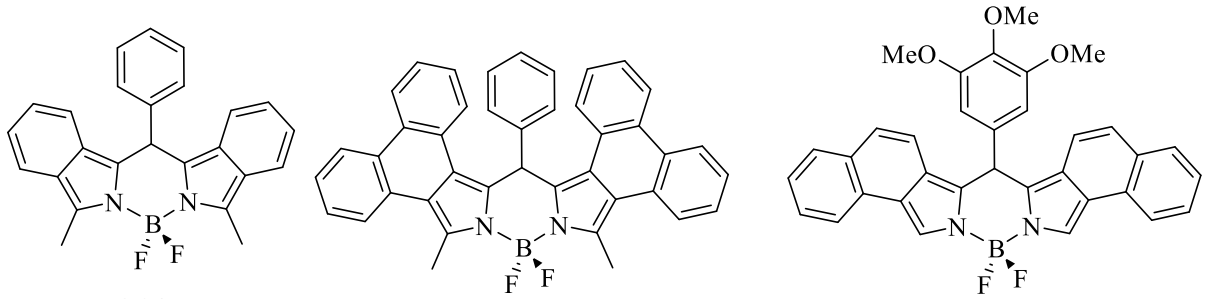

3.24 $\lambda_{abs/emi}$ = 596/604 nm

3.25 $\lambda_{abs/emi}$ = 630/648 nm

3.26 $\lambda_{abs/emi}$ = 596/604 nm

Figure 3.11: Examples of [a]-fused BODIPYs.

Free rotation of aryl substituents can be restricted by fusing the substituent to the BODIPY core with sp^3 or sp^2 hybridised carbon. If it is done by sp^3 hybridised carbons, then the aryl rings will obtain co-planarity with the BODIPY plane and delocalisation of π-electron will be more facile. This reduces HOMO-LUMO gap and thus bathochromic shift in absorption and emission spectra is observed. Due to restricted movement, fluorescence quantum yield also increases.[32] If the [*b*] bonds are fused with heterocycles like furan, thiophene or benzofuran etc. then optical properties differ dramatically. **3.28** is having more red shifted absorption and emission relative to **3.27** due to extended conjugation. But reduction of quantum yield in case of **3.28** can be attributed to presence of heavy atom iodine on the *meso* phenyl group.[32.33] A

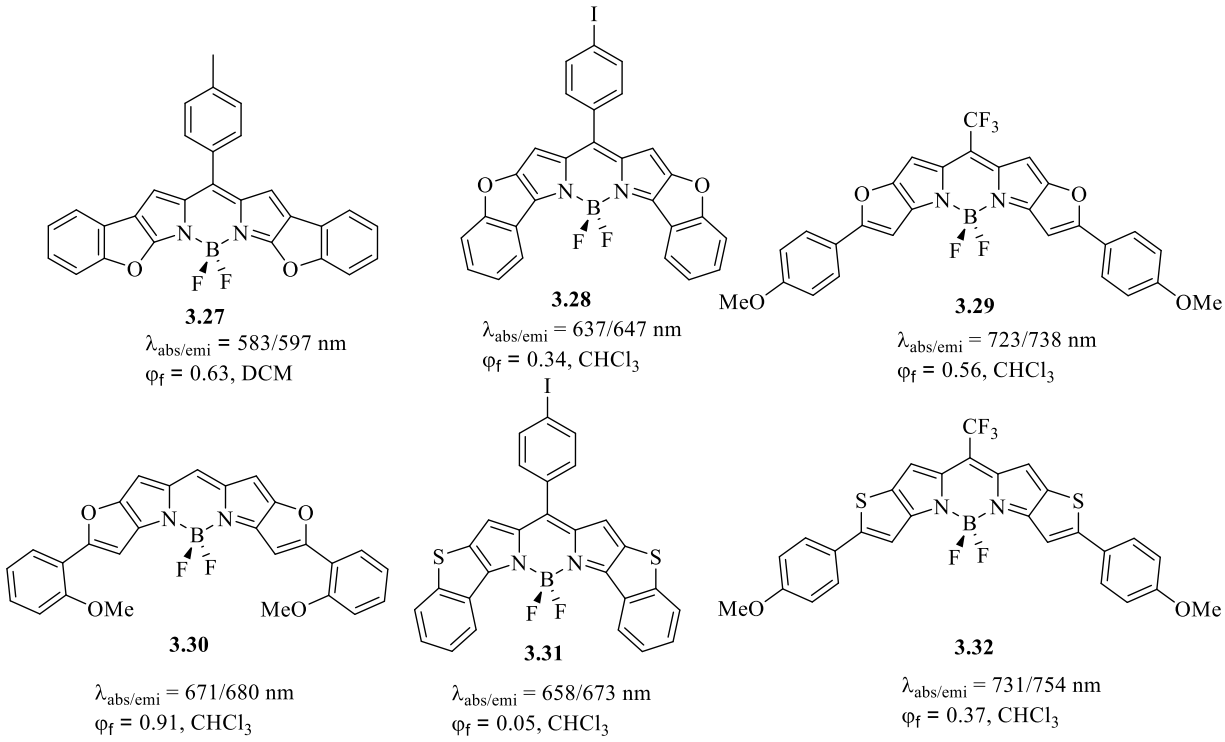

3.27 $\lambda_{abs/emi}$ = 583/597 nm, φ_f = 0.63, DCM

3.28 $\lambda_{abs/emi}$ = 637/647 nm, φ_f = 0.34, $CHCl_3$

3.29 $\lambda_{abs/emi}$ = 723/738 nm, φ_f = 0.56, $CHCl_3$

3.30 $\lambda_{abs/emi}$ = 671/680 nm, φ_f = 0.91, $CHCl_3$

3.31 $\lambda_{abs/emi}$ = 658/673 nm, φ_f = 0.05, $CHCl_3$

3.32 $\lambda_{abs/emi}$ = 731/754 nm, φ_f = 0.37, $CHCl_3$

Figure 3.12: Examples of [*b*] fused BODIPY showing NIR absorption and emission.

series of BODIPYs fused with furan named Keio Fluors, **3.29** and **3.30** were reported with enhanced photophysical properties. They exhibit high molar absorption coefficient and high quantum yield.[34] Quantum yield of **3.30** is more relative to **3.29** due to restricted movement of 2-methoxy groups in phenyl substituent due to steric repulsion.

3.1.3.4. Application of BODIPY

Before discussing imaging-based applications of BODIPY, it is important to discuss briefly different charge transfer mechanisms like photo-induced electron transfer (PET), intramolecular charge transfer (ICT), and Förster resonance energy transfer (FRET) mechanism, or the coupled mechanisms on which BODIPY can be designed.[35] PET mechanism works where the fluorophore is designed as **fluorophore-spacer-Donor/receptor**, where spacer disconnects any electronic communications and takes place through space. Fluorophore acts as a donor in case of oxidative PET and acceptor in reductive PET. But, in ICT fluorophore possesses an EDG and conjugated to EWG or vice versa. In this type of system electronic communication takes place through π-conjugation. This will create a change in dipole moment on photoexcitation. On the other hand, FRET exhibits interaction between two fluorophores joined together in the same molecule. BODIPY undergoes these types of mechanisms for fluorescence on-off procedure in presence of the different analytes and can be used as a sensor or for imaging.

As pH is one of the important factors to consider while checking cellular event to locate abnormal cell growth or division in inflammation or cancer, examining this with different fluorescent probes is a major concern. There are many reports for BODIPY based fluorescent probes. BODIPY based fluorescent probes have N-alkylated donor attached to it, mostly on *meso* carbon.[35] This acts as a strong EDG which quenches emission by the mechanism of photo electron transfer (PET) or photo-induced charge transfer (ICT). Protonation inhibits PET or ICT and recovers emission. This is called as fluorescence *turn-on* sensing. For example, **3.33** is very weakly emissive in polar solvent like acetonitrile. But after protonation 2000-fold enhancement of fluorescence is observed accompanied with a spectral change.[36] Emission of **3.34** is quenched in polar protic solvent like ethanol/water mixture but upon protonation, emission is recovered with enhancement factor of 150 in 650 nm region.[31b]

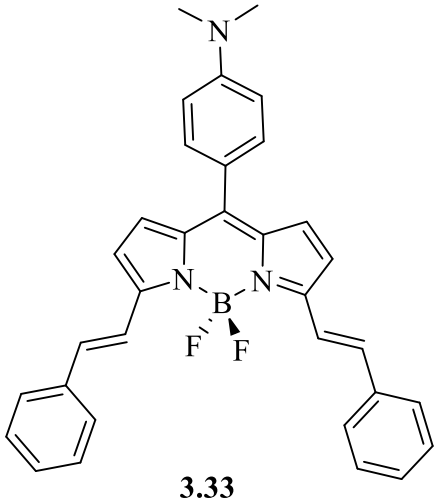

3.33

$\lambda_{abs/emi}$ = 620/636 nm
φ_f = 0.0004, CH_3CN

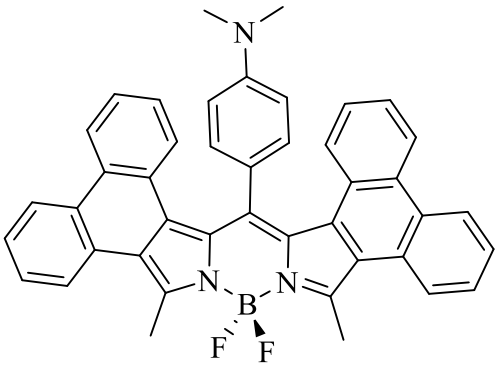

3.34

$\lambda_{abs/emi}$ = 621/636 nm
φ_f = 0.96, dibutyl ether

Figure 3.13: Examples of BODIPY as potential fluorescence probe for pH.

Bio-imaging of metal ions has been a challenging topic due to poor solubility of fluorophores in aqueous medium. Few of the BODIPYs have shown good potential for metal ion sensing in cell lines. Peng *et al.* reported **3.35** as a sensor for Cd^{2+} in living cells.[37] N,N-Bis(pyridin-2-ylmethyl)-benzenamine was attached to BODIPY moiety as Cd^{2+} receptor, which behaves as ICT donor. **3.35.3HCl** exhibits emission spectrum with max at 656 nm in acetone-water mixture with a quantum yield of 0.12. But in presence of Cd^{2+} emission maxima show a hypsochromic shift and appears at 597 nm with quantum yield of 0.59. Along with it,

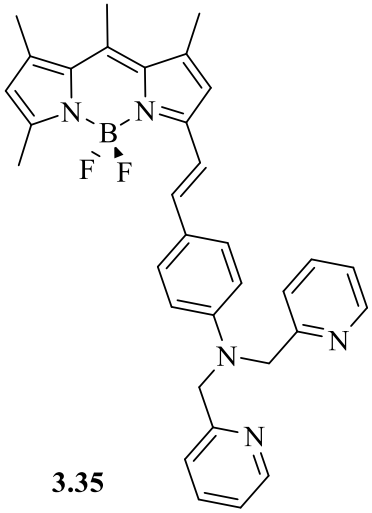

3.35

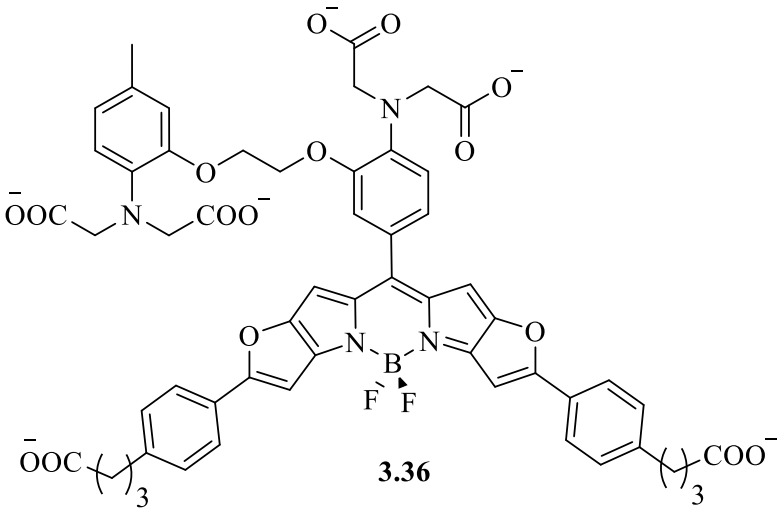

3.36

Figure 3.14: Examples of BODIPY showing potential application in bio-imaging for metal ions.

another emission peak appears at 673 nm (**Figure 3.15**). Suzuki and co-workers reported Keio fluors based fluorescent probe, **3.37** for Ca^{2+} ions. BAPTA (O,O-bis(2-aminophenyl) ethyleneglycol-N,N,N,N′ -tetra acetic acid) is attached to *meso* carbon of Keio Fluor BODIPY as Ca^{2+} receptor. Though absorption spectrum of the fluorophore is not affected by presence of Ca^{2+}, emission is recovered by 120 fold after addition of Ca^{2+} due to inhibition of PET.[38]

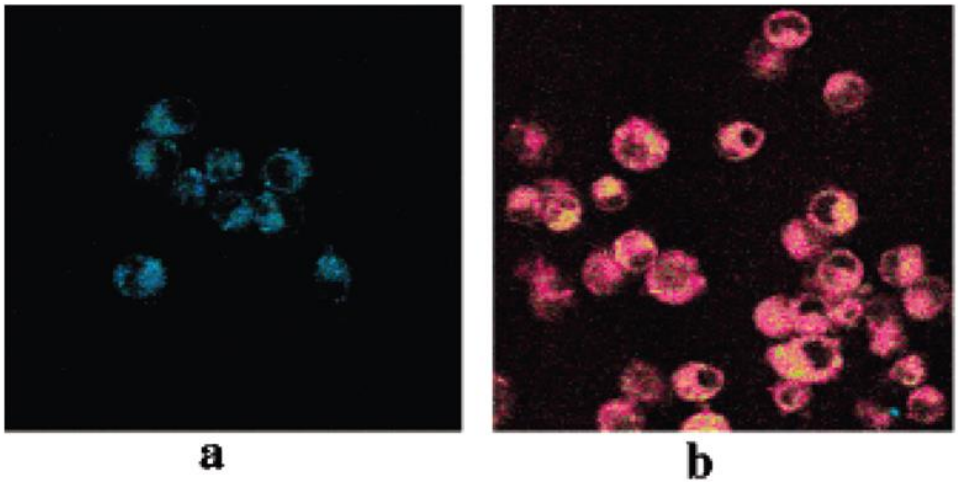

Figure 3.15: (a) DC cells (Leica TCS-SP2 confocal fluorescence microscope, 20× objective lens) incubated with **3.35** (5 μM); (b) DC cells incubated with **3.35** and then further incubated with 5 μM $CdCl_2$.[37]

BODIPY based fluorescent probes for small biological molecules like cysteine and homocysteine has been reported by Ravikanth and co-workers.[39] The free probe exhibits an absorption band at 596 nm in buffer. Upon addition of cysteine or homocysteine it shows a hypsochromic shift and new band appears at 552 nm. In addition, emission spectrum also exhibits blue shift from 612 nm to 567 nm.

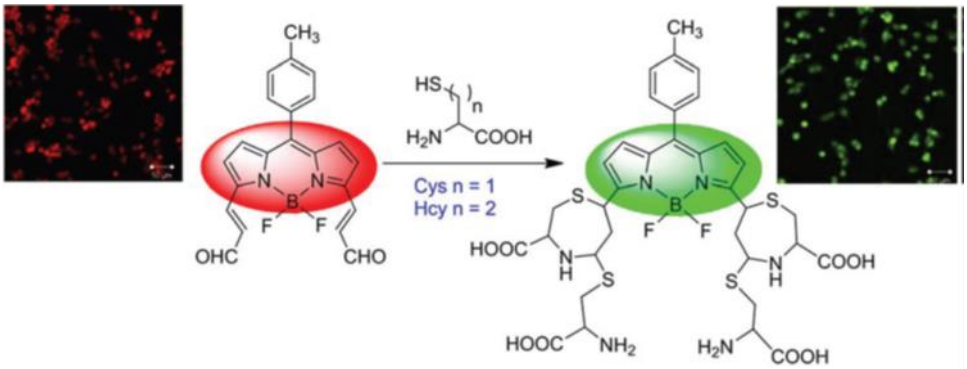

Figure 3.16: Reaction based detection of cysteine and homocysteine along with bio-imaging.[39]

3.2. Scope of the Present Work

From the above discussions, it is understandable that still there is a huge demand for NIR active fluorophore, which may have lower energy absorption and emission in the NIR region with good fluorescence quantum yield. Lots of developments need to be explored in this research area. About this, we have designed and synthesized new NIR BODIPY dyes which are explored for their unique photophysical properties. These details will be discussed in the coming chapters.

3.3. References

1. Qian, G.; Wang, Z. Y. Near-Infrared Organic Compounds and Emerging Applications. *Chem. Asian J.,* **2010**, *5*, 1006.
2. Hong, G.; Antaris, A. L.; Dai, H. Near-infrared fluorophores for biomedical imaging. *Nat. Biomed. Eng.,* **2017**, *1*, 10.
3. Frangioni, J. In vivo near-infrared fluorescence imaging. *Curr. Opin. Chem. Biol.* **2003**, *7*, 626.
4. Swamy, P. C. A.; Sivaraman, G.; Priyanka, R. N.; Raja, S. O.; Ponnuvel, K.; Shanmugpriya, J.; Gulyani, A. Near Infrared (NIR) absorbing dyes as promising photosensitizer for photo dynamic therapy. *Coord. Chem. Rev.* **2020**, *411*, 213233.
5. Treibs, A. Jacob, K. Cyclotrimethine dyes derived from squaric acid. *Angew. Chem. Int. Ed.,* **1965**, *4*, 694.
6. [a] Oswald, B.; Lehmann, F.; Simon, L.; Terpetschnig, E.; Wolfbeis, O.S. Red laser-induced fluorescence energy transfer in an immunosystem. *Anal. Biochem.,* **2000,** *280*, 272. [b] Wang, B.; Fan, J.; Sun, S.; Wang, L.; Song, B.; Peng, X. 1-(Carbamoylmethyl)-3H-indolium squaraine dyes: synthesis, spectra, photo-stability and association with BSA. *Dyes Pigm.,* **2010**, *85*, 43. [c] Terpetschnig, E.; Szmacinski, H.; Lakowicz, J.R. Synthesis, spectral properties and photostabilities of symmetrical and unsymmetrical squarines; a new class of flourophores with long-wavelength excitation and emission. *Anal. Chim. Acta,* **1993,** *282*, 633.
7. Ghosh, A. Donor–acceptor type low band gap polymers: polysquaraines and related systems. *Chem. Soc. Rev.,* **2003**, *32*, 181.
8. Ilina, K.; MacCuaig, W.; Laramie, M.; Jeouty, J. N.; McNally, L. R. Henary, M. Squaraine dyes: Molecular design for different applications and remaining challenges. *Bioconjugate Chem.,* **2020**, *31*, 194.
9. Sreejith, S.; Joseph, J.; Lin, M.; Menon, N. V.; Borah, P.; Ng, H. J.; Loong, Y. X.; Kang, Y.; Yu, S. W.-K.; Zhao, Y. Near-infrared squaraine dye encapsulated micelles for in vivo fluorescence and photoacoustic bimodal imaging. *ACS Nano,* **2015**, *9*, 5695.
10. Dong, S.; Teo, J. D. W.; Chan, L. Y.; Lee, C.-L. K.; Sou, K. Far-Red Fluorescent Liposomes for Folate Receptor-targeted Bioimaging. *ACS Appl. Nano Mater.,* **2018**, *1*, 1009.
11. [a] Collins, C. G.; Baumes, J. M.; Smith, B. D. Thermally-activated chemiluminescent squaraine rotaxane endoperoxide with green emission. *Chem. Commun.,* **2011**, *47*, 12352.

[b] Jarvis, T. S.; Collins, C. G.; Dempsey, J. M.; Oliver, A. G.; Smith, B. D. Synthesis and Structure of 3, 3-Dimethylindoline Squaraine Rotaxanes. *J. Org. Chem.*, **2017**, *82*, 5819.

12. Umezawa, K.; Citterio, D.; Suzuki, K. Water-soluble NIR fluorescent probes based on squaraine and their application for protein labeling. *Anal. Sci.*, **2008**, *24*, 213.
13. [a] Ramaiah, D.; Eckert, I.; Arun, K. T.; Weidenfeller, L.; Epe, B. Squaraine dyes for photodynamic therapy: mechanism of cytotoxicity and DNA damage induced by halogenated squaraine dyes plus light (>600 nm). *Photochem. Photobiol*., **2004**, *79*, 99. [b] Lima, E.; Ferreira, O.; Gomes, V. S. D.; Santos, A. O.; Boto, R. E.; Fernandes, J. R.; Almeida, P.; Silvestre, S. M.; Reis, L. V. Synthesis and *in vitro* evaluation of the antitumoral phototherapeutic potential of squaraine cyanine dyes derived from indolenine. *Dyes Pigm*., **2019**, *167*, 98. [c] Sun, P.; Wu, Q.; Sun, X.; Miao, H.; Deng, W.; Zhang, W.; Fan, Q.; Huang, W. J-Aggregate squaraine nanoparticles with bright NIR-II fluorescence for imaging guided photothermal therapy. *Chem. Comm*., **2018,** *54*, 13395.
14. Ilina, K. Henary, M. Cyanine Dyes Containing Quinoline Moieties: History, Synthesis, Optical Properties, and Applications. *Chem. Eur. J.*, **2021**, *27*, 4230.
15. F. M. Hamer, The Chemistry of Heterocyclic Compounds, Wiley, Hoboken, **2009**, Vol 18.
16. Zhytniakivska, O.; Girych, M.; Trusova, V.; Gorbenko, G.; Vasilev, A.; Kandinska, M.; Kurutos, A. Baluschev, S. B. Spectroscopic and molecular docking studies of the interactions of monomeric unsymmetrical polycationic fluorochromes with DNA and RNA. *Dyes Pigm.*, **2020**, *180*, 108446.
17. Gopika, G. S.; Prasad, P. M. H.; Lekshmi, A. G.; Lekshmypriya, S.; Sreesaila, S.; Arunima, C.; Kumar, M. S.; Anil, A.; Sreekumar, A.; Pillai. Z. S. Chemistry of cyanine dyes-A review. *Materials Today: Proceedings*, **2021**, *46*, 3102.
18. Gorka, A. P.; Nani, R. R.; Schnermann, M. J. Cyanine polyene reactivity: scope and biomedical applications. *Org. Biomol. Chem.*, **2015**, *13*, 7584.
19. Treibs, A.; Kreuzer, F. H. Difluorboryl-komplexe von di-und tripyrrylmethenen. *Justus Liebigs Ann. Chem.* **1968**, *718*, 208.
20. [a] Boens, N.; Leen V.; Dehaen, W. Fluorescent indicators based on BODIPY. *Chem. Soc. Rev.*, **2012**, *41*, 1130. [b] Bessette A.; Hanan, G. S. Design, synthesis and photophysical studies of dipyrromethene-based materials: insights into their applications in organic photovoltaic devices. *Chem. Soc. Rev.*, **2014**, *43*, 3342. [c] Kowada, T.; Maeda, H.; Kikuchi, K. BODIPY-based probes for the fluorescence imaging of biomolecules in living cells. *Chem. Soc. Rev.*, **2015**, *44*, 4953.

21. Wagner, R. W.; Lindsey, J. S. Boron-dipyrromethene dyes for incorporation in synthetic multi-pigment light-harvesting arrays. *Pure Appl. Chem.*, **1996**, *68*, 1373.
22. Loudet, A.; Burgess, K. BODIPY Dyes and Their Derivatives: Syntheses and Spectroscopic Properties. *Chem. Rev.*, **2007,** *107*, 4891.
23. Lu, H.; Mack, J.; Yanga, Y.; Shen, Z. Structural modification strategies for the rational design of red/NIR region BODIPYs. *Chem. Soc. Rev.*, **2014**, *43*, 4778.
24. [a] Qin, W.; Rohand, T.; Dehaen, W.; Clifford, J. N.; Driessen, K.; Beljonne, D.; Averbeke, B. V.; Auweraer M. V.; Boens, N. Boron dipyrromethene analogs with phenyl, styryl, and ethynylphenyl substituents: synthesis, photophysics, electrochemistry, and quantum-chemical calculations. *J. Phys. Chem. A*, **2007**, *111*, 8588. [b] Rohand, T.; Lycoops, J.; Smout, S.; Braeken, E.; Sliwa, M.; Auweraer, M. V.; Dehaen, W.; Borggraeve, W. M. D.; Boens, N. Photophysics of 3,5-diphenoxy substituted BODIPY dyes in solution. *Photochem. Photobiol. Sci.*, **2007**, *6*, 1061.
25. Xuan, S.; Zhao, N.; Ke, X.; Zhou, Z.; Fronczek, F. R.; Kadish, K. M.; Smith K. M.; Vicente, M. G. H. Synthesis and Spectroscopic Investigation of a Series of Push-Pull Boron Dipyrromethenes (BODIPYs). *J. Org. Chem.*, **2017**, *82*, 2545.
26. Killoran, J.; Allen, L.; Gallagher, J. F.; Gallagher, W. M.; O′Shea D. F. Synthesis of BF_2 chelates of tetraarylazadipyrromethenes and evidence for their photodynamic therapeutic behaviour. *Chem. Commun.*, **2002**, 1862.
27. Kritskaya, A. Y.; Berezin, M. B.; Antina, E. V.; Vyugin A. I. Effect of Aryl-, Halogen-, and Ms-Aza-Substitution on the Luminescent Properties and Photostability of Difluoroborates of 2,2′-Dipyrrometenes. *J. Fluoresc.*, **2019**, *29*, 911.
28. [a] Gorman, A.; Killoran, J.; O'Shea, C.; Kenna, T.; Gallagher, W. M.; O'Shea, D. F. In Vitro Demonstration of the Heavy-Atom Effect for Photodynamic Therapy. *J. Am. Chem. Soc.* **2004**, *126*, 10619. [b] McDonnell, S. O.; O'Shea, D. F. Near-Infrared Sensing Properties of Dimethlyamino-Substituted BF_2−Azadipyrromethenes. *Org. Lett.* **2006**, *8*, 3493.
29. [a] Zhao, W.; Carreira, E. M. Conformationally restricted aza-bodipy: a highly fluorescent, stable, near-infrared-absorbing dye. *Angew. Chem., Int. Ed.* **2005**, *44*, 1677. [b] Zhao, W.; Carreira, E. M. Conformationally Restricted Aza-BODIPY: Highly Fluorescent, Stable Near-Infrared Absorbing Dyes. *Chem. Eur. J.*, **2006**, *12*, 7254.
30. Wang, J.; Boens, N.; Jiao, L.; Hao, E. Aromatic [b]-fused BODIPY dyes as promising near-infrared dyes. *Org. Biomol. Chem.*, **2020**, *18*, 4135.

31. [a] Shen, Z.; Röhr, H.; Rurack, K.; Uno, H.; Spieles, M.; Schulz, B.; Reck, G.; Ono, N. Boron–Diindomethene (BDI) dyes and their tetrahydrobicyclo precursors—en route to a new class of highly emissive fluorophores for the red spectral range. *Chem. – Eur. J.*, **2004**, *10*, 4853. [b] Descalzo, A. B.; Xu, H.; Xue, Z.; Hoffmann, K.; Shen, Z.; Weller, M. G.; You X.; Rurack, K. Phenanthrene-Fused Boron−Dipyrromethenes as Bright Long-Wavelength Fluorophores. *Org. Lett.*, **2008**, *10*, 1581. [c] Swavey, S.; Quinn, J.; Coladipietro, M.; Cox, K. G.; Brennaman. M. K. Tuning the photophysical properties of BODIPY dyes through extended aromatic pyrroles. *RSC Adv.*, **2017**, *7*, 173.
32. Chen, J.; Burghart, A.; Derecskei-Kovacs, A.; Burgess, K. 4,4-Difluoro-4-bora-3a,4a-diaza-s-indacene (BODIPY) Dyes Modified for Extended Conjugation and Restricted Bond Rotations. *J. Org. Chem.*, **2000**, *65*, 2900.
33. Leen, V.; Qin, W.; Yang, W.; Cui, J.; Xu, C.; Tang, X.; Liu, W.; Robeyns, K.; Meervelt, L. V.; Beljonne, D.; Lazzaroni, R.; Tonnelé, C.; Boens N.; Dehaen, W. Synthesis, Spectroscopy, Crystal Structure Determination, and Quantum Chemical Calculations of BODIPY Dyes with Increasing Conformational Restriction and Concomitant Red-Shifted Visible Absorption and Fluorescence Spectra. *Chem. – Asian J.*, **2010**, *5*, 2016.
34. [a] Umezawa, K.; Nakamura, Y.; Makino, H.; Citterio D.; Suzuki, K.; *J. Am. Chem. Soc.*, **2008**, *130*, 1550. [b] Umezawa, K.; Matsui, A.; Nakamura, Y.; Citterio D.; Suzuki, K. Bright, color-tunable fluorescent dyes in the Vis/NIR region: establishment of new "tailor-made" multicolor fluorophores based on borondipyrromethene. *Chem. – Eur. J.*, **2009**, *15*, 1096.
35. Nia, Y.; Wu, J.; Far-red and near infrared BODIPY dyes: synthesis and applications for fluorescent pH probes and bio-imaging. *Org. Biomol. Chem.*, **2014**, *12*, 3774.
36. Rurack, K.; Kollmannsberger M.; Daub, J. A highly efficient sensor molecule emitting in the near infrared (NIR): 3,5-distyryl-8-(*p*-dimethylaminophenyl)difluoroboradiaza-*s*-indacene. *New J. Chem.*, **2001**, *25*, 289.
37. Peng, X.; Du, J.; Fan, J.; Wang, J.; Wu, Y.; Zhao, J.; Sun, S.; Xu, T. A Selective Fluorescent Sensor for Imaging Cd^{2+} in Living Cells. *J. Am. Chem. Soc.*, **2007**, *129*, 1500.
38. Matsui, A.; Umezawa, K.; Shindo, Y.; Fujii, T.; Citterio, D.; Oka, K.; Suzuki, K. A near-infrared fluorescent calcium probe: a new tool for intracellular multicolour Ca^{2+} imaging. *Chem. Commun.*, **2011**, *47*, 10407.
39. Madhu, S.; Gonnade, R.; Ravikanth, M. Synthesis of 3,5-bis(acrylaldehyde) boron-dipyrromethene and application in detection of cysteine and homocysteine in living cells. *J. Org. Chem.*, **2013**, *78*, 5056.

Chapter 4

Functionalization of Napthobipyrrole Derived BODIPY

4.1. Introduction

The ever-growing success in developing new BODIPYs with enhanced optical properties has kept interest in this research area intact for years. BODIPY dye, a small organic molecule with interesting properties like intense absorption and emission with better fluorescence quantum yield, photostability has inspired many researchers to explore this for many applications like fluorescent sensors,[1] fluorescent labels for bioimaging,[2] photovoltaics,[3] organic light-emitting devices[4] etc. Over the past two decades, there is a surge in demand for NIR active fluorophores as these can be explored as potential candidates for bio imaging or photosensitizers in solar cells. As structural tuning of BODIPY dyes has been facile, they can be modified in several ways to tune the optical properties.

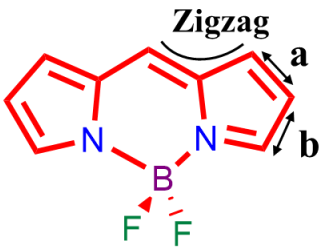

Among different strategies, fusing the periphery of BODIPY dyes has been more encouraging as it provides a large red shift to the absorption and emission wavelength. Fusion can be done with three different bonds like [*a*] bonds, [*b*] bonds or *zig zag* bonds. Among these three possibilities, [*b*] bond fusion has been more efficient in narrowing the HOMO-LUMO energy gap.[5] There have been many reports in the literature showing the synthesis of [b] fused BODIPY with aromatic compounds like benzene, naphthalene, phenanthrene, furan or thiophene. Though almost all types of annulations create bathochromic shift, few of them only could reach up to NIR region. As naphthalene and phenanthrene exhibits larger π-extension they result in more bathochromic shift.

4.1.1. [b]-Fused BODIPY

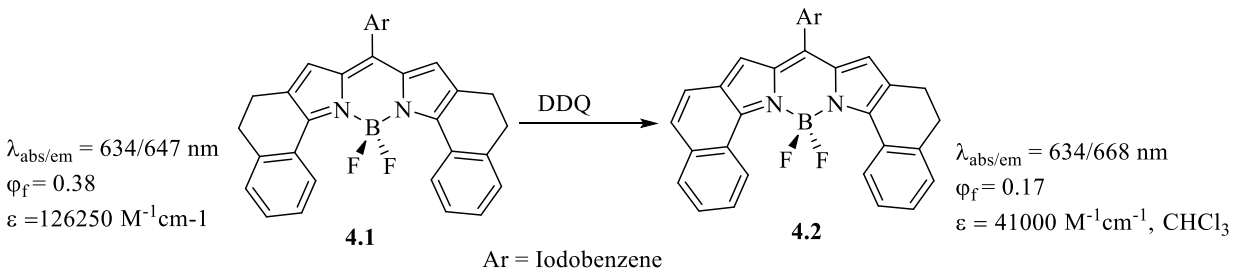

Scheme 4.1: Synthesis and optical properties of naphtho-fused BODIPY, **4.2**.

Burgess and co-workers reported synthesis of **4.1**, which on oxidation with DDQ could only produce partially oxidized **4.2** instead of a fully oxidized symmetrical naptho-fused BODIPY.[6] Though **4.2** is expected to produce bathochromic shift in the absorption maxima

owing to the extended π-conjugation, it appears at same wavelength as that of **4.1**, however it results in a large Stokes shift. Despite of increased conjugation, extinction coefficient and fluorescence quantum yield are drastically reduced in **4.2**. Wu and co-workers also synthesised naphtho-fused BODIPY **4.3**, which shows red shifted absorption and emission with a large Stokes shift of 120482 cm^{-1}.[7] Both the naphtho-fused BODIPYs (**4.2** and **4.3**) show less extinction coefficient and very less fluorescence quantum yield.

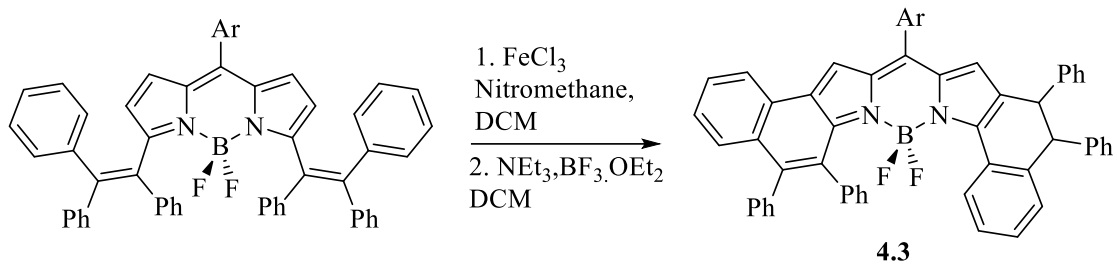

$\lambda_{abs/em}$ = 674/757 nm
ε = 57631$M^{-1}cm^{-1}$, THF

Scheme 4.2: Synthesis of naphtho-fused BODIPY **4.3**.

Naphtho[*b*]-fused BODIPY, **4.4** was synthesized by Shen and co-workers by one pot Suzuki–Miyaura–Knoevenagel conditions, shows absorption in red region with absorption maxima at 630 nm.[8] The compound is weakly emissive like above two naphtho-fused BODIPY but, it shows less Stokes shift with emission at 640 nm.

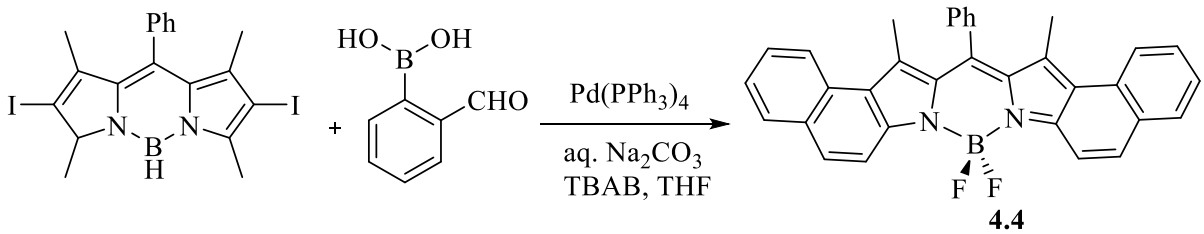

$\lambda_{abs/em}$ = 630/640 nm
φ_f = 0.06
ε = 175660 $M^{-1}cm^{-1}$, DCM

Scheme 4.3: Synthesis of naphtho-fused BODIPY, **4.4**.

Recently, a series of phenanthro-fused BODIPYs (**4.5**-**4.8**) have been synthesized by Hao and Jiao group, which shows NIR absorption and emission with very high molar extinction coefficient.[9] Substituting electron donating group causes a bathochromic shift and enhancement in absorption coefficient in the series. But due to increase in non-radiative decay, fluorescence quantum yield decreases dramatically.

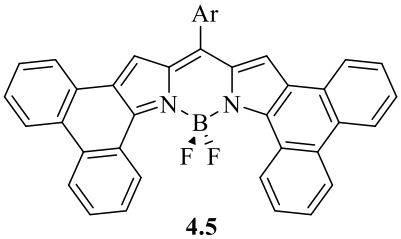

4.5

$\lambda_{abs/emi}$ =680/697 nm
φ_f = 0.51
ε = 166000 $M^{-1}cm^{-1}$

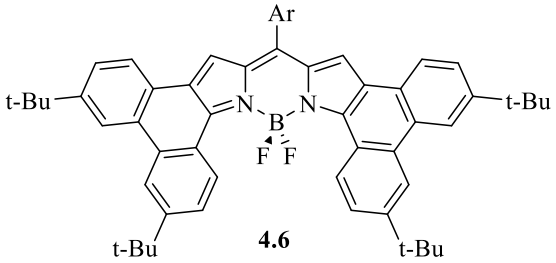

4.6

$\lambda_{abs/emi}$ = 698/715 nm
φ_f = 0.29
ε = 173800 $M^{-1}cm^{-1}$

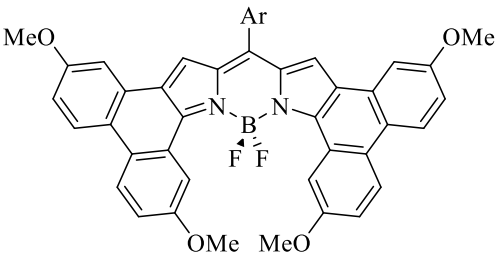

4.9

$\lambda_{abs/emi}$ = 682/717 nm
φ_f < 0.01
ε = 144500 $M^{-1}cm^{-1}$

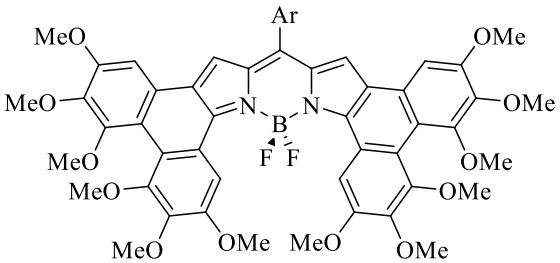

4.8

$\lambda_{abs/emi}$ = 740/767 nm
φ_f < 0.01
ε = 195000 $M^{-1}cm^{-1}$

Figure 4.1: Few examples of phenanthro-fused BODIPY.

In chapter 3, we have discussed about how fusion of heterocyclic aromatic compounds to the periphery causes bathochromic shifts in absorption and emission spectra.[10] Similarly, heterocycle incorporated benzo or naphtho groups also have shown dramatic effect in changing the optical properties of BODIPY. Dithiophenebenzo[b]-fused BODIPYs, **4.9** and **4.10** show absorption maxima at 719 and 758 nm, respectively with a very high absorption coefficient.[11] But, these molecules are weak or non-emissive in nature owing to its large inter system crossing populating the triplet state.

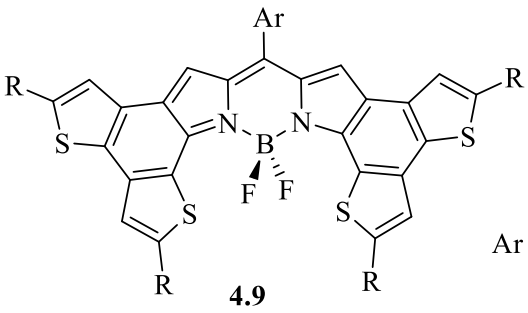

4.9

$\lambda_{abs/emi}$ = 719/730 nm
ε = 229000 $M^{-1}cm^{-1}$

Ar = Toluene

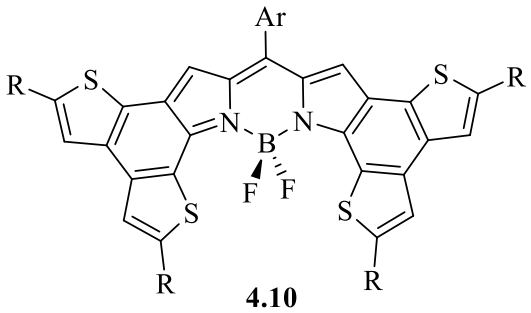

4.10

λ_{abs} = 758 nm
ε = 122000 $M^{-1}cm^{-1}$

Figure 4.2: Example of benzobithiophene-fused BODIPY.[11]

Panda and co-workers reported an excellent bis-pyrrolylnaphtho[b]-fused BODIPY dye **A10**, which exhibits absorption and emission spectra in NIR region, with excellent molar absorption coefficient, fluorescence quantum yield and photostability owing to its rigid framework with extended π-conjugation.[12] Combination of all these desired characteristics makes it a better candidate for bioimaging.

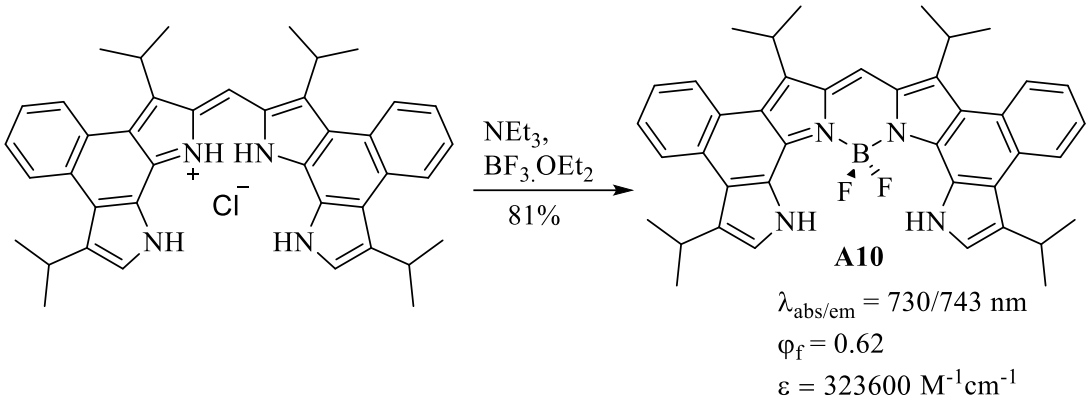

Scheme 4.4: Synthesis and optical properties of.

4.2. Research Goal

Owing to its better yield, bis(naphthobipyrrolyl)-BODIPY, **A10** can be further explored for functionalization to tune optical properties. The dye has two active and free positions for functionalization i.e., *α* and *meso*. As we have discussed the effect of *meso* substitution does not affect the frontier orbitals efficiently, we are left with α positions. Though, the above dye has two α-free positions, they show good photostability. So, functionalization at *α*-positions is expected to enhance the optoelectronic properties along with tuning its photostability further. We have chosen different functional groups like formyl, nitrile, nitro and bromo.

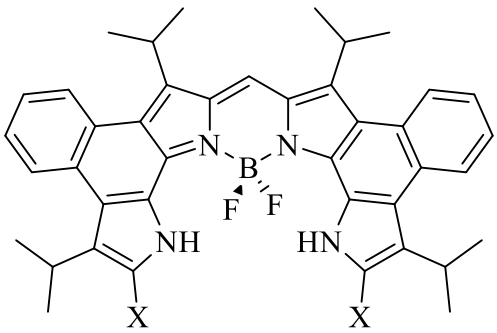

X = -CHO, -CN, -NO_2, -Br, -Ph

Figure 4.3: Structure of target molecules.

4.3. Result and Discussion

4.3.1. Synthesis

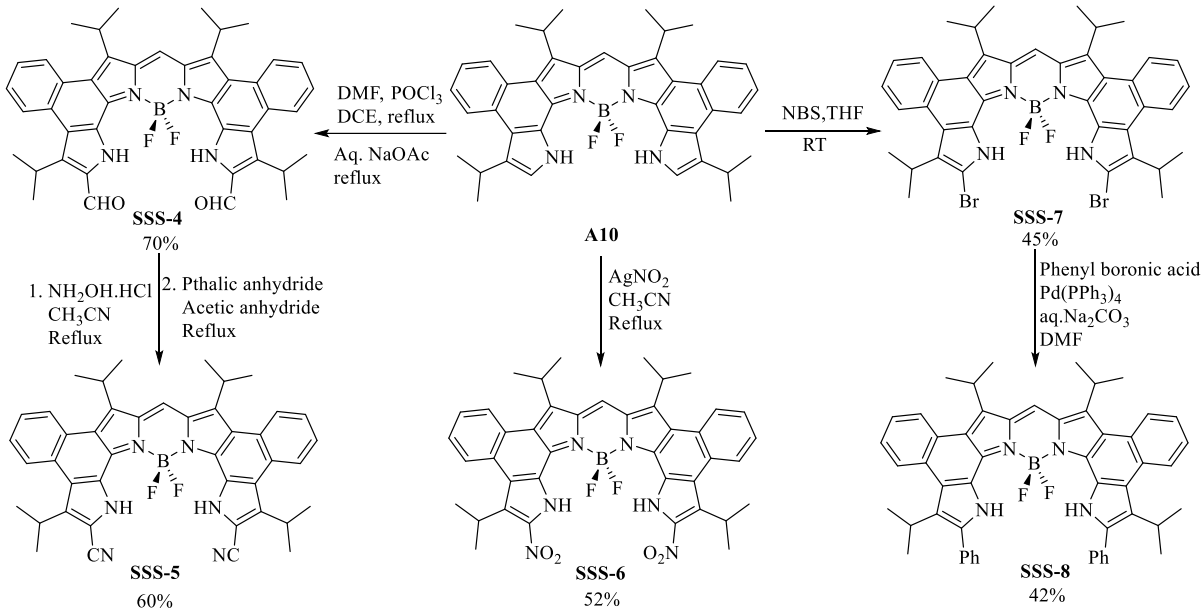

Scheme 4.5: Synthesis of all the designed BODIPY molecules.

As naphthobipyyrole shows facile formylation with Vilsmeier-Haack reaction, we tried formylation of bis-(napthobipyrrolyl)methene-BODIPY with DMF-$POCl_3$ adduct in DCE under reflux condition. We obtained diformyl-BODIPY, **SSS-4** successfully with 70% yield. **SSS-4** was then subjected to Beckmann-rearrangement, which on subsequent dehydration with desiccating reagent like acetic anhydride and pthalic anhydride resulted in dicyano-BODIPY, **SSS-5** with 60% yield. Dinitro-BODIPY, **SSS-6** was synthesized by treating **A10** with silver nitrite with 52% yield. Bromination of BODIPY was a very facile reaction with NBS. But dibromo-BODIPY, **SSS-7** was not very stable in solution medium, due to which it was difficult for rigorous purification and further characterization. We could obtain only UV-Vis-NIR absorption spectrum and ^{1}H NMR spectrum for dibromo product. So, we carried out a Suzuki-coupling of **SSS-7** with phenyl boronic acid to obtain diphenyl-BODIPY, **SSS-8**. All the derivatives, except **SSS-7** are fully characterized with standard spectroscopic characterization techniques like ^{1}H NMR, ^{13}C NMR, ^{19}F NMR, ^{11}B NMR, UV-Vis-NIR, fluorescence spectroscopy, HRMS analysis. SCXRD analysis has been performed for **SSS-4**, **SSS-5** and **SSS-6**.

4.3.2. Characterization

4.3.2.1. Optical Properties

Absorption and emission of all the BODIPY derivatives are studied in different solvents. All the derivatives show less pronounced solvent effect except NO_2-derivatives. Diformyl BODIPY, **SSS-4** exhibits bathochromic shift in the absorption spectra with absorption maxima at 735 nm in toluene with a slight reduction in molar extinction coefficient from parent BODIPY, **A10**.[12] It also exhibits bathochromic shift in emission spectra with emission maxima at 745 nm. Solvent effect on absorption and emission spectra is not very much significant.

Table 4.1: Summary of photophysical properties of **SSS-4** in different solvents.

Solvents	**Absorption**			**Emission**				
	λ_{max} (nm)	ε ($M^{-1}cm^{-1}$ x10^5)	FWHM (cm^{-1})	λ_{exc} (nm)	λ_{max} (nm)	FWHM (cm^{-1})	Stokes Shift (cm^{-1})	τ_f (ns)
Hexane	730	2.42	395	655	736	426	93	4.35
Toluene	735	1.65	502	655	745	504	165	4.02
$CHCl_3$	733	1.63	503	655	743	507	165	-
Methanol	721	0.6	697	655	732	633	208	3.07
Acetonitrile	717	1.26	703	655	732	633	286	4.36
DMSO	726	0.64	1154	655	742	655	297	-

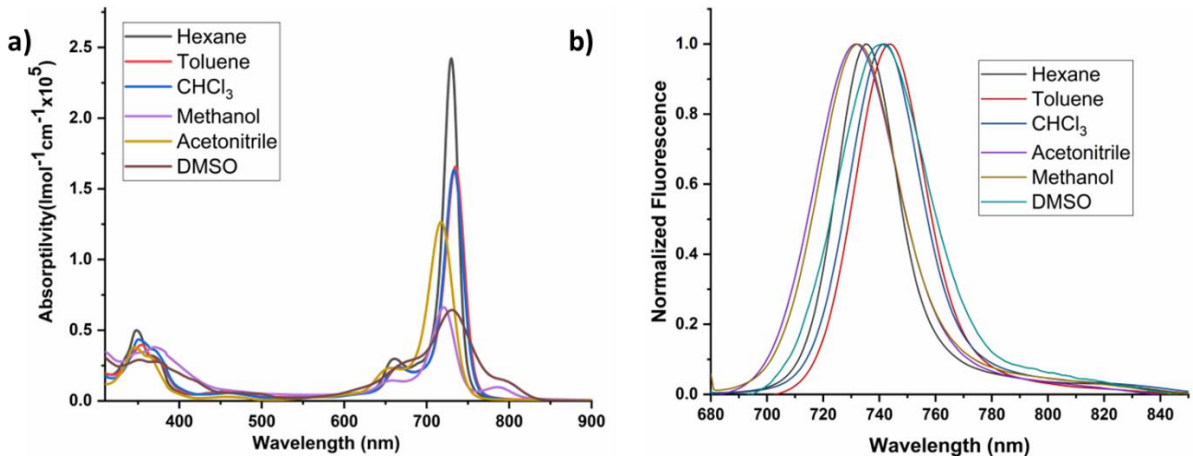

Figure 4.4: a) Absorption and b) emission spectra of **SSS-4** in different solvents.

Surprisingly, nitrile derivative shows a hypsochromic shift in the absorption and emission spectra with maxima at 717 and 726 nm, respectively. Solvent effect on absorption and emission spectra are very less. In DMSO this shows aggregation effect.

Table 4.2: Summary of photophysical properties of **SSS-5**.

Solvents	**Absorption**			**Emission**				
	λ_{max} (nm)	ε ($M^{-1}cm^{-1}$ x10^5)	FWHM (cm-1)	λ_{exc} (nm)	λ_{max} (nm)	FWHM (cm^{-1})	Stokes Shift (cm^{-1})	τ_f (ns)
Toluene	717	1.83	507	640	726	494	173	4.21
$CHCl_3$	712	1.74	495	640	721	482	175	-
Methanol	703	1.06	731	640	714	570	219	3.85
Acetonitrile	698	1.35	700	640	712	631	282	4.47

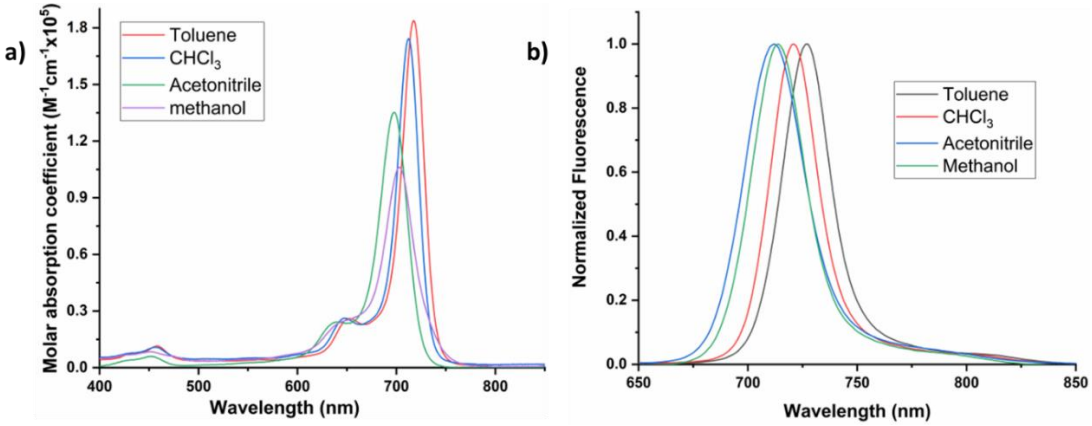

Figure 4.5: a) UV-Vis-NIR absorption and b) emission spectra of **SSS-5** in different solvents.

Table 4.3: Summary of photophysical properties of **SSS-6**.

Solvents	**Absorption**			**Emission**				
	λ_{max} (nm)	ε ($M^{-1}cm^{-1}$ x10^5)	FWHM (cm^{-1})	λ_{exc} (nm)	λ_{max} (nm)	FWHM (cm^{-1})	Stokes Shift (cm^{-1})	τ_f (ns)
Hexane	725	1.55	382	655	730	395	95	4.7
Toluene	733	2.38	503	655	741	510	147	4.08
$CHCl_3$	733	2.12	503	655	742	509	165	-
Acetonitrile	721	1.47	674	655	734	632	246	3.86
DMSO	803	0.94	606	709	816	broad	199	-

SSS-6 does not show much difference in absorption and emission spectra from parent α-free BODIPY, **A10**. Solvent effect on absorption and emission is not very much different for non-polar or slightly polar solvents. But, highly polar solvents like DMSO causes a dramatic change in both absorption and emission spectra. There is a 70 and 75 nm bathochromic shifts in the absorption and emission spectra, respectively when solvent changed from toluene to DMSO.

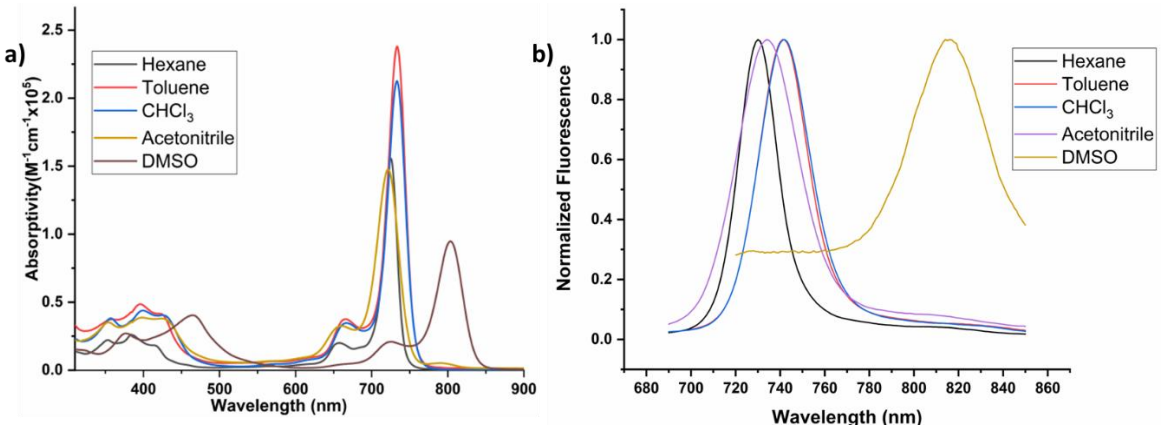

Figure 4.6: UV-Vis-NIR absorption; b) emission spectra of **SSS-6** in different solvents.

SSS-7 exhibits absorption maxima at 735 nm in chloroform. But due to less stability further studies like molar extinction coefficient, emission could not be examined. **SSS-8** exhibits highest bathochromic shift in both absorption and emission spectra.

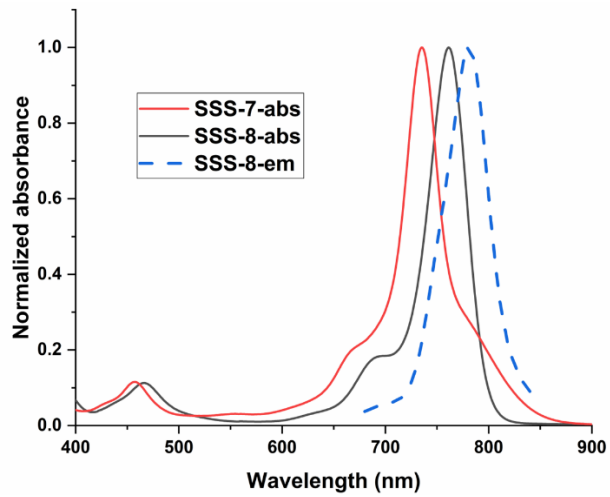

Figure 4.7: Absorption and emission spectra of **SSS-7** and **SSS-8** in chloroform.

The photostability of all the BODIPY derivatives were examined by irradiating the air saturated solution of BODIPYs with 365 nm lamp (8 W) for 72 h. Nitrile derivative, **SSS-5** shows highest photostability with ~0.05% degradation per hour followed by **SSS-4** and **SSS-8**

with 0.2 % degradation per hour. **A10** shows 0.7% degradation per hour. But nitro derivative **SSS-6** shows minimum stability with 4% degradation per hour.

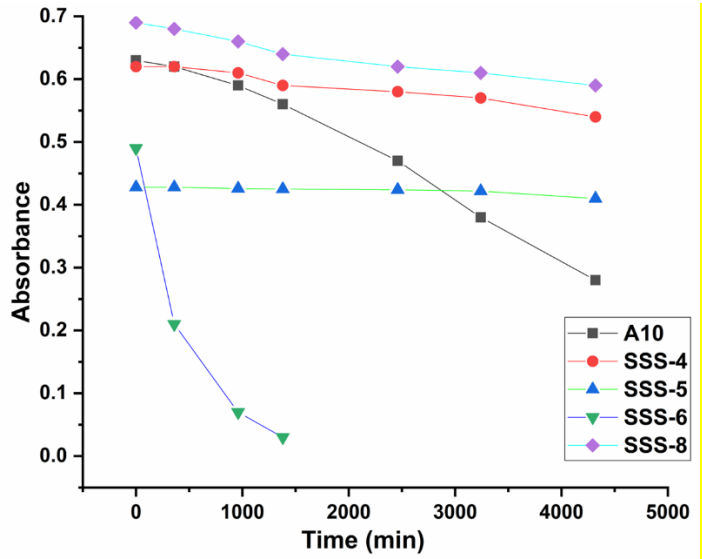

Figure 4.8: Change in optical density with time on irradiation with 8W lamp at 365 nm (monitored at absorption maxima).

4.3.2.2. Structural analysis

SCXRD analysis of a diffraction grade crystal (obtained from diffusion of methanol into chloroform solution) confirmed the structure of **SSS-4**. **SSS-4** exhibits a twisted structure unlike **A10**, which shows a relatively planar structure. Two molecules are present in an asymmetric unit with a dihedral angle of 71.09°. They possess unidirectional twist but different twist angle at *meso*-position (named as A and B in **figure 4.9d**). Dihedral angles between both the naphthobipyrrole moiety 17.54° and 12.49° for A and B, respectively. Two NHs of BODIPY are found to be above and below the mean molecular plane of BODIPY (defined by bis(napthobipyrrolyl)BODIPY) and fused *o*-phenylene moieties are deviated in the opposite direction. One formyl group is 0.987 Å below the molecular plane and another is 0.874 Å above the plane in A. Same has been observed in B with a distance of 1.001 Å and 0.501 Å. Interestingly, there are no existing π-π stacking in the solid state as usually observed in BODIPY molecules owing to its distorted structure. In crystal packing diagram, bidirectional helices are present with equal numbers and placed alternate to each other.

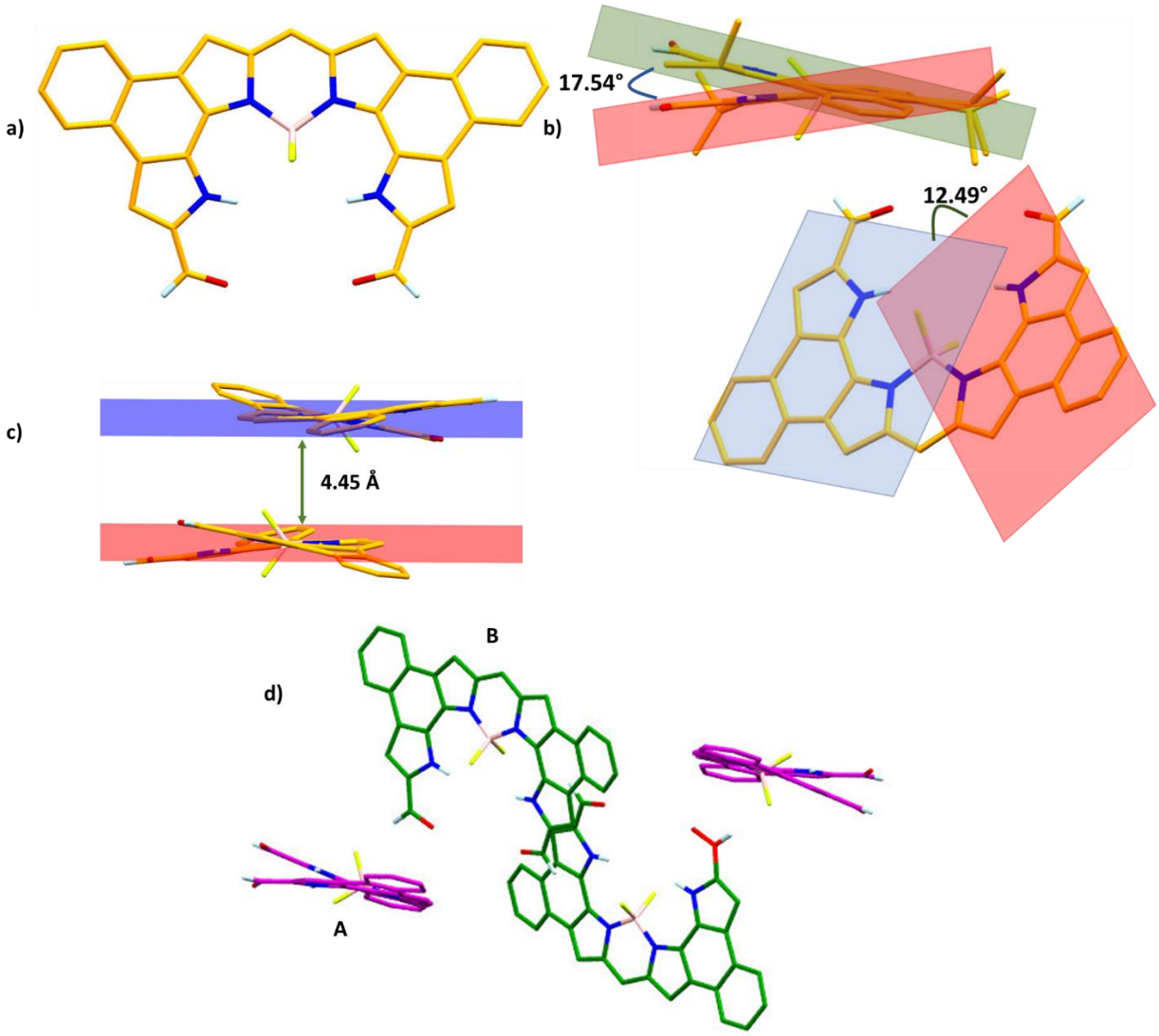

Figure 4.9: SCXRD structure of **SSS-4**: a) front view: b) asymmetry unit showing dihedral angle between naphthobipyrroles; c) Side view showing interplanar distance; d) packing diagram showing opposite twists (peripheral *i*-Pr and hydrogens removed for clarity).

Crystal structure of **SSS-5** also consists of two molecules in the asymmetry unit. They are aligned with a dihedral angle of 74.07°. Both the molecules deviate from planarity but to different extents. One molecule (B) shows less deviation from planarity while another (A) shows much more distorted structure. One outer NH (0.25 Å) of naphthobipyrrole is above and another (0.07 Å) is below the mean molecular plane in molecule B. Same is followed for CN substituent (0.39 and 0.37 Å). But in A, both the NHs (0.05 and 0.15 Å) are above the mean plane with relatively lesser deviation from mean plane. Also, CN substituent is very less deviated from mean plane (0.07 and 0.10 Å) in A.

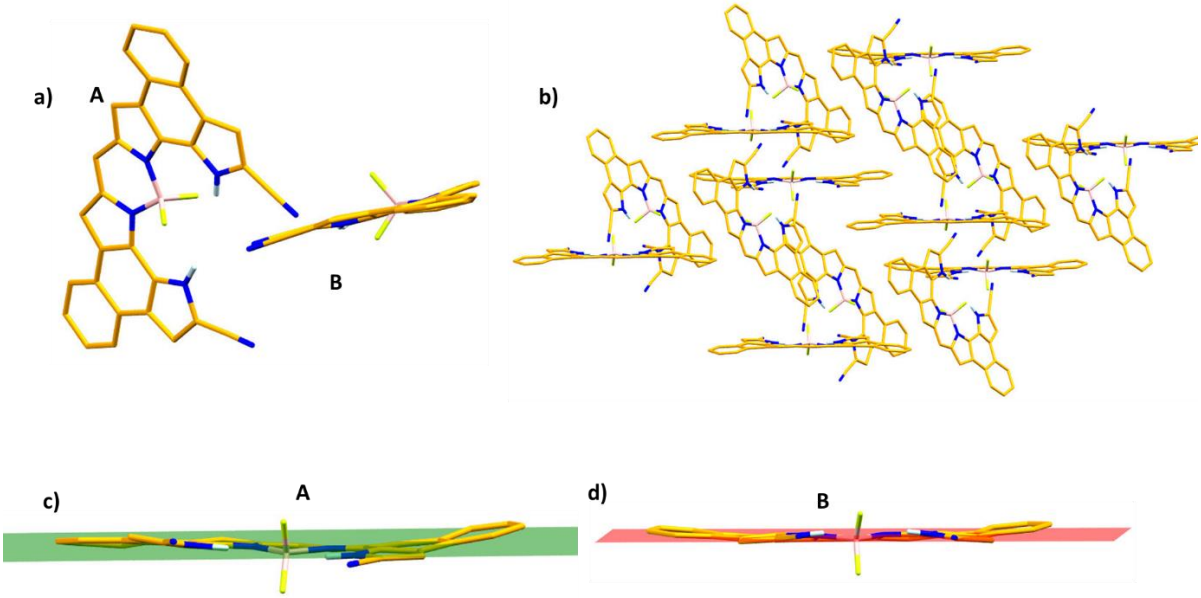

Figure 4.10: SCXRD structure of **SSS-5**: a) Asymmetry unit; b) crystal packing; c) side view of A; d) side view of B (peripheral *i*-Pr and hydrogens are removed for clarity).

Structure of **SSS-6** is also elucidated by SCXRD analysis of a diffraction grade crystal (obtained by diffusion of methanol into the chloroform solution). Nitro-derivative shows less but pronounced distortion relative to **SSS-4**. The dihedral angle between both the naphthobipyrroles is reduced to 5.73°. One nitro group is present at 0.44 Å above and another at 0.40 Å below mean molecular plane.

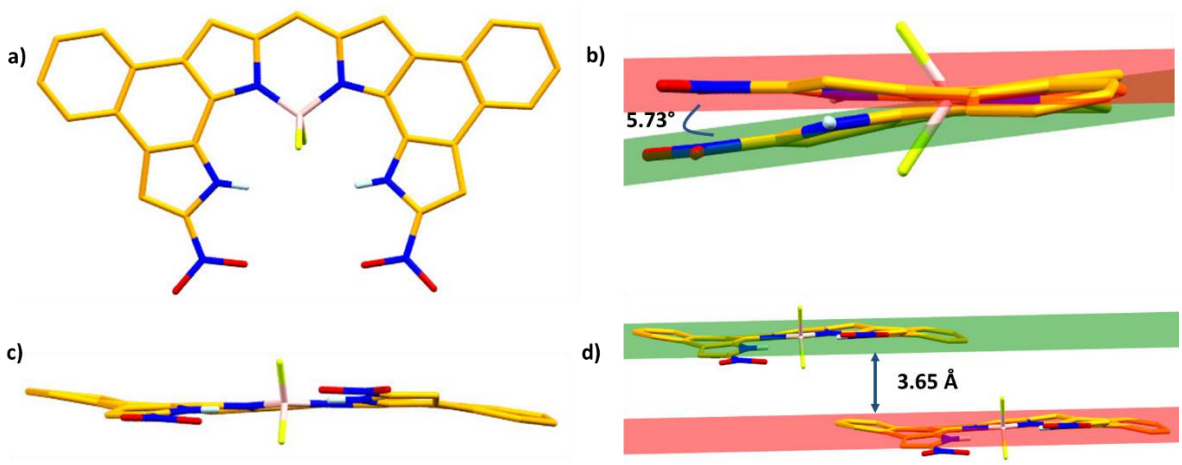

Figure 4.11: SCXRD structure of **SSS-6**: a) Front view; b) side view showing dihedral angle between naphthobipyrroles; c) another side view; d) interplanar distance (peripheral *i*-Pr and hydrogens removed for clarity).

Owing to its small distortion from plane there exist a π-π stacking with an interplanar distance 3.65 Å. Packing diagram of **SSS-6** shows that it consists of equal number molecules with opposite helix.

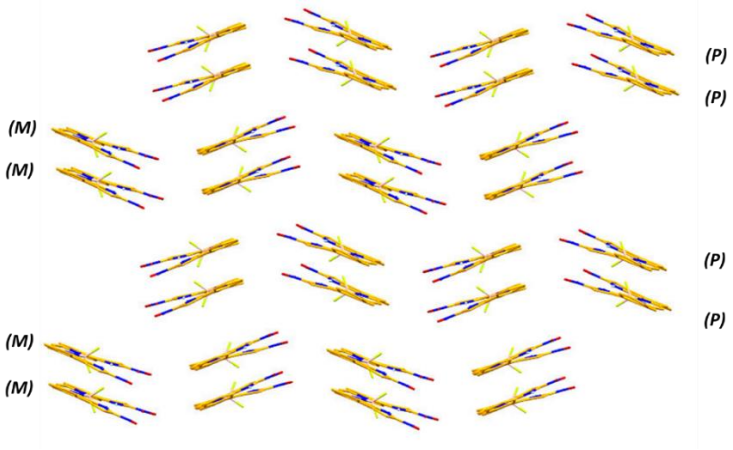

Figure 4.12: Packing diagram of **SSS-6** showing alternate arrangement of opposite helices.

4.3.2.3. Computational analysis

All structures are optimized using DFT-B3LYP/6-31G(d,p). All structures show slightly boat shaped conformation. With both o-phenylene carbons away from plane in same direction. But, **SSS-8** exhibits a highly distorted helical structure. Phenyl groups are not in plane with naphthobipyrrole moiety, restricting extended conjugation.

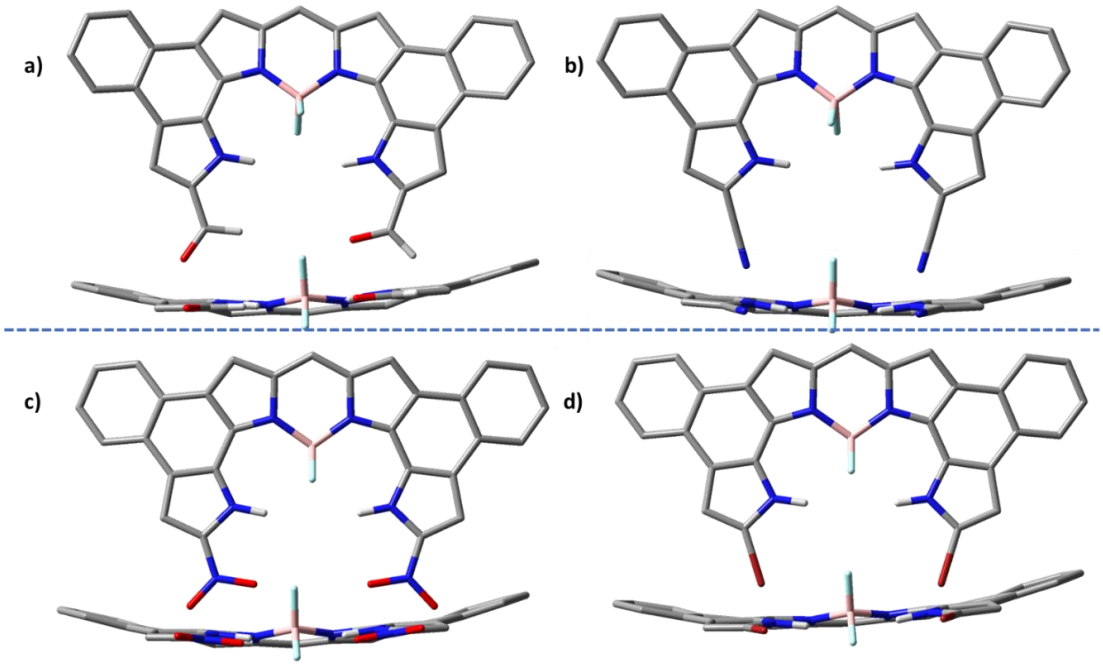

Figure 4.13: DFT optimized structures of a) **SSS-4**; b) **SSS-5**; c) **SSS-6**: d) **SSS-7.**

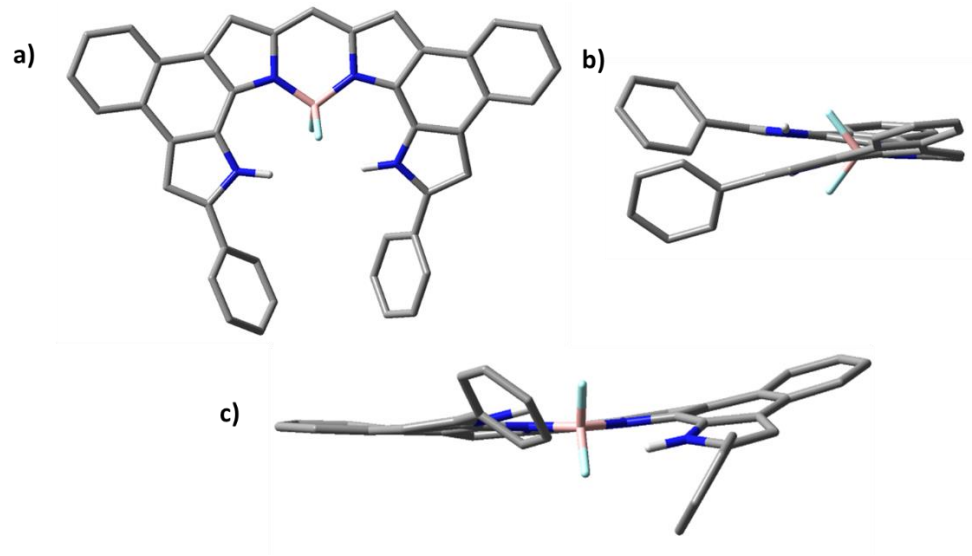

Figure 4.14: DFT-optimized geometry of **SSS-8** showing helical conformation: a) front view; b) and c) side views.

Frontier orbital diagram of all the derivatives display HOMO-LUMO energy gap, which is in accord with experimentally obtained spectral values. It shows electron withdrawing group on α-position decreases both HOMO and LUMO energy. Nitrile being strong electron withdrawing group lowers HOMO energy more than LUMO energy causing increased HOMO-LUMO energy gap and supported the hypsochromic shift noticed in its absorption spectrum. **SSS-8** is having minimum HOMO-LUMO energy gap presumably owing to its structural distortion.

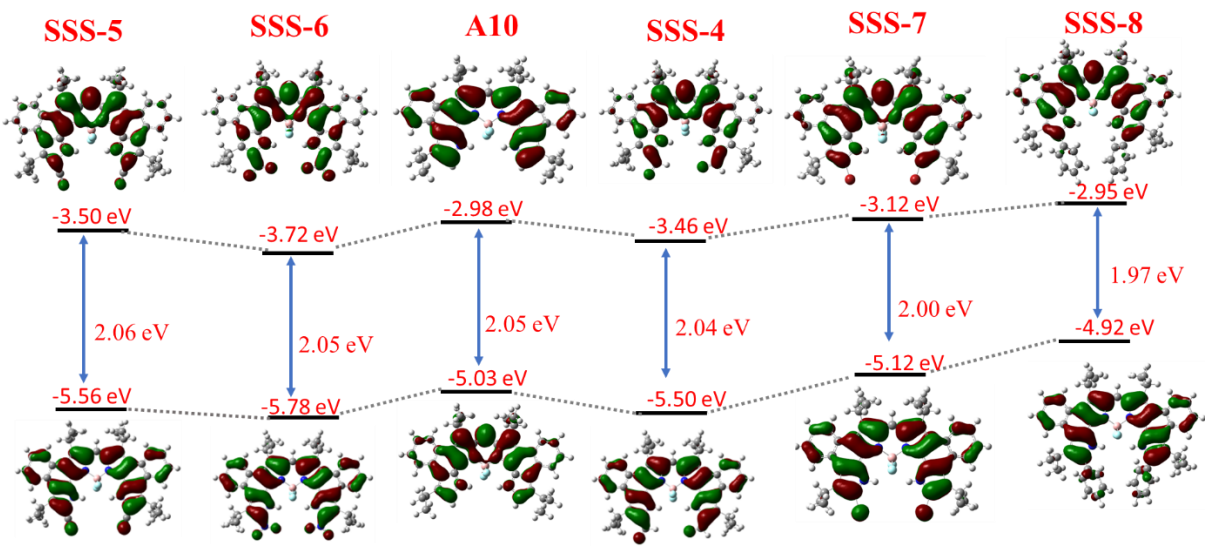

Figure 4.15: Frontier orbital diagrams of all BODIPY derivatives showing HOMO-LUMO energy gap.

4.4. Conclusion

We have successfully functionalized both the terminal α-free positions of naphthobipyrrole-derived BODIPY with different functional groups like formyl, nitrile, nitro, bromo and phenyl. Except nitrile-BODIPY all other show slight bathochromic shift in the absorption and emission spectra with respect to α-free BODIPY. Nitrile-BODIPY displays hypsochromic shift in both absorption and emission spectra. Formyl and nitrile-BODIPY show excellent photostability. But bromo derivative is found to be very less stable, therefore, it was further derivatized with phenyl groups. Phenyl substituted BODIPY revealed largest bathochromic shift in absorption and emission with respect to all other derivatives. Optimized geometry of phenyl derivative shows a helical conformation causing reduction in HOMO-LUMO energy gap.

4.5. Experimental

Synthesis of diformyl BODIPY, SSS-4

DMF (0.31 mL) was taken in a properly dried two necked RB fitted with condenser under N_2 atmosphere and kept in ice bath. Freshly distilled $POCl_3$ (0.36 mL) was added to it and stirred at room temperature for 30 min. After that DCE (5 mL) solution of bis(naphthobipyrrolyl)BODIPY, **A10** (50 mg) was added to it slowly and kept for reflux in a preheated oil-bath for 7 h. Reaction was cooled to room temperature and saturated aqueous solution of NaOAc was added to it. Again, it was refluxed for 2 h. Then organic layer was extracted with EtOAc and passed over anhyd. Na_2SO_4. Solvent was removed under reduced pressure. Crude reaction mixture was purified by silica gel column chromatography by hexane:EtOAc (9:1) to get pure green colour solid. Yield Obtained: 70%

^{1}H NMR (500 MHz, $CDCl_3$) δ in ppm: 10.88 (br, 2H, NH), 10.41 (s, 2H, CH aldehyde), 8.40 (d, *J*=6.02 Hz, 2H, CH naphthalene), 8.36 (d, *J*=7.99 Hz, 2H, CH naphthalene), 8.24 (s, 1H, CH *meso*), 7.55 (m, 2H, CH naphthalene), 7.51(m, 2H, CH naphthalene), 4.26 (m, 2H, -CH alkyl), 4.18 (m, 2H, -CH alkyl), 1.74 (d, *J*=7.13 Hz, 12H, -CH_3 alkyl), 1.70 (d, *J*=7.09 Hz, 12H, -CH_3 alkyl); ^{13}C NMR (125.83 MHz, $CDCl_3$) δ in ppm: 180.8, 147.8, 139.7, 136.7, 136.3, 134.8, 129.1, 127.2, 126.3, 125.8, 125.5, 125.4, 125.3, 124.0, 100.0, 27.8, 27.2, 24.9, 24.4; ^{19}F NMR (376.42 MHz, $CDCl_3$,) δ in ppm: -139.01 (m, 2F); HRMS (ESI+): m/z calculated for $C_{43}H_{42}BF_2N_4O_2$ ($M+H^+$): 695.3368; found: 695.3367

Synthesis of dicyano BODIPY, SSS-5

SSS-4 (10 mg) and hydroxyl amine hydrochloride (13 mg) were taken in a two necked RB and dissolved in acetonitrile (5 mL). To this NEt_3 (30 µL) was added and heated at 60 °C for 45 min. Then reaction was stopped and washed with water. The organic layer was passed over Na_2SO_4 and dried under reduced pressure. Then the crude mixture and pthalic anhydride (100 mg) were taken in a two necked RB and dissolved in acetonitrile under N_2 atmosphere. To this acetic anhydride (2 mL) was added and refluxed for 24 h. After that it was cooled to room temperature and washed with aq. ammonia solution. Then organic layer was extracted with EtOAc and passed over anhyd. Na_2SO_4. Solvent was removed under reduced pressure. Crude mixture was purified by silica gel column chromatography by hexane:EtOAc (9:1) to get pure green colour solid. Yield Obtained: 60%

^{1}H NMR (500 MHz, $CDCl_3$) δ in ppm: 10.46 (br, 2H, NH), 8.37 (d, *J*=7.65 Hz, 4H, CH naphthalene), 8.29 (s, 1H, CH *meso*), 7.56 (m, 4H, CH naphthalene), 4.28 (m, 2H, -CH alkyl),

3.99 (m, 2H, -CH alkyl), 1.75 (d, *J*=7.17 Hz, 12H, -CH_3 alkyl), 1.67 (d, *J*=6.99 Hz, 12H, -CH_3 alkyl); ^{13}C NMR (125.78 MHz, $CDCl_3$) δ in ppm: 148.1, 139.0, 138.5, 135.9, 128.1, 127.0, 126.4, 125.8, 125.7, 125.4, 124.7, 124.2, 123.6, 115.1, 105.8, 27.8, 27.0, 24.4, 22.5; ^{19}F NMR (376.42 MHz, $CDCl_3$) δ in ppm: -138.25 (2F); HRMS(ESI+): m/z calculated for $C_{43}H_{40}BF_2N_6$ ($M+H^+$): 689.3376; found: 689.3373.

Synthesis of dinitro BODIPY, SSS-6

Bis(naphthobipyrrolyl)BODIPY, **A10** (10 mg) was dissolved in chloroform under N_2 atmosphere. To this, acetonitrile solution of $AgNO_2$ (100 mg) was added and refluxed for 7 h. Then it was cooled and solvent was removed under reduced pressure. The crude mixture was purified by silica gel column chromatography with hexane:EtOAc (9:1) mixture. Yield obtained: 52%

^{1}H NMR (500 MHz, $CDCl_3$) δ in ppm: 11.12 (br, 2H, NH), 8.40 (dd, *J* = 7.36 Hz, 2H, CH naphthalene), 8.39 (dd, *J*=7.36 Hz, 2H, CH naphthalene), 8.32 (s, 1H, CH *meso*), 7.58 (m, 4H, CH naphthalene), 4.40 (m, 2H, -CH alkyl), 4.26 (m, 2H, -CH alkyl), 1.75 (d, *J*=7.15 Hz, 12H, -CH_3 alkyl), 1.64 (d, *J*=7.17 Hz, 12H, -CH_3 alkyl); ^{13}C NMR (125.78 MHz, $CDCl_3$) δ in ppm: 148.7, 140.0, 139.2, 136.6, 129.4, 128.2, 127.3, 126.9, 126.6, 126.4, 125.9, 125.8, 125.4, 120.6, 31.6, 27.9, 24.4, 19.6; ^{19}F NMR (470.59 MHz, $CDCl_3$,) δ in ppm: -138.79 (m, 2F); ^{11}B NMR (160.5 MHz, $CDCl_3$) δ in ppm: 2.11 (t, 1B); HRMS (ESI+): m/z calculated for $C_{41}H_{40}BF_2N_6O_4$ ($M+H^+$): 729.3172; found: 729.3171.

Synthesis of dibromo BODIPY, SSS-7

Bis(naphthobipyrrolyl)BODIPY, **A10** (30 mg) was dissolved in THF (10 mL) under N_2 atmosphere. NBS (21 mg) was added to it portion wise and stirred at room temperature for 45 minutes. Then reaction was quenched with aq $NaHCO_3$ solution. Then organic layer was extracted with EtOAc and passed over anhyd. Na_2SO_4. Solvent was removed under reduced pressure. Crude mixture was roughly purified by a quick silica gel filter column chromatography by hexane:EtOAc (19:1). Then it was used for next step reaction. Yield Obtained: 45%

^{1}H NMR (500 MHz, $CDCl_3$) δ in ppm: 9.94 (br, 2H, NH), 8.41 (d, *J* = 7.81 Hz, 2H, CH naphthalene), 8.37 (dd, *J*=8.11 Hz, 2H, CH naphthalene), 8.13 (s, 1H, CH *meso*), 7.51 (m, 4H, CH naphthalene), 4.26 (m, 2H, -CH alkyl), 3.96 (br, 2H, -CH alkyl), 1.73 (d, *J*=7.18 Hz, 12H, -CH_3 alkyl), 1.60 (d, *J*=7.23 Hz, 21H, -CH_3 alkyl merged with H_2O).

Synthesis of diphenyl BODIPY, SSS-8

Dibromo BODIPY (17 mg), phenyl boronic acid (20 mg), $Pd(PPh_3)_4$ (2.5 mg) were taken in a two necked RB and kept under vacuum for some time. Degassed DMF (1.5 mL) was added to it under N_2 atmosphere. To it degassed aq. Na_2CO_3 (25 mg in 0.5 mL) was added and heated at 80 °C for 24 h. It was purified with preparative silica gel TLC with hexane:DCM (9:1). Yield obtained: 42%

^{1}H NMR (500 MHz, $CDCl_3$) δ in ppm: 9.85 (br, 2H, NH), 8.49 (d, *J* = 7.73 Hz, 2H, CH naphthalene), 8.42 (d, *J* = 7.82 Hz, 2H, CH naphthalene), 8.12 (s, 1H, CH *meso*), 7.54 (m, 6H CH phenyl), 7.48 (m, 4H, CH phenyl), 7.36 (m, 4H, CH naphthalene), 4.30 (m, 2H, -CH alkyl), 3.87 (m, 2H, -CH alkyl), 1.76 (d, *J* = 7.14 Hz, 12H, CH_3 alkyl), 1.50 (d, *J* = 7.23 Hz, 12H, CH_3 alkyl); ^{19}F NMR (470.59 MHz, $CDCl_3$,) δ in ppm: -137.25 (s, 2F); ^{11}B NMR (160.5 MHz, $CDCl_3$) δ in ppm: 2.34: HRMS (ESI+): m/z calculated for $C_{53}H_{50}BF_2N_4$ ($M+H^+$): 791.4097; found: 791.4093.

4.6. References

1. [a] Boens, N.; Leen, V.; Dehaen, W. *Chem. Soc. Rev.*, **2012**, *41*, 1130. [b] Kaur, P.; Singh, K. Recent advances in the application of BODIPY in bioimaging and chemosensing. *J. Mater. Chem. C*, **2019**, *7*, 11361.

2. Kowada, T.; Maeda, H.; Kikuchi, K. BODIPY-based probes for the fluorescence imaging of biomolecules in living cells. *Chem. Soc. Rev.*, **2015**, *44*, 4953.

3. [a] Bessette, A.; Hanan, G. S. Design, synthesis and photophysical studies of dipyrromethene-based materials: insights into their applications in organic photovoltaic devices. *Chem. Soc. Rev.*, **2014**, *43*, 3342. [b] Klfout, H.; Stewart, A.; Elkhalifa, M.; He, H. BODIPYs for dye-sensitized solar cells. *ACS Appl. Mater. Interfaces*, **2017**, *9*, 39873.

4. Chapran, M.; Angioni, E.; Findlay, N. J.; Breig, B.; Cherpak, V.; Stakhira, P.; Tuttle, T.; Volyniuk, D.; Grazulevicius, J. V.; Nastishin, Y. A.; Lavrentovich, O. D.; Skabara, P. J. An ambipolar BODIPY derivative for a white exciplex OLED and cholesteric liquid crystal laser toward multifunctional devices. *ACS Appl. Mater. Interfaces*, **2017**, *9*, 4750.

5. Wakamiya, A.; Murakami, T.; Yamaguchi, S. Benzene-fused BODIPY and fully-fused BODIPY dimer: impacts of the ring-fusing at the b bond in the BODIPY skeleton. *Chem. Sci.*, **2013**, *4*, 1002.

6. Chen, J.; Burghart, A.; Derecskei-Kovacs, A.; Burgess, K. 4,4-Difluoro-4-bora-3a,4a-diaza-s-indacene (BODIPY) Dyes Modified for Extended Conjugation and Restricted Bond Rotations. *J. Org. Chem.*, **2000**, *65*, 2900.

7. Chua, M. H.; Huang, K.-W.; Xu, J.; Wu, J. Unusual Intramolecular Hydrogen Transfer in 3,5-Di(triphenylethylenyl) BODIPY Synthesis and 1,2-Migratory Shift in Subsequent Scholl Type Reaction. *Org. Lett.*, **2015**, *17*, 4168.

8. Zhou, Z.; Zhou, J.; Gai, L.; Yuan, A.; Shen, Z. Naphtho[b]-fused BODIPYs: one pot Suzuki–Miyaura–Knoevenagel synthesis and photophysical properties. *Chem. Commun.* **2017**, *53*, 6621.

9. Miao, W.; Feng, Y.; Wu, Q.; Sheng, W.; Li, M.; Liu, Q.; Hao, E.; Jiao, L. Phenanthro[b]-Fused BODIPYs through Tandem Suzuki and Oxidative Aromatic Couplings: Synthesis and Photophysical Properties. *J. Org. Chem.*, **2019**, *84*, 9693.

10. [a] Chen, J.; Burghart, A.; Derecskei-Kovacs, A.; Burgess, K. 4,4-Difluoro-4-bora-3a,4a-diaza-s-indacene (BODIPY) Dyes Modified for Extended Conjugation and Restricted Bond Rotations. *J. Org. Chem.*, **2000**, *65*, 2900. [b] Umezawa, K.; Nakamura, Y.; Makino, H.; Citterio, D.; Suzuki, K.; *J. Am. Chem. Soc.*, **2008**, *130*, 1550. [c] Umezawa, K.; Matsui, A.; Nakamura, Y.; Citterio, D.; Suzuki, K. Bright, color-tunable fluorescent dyes in the Vis/NIR region: establishment of new "tailor-made" multicolor fluorophores based on borondipyrromethene. *Chem. – Eur. J.*, **2009**, *15*, 1096. [d] Leen, V.; Qin, W.; Yang, W.; Cui, J.; Xu, C.; Tang, X.; Liu, W.; Robeyns, K.; Meervelt, L. V.; Beljonne, D.; Lazzaroni, R.; Tonnelé, C.; Boens, N.; Dehaen, W. Synthesis, Spectroscopy, Crystal Structure Determination, and Quantum Chemical Calculations of BODIPY Dyes with Increasing Conformational Restriction and Concomitant Red-Shifted Visible Absorption and Fluorescence Spectra. *Chem. – Asian J.*, **2010**, *5*, 2016.

11. Huaulmé, Q.; Sutter, A.; Fall, S.; Jacquemin, D.; Lévêque, P.; Retailleau, P.; Ulrich, G.; Leclerc, N. Versatile synthesis of α-fused BODIPY displaying intense absorption in the NIR region and high electron affinity. *J. Mater. Chem. C*, **2018**, *6*, 9925.

12. Sarma, T.; Panda P. K.; Setsune, J.-I. Bis-naphthobipyrrolylmethene derived BODIPY complex: an intense near-infrared fluorescent dye. *Chem. Commun.*,**2013**, *49*, 9806.

4.7. Spectra

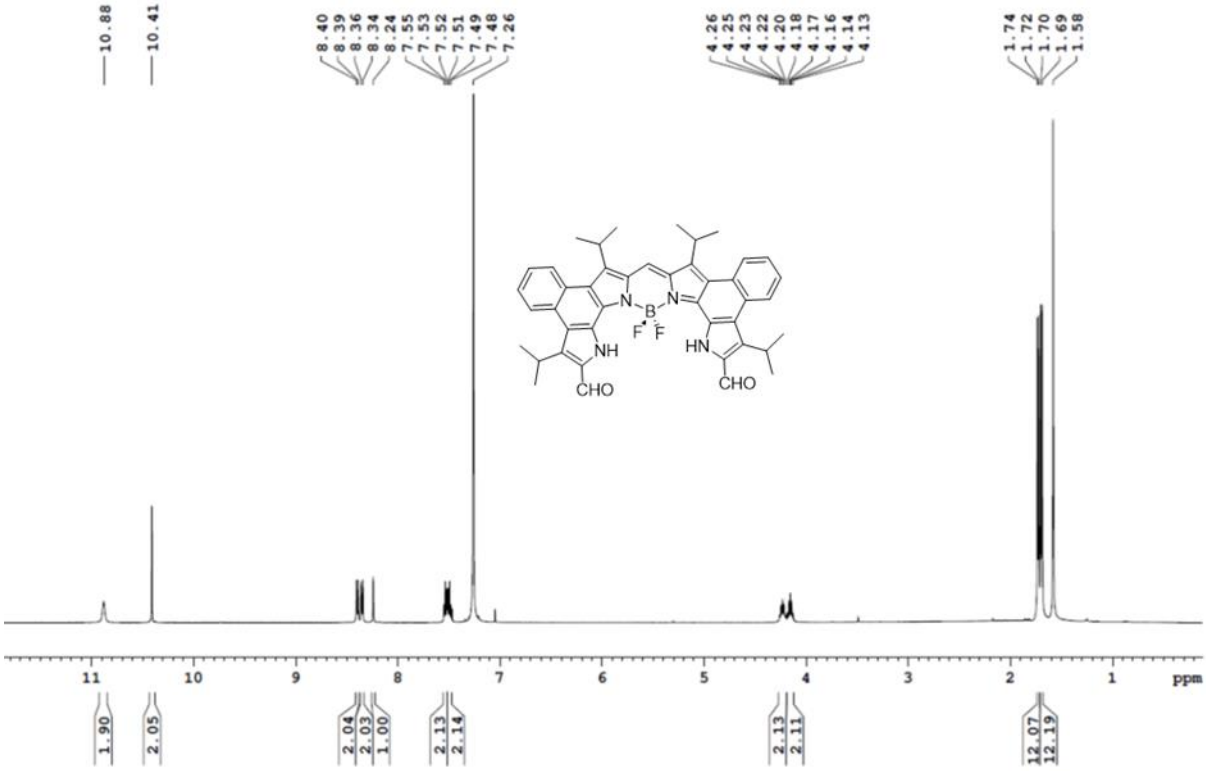

Figure 4.16: ^{1}H NMR spectrum of **SSS-4** in $CDCl_3$.

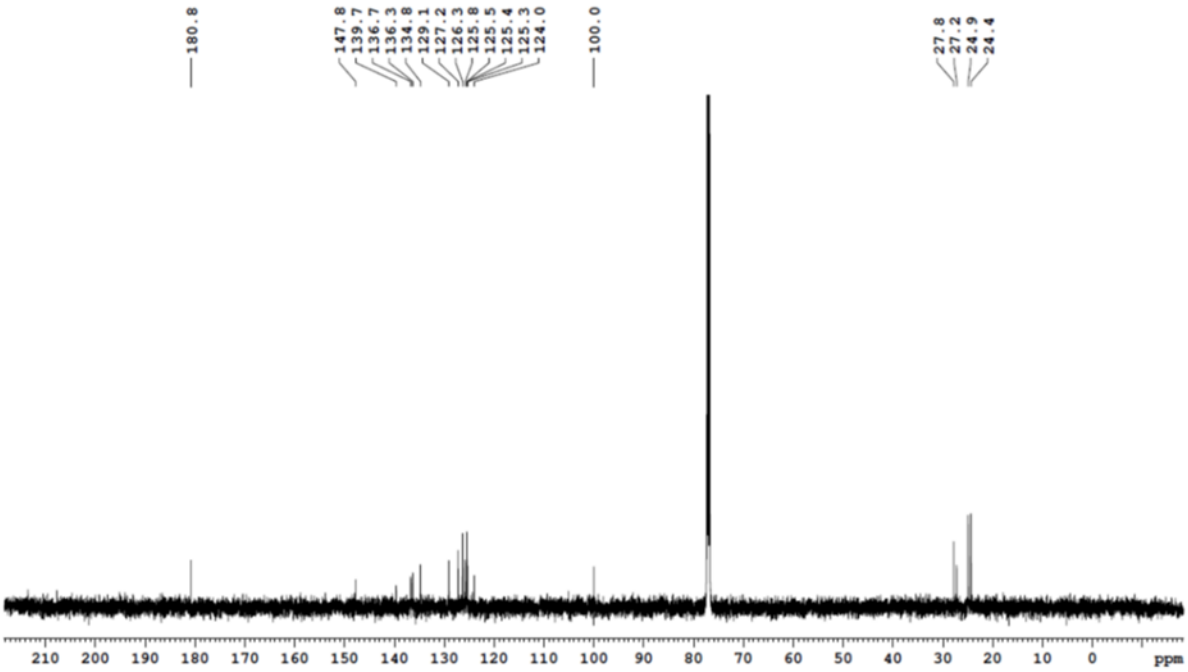

Figure 4.17: ^{13}C NMR spectrum of **SSS-4** in $CDCl_3$.

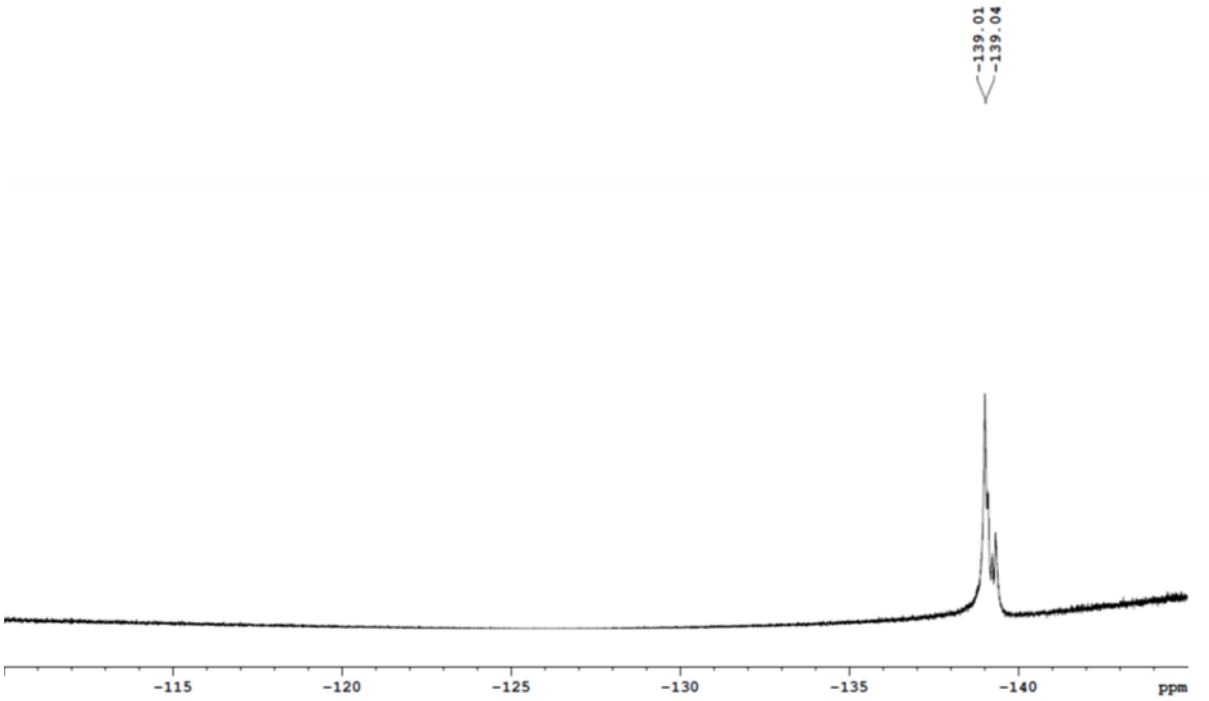

Figure 4.18: ^{19}F NMR spectrum of **SSS-4** in $CDCl_3$.

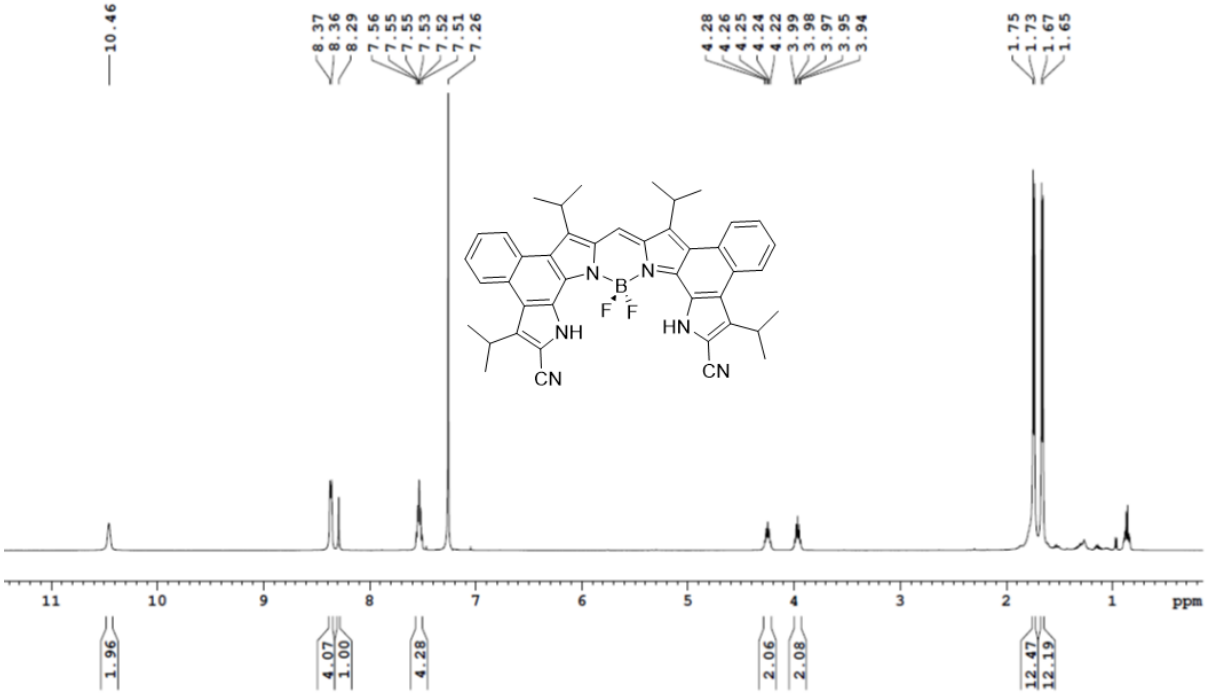

Figure 4.19: ^{1}H NMR spectrum of **SSS-5** in $CDCl_3$.

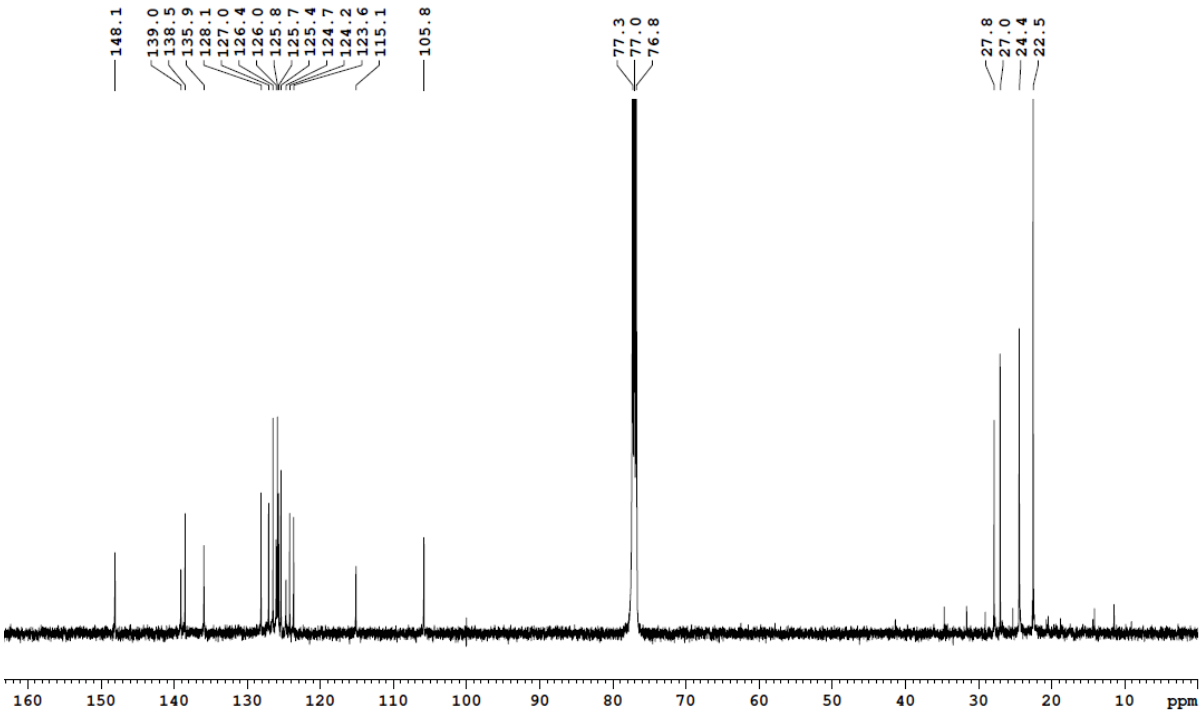

Figure 4.20: ^{13}C NMR spectrum of **SSS-5** in $CDCl_3$.

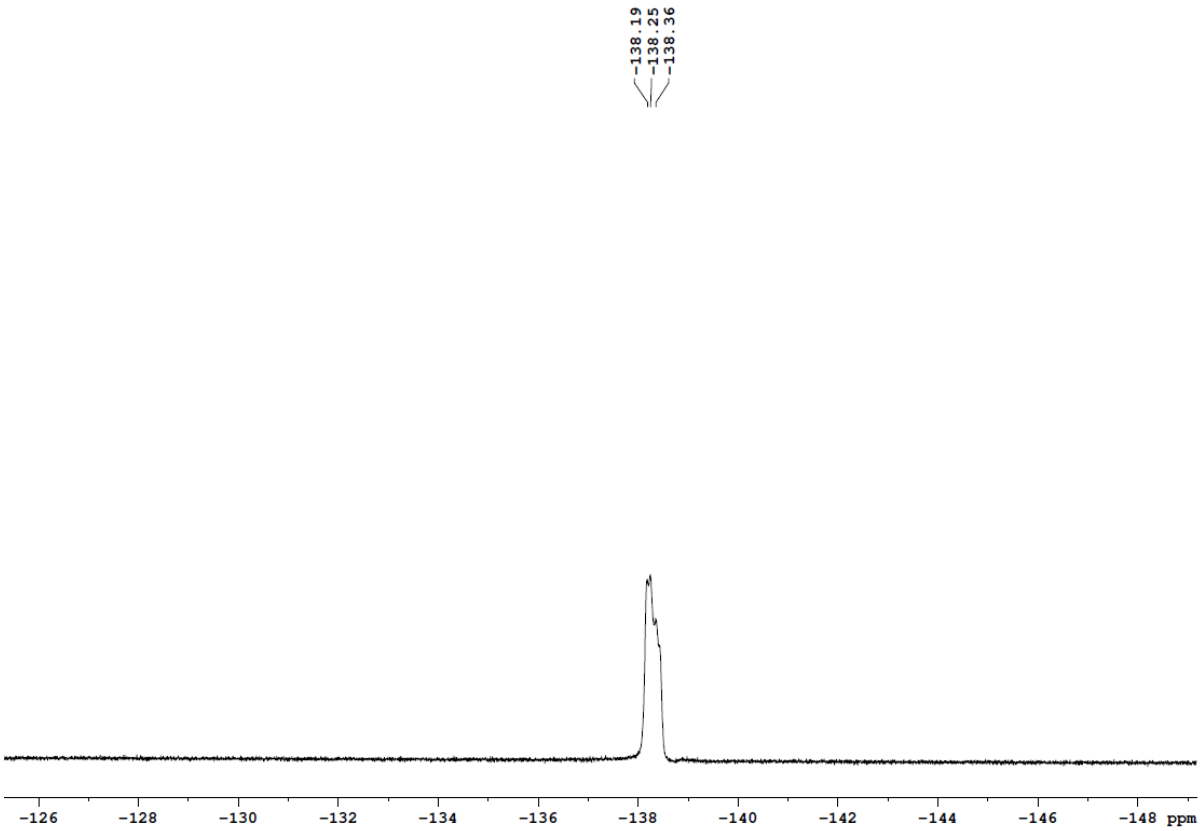

Figure 4.21: ^{19}F NMR spectrum of **SSS-5** in $CDCl_3$.

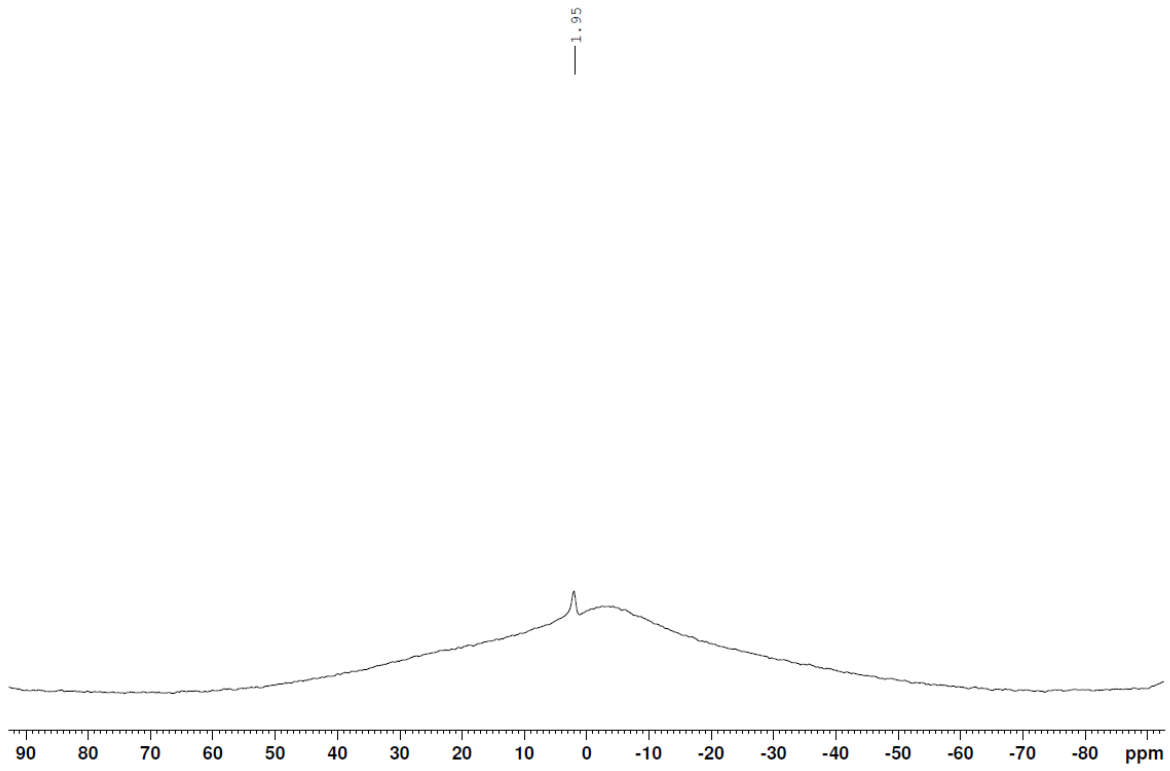

Figure 4.22: ^{11}B NMR spectrum of **SSS-5** in $CDCl_3$.

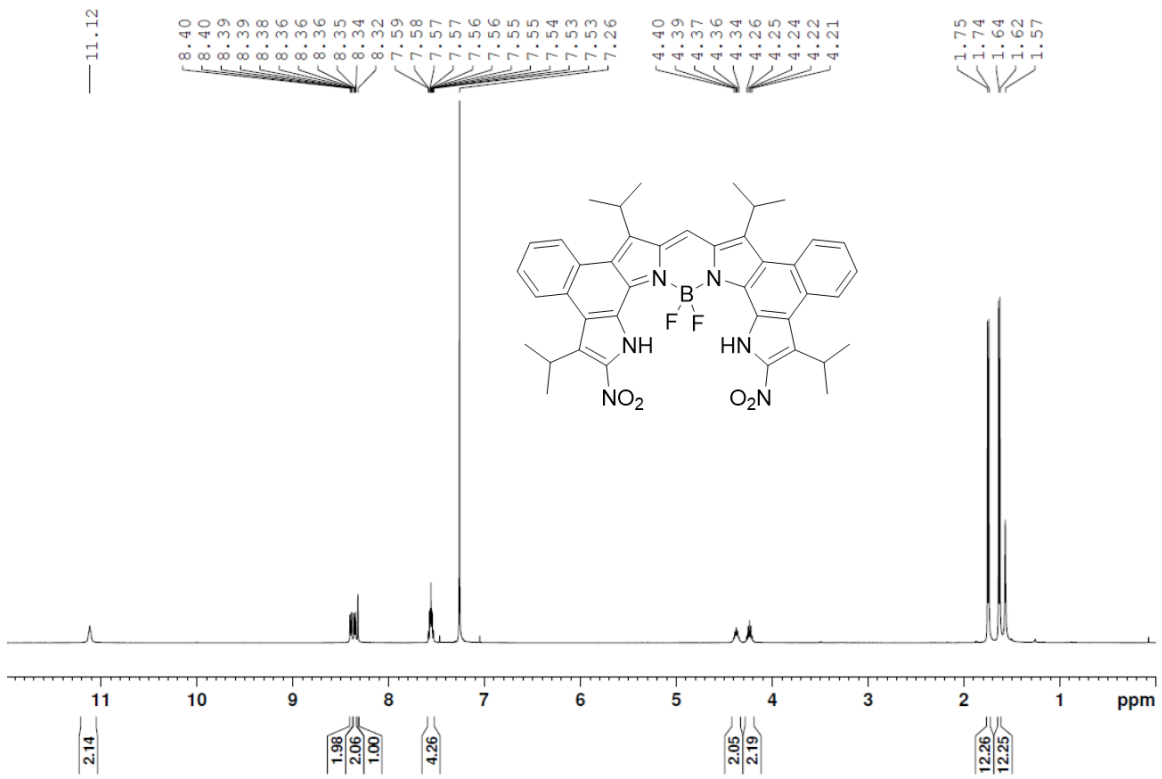

Figure 4.23: ^{1}H NMR spectrum of **SSS-6** in $CDCl_3$.

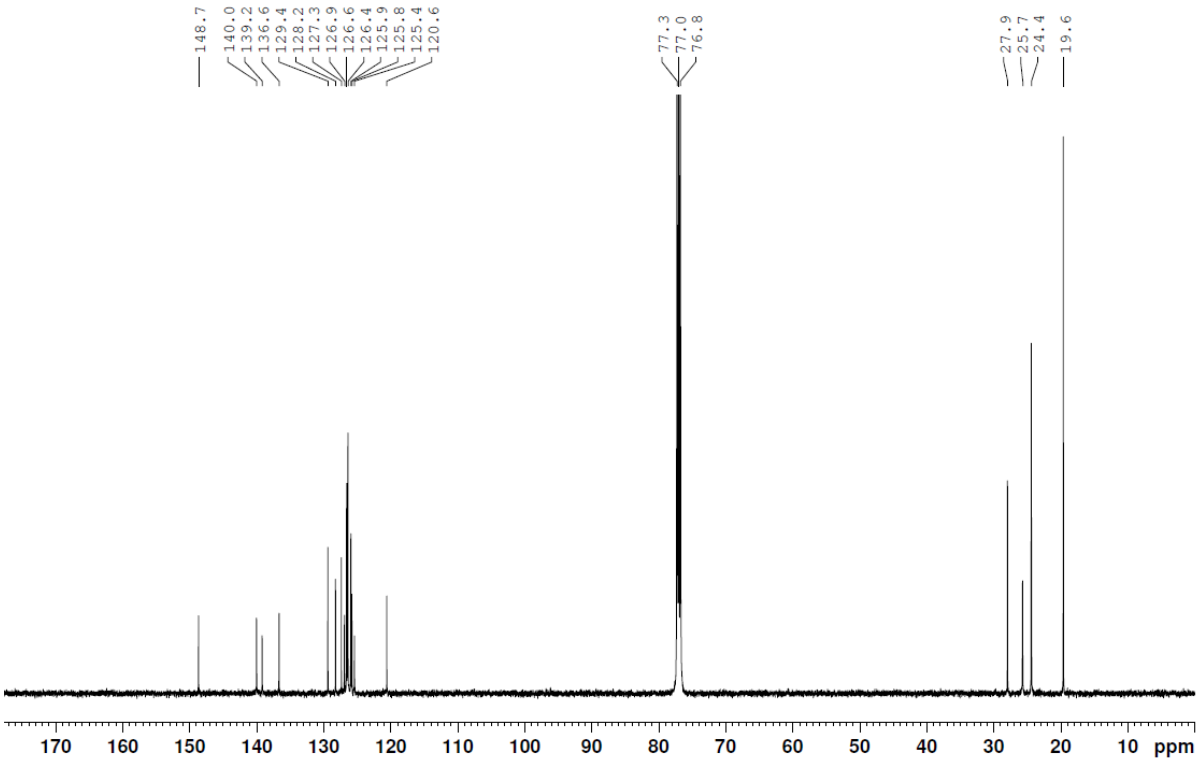

Figure 4.24: ^{13}C NMR spectrum of **SSS-6** in $CDCl_3$.

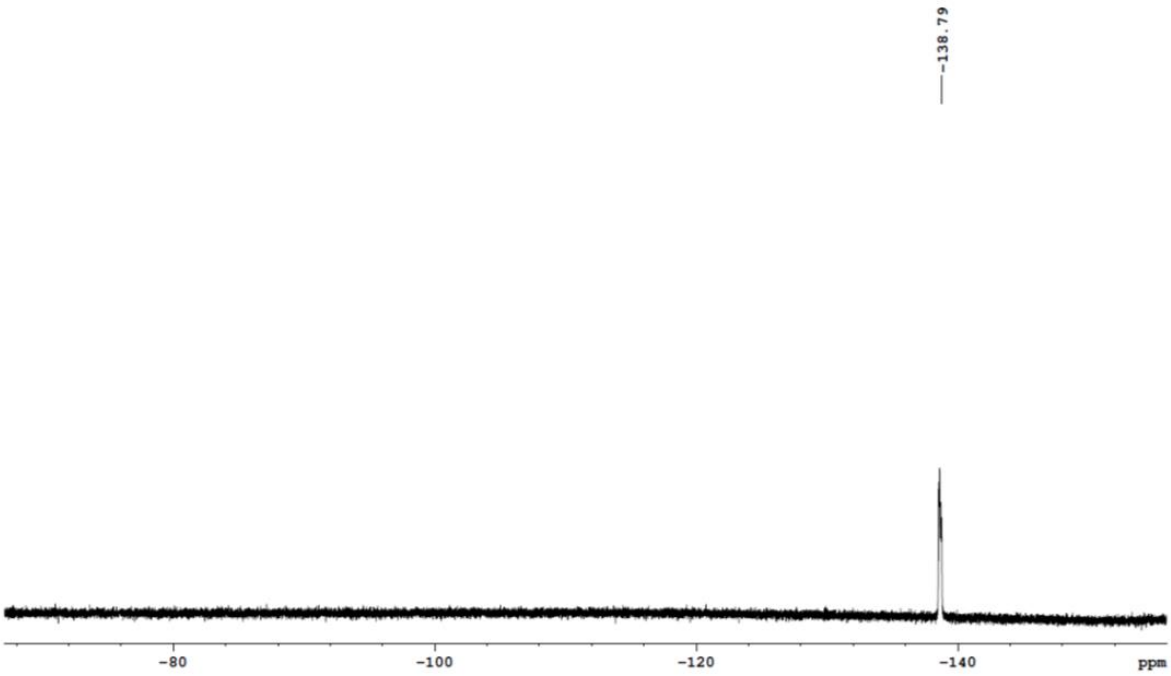

Figure 4.25: ^{19}F NMR spectrum of **SSS-6** in $CDCl_3$.

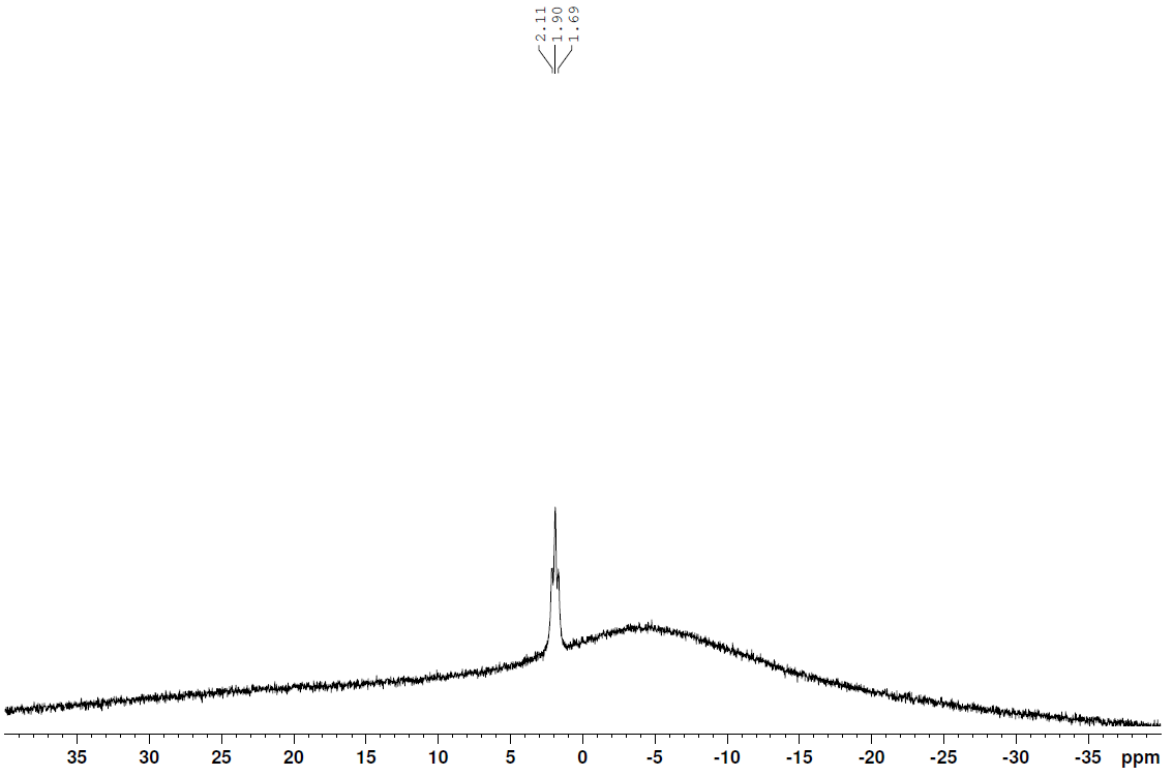

Figure 4.26: ^{11}B NMR of **SSS-6** in $CDCl_3$.

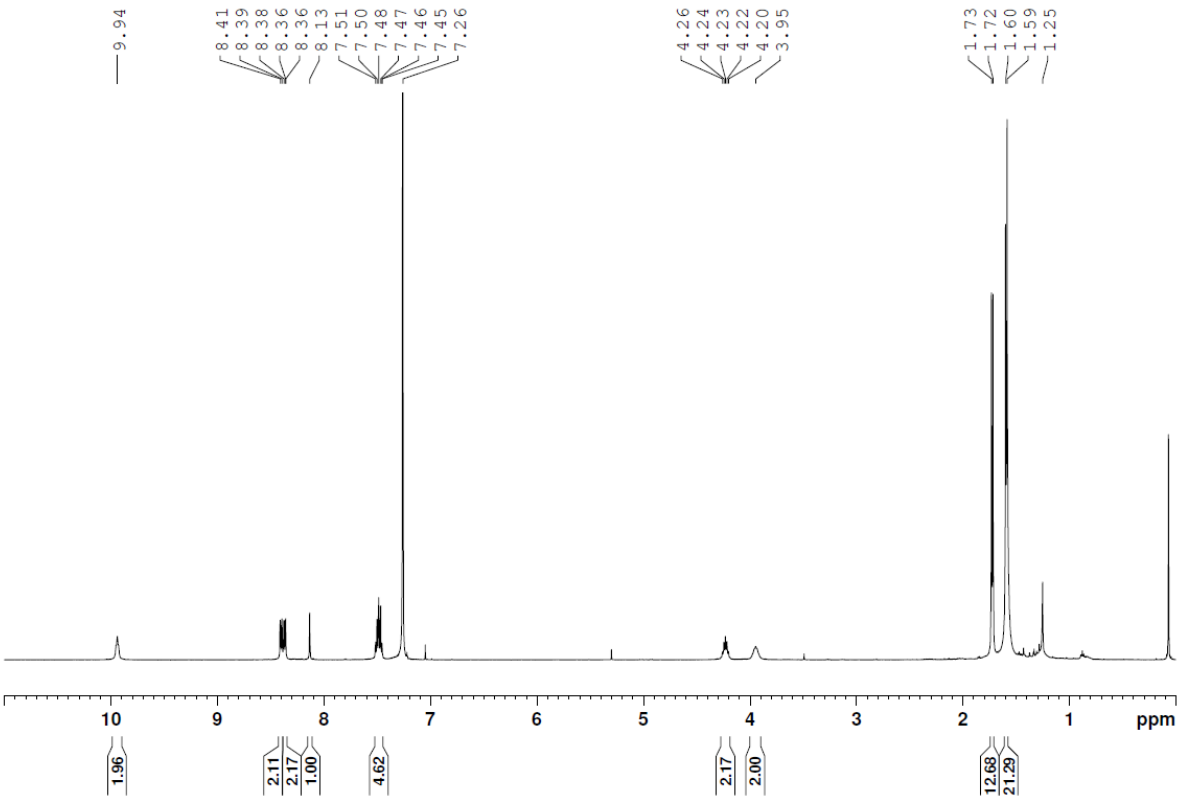

Figure 4.27. ^{1}H NMR spectrum of **SSS-7** in $CDCl_3$.

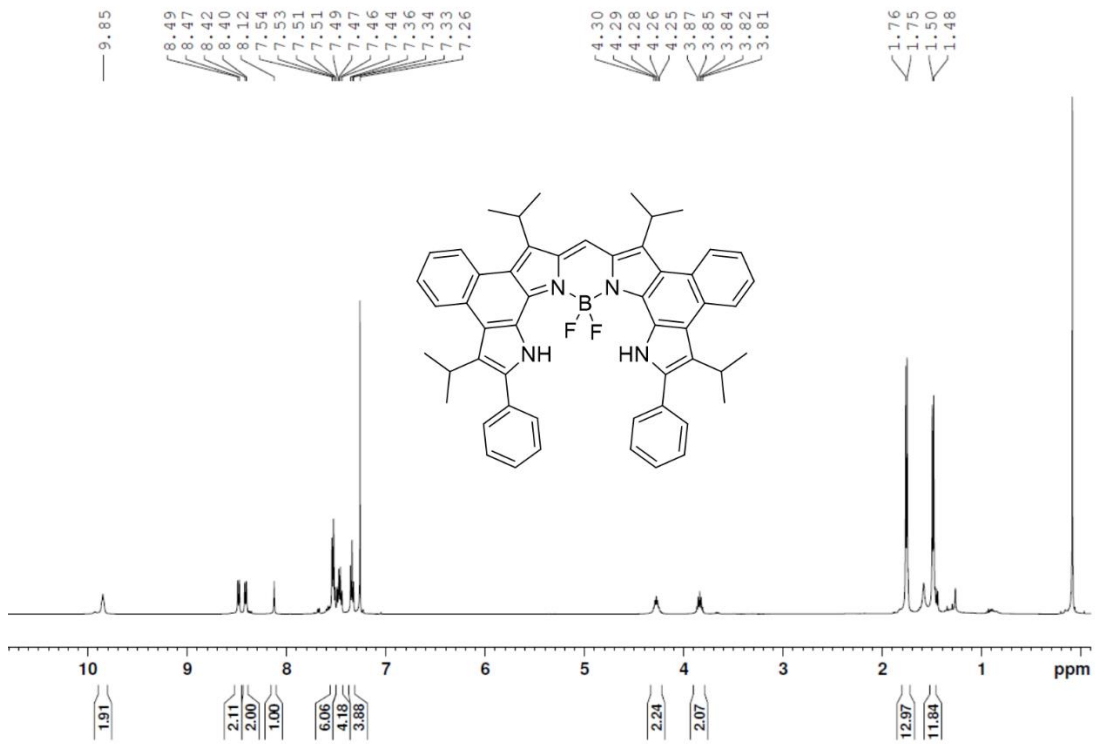

Figure 4.28: ^{1}H NMR spectrum of **SSS-8** in $CDCl_3$.

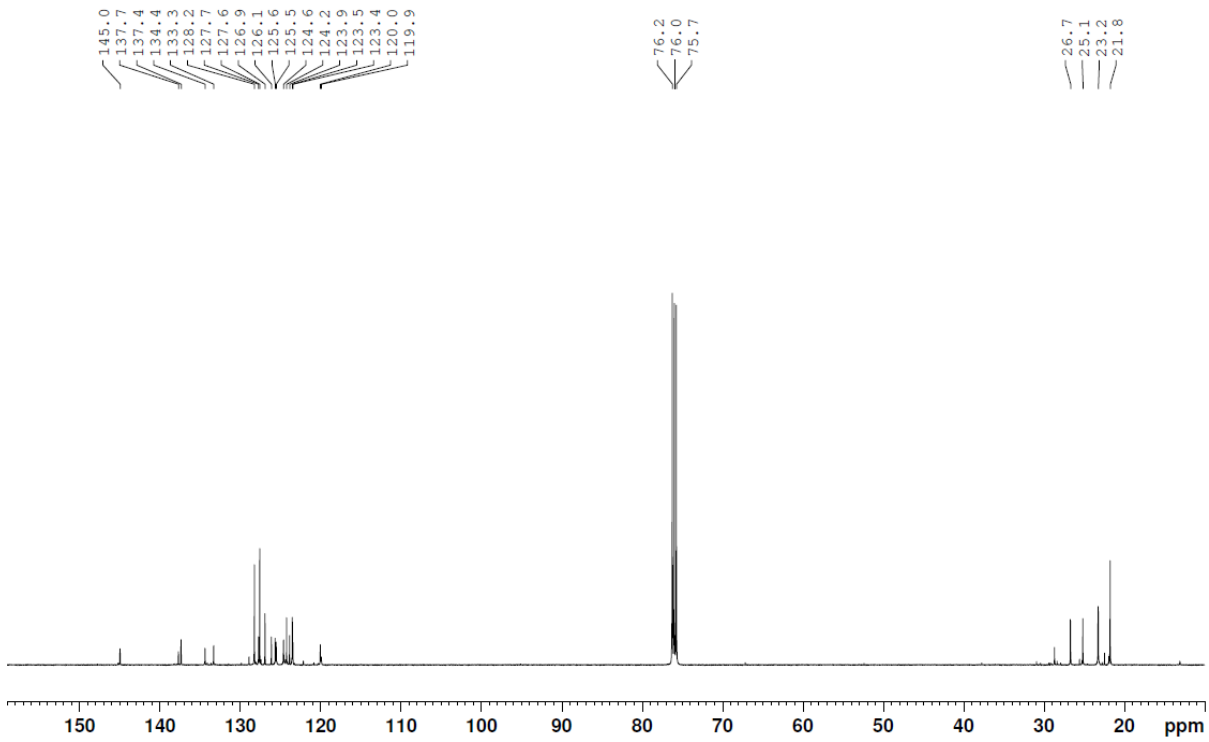

Figure 4.29. ^{13}C NMR spectrum of **SSS-8** in $CDCl_3$.

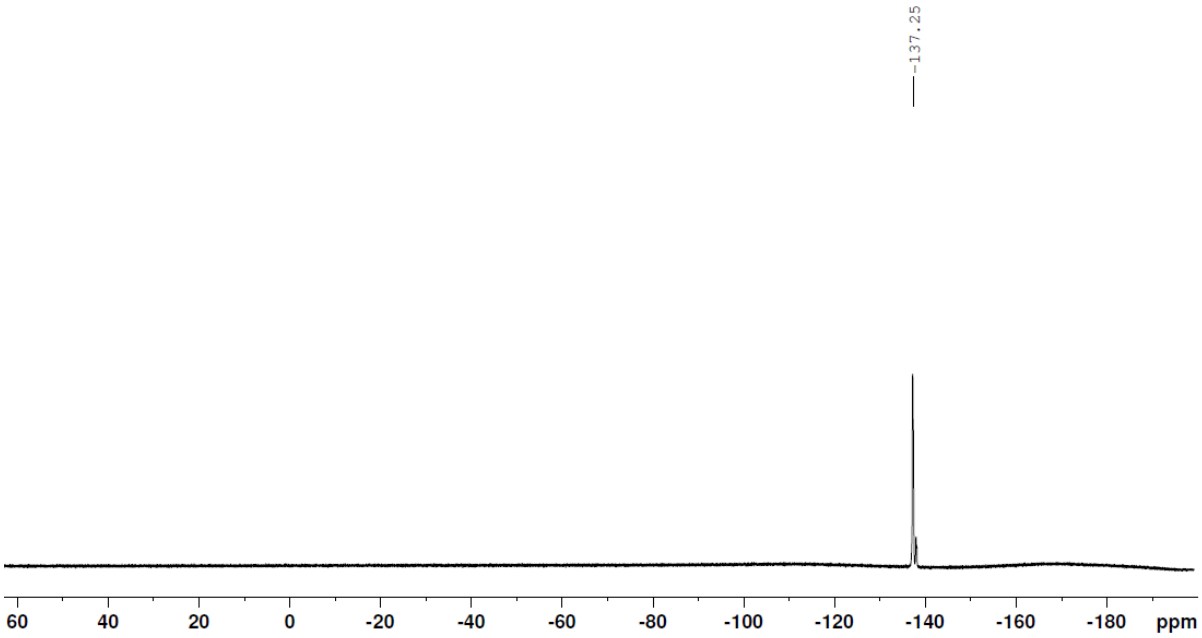

Figure 4.30: ^{19}F NMR spectrum of **SSS-8** in $CDCl_3$.

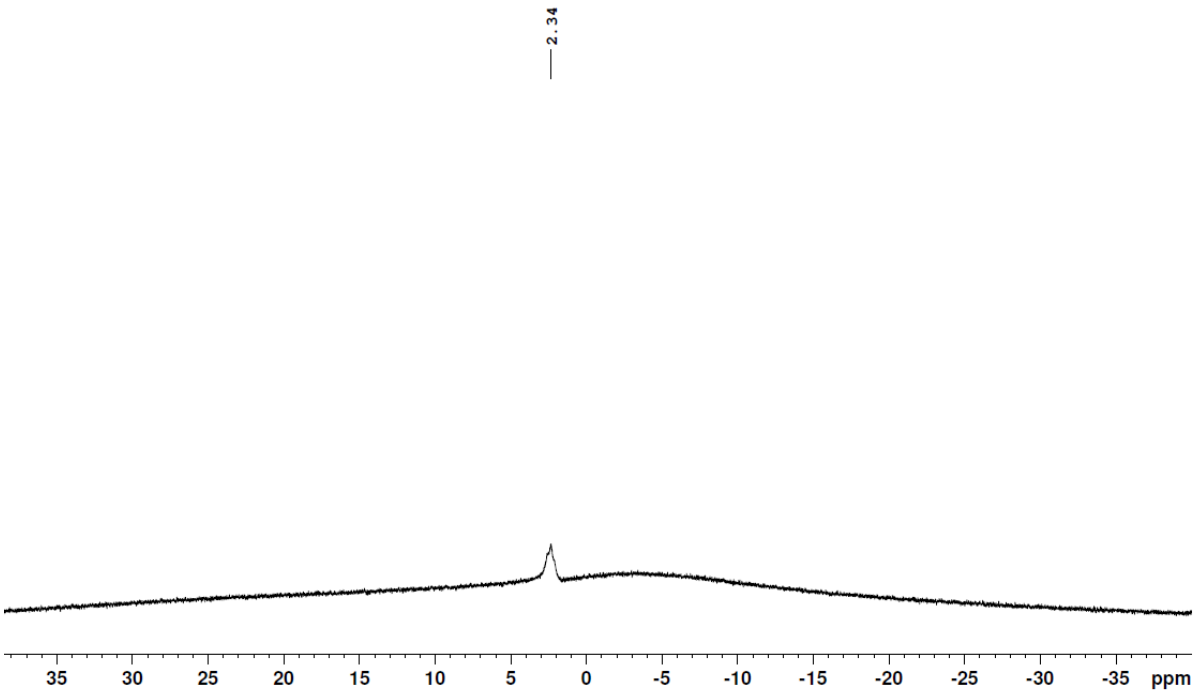

Figure 4.31: ^{11}B NMR spectrum of **SSS-8** in $CDCl_3$.

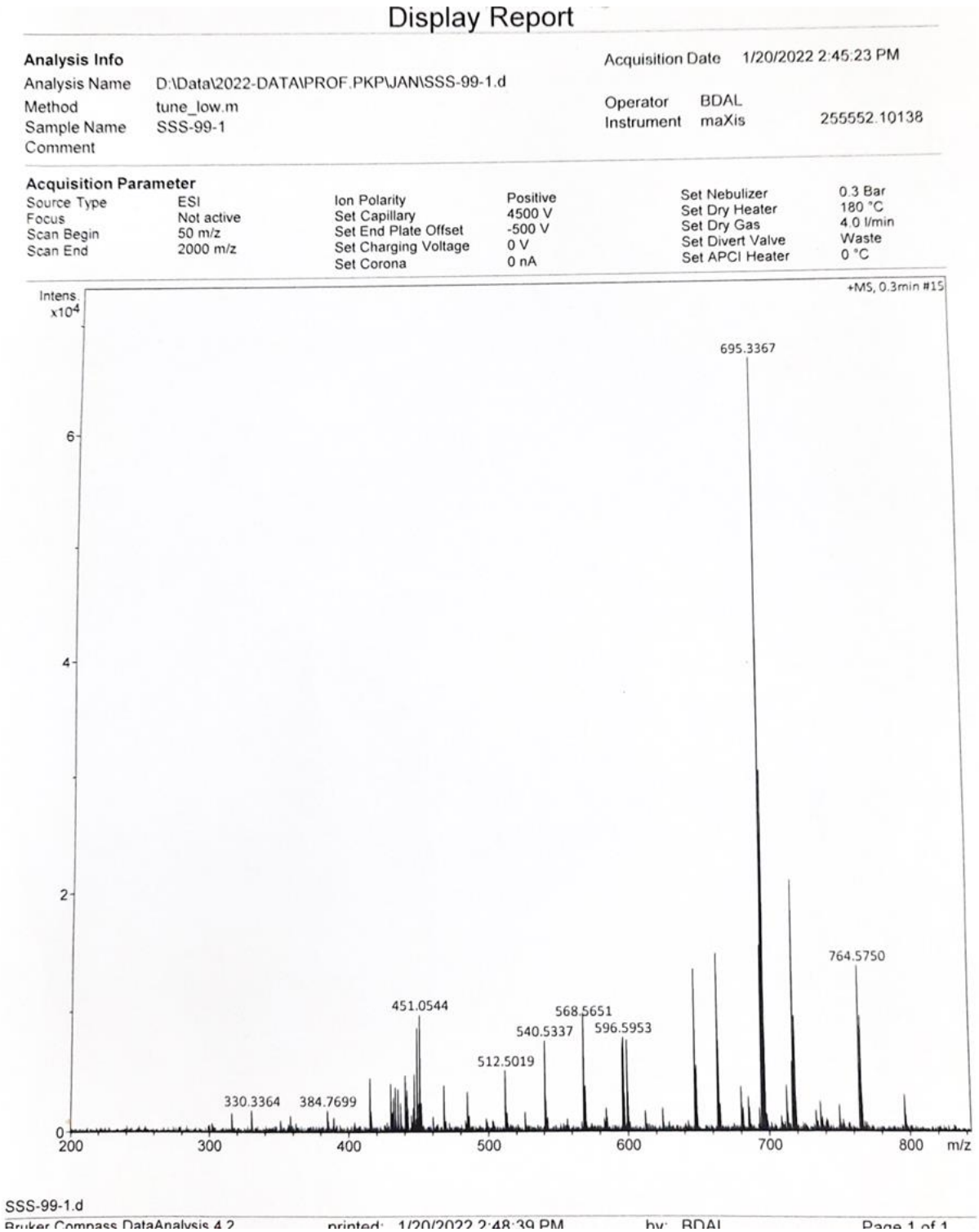

Figure 4.32. HRMS data of **SSS-4** (m/z calculated for $C_{43}H_{42}BF_2N_4O_2$ ($M+H^+$): 695.3368; found: 695.3367).

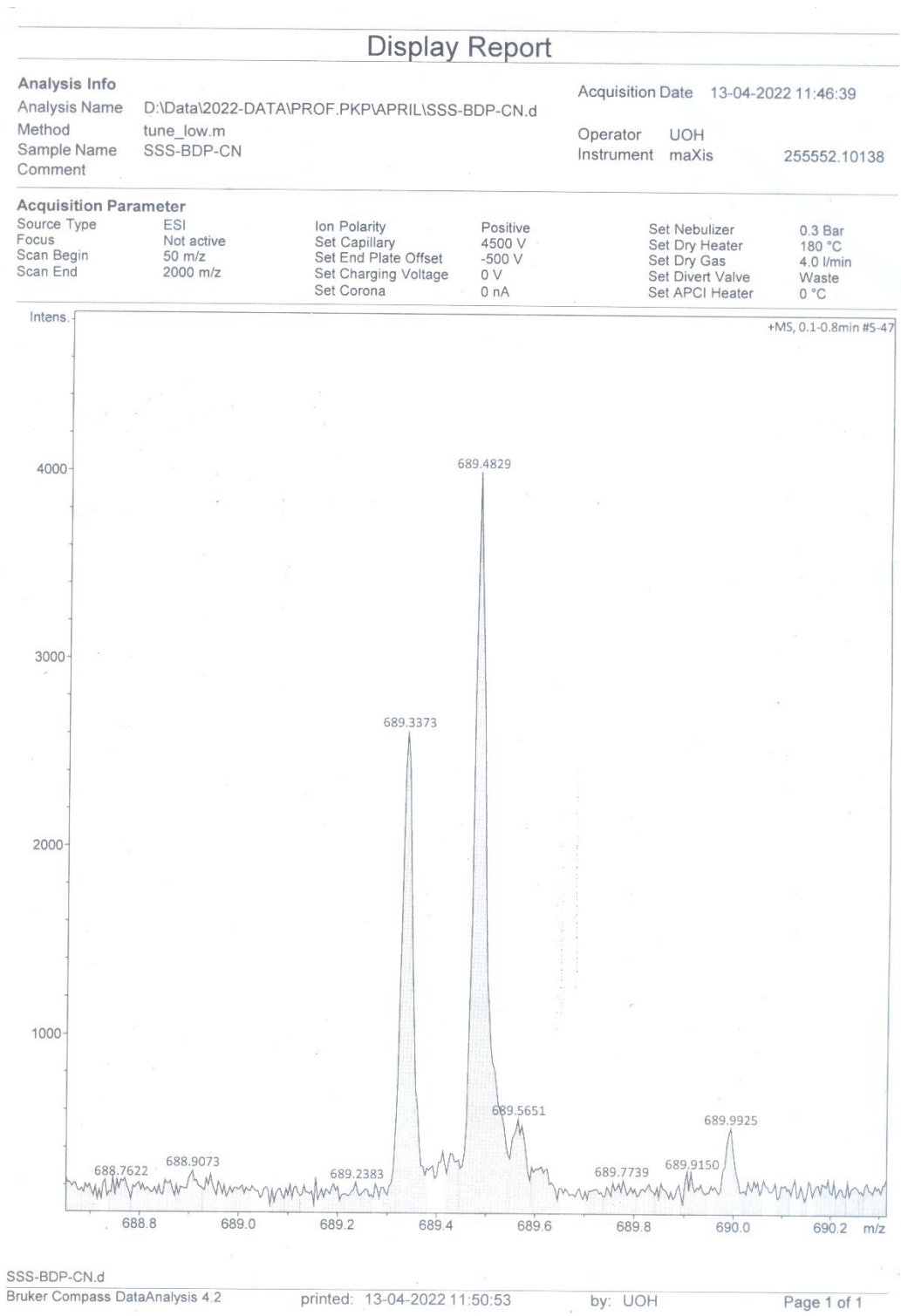

Figure 4.33. HRMS data of **SSS-5 (**m/z calculated for $C_{43}H_{40}BF_2N_6$ ($M+H^+$): 689.3376; found: 689.3373**)**.

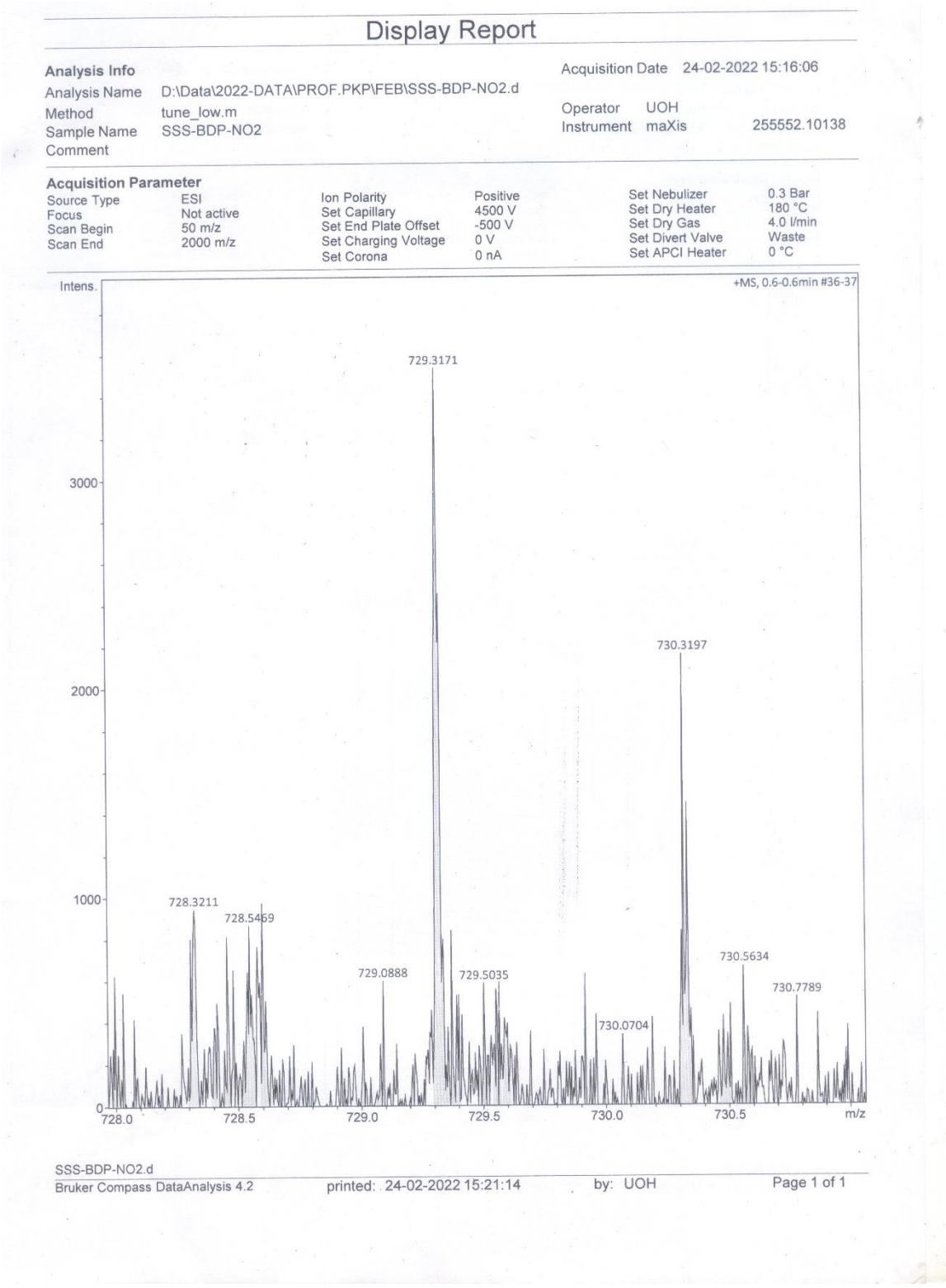

Figure 4.34: HRMS data of **SSS-6** (m/z calculated for $C_{41}H_{40}BF_2N_6O_4$ ($M+H^+$): 729.3172; found: 729.3171).

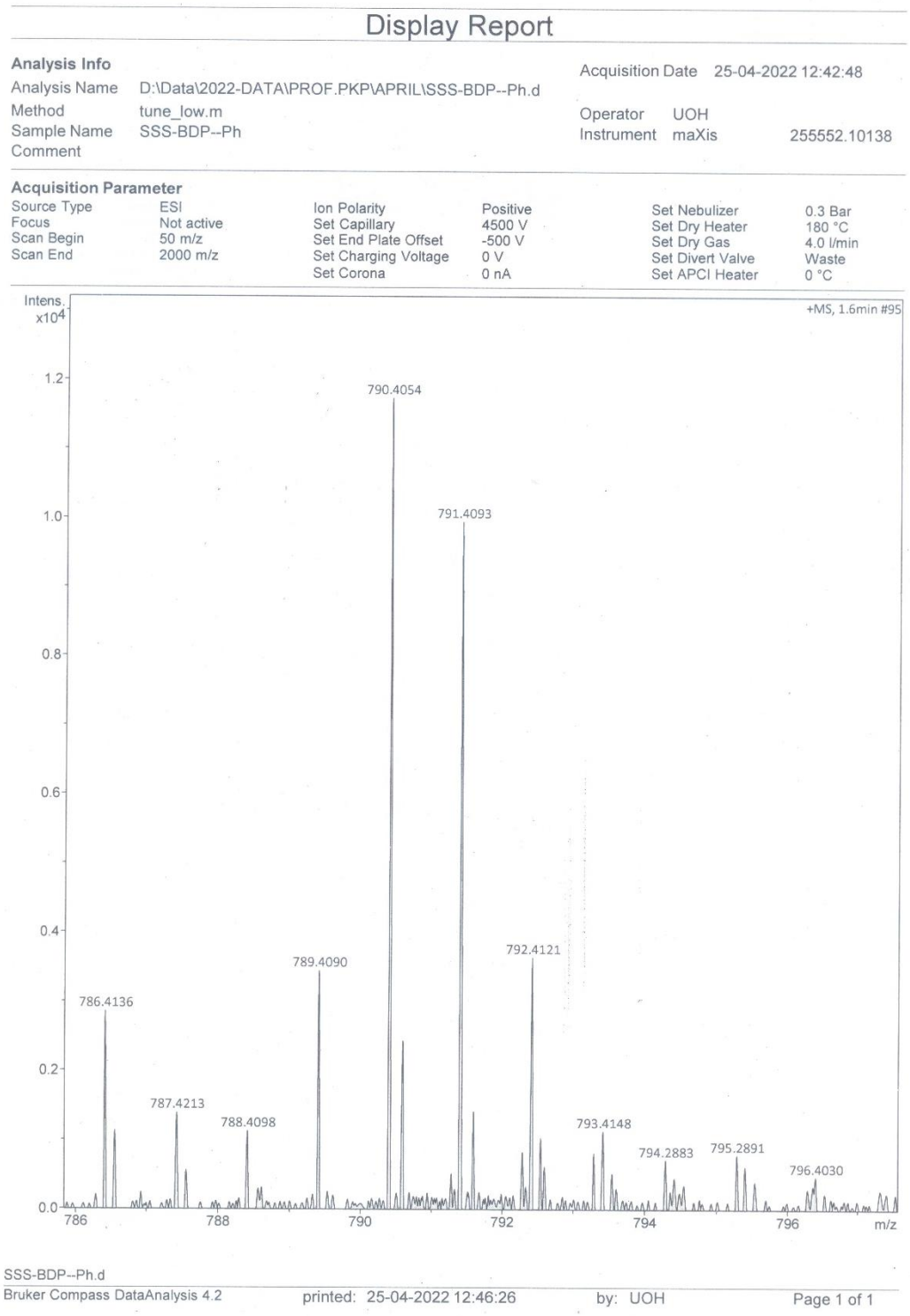

Figure 4.35: HRMS data of **SSS-8** (m/z calculated for $C_{53}H_{50}BF_2N_4$ ($M+H^+$): 791.4097; found: 791.4093).

Chapter 5

Bis(napthobipyrrolyl) methene derived helical BODIPY

5.1. Introduction

Nature has adopted chirality from the molecular level for biological system like L-amino acid as a major component for protein to right-handed double helical DNA or RNA.[1] Chiral molecules in general have a stereogenic centre or sp^3 carbon attached to 4 non-equivalent groups. Helical chirality is a completely different area to explore. They lack any stereogenic centre, instead exhibits axial chirality due to the presence of stereogenic axis. *ortho*-fused aromatic rings form helicene due to steric repulsion between terminal groups. Helicenes are stabilized by two types of driving forces.[2] If the molecule is rigid then steric repulsion is the main driving force for adopting helical conformation. In flexible molecules, noncovalent interactions like hydrogen bonding are responsible for helicity. When these forces balance torsional strain induced in the molecule due to twisting, then their helicene will be stable adopted conformation.

Historically, synthesis of the first aza-helicine, namely 7H-dibenzo[*c*,*g*]carbazole (**5.1**) and benzo[f]naphtho[2,1-*c*]cinnoline (**5.2**) was reported by Meisenheimer and Witte.[3] But the synthesis of enantio-enriched carbo[6]helicene in 1968 by Newman and Lednicer was a landmark discovery in helicene chemistry.[4] According to IUPAC nomenclature, helicenes are named as carbo[n]helicenes for n number of fused benzene.[5] For heterohelicene i.e., the heteroatom is incorporated into the skeleton of helicene, then it can be named as hetero[n]helicenes. Hetero here is referred to 'aza', 'oxa', 'phospa' or 'thia'. As the name aza[n]helicene can represent both pyrrolo- or pyrido- derivatives, it can be mentioned accordingly, pyrrolo[n]helicene or pyrido[n]helicene. According to the helicity rule, a left-handed helix can be denoted as *M*-helix and a right-handed helix as *P*-helix.

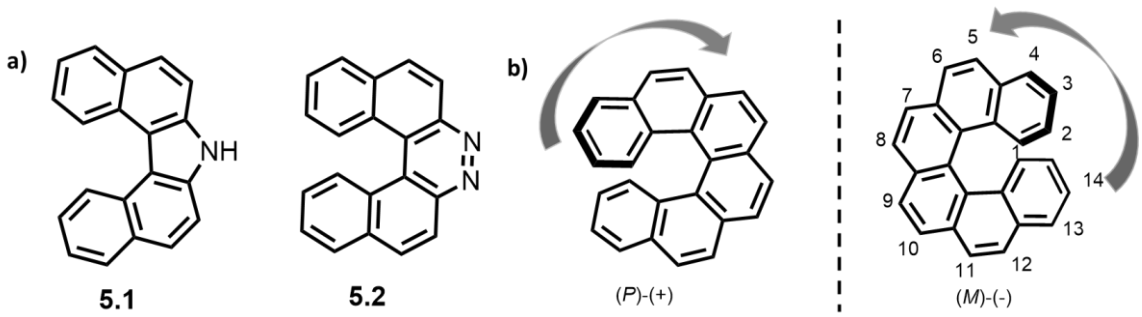

Figure 5.1: Structure of first aza-helicene; (*P*) and (*M*) chirality in carbo helicene.

As most of the helicenes are aromatic, its highly delocalized π-electrons furnish it with interesting optical properties. They mostly absorb and emit in the UV-Vis region and some polycyclic aromatic hydrocarbons (PAH) exhibit absorption maxima in NIR region. PAHs

emitting in NIR region needs very large π-extended systems like hexa-peri-hexabenzocoronene- based [7]helicene ($C_{111}H_{30}(CO)_2(^tBu)_8$) with λ_{em} at 610 nm (φ_f = 0.09)[6] or [9]helicene ($C_{198}H_{72}(^tBu)_6(^nhex)_{12}$) with λ_{em} at 870 nm (φ_f = 0.04).[7] As they are having such a large π-extended systems, bulkier groups are needed to incorporate into the skeleton for solubility. This makes synthesis lengthier. Chiral molecules having NIR emission can be explored for use in circularly polarized luminescence (CPL) devices.[8] Introduction of heteroatoms to core can tune optoelectronic properties due to their vacant orbital or lone pairs which can participate in conjugation. They can reduce the HOMO-LUMO energy gap.[5]

5.1.1. Pyrrole-based helicene

Heterohelicenes based on pyrrole are stabilized by inter or intramolecular hydrogen bonding due to higher number of NHs,[9] by anion binding[10] or metal complexation.[11] Sessler and co-workers synthesized one oligopyrrole amide, **5.3** which shows a helical conformation in solid state.[9a] The conformation was stabilized by ten intramolecular hydrogen bonding formed between two pyrrole NHs, amide NHs and nitrile nitrogens and isoindoline nitrogens. Crystal structure comprised of both the enantiomers (*P* and *M*).

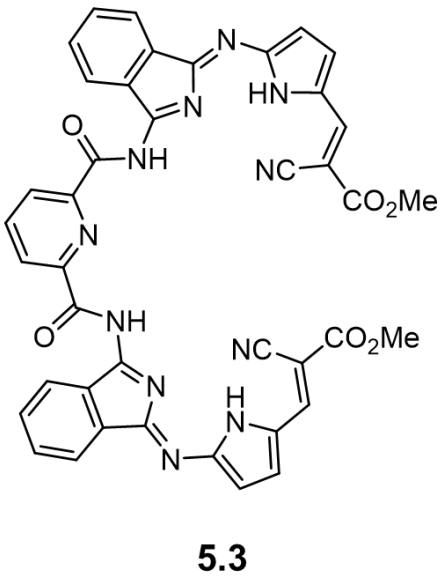

5.3

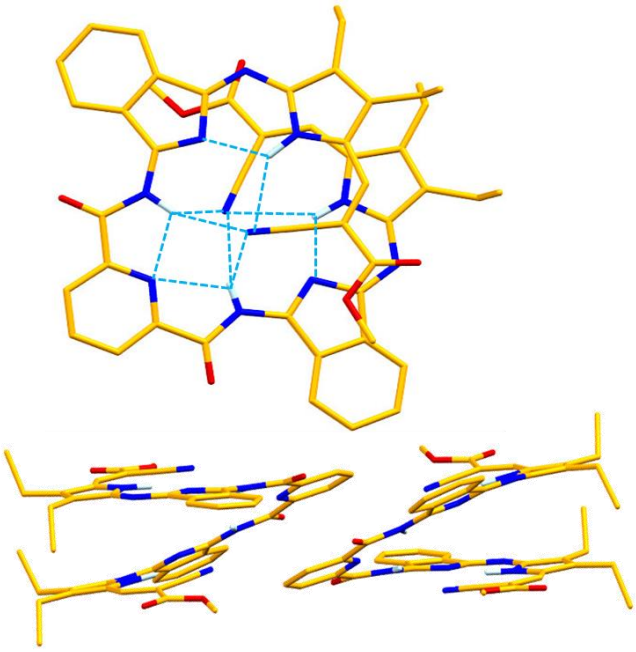

(*P*) (*M*)

Figure 5.2: Example of pyrrole based helicene stabilized by hydrogen bonding.[9a]

Guest responsive conformation change to a helix can be obtained owing to hydrogen bonding or van der Waals forces between host-guest. In this context, π-conjugated oligomers

show interesting response towards positively charged metal ions[12] or anions.[10b] They exhibit tunable optoelectronic properties. Oligomers exhibit electrostatic or hydrogen bonding interaction with anions like halides yielding different molecular assemblies. But there are few reports for anion driven helicene formation in case of pyrrole-based oligomers. Haketa and Maeda reported anion driven conformation change of BF_2 complex of oligomer **5.4** to helical conformation (**5.4.Cl**) by multiple inversions of pyrroles, which was otherwise a linear conformation (**scheme 5.1**).[10a] In solid state structure it shows a [2+2] type double helical assembly where two strands binds to chloride ions by hydrogen bonding (**figure 5.3**). Two strands of helicene are stabilized by π-π stacking. Crystal structure shows racemisation with equal intensity of *P* and *M* enantiomers. But, in solution phase it forms [1+1] binding with single helix due to lack of π-π stacking.

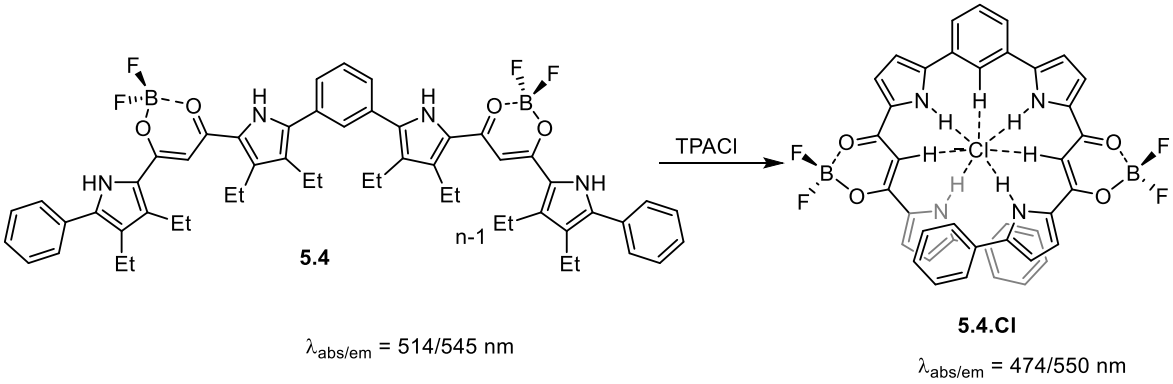

Scheme 5.1: Example of pyrrole based helicene stabilized by anion binding.

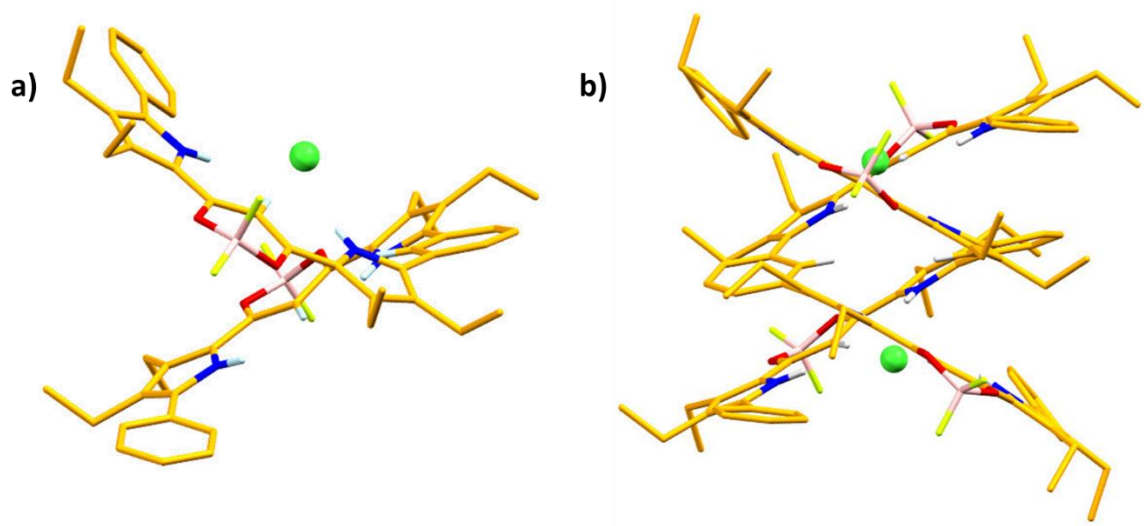

Figure 5.3: Example of pyrrole based helicene **5.4** stabilized by two chloride ions binding.

Setsune and co-workers reported monodirectional single helicates of long oligopyrrole consisting of six pyrroles coordinated to palladium. Coordination of Pd lead the oligopyrrole moiety has a chiral and monodirectional twist.[11b]

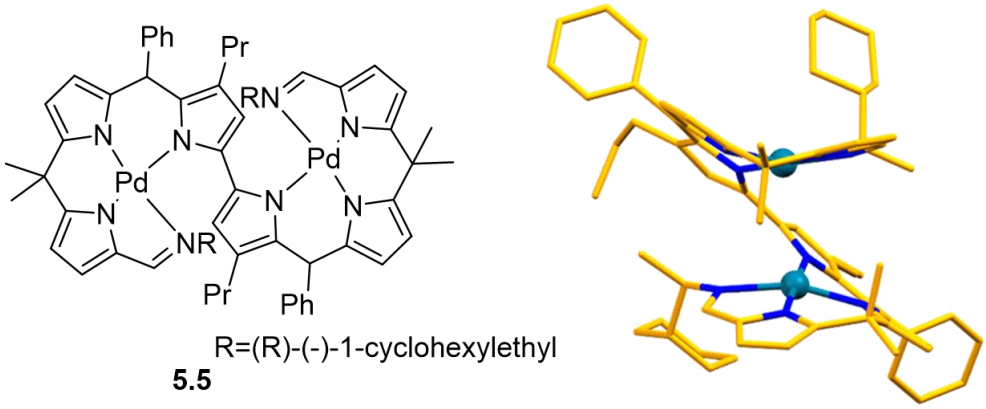

Figure 5.4: Examples of pyrrole based helicene stabilized by coordination.

5.1.1.1. BODIPY based helicates

As BODIPY dyes are promising candidates in material science due to its unique optical properties like sharp and intense absorption and emission with good fluorescence quantum yield, their combination with chirality have been explored for circularly polarized luminescent (CPL) materials also. Though BODIPY is an achiral system, studies are going on to induce chirality by attaching chiral substituents[13] or fusing chiral helicenes.[14] Few of the annulated BODIPYs show twisted structure owing to steric repulsion from which some have been studied for chiral behaviour. Naphtho[*b*]-fused BODIPY (**4.4**) shows deviation of planarity in crystal and exhibits a twist in the structure.[15] Dihedral angle between two fused naphthalene ring is 14.5° and that between two indole planes (AB and CD) is 12.6°. With this slight twist in the molecule **4.4** is considered as helical BODIPY and exhibits intersystem crossing (ISC).[16] It manifests long lived triplet state (492 μs) with triplet state quantum yield of 52%. Thus, it can act as a good photosensitizer for photodynamic therapy.

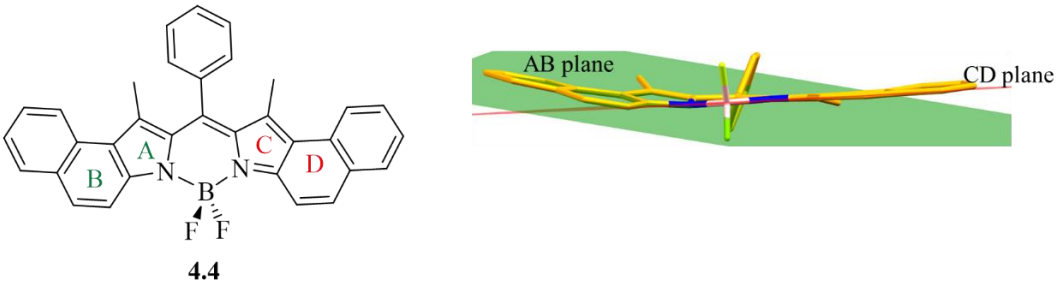

Figure 5.5: Naphthofused BODIPY showing helicity.

Incorporation of aza[7]helicene to a BODIPY framework induces chirality into BODIPY.[14] Crystal structure of **5.6** shows both (*P*) and (*M*) are arranged alternate to each other. Optical resolution through chiral column gave two fractions of different chirality which exhibits mirror image CD spectra. Alternatively, they converted racemic **5.6** to diastereomeric **5.7** by substituting binaphthyl unit onto boron. They can be separated with chiral HPLC. Then optically pure **5.7** can be converted to enantiomerically pure **5.6** through standard BF_2-complexation condition with $BF_3.OEt_2$.

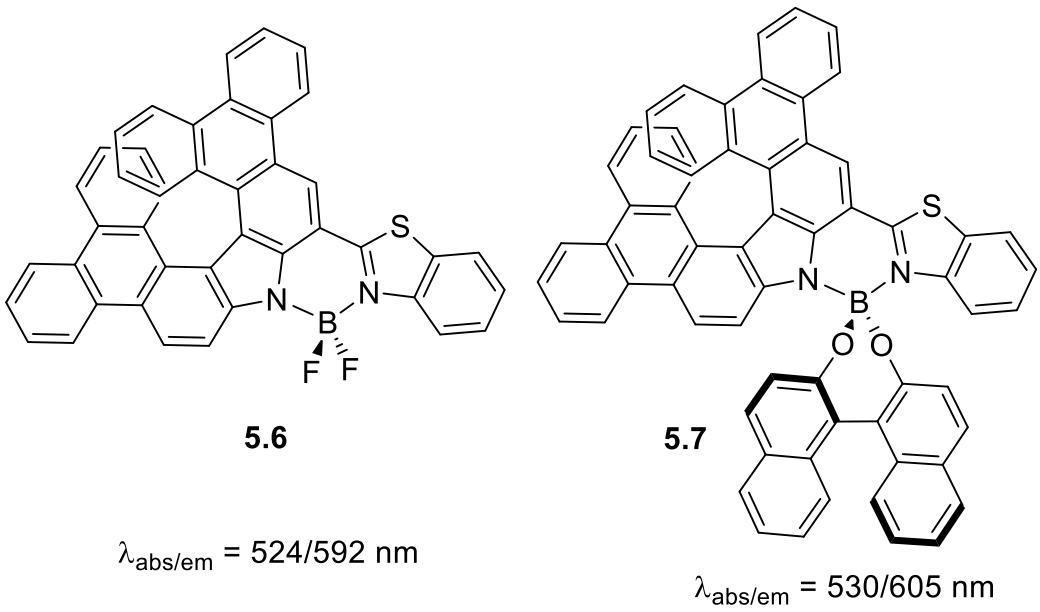

Figure 5.6: Examples of helical BODIPY showing chirality.

5.2. Research Goal

From the perspective of recent developments, helicenes can be incorporated to BODIPY frame work to induce chirality and their unique photophysical properties like intense absorption and emission with good extinction coefficient and fluorescence quantum yield can be used in material science. They can be tuned to have absorption and emission in NIR region which is expected to be better candidates for CPL emitting devices. But hardly there are any example where helical BODIPYs absorb in NIR region. Our aim is to explore naphthobipyrrole derived BODIPY having NIR absorption and emission, as a candidate for adopting helical conformation. Our serendipitous encounter with HCl salt of hexapyrrolic oligomer showing a helical conformation prompted us to synthesize its BF_2 complex which enhanced its emission property.

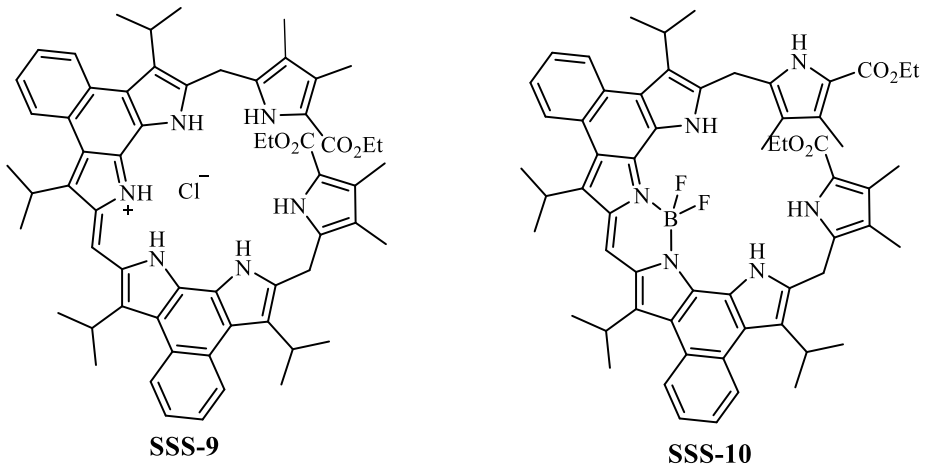

Figure 5.7: Structure of target molecules.

5.3. Result and Discussion

5.3.1. Synthesis of Hexapyrrole Hydrochloride Salt

SSS-9 was an unexpected byproduct while synthesizing tetrapyrrole (**Scheme 5.2**). *p*-TSA catalyzed condensation of diisopropyl naphthobipyrrole **A8** with **A13** results **SSS-11** along with byproducts **SSS-12** and **SSS-9**. But due to similar polarity and melting points of **SSS-11** and **SSS-12**, they could not be isolated for further use. **SSS-9** could be isolated with recrystallization from methanol. Initially, it was difficult to analyse the structure from ^{1}H NMR spectrum and HRMS data. Fortunately, we got the crystal for **SSS-9** which on SCXRD analysis revealed the structure.

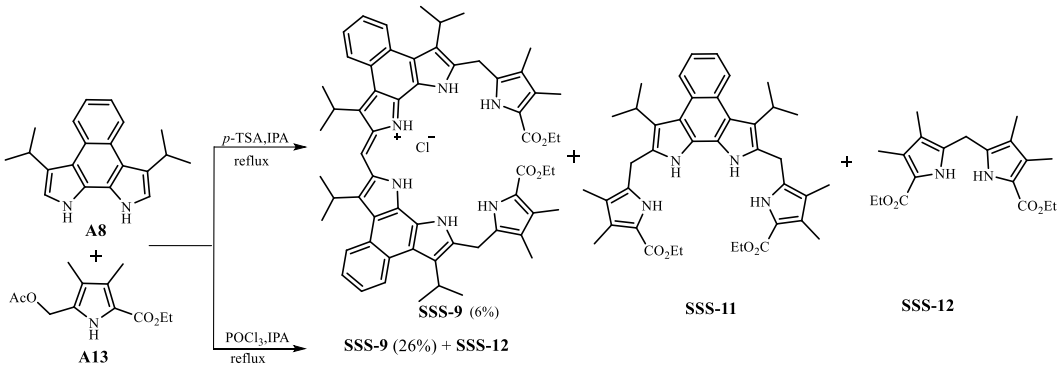

Scheme 5.2: Synthesis of **SSS-9**.

Interestingly, we found out it to be HCl salt of hexapyrrolic oligomer with helical conformation. Accordingly, all other spectroscopic data are compiled with. After structural conformation yield was calculated to be very less (6%). As the structure was stabilized by Cl^{-}

ion binding, we changed *p*-TSA catalyst to $POCl_3$ keeping other conditions identical. Then we got enhancement in the yield to 26%. But through this method **SSS-11** was not formed.

5.3.1.1. Characterization

^{1}H NMR spectrum of **SSS-9** exhibits 3 sets of deshielded NH protons at 12.60, 11.72 and 11.29 ppm. Along with 4 sets of naphthalene peaks, one singlet (1 H) appears at 7.95 ppm. Another singlet (4 protons) appears at 4.43 ppm along with *i*-Pr CH and ester CH_2 protons. This indicates one *meso*-carbon is oxidized while other two remain unoxidized. HRMS data match with M-Cl$^-$ mass.

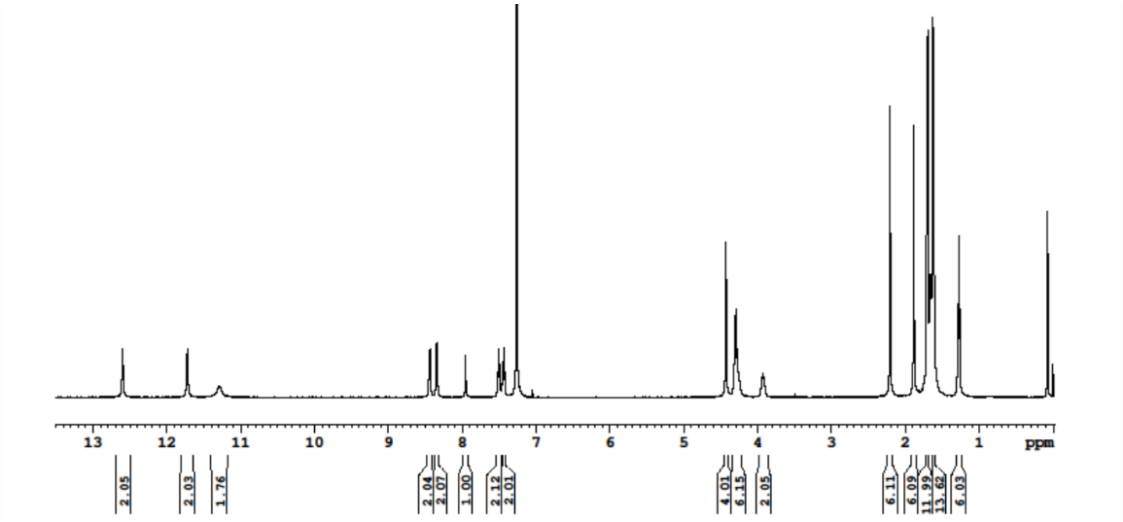

Figure 5.8: ^{1}H NMR spectrum of **SSS-9** in $CDCl_3$.

5.3.1.2. Optical properties

SSS-9 exhibits intense absorption at 758 nm accompanied by shoulder in higher energy side in chloroform. Absorption spectrum of **SSS-9** is highly solvent dependent (**Table 5.1**). While in hexane, it exhibits a more sharp and red shifted absorption λ_{abs} at 762 nm with high molar extinction coefficient (ε = 1.9 x 10^5 $M^{-1}cm^{-1}$), with increasing polarity it shows hypsochromic shift with reduced absorption coefficient. But, in highly polar solvents like methanol it manifests a spectrum which loses its characteristic sharp and intense peak, and appears as a broad and less intense (ε = 5 x 10^4 $M^{-1}cm^{-1}$) peak at 662 nm. This may be attributed to solvent induced deprotonation of **SSS-9**. To check for this hypothesis, we examined changes in spectrum of **SSS-9** with addition of excess of NEt_3 in chloroform. It resulted in similar type of spectra that obtained in methanol. We examined fluorescence property of **SSS-9**, which shows it to be non-emissive.

Table 5.1: Summary of absorption properties of **SSS-9**.

Sl. No	Solvent	λ_{abs} (nm)	Molar Extinction Coefficient ε ($M^{-1}cm^{-1}$ x 10^5)	FWHM (cm^{-1})
1	Hexane	762	1.91	623
2	Toluene	758	1.67	698
3	$CHCl_3$	758	1.70	808
4	DCM	752	1.58	855
5	Acetonitrile	739	0.27	1075
6	Methanol	660	0.41	2745
7	DMF	662	0.56	2788

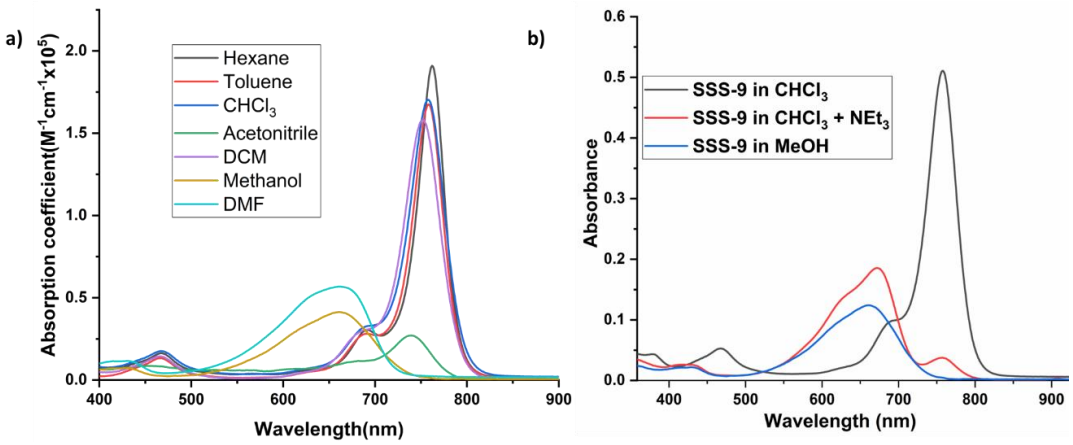

Figure 5.9: Changes in UV-Vis-NIR spectra of **SSS-9**: a) in different solvents; b) in $CHCl_3$ upon addition of NEt_3.

5.3.1.3. Structural Analysis

SCXRD structure reveals a helical conformation for **SSS-9**. Structure shows two naphthobipyrroles tethered together by a *meso* methine bridge and two dimethyl pyrrole esters are attached to both end of the bisnaphthobipyrrolyl methene with two *meso* methane bridge. The conformation is stabilized by six intramolecular hydrogen bonding, four between naphthobipyrrole NHs and Cl^- ion, and other two between ester carbonyl oxygens and pyrrole NHs. There exists a twist in the *meso* methine bridge for which the structure adopts helical conformation. Dihedral angle between two naphthobipyrrole is 20.66°. Chloride ion is positioned at 3.18 Å from the inner two nitrogens (N4) and at 3.09 Å from outer two nitrogens (N5) of bisnaphthobipyrrolyl methene. Outer two pyrrole esters are facing each other with

carbonyl oxygen directly above pyrrole nitrogen with a O-N distance of 2.82 Å which can be considered as outer pitch of the helix.

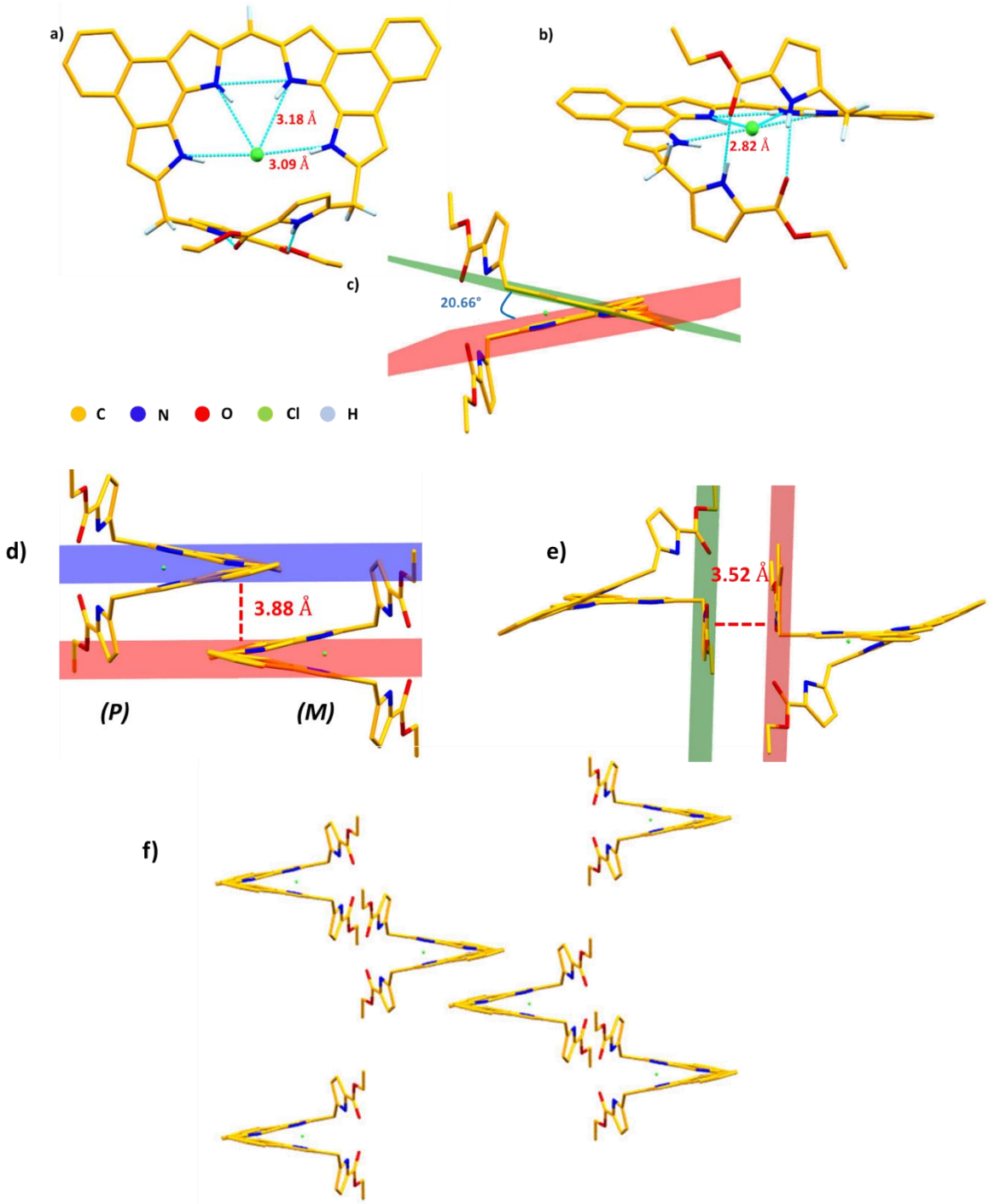

Figure 5.10: SCXRD diagram of **SSS-9** displaying: a) front view; b) side view showing hydrogen bonds; c) side view showing dihedral angle between naphthobipyrroles; d) π-π stacking of BODIPY units; e) outer pyrroles; f) packing diagram (peripheral *i*-Pr are removed for clarity).

Packing diagram demonstrates both *P* and *M* helix are placed alternately making the system racemic mixture. There exist π-π stacking interaction between outer pyrroles of two oppositely placed helices with interplanar distance of 3.52 Å and between two bisnaphthobipyrrolylmethene planes with interplanar distance of 3.88 Å.

5.3.2. BF_2 complexation of SSS-9

Attempt to further oxidize **SSS-9** failed presumabley due to involvement of pyrrole NHs in hydrogen bonding, which will be disrupted once oxidized. **SSS-9** was treated with NEt_3 and subsequently with $BF_3.OEt_2$ to convert it to its corresponding mono-BF_2 complex **SSS-10** in 60% yield. Hoping for better yield, we tried alternate route of acid mediated condensation of **A10** with acetoxy pyrrole derivative **A13**. Though we were successful in getting the desired product, but overall yield calculated from naphthobipyrrole were less for this synthetic route. So, strategy of going through hexapyrrole hydrochloride as building block is more suitable due to less no of steps involved and higher overall yield. The complex was fully characterized with standard spectroscopic characterization techniques like ^{1}H NMR, ^{13}C NMR, ^{19}F NMR, UV-Vis-NIR, fluorescence spectroscopy, HRMS and SCXRD analysis.

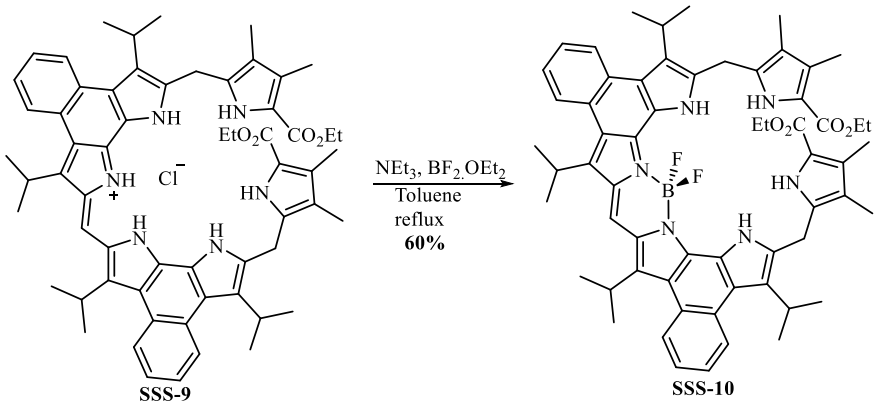

Scheme 5.3: Synthesis of **SSS-10** from **SSS-9**.

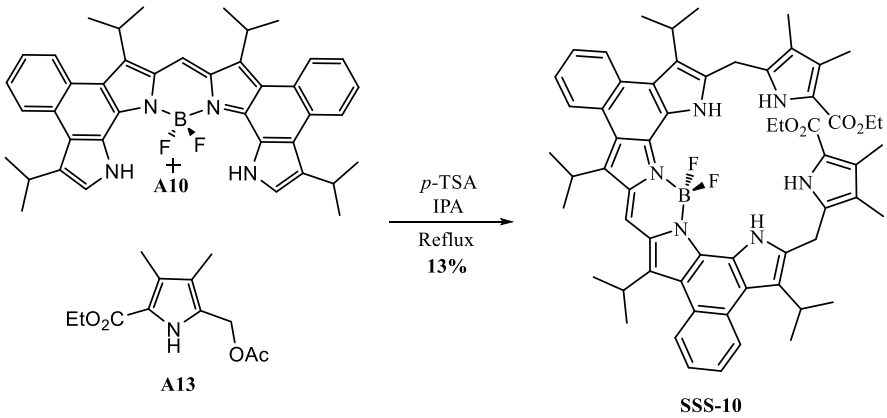

Scheme 5.4: Synthesis of **SSS-10** from bis(naphthobipyrrolyl)BODIPY.

5.3.2.1. Characterization

^{1}H NMR spectrum of **SSS-10** doesn't differ much from **SSS-9** except for NHs. Two non-equivalent NHs are present in the system. Naphthobipyrrole NHs lose hydrogen bonding due to loss of Cl^- ion. Two NHs appear at 10.51 and 9.41 ppm, which are upfield shifted relative to **SSS-9**. HRMS data also matches corresponding to molecular ion peak, m/z = 996.5285.

5.3.2.2. Optical Properties

SSS-10 exhibits similar absorption maxima as **SSS-9** but with enhanced molar extinction coefficient and small FWHM as typically seen in BODIPYs. We carried out solvent dependent absorption and emission for **SSS-10**, which has been summarized in **Table 5.2**.

Table 5.2: Summary of photophysical properties of **SSS-10**.

Solvents	Absorption			Emission[a]			
	λ_{abs} (nm)	Molar Extinction Coefficient ε ($M^{-1}cm^{-1}$x 10^5)	FWHM (cm^{-1})	λ_{em} (nm)	Stokes Shift (cm^{-1})	FWHM (cm^{-1})	τ_f (ns)
Hexane	758	2.92	419	763	86	463	3.65
Toluene	759	2.57	541	768	155	593	3.36
$CHCl_3$	757	2.31	633	767	173	698	-
DCM	754	2.01	708	769	259	728	-
Acetonitrile	756	1.99	834	765	155	837	-
Methanol	745	1.93	752	766	368	750	-
DMF	750	1.65	845	775	430	831	-
DMSO	761	1.86	852	782	353	885	2.65

[a] λ_{exc} = 670 nm

Unlike **SSS-9**, it doesn't show large solvatochromism for ground state absorption spectra. But effect of solvent polarity is more noticeable on emission spectra. It shows a positive solvatochromism, where emission maxima are red shifted in polar solvents like DMF and DMSO. This indicates there is an excited state stabilization in polar solvents. Stokes shift is relatively more in polar solvents like methanol, DMF and DMSO. However, singlet state lifetimes are reduced in polar solvents compared to nonpolar solvents. Though there is no extra extended conjugation relative to **A10,** still **SSS-10** exhibits large red shift in absorption and emission maxima which may be attributed to large structural distortion caused from planarity to helicity.

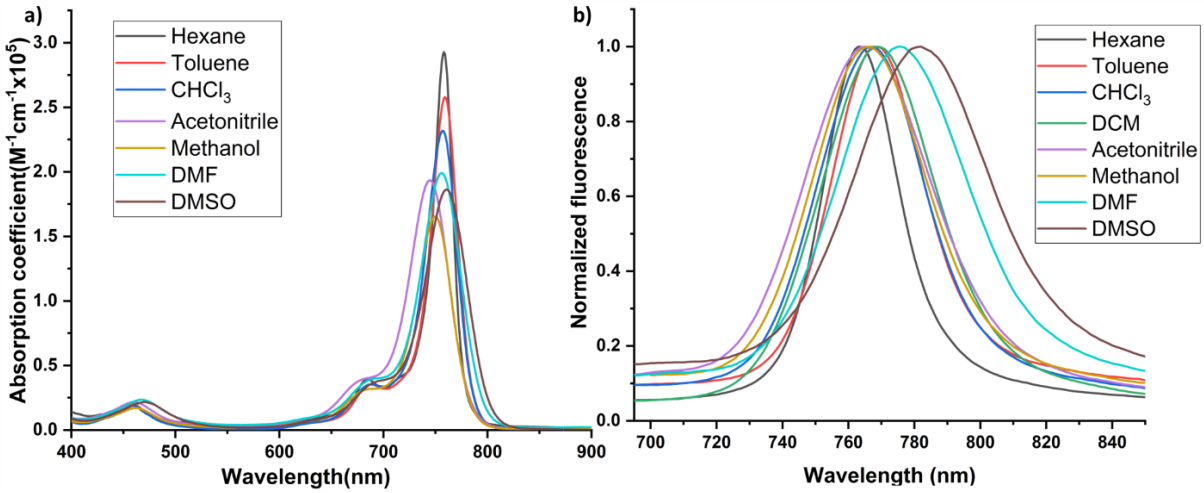

Figure 5.11: a) UV-Vis-NIR absorption spectra; b) emission spectra of **SSS-10** in different solvents.

5.3.2.3. Structural Analysis

Crystal structure of **SSS-10** displays a helical conformation with greater distortion relative to **SSS-9**. Naphthobipyrroles are more twisted with dihedral angle of 45.18°. Two hydrogen bonds are present between oppositely faced pyrrole NHs and ester carbonyl oxygen with NH⋯O distances of 2.86 and 2.87 Å. Napthobipyrrole NHs are also experiencing a weak

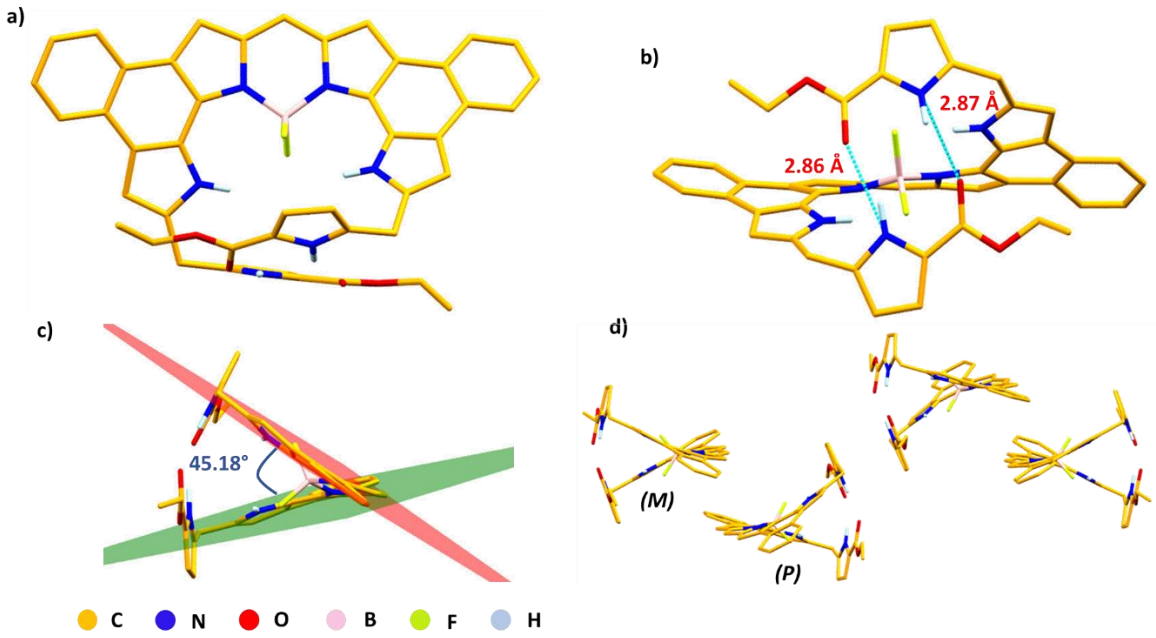

Figure 5.12: SCXRD structure of **SSS-10**: a) front view; b) side view showing hydrogen bonding; c) side view showing dihedral angles between naphthobipyrroles; d) packing diagram (peripheral substitutions are removed for clarity).

hydrogen bonding with fluorine. Crystal structure shows both *P* and *M* helices are present in the crystal with an alternate arrangement.

5.3.2.4. Theoretical calculation

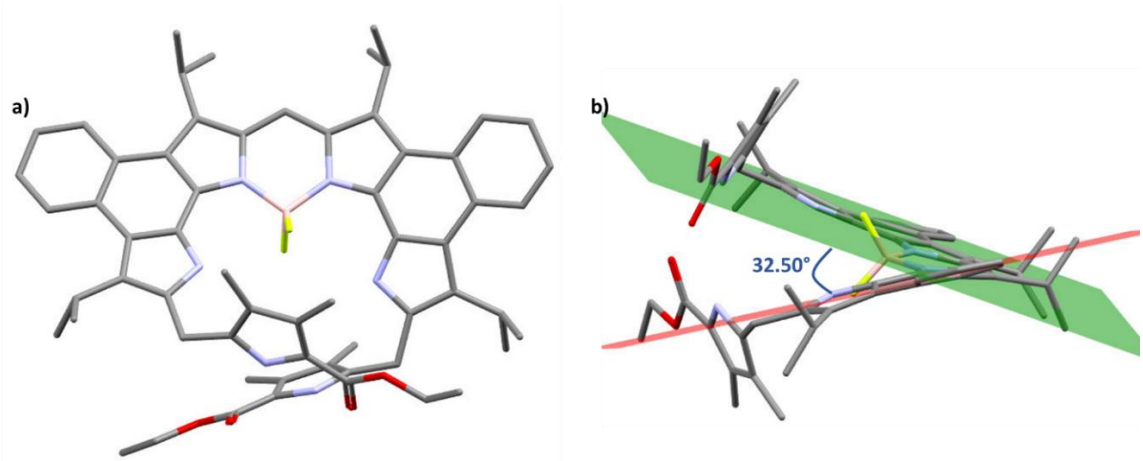

Figure 5.13: Gas phase optimized structure of **SSS-10**: a) front view and b) side view showing dihedral angle between naphthobipyrroles (Optimized by DFT/B3LYP/6-31G(d,p); hydrogens are removed for clarity).

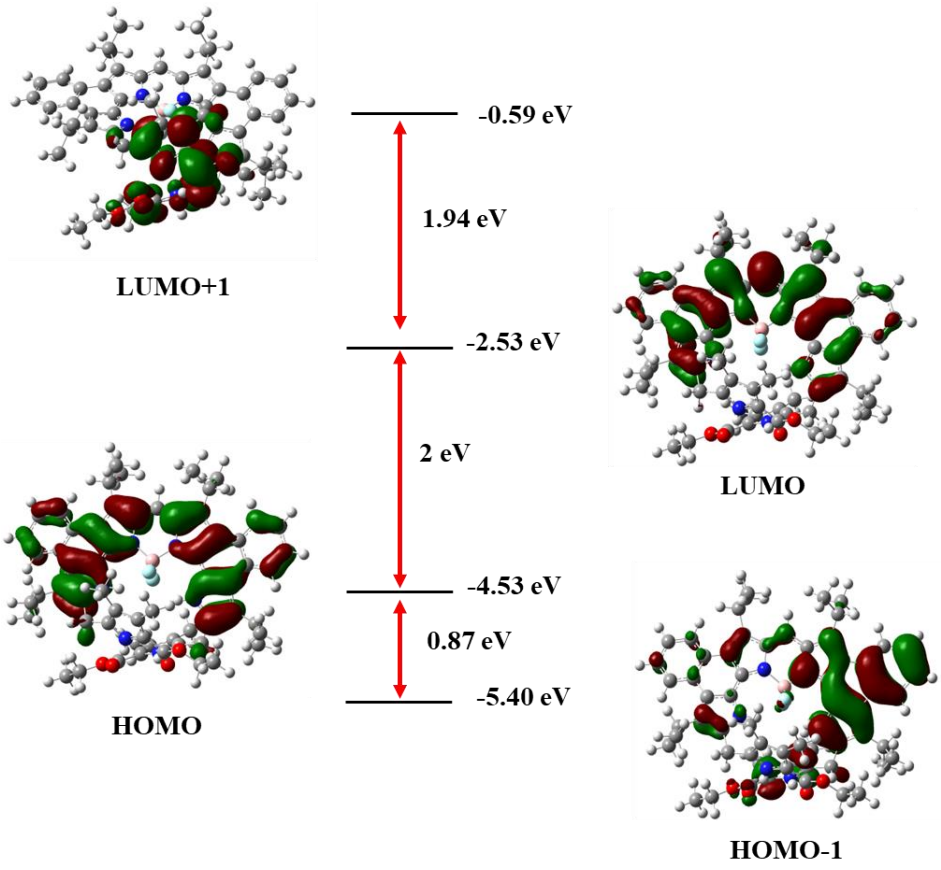

Figure 5.14: Frontier orbital diagram of **SSS-10** with their energies.

Gas-phase optimization of **SSS-10** resembles the solid state structure but the dihedral angle between the naphthobipyrroles is reduced in the optimized structure to 32.5°. Pyrrole NH and ester carbonyls displays similar N···O distance of 2.87 and 2.88 Å owing to hydrogen bonding. **Figure 5.14** shows frontier orbital diagram of **SSS-10**, Where both HOMO and LUMO coefficients are concentrated on bis(naphthobipyrrolyl)methene unit. It shows a reduced HOMO-LUMO energy gap compared to α-free bis(napthobipyrrolyl) BODIPY **A10** (2.05 eV) possibly due to the inherent distortion.

5.4. Conclusion

In conclusion, we have realized a novel naphthobipyrrole derived oligomer as its hydrochloride salt and BF_2 complex with a helical conformation and the latter absorbs and emits in NIR region. They consist of racemic mixture, and BF_2 complex can be further explored to achieve chirality and can serve as a potential candidate in CPL emitting devices.

5.5. Experimental

Synthesis of SSS-9

A8 (200 mg) and **A13** (247 mg) were taken in two necked RB fitted with a condenser. Then degassed isopropanol was added to it under N_2 atmosphere. After dissolving the compounds, $POCl_3$ (63 µL) was added and refluxed for 4-5 h. Then it was cooled to room temperature and quenched with excess triethyl amine. Precipitate formed was filtered and washed with cold methanol. The residue was recrystallised with chloroform and methanol to obtain the desired product as pure green colour solid. Yield obtained: 26%

^{1}H NMR (500 MHz, $CDCl_3$) δ in ppm: 12.60 (s, 2H), 11.72 (s, 2H), 11.29 (br, 2H), 8.45 (d, J=8.03 Hz, 2H), 8.35 (d, J=8.09 Hz, 2H), 7.95 (s, 1H), 7.52 (t, J=7.22 Hz, 2H), 7.45 (t, J=7.55 Hz, 2H), 4.43 (s, 4H), 4.32 (m, 6H), 3.94 (m, 2H), 2.21 (s, 6H), 1.88 (s, 6H), 1.71 (d, J=7.07Hz, 12H), 1.63 (d, J=7.16 Hz, 12H), 1.29 (t, J=7.01 Hz, 6H). ^{13}C NMR (125.7 MHz, $CDCl_3$) δ in ppm: 163.3, 148.0, 137.1, 136.9, 130.8, 129.3, 126.9, 126.4, 125.9, 125.7, 125.5, 124.4, 121.5, 119.5, 118.1, 117.6, 116.9, 59.7, 27.3, 26.1, 25.2, 23.8, 22.7, 14.5, 11.0, 8.9. HRMS (ESI+): m/z calculated for $C_{61}H_{69}N_6O_4$ (M-Cl^-): 949.5380, found: 949.5383.

Synthesis of SSS-10

SSS-9 (10 mg) was dissolved in dry toluene (7 mL) under N_2 atmosphere. After it gets dissolved, triethyl amine (46 µL) was added to it and stirred at room temperature for 15 min. To this, $BF_3.OEt_2$ (80 µL) was added and refluxed for 30 min. After that the reaction mixture was cooled to room temperature and washed with water to remove any salt formed. Organic layer was passed over anhyd. Na_2SO_4 and concentrated under reduced pressure. It was purified by silicagel column chromatography (EtOAc:hexane :: 1:19). Yield obtained: 60%

^{1}H NMR (500 MHz, $CDCl_3$) δ in ppm: 10.51 (br, 2H), 9.41 (s, 2H), 8.39 (d, J=8.06 Hz, 2H), 8.31 (d, J=7.88 Hz, 2H), 7.96 (s, 1H), 7.48 (t, J=7.27 Hz, 2H), 7.44 (t, J=7.39 Hz, 2H), 4.35 (s, 4H), 4.18 (m, 6H), 3.97 (br, 2H), 2.14 (s, 6H), 1.77 (s, 6H), 1.67 (d, J=7.07 Hz, 12H), 1.56 (d, J=7.27 Hz, 12H), 1.24 (t, J=7.16 Hz, 6H). ^{13}C NMR (125.8 MHz, $CDCl_3$) δ in ppm: 163.3, 145.1, 135.3, 135.0, 130.0, 128.7, 127.9, 127.0, 125.9, 125.6, 125.3, 124.4, 123.8, 120.5, 117.8, 117.4, 60.0, 27.4, 26.0, 25.7, 24.3, 22.5, 14.4, 10.8, 8.6. ^{19}F NMR (376.4 MHz, $CDCl_3$) δ in ppm: -139.77. HRMS (ESI+): m/z calculated for $C_{61}H_{67}N_6O_4BF_2$ (M^+): 996.5284, found: 996.5285.

5.6. Reference

1. Bonner, W. A. Chirality and Life. *Orig. Life Evol. Biosph.*, **1995**, *25*, 175.

2. Rickhaus, M.; Mayor, M.; Juríčeka, M. Strain-induced helical chirality in polyaromatic systems. *Chem. Soc. Rev.*, **2016**, *45*, 1542.

3. Meisenheimer, J.; Witte, K. Reduction von 2-Nitronaphtalin. *Ber. Dtsch. Chem. Ges.*, **1903**, *36*, 4153.

4. Newman, M. S.; Lednicer, D. The Synthesis and Resolution of Hexahelicene. *J. Am. Chem. Soc.*, **1956**, *78*, 4765.

5. Dhbaibi, K.; Favereau, L.; Crassous, J. Enantioenriched Helicenes and Helicenoids Containing Main-Group Elements (B, Si, N, P). *Chem. Rev.*, **2019**, *119*, 8846.

6. Cruz, C. M.; Castro-Fernández, S.; Maçôas, E.; Cuerva, J. M.; Campaña, A. G. Undecabenzo[7]superhelicene: A Helical Nano-graphene ribbon as a Circularly Polarized Luminescence emitter. *Angew. Chem. Int. Ed.*, **2018**, *57*, 14782.

7. Furche, F.; Ahlrichs, R.; Wachsmann, C.; Weber, E.; Sobanski, A.; Vögtle, F.; Grimme, S. Circular dichroism of helicenes Investigated by Time-dependent Density Functional Theory. *J. Am. Chem. Soc.*, **2000**, *122*, 1717.

8. Xue, J.; Liang, Q.; Zhang, Y.; Zhang, R.; Duan, L.; Qiao, J. High-Efficiency Near-Infrared Fluorescent Organic Light Emitting Diodes with Small Efficiency Roll-Off: A Combined Design from Emitters to Devices. *Adv. Funct. Mater.*, **2017**, *27*, 1703283.

9. [a] Pantoş, G. D.; Rodríguez-Morgade, M. S.; Torres, T.; Lynch, V. M.; Sessler, J. L. 2-Amino-3,4-diethylpyrrole derivatives: new building blocks for coiled structures. *Chem. Commun.*, **2006**, 2132. [b] Ueta, K.; Umetani, M.; Osuka, A.; Pantoş, G. D.; Tanaka, T. Single- and double-helices of α,α'-dibenzylaminotripyrrin: solution and solid state studies. *Chem. Commun.*, **2021**, *57*, 2617.

10. [a] Haketa, Y.; Maeda, H. From Helix to Macrocycle: Anion-Driven Conformation Control of π-Conjugated Acyclic Oligopyrroles. *Chem. Eur. J.*, **2011**, *17*, 1485. [b] Haketa, Y.; Bando, Y.; Takaishi, K.; Uchiyama, M.; Muranaka, A.; Naito, M.; Shibaguchi, H.; Kawai, T.; Maeda, H. Asymmetric Induction in the Preparation of Helical Receptor–Anion Complexes: Ion-Pair Formation with Chiral Cations. *Angew. Chem. Int. Ed.*, **2012**, *51*, 7967.

11. [a] Maeda, H.; Nishimura, T.; Akuta, R.; Takaishi, K.; Uchiyama M.; Muranaka, A. Two double helical modes of bidipyrrin–Zn^{II} complexes. *Chem. Sci.*, **2013**, *4*, 1204. [b] Eerdun, C.; Hisanaga, S.; Setsune, J.-I. Single Helicates of Dipalladium(II) Hexapyrroles: Helicity Induction and Redox Tuning of Chiroptical Properties. *Angew. Chem. Int. Ed.*, **2013**, *52*, 929.

12. Yamanishi, K.; Miyazawa, M.; Yairi, T.; Sakai, S.; Nishina, N.; Kobori, Y.; Kondo, M.; Uchida, F. Conversion of Cobalt(II) Porphyrin into a Helical Cobalt(III) Complex of Acyclic Pentapyrrole. *Angew. Chem. Int. Ed.*, **2011**, *50*, 6583.

13. Liu, Z.; Jiang, Z.; He, C.; Chen, Y.; Guo, Z. Circularly polarized luminescence from axially chiral binaphthalene-bridged BODIPY, *Dyes Pigm.*, **2020**, *181*, 108593.

14. Maeda, C.; Nagahata, K.; Shirakawa, T.; Ema, T. Azahelicene-Fused BODIPY Analogs Showing Circularly Polarized Luminescence. *Angew. Chem. Int. Ed.*, **2020**, *59*, 7813.

15. Zhou, Z.; Zhou, J.; Gai, L.; Yuan, A.; Shen, Z. Naphtho [b]-fused BODIPYs: one pot Suzuki–Miyaura–Knoevenagel synthesis and photophysical properties. *Chem. Commun.*, **2017**, *53*, 6621.

16. Wang, Z.; Huang, L.; Yan, Y.; El-Zohry, A.M.; Toffoletti, A.; Zhao, J.; Barbon, A.; Dick, B.; Mohammed, O. F.; Han, G. Elucidation of the Intersystem Crossing in a Helical BODIPY for Low Dose Photodynamic Therapy. *Angew. Chem. Int. Ed.* **2020**, *59*, 16114.

5.7. Spectra

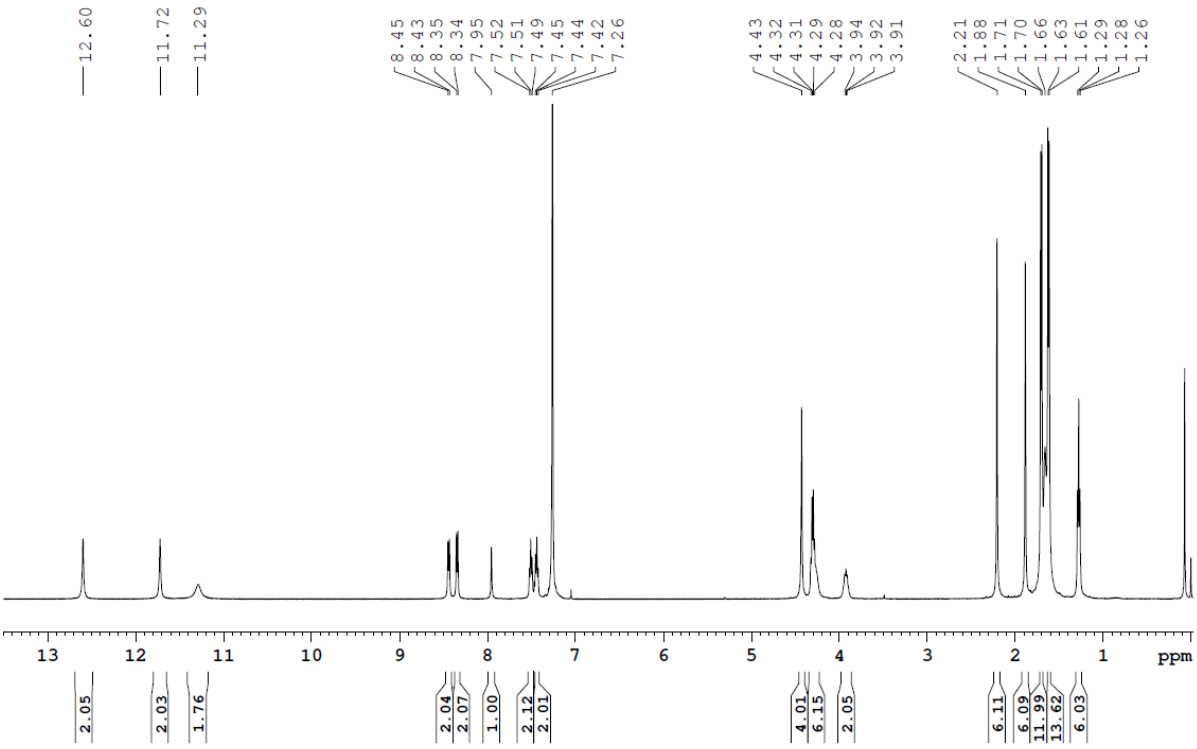

Figure 5.15: ^{1}H NMR spectrum of **SSS-9** in $CDCl_3$.

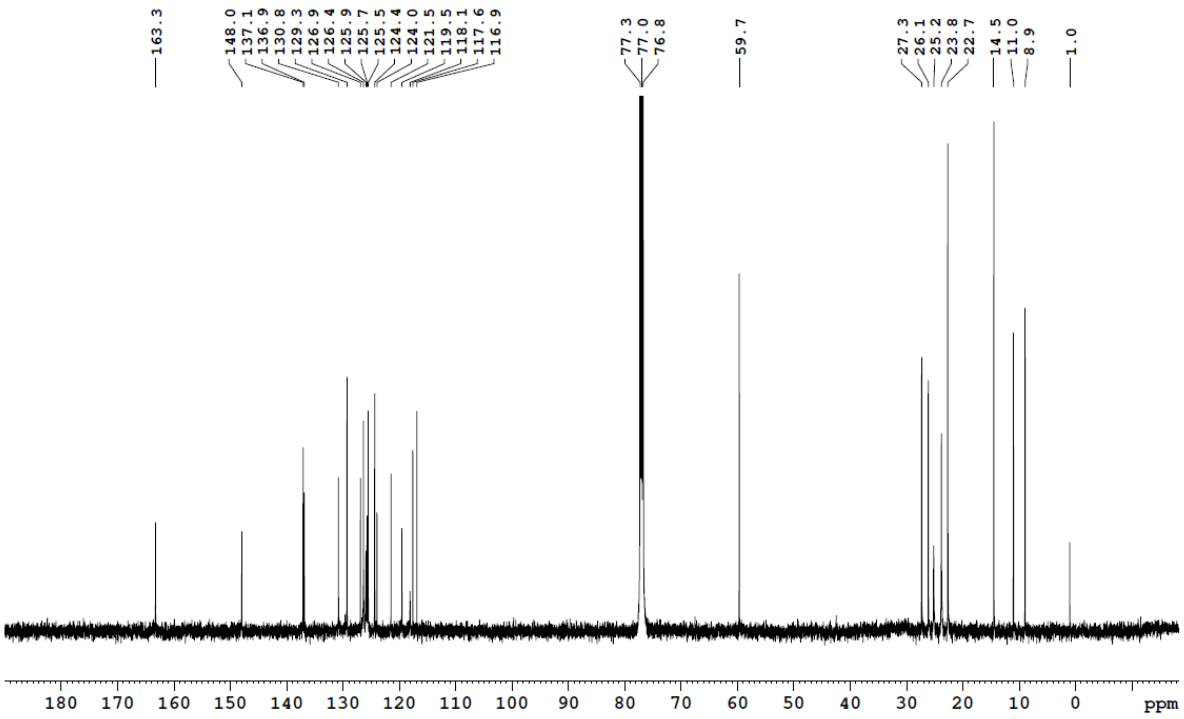

Figure 5.16: ^{13}C NMR spectrum of **SSS-9** in $CDCl_3$.

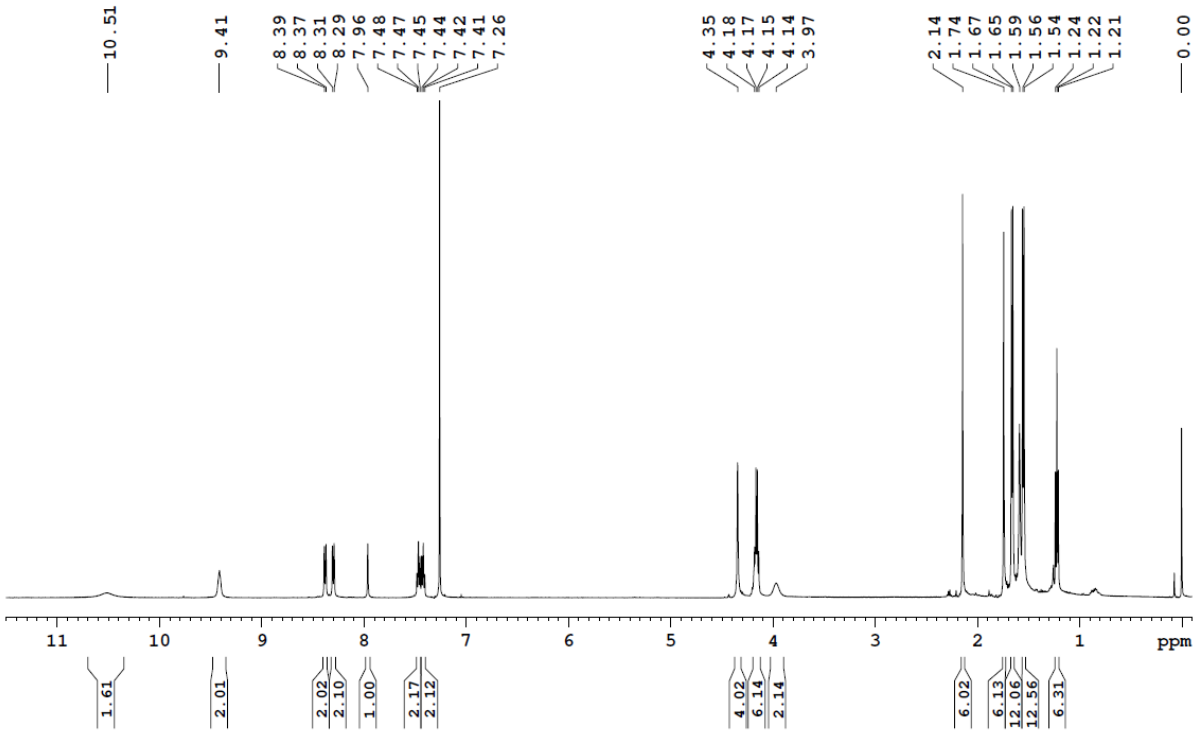

Figure 5.17: ^{1}H NMR spectrum of **SSS-10** in $CDCl_3$.

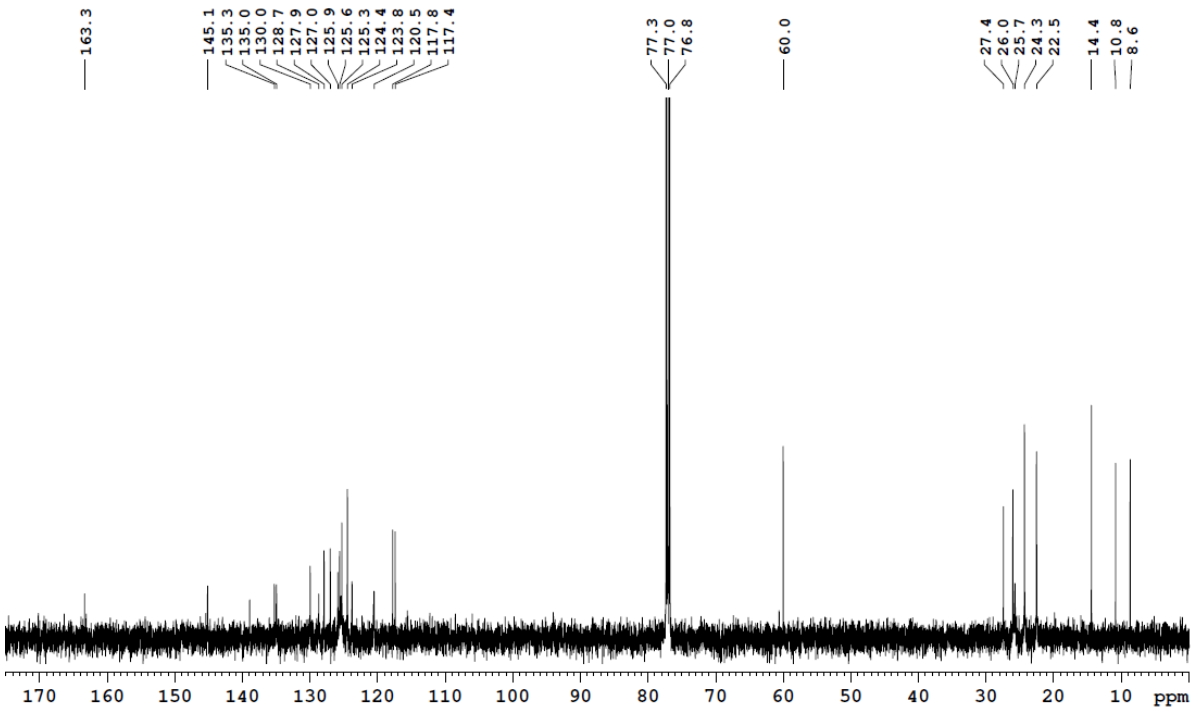

Figure 5.18: ^{13}C NMR spectrum of **SSS-10** in $CDCl_3$.

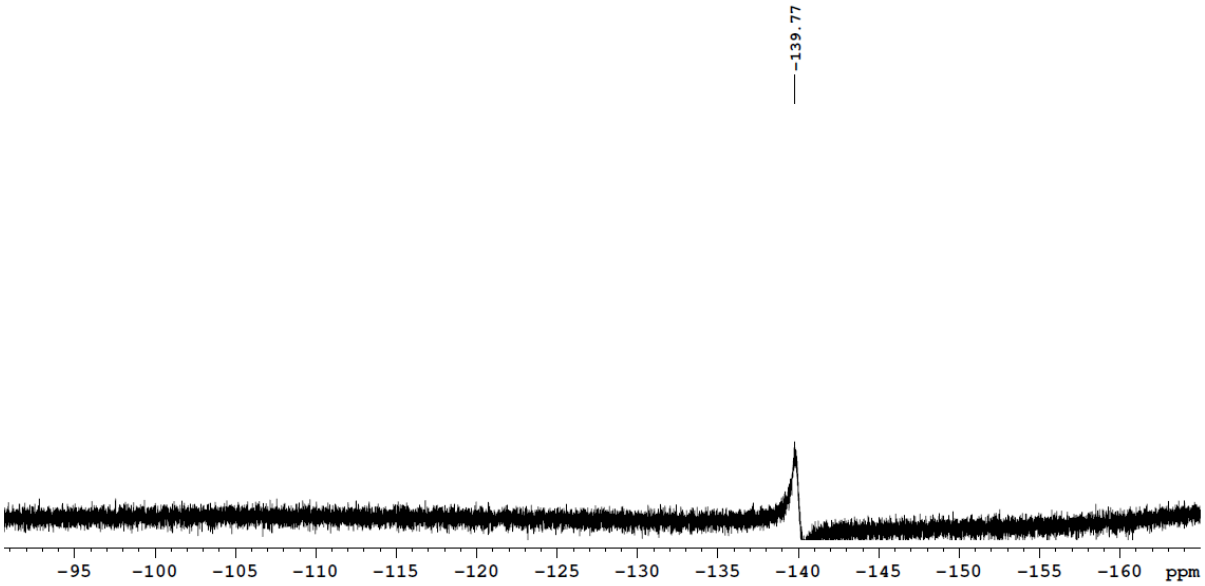

Figure 5.19: ^{19}F NMR spectrum of **SSS-10** recorded in $CDCl_3$.

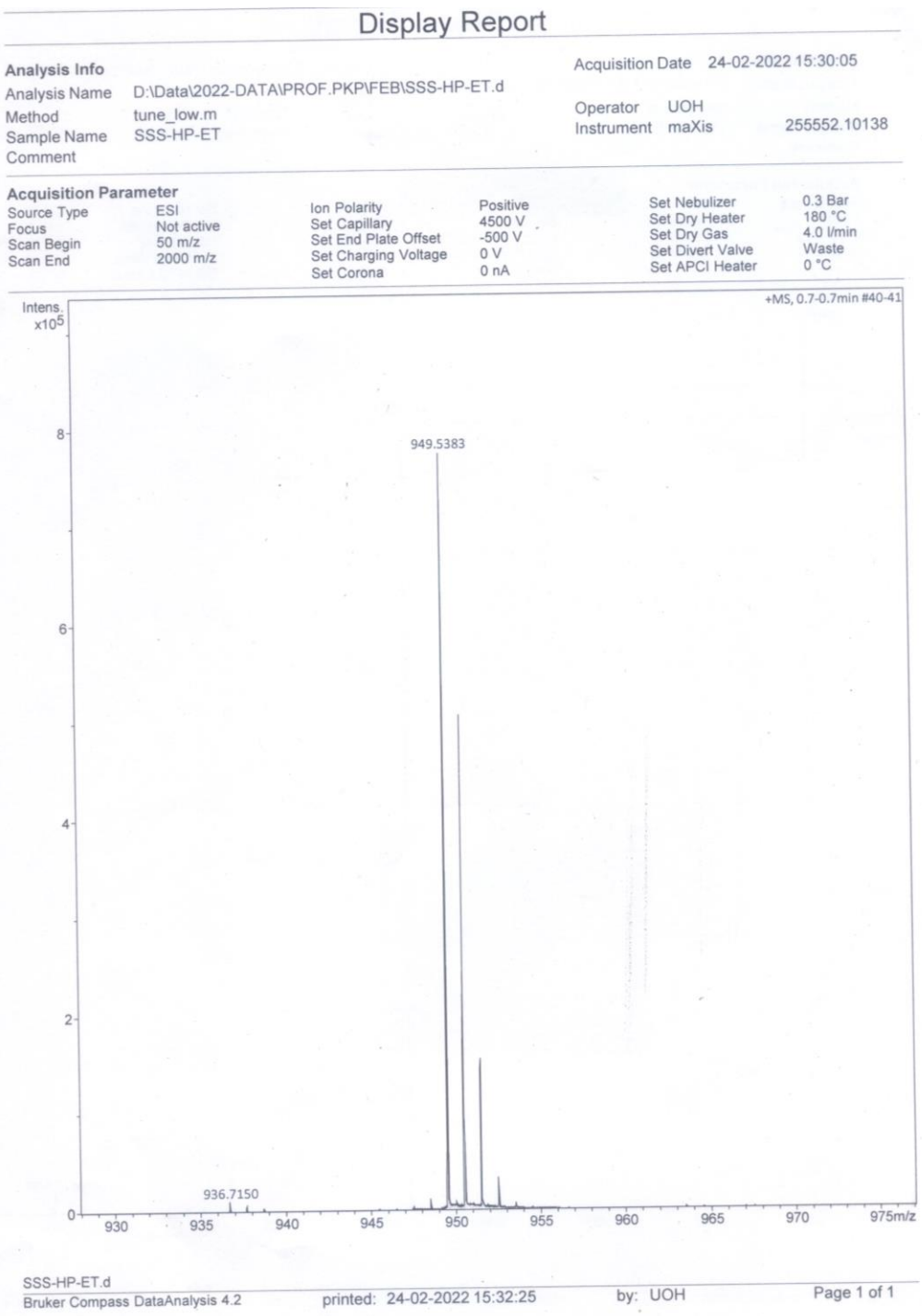

Figure 5.20: HRMS data of **SSS-9** (m/z calculated for $C_{61}H_{69}N_6O_4$ ($M-Cl^-$): 949.5380, found: 949.5383).

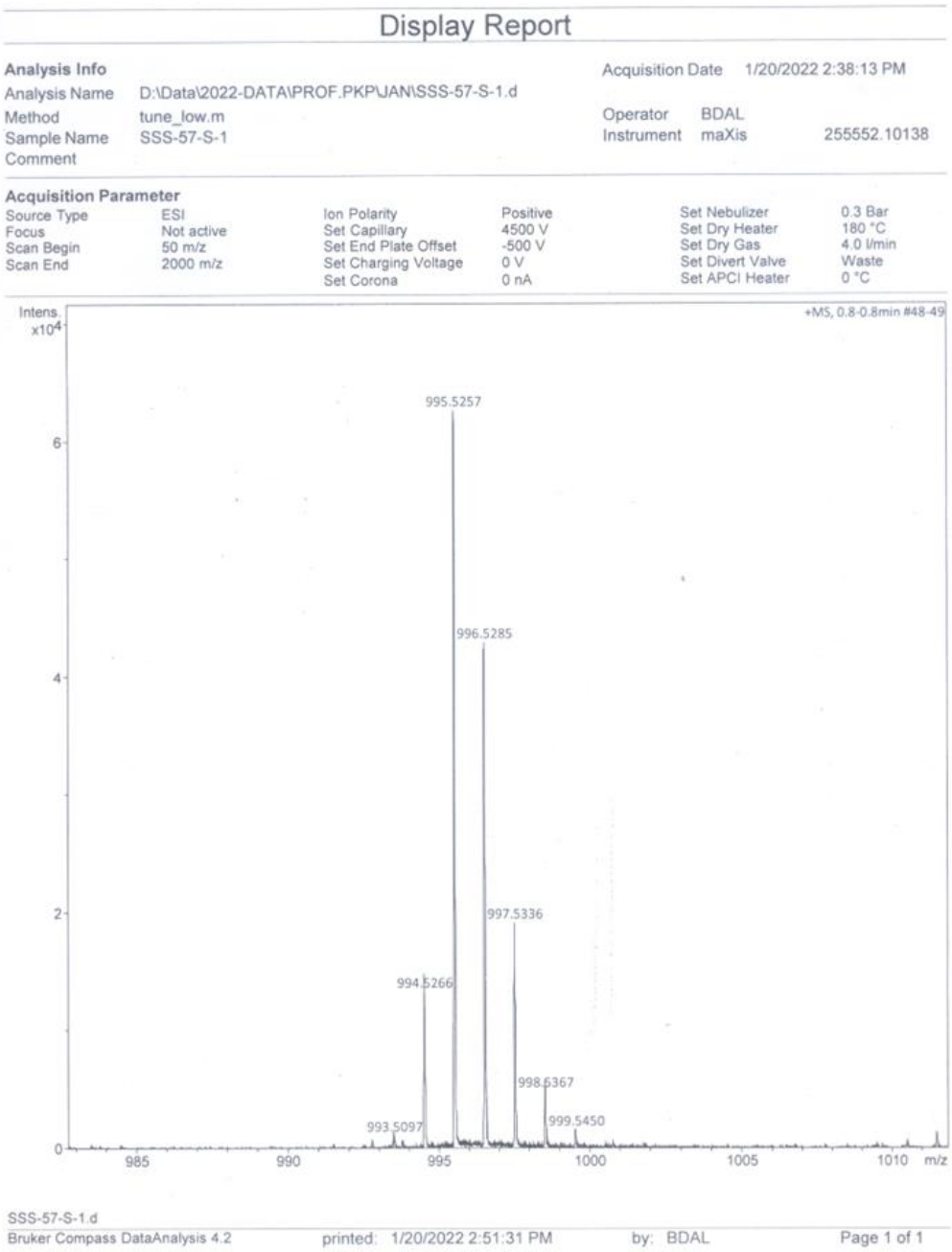

Figure 5.21: HRMS data of **SSS-10** (m/z calculated for $C_{61}H_{67}N_6O_4BF_2$ (M^+): 996.5284, found: 996.5285).

Chapter 6

Conclusion

6.1. Summary

The thesis entitled "**Exploration of Novel Sapphyrin Isomer through Design, its Coordination Chemistry and Naphthobipyrrole-Derived BODIPYs as NIR Emitting Dyes**" consists of six chapters including three working chapters along with two introductory chapter and the conclusion. The thesis is divided into two parts. Part A is about expanded porphyrin and part B includes NIR emitting BODIPY dyes. Part A deals with the design, synthesis and exploration of anion binding and coordination properties of a new sapphyrin isomer. Synthesis and optical properties of NIR emitting naphthobipyrrole derived BODIPY dyes have been studied in details in part B. In this chapter, we will be summarising briefly all the works discussed in the previous chapters.

Porphyrin which has been considered as 'pigment of life' owing to its vital roles played in many essential biological functions, has vast chemistry. Since the discovery of the structure of porphyrin by Fischer, this chemistry has neither been ignored nor exhausted. Most of the research plays around its optical properties and rich coordination chemistry. Along with porphyrin, various structural isomers have been reported among which, porphycene is the most widely explored one. This shows interesting optical and coordination properties different from porphyrin owing to its structural differences. The presence of direct pyrrole-pyrrole bond and ethene bridge causes a dramatic change in its electronic properties, core shape and size. The porphyrin chemistry is not only limited to tetrapyrrolic systems with four bridges. This has been expanded to many other structural analogues like contracted and expanded porphyrins. As the name suggests contracted porphyrins have less no of heterocycles or *meso* bridges and expanded ones have more no. of heterocycles or *meso* bridges.

Expanded porphyrin was discovered by Woodward in 1966 as a pentapyrrolic analogue and named as sapphyrin owing to its bright green colour crystals like sapphire. Expanded porphyrins are more interesting due to their flexible conformation, higher aromaticity, coordination chemistry, anion binding and many other properties. Among innumerable reports on various expanded porphyrins, sapphyrin remains most widely explored one due its interesting properties. Its interesting anion binding properties with halides, phosphates, carbonates, nucleotides and DNA and also as a photosensitizer for photodynamic therapy make it a unique class of molecule. Despite of so many studies on sapphyrin, its structural isomers were not explored to a greater extend like porphyrin. Rich chemistry of sapphyrin demands studies on its isomerism also.

Our thought of putting structural aspects of porphycene into skeleton of sapphyrin arouse due to our strong encounter with porphycene and related systems. Putting an ethene bridge into pentapyrrolic molecule was expected to bring changes in electronic properties causing spectral changes and also core shape and size bringing an interesting twist to coordination chemistry. With a primary theoretical calculation for possible isomers of sapphyrin which shows our designed molecule is more stable than sapphyrin, we started making strategy to realize that. Taking a core modified structure with a thiophene as one of the heterocycles as our target added some more interesting properties like stability, larger core and more red shifted absorption. We realized the target molecule with our expected outcomes. It exhibits lower energy absorption like sapphyrin along with enhanced intensity like porphycene. It exhibits strong NH⋯N hydrogen bonding like porphycene along with NH⋯S hydrogen bonding. Properties studied show similarity with porphycene and sapphyrin. We named the novel molecule as sapphycene. The molecule is weakly NIR emissive, which is not so common character in expanded porphyrins. This molecule is also studied for fluoride binding.

Its interesting structural attributes lead us to explore its coordination chemistry. We realized stable Pd(II) complex, which manifests the neutral binding mode of sapphycene. It acts as a bidentate neutral ligand showing an out-of-plane complexation mode. It forms a seven membered metallacycle, which is a very rare phenomenon in expanded porphyrins. Both the freebase and metal complex has also been studied theoretically for its electronic transition, aromaticity, existing hydrogen bonding. They correlate well with our experimental results.

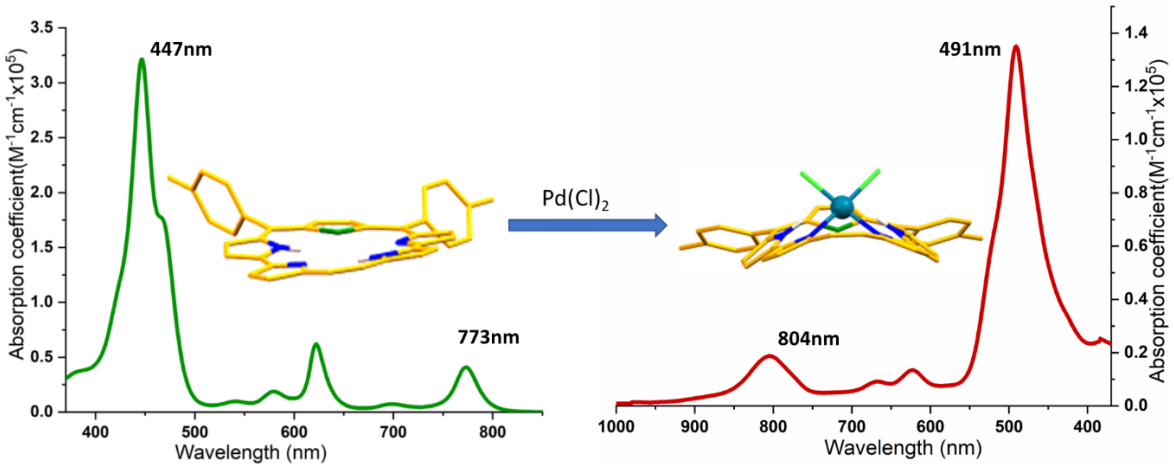

Figure 6.1: Metalation of sapphycene with $Pd(Cl)_2$ with their absorption spectra.

BODIPY, also considered as "porphyrin's little sister" is one of the widely used fluorescent dye. This can be considered as a rigidified monomethine cyanine dyes forming a

planar tricyclic system, which restricts *cis-trans* isomerisation. This allows effective π-delocalization as a consequence of which it shows intense absorption. On account of its versatile structural modification, intense absorption, emission with high quantum yield and specifically its excellent photostability and thermal stability, this has been a dye of choice for many applications like fluorescent sensors, labels for bioimaging, photovoltaics etc. But most of the application field needs absorption in NIR region, which is an emerging field of research. As BODIPY provides easy structural modification for fine tuning its photophysical properties, many strategies have been followed to get its absorption and emission profile in NIR region. There is a plethora of examples of BODIPY dyes in literature showing structural modification to have enhanced optical properties. Among them annulation of the periphery of BODIPY with other aromatic systems is the most followed strategy. But few of them could only reach up to NIR region. Fusing the system with electron-rich heterocyclic aromatic system alters the electronic effect efficiently affecting the frontier orbitals and reducing the HOMO-LUMO energy gap. Our group has already reported many novel naphthobipyrrole derived macrocycles, which shows interesting structural and optical properties owing to its rigidified system. BODIPY derived from naphthobipyrrole was also reported, which shows excellent optical properties with absorption and emission in NIR region i.e., > 720 nm, high fluorescent quantum yield (~ 0.6), large molar extinction coefficient and excellent photostability.

In this context, we have functionalized the naphthobipyrrole-derived BODIPY at its terminal α-free positions to check the effect on optical properties and photostability. We have successfully functionalized the BODIPY with various functional groups like formyl, nitrile, nitro, and bromo.

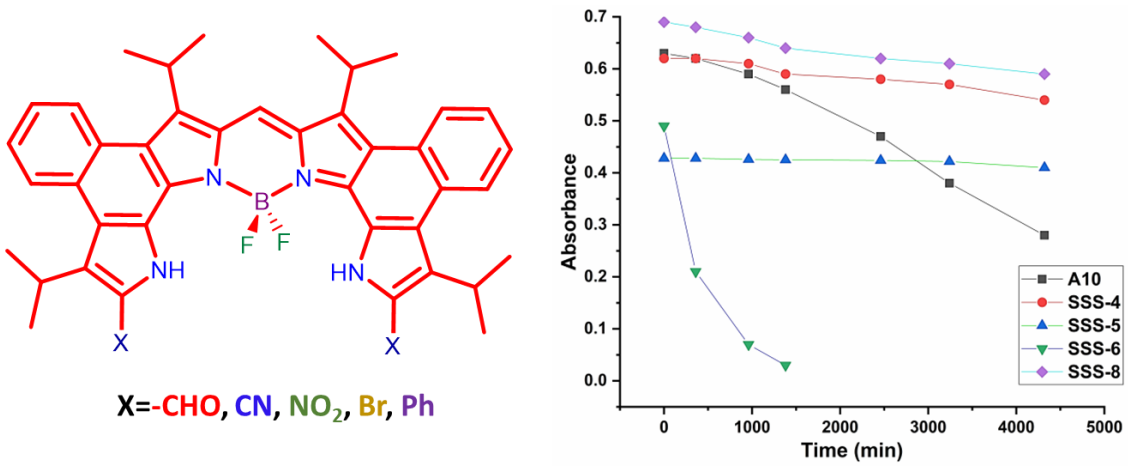

Figure 6.2: Structure of synthesized BODIPY derivatives along with their photostability.

Though they don't exhibit drastic changes in absorption and emission spectra with respect to parent naphtobipyrrole-derived BODIPY, they provide excellent photostability to formyl and nitrile derivatives. They are relatively less sensitive to solvent polarity except for nitro derivative, which shows a dramatic change in absorption and emission profile in polar solvents like DMSO. Due to less stability of bromo derivative, we have further derivatized it with phenyl groups. Phenyl substitution on α-positions caused a significant change in frontier orbitals reducing the HOMO-LUMO gap thus causing a large bathochromic shift in absorption (761 nm) and emission profile (781 nm).

Discovery of the double-helical structure of DNA has shown the importance of helical chirality in complex biological systems. Helical polyaromatic systems form many types of supramolecular assemblies, which may be a chiral or racemic mixture. Helical chirality is a property of a class of chiral molecules devoid of any stereogenic center, i.e., sp^3 atom with all four non-equivalent substituents. This possesses a stereogenic axis and this type of chirality is known as axial chirality. Classically, helicenes are ortho-fused polyaromatic systems possessing steric hindrance between terminal positions. Generally, they have a long π-conjugation and exhibit absorption in the visible region due to π-π* conjugation. Incorporating hetero atoms into the skeleton of helicene alters the electronic properties thus, changing the absorption and emission profile. Inducing helicity in nonhelical or planar aromatic system will enhance its optical and chiroptical properties. Though, chemistry of carbo[n]helicene is much more developed and already used for many applications, growth of helicenes having other main group elements is limited. There are a few reports about pyrroles directly incorporated or fused to helicene skeleton.

Blending unique chiroptical properties to the exceptionally enhanced photophysical properties of BODIPY may meet demands of candidate for NIR CPL (chiral photo luminescent) devices. But inducing chirality in BODIPY has been done by substituting BODIPY periphery or boron with chiral substituents. There are very few reports of direct involvement of BODIPY for helicity formation, which have been discussed in the preceding chapters. We have realized novel helical BODIPY dye from a hexapyrrolic helical oligomer derived from naphthobipyrroles. From the crystal structure analysis, it is evident that steric hindrance among terminal groups and possible hydrogen bonding, the oligomer and the BODIPY molecules adopt a stable helical conformation. Though the molecules are not fully oxidised and π-electron delocalisation is not global on whole molecule, both the oligomer and its BODIPY derivative exhibit absorption in NIR region (758 nm) owing to their large

distortion, which reduces HOMO-LUMO energy gap. Also, latter one emits in the NIR region. Though, it consists of bidirectional helices and exhibit racemisation, its large bathochromic shift in absorption and emission with easy structural modification made the system more interesting for further exploration.

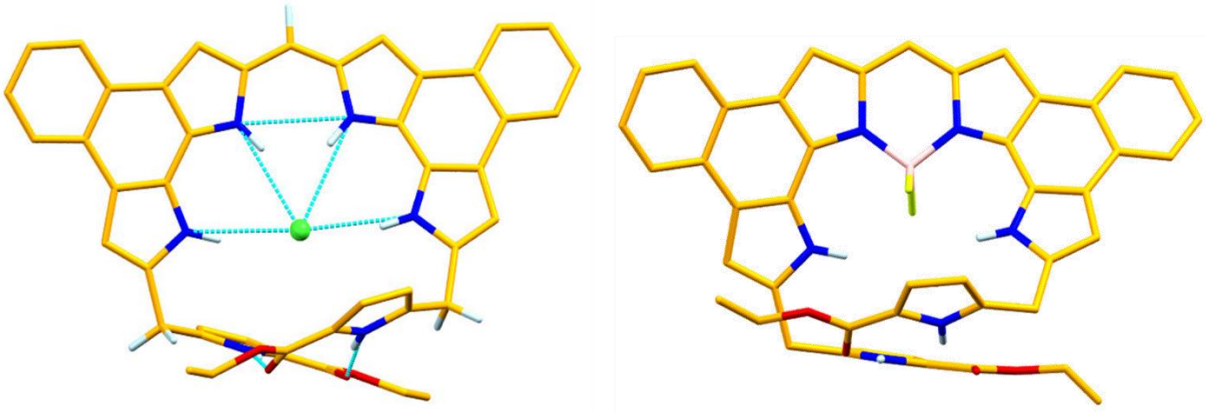

Figure 6.3: SCXRD structure of hexapyrrole as HCl salt and its BODIPY derivative.

In summary, an attempt has been made to synthesize novel core-modified sapphyrin isomer, which shows enhanced photophysical properties compared to its structural analogues. Also, its coordination chemistry demonstrates rare neutral binding mode in expanded porphyrin chemistry. A few NIR emitting BODIPY dyes have been synthesized and explored for its unique structural and optical properties.

These systems can be explored further to get better insight into structure-property relationships. They can be fine-tuned for best optical properties, which are desirable for their practical application.

Appendix

General Experimental Methods and Techniques

This chapter deals with the materials utilized and the purification procedures employed for the solvents and chemicals used along with a brief summary of the various physicochemical methods. Additionally, we have elaborated about the synthetic procedure of formally known compounds utilized during the course of our investigation.

A.1. Materials Employed

A.1.1. Solvents

The purification procedures described below for different solvents are essentially the same as reported elsewhere.[1]

I. DCE, DCM and DMF were dried by distillation over calcium hydride.

II. THF and hexane was refluxed over benzophenone and sodium till deep blue color continues and then distilled instantly before use.

III. Methanol was dried by refluxing with magnesium activated with iodine followed by distillation.

IV. Toluene was refluxed with sodium and benzophenone until blue color persists and followed by distillation before use and $POCl_3$ was distilled before use.

V. Ethylene glycol was dried by distillation over sodium.

A.1.1.1. NMR solvents

DMSO-d_6, MeOH-d_4, chloroform-d and D_2O were purchased from Sigma Aldrich/ Acros Organic/ Chembridge Inc.

A.1.1.2. Solvents for optical measurement

All required solvents are purchased from FINAR and then dried according to above procedure before use.

A.1.2. Chemicals

I. Pyrrole (SPECTROCHEM) was distilled over calcium hydride before use.

II. Mineral acids (HNO_3, H_2SO_4 and HCl) and NH_3 (aq.) procured from Finar Chemicals (India) were of AR grade and used as received.

III. Anhydrous sodium sulphate, potassium carbonate, sodium bicarbonate, sodium carbonate, sodium hydroxide pellets and anhydrous calcium chloride procured, (India) and were used as received.

IV. N-iodosuccinimide, Pd/C (5%), $BF_3.OEt_2$, TFA, $Ni(acac)_2$, $Zn(OAc)_2.2H_2O$ and $Pd(OAc)_2$ were purchased from Sigma-Aldrich® and used as such.

V. $TiCl_4$, Zn powder and sodium were purchased from Finar chemicals.

A.2. Chromatography

Thin layer chromatography was performed on pre-coated TLC Silica gel 60 F254 on aluminum sheet, purchased from Merck. Column chromatography was carried out on silica gel (100-200 mesh) purchased from Merck/SRL India.

A.3. Physico-Chemical Techniques:

The various instrumental techniques employed in the present study are as given below:

A.3.1. ^{1}H NMR Spectroscopy:

Nuclear magnetic resonance (NMR) spectra were obtained on Bruker 400 MHz and 500 MHz FT- NMR spectrometers operating at ambient temperature. In $CDCl_3$, TMS (δ = 0 ppm) was used as internal standard for ^{1}H NMR spectra and for other deuterated solvents, solvents residual peak was taken as standard. Similarly, for ^{13}C NMR spectra solvent peak was taken as standard for all deuterated solvent for calibration purpose.

A.3.2. Electronic spectra

The optical absorption spectra were recorded in Perkin Elmer Lambda-750 UV-VIS spectrophotometer.

A.3.3. Infrared Spectra (IR-Spectra)

IR spectra were recorded on NICOLET Is5 FT-IR spectrometer by neat sample.

A.3.4. High-resolution mass spectrometry (HRMS) analysis

The mass spectral determinations were carried out by Bruker Maxis HRMS by ESI techniques and LCMS were recorded by Shimadzu-LCMS-2010 mass spectrometer by both positive and negative ionization methods.

A.3.5. Melting points determination

Melting points determination were carried out in Lab India MR-VIS+ visual melting point apparatus.

A.3.6. Fluorescence

Fluorescence spectra were recorded on a JASCO FP-8500 spectrofluorometer.

A.3.7. Fluorescence life time analysis

Fluorescence lifetime measurements were carried out using a time-correlated single-photon counting (TCSPC) spectrometer (Horiba Jobin Yvon IBH). PicoBrite diode laser source (λ_{exc} 485 nm) was used as the excitation source and an MCP photomultiplier (Hamamatsu R3809U-50) as the detector. The pulse repetition rate of the laser source was 10 MHz. The width of the instrument response function, which was limited by the FWHM of the exciting pulse, was around 55 ps. The lamp profile was recorded by placing a scatterer (Ludox solution in water)

in place of the sample. The time-resolved emission decay profiles were collected at steady-state emission spectrum maxima's 630 nm and 680 nm. Decay curves were analyzed by nonlinear least-squares iteration procedure using IBH DAS6 (Version 2.2) decay analysis software. The quality of the fit was assessed by inspection of the χ^2 values and the distribution of the residuals.

A.3.8. Single crystal X-ray Diffraction analysis (SCXRD)

Some of the crystallographic data was collected on BRUKER APEX-II CCD microfocus diffractometer, Mo-Kα (λ = 0.71073 Å) radiation and Cu-Kα (λ = 1.54184 Å) radiation was used to collect the X-ray reflections of the crystal. Data reduction was performed using Bruker SAINT Software.[2] Intensities for absorption were corrected using SADABS 2014/5,[3] refined using SHELXL2014/7 [4,5] with anisotropic displacement parameters for non-H atoms. Hydrogen atoms on O and N were experimentally located in difference electron density maps. All C−H atoms were fixed geometrically using HFIX command in SHELX-TL. A check of the final CIF file using PLATON [6,7] did not show any missed symmetry. Remaining other crystallographic data were collected in Rigaku XtaLAB Synergy, single source X-ray diffractometer. Mo-Kα (λ = 0.71073 Å) radiation was used to collect the X-ray reflections of the crystal. Data reduction was performed using CrysAlisPro 1.171.40.35a.[8] Intensities for absorption were corrected using CrysAlisPro 1.171.40.35a and refined using SHELXL2014/7 [4,5] with anisotropic displacement parameters for non-H atoms. All H atoms were fixed geometrically using the HFIX command in SHELX-TL. A check of the final CIF file using PLATON[5] did not show any missed symmetry.

A.3.9. Computational studies

All quantum mechanical calculations are performed by Gaussian 09 programme[9] provided by CMSD facility at University of Hyderabad. Ground state optimisation has been performed by DFT using Becke's three-parameter hybrid exchange functional and the Lee-Yang-Parr correlation functional (B3LYP) employing 6-31G+(D,P) basis set. The NICS values were obtained with gauge independent atomic orbital (GIAO) method based on the optimized geometries.[10] HOMA (Harmonic Oscillator Model of Aromaticity) indices were calculated by using Ropt (C-C) = 1.388 Å and Ropt = 1.334 Å.[11-13] NBO analysis were performed upon optimized geometries. The molecular orbitals were visualized using Gauss view 5. The molecular orbitals were visualized using Gaussview 5.

A.4. Preparation of starting materials

A.4.1. Synthesis of 1H,1'H-[2,2'-bipyrrole]-5-carbaldehyde[14-15]

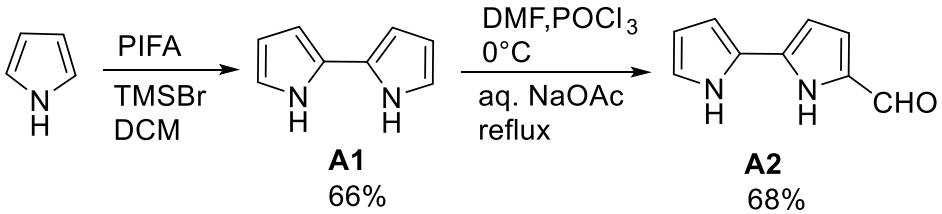

Scheme A1: Synthetic pathway for bipyrrole monoaldehyde.

A.4.1.1. Synthesis of A1

Dry pyrrole was added to dry DCM and cooled to -78 °C under N_2 atmosphere. To this, TMSBr and PIFA were added simultaneously. Then temperature was increased to -40 °C and stirred for 1 h more. Then reaction was quenched with saturated aq. $NaHCO_3$. Organic layer was extracted with DCM and dried over Na_2SO_4, evaporated and a quick filter column was carried out and then distilled under reduced pressure at 100 °C to get pure white solid.

Yield obtained: 66% (Reported yield: 78%)[14]

A.4.1.2. Synthesis of A2

A1 was dissolved in DMF and cooled to 0 °C under N_2 atmosphere. Then to it $POCl_3$ was added slowly and kept for stirring for 1 h. Then it was quenched with aq. Na_2CO_3 and kept for reflux for 1 h. Reaction mixture was cooled and organic layer was washed with EtOAc. Organic layer was dried under reduced pressure and purified with silica gel column to get pure **A2**.

Yield obtained: 68% (Reported Yield: 65%)[15]

A.4.2. Synthesis of thiophene-2,5-diylbis(*p*-tolylmethanol)[16]

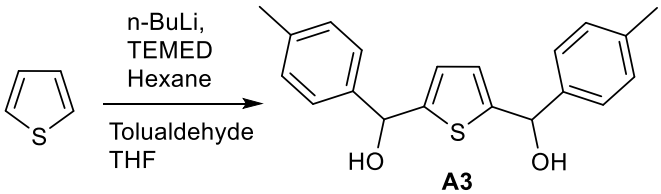

Scheme A2: Synthesis of **A3**.

To a three necked RB, anhydrous hexane was added under N_2 atmosphere. To this, n-BuLi and TEMED were added and stirred. Thiophene was added and refluxed for 1 h. A white turbid solution formed indicating formation of dilithiated salt of thiophene. Then, reaction mixture was cooled with ice bath. To this, *p*-tolualdehyde in dry THF was added slowly. Then the reaction was stirred at 0 °C for 15 min. Then, it was quenched with cold saturated NH_4Cl solution. Then organic layer was washed with brine. Then it was concentrated under reduced

pressure to get crude product. It was purified in silica gel column chromatography EtOAc:hexane (20:80) mixture to obtain white colour product.

Yield obtained:80% (Reported yield: 89%)[16]

A.4.3. Synthesis of ethyl 4-methyl-2-oxo-pentanoate (A4)[17]

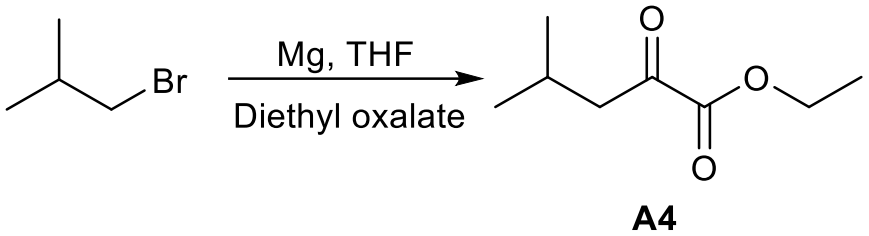

Scheme A3: Synthesis of ethyl 4-methyl-2-oxo-pentanoate.

Mg turnings (20 g) and iodine were taken in a dry 3-necked RB and stirred for some time under N_2 atmosphere till it looks brown coloured indicating Mg is activated. To this, dry THF (184 mL) was added followed by slow addition of isobutyl bromide (26 mL). Addition is done maintaining low temperature by keeping it in ice bath. It was stirred for 2 h. Then this mixture was added through cannula to solution of diethyl oxalate (27.8 mL) in THF (105 mL) at -78 °C. It was further stirred for 3 h. Then reaction was quenched with dil. HCl. Organic layer was extracted with EtOAc and dried under reduced pressure. Crude mixture was distilled under reduced pressure to get pure yellow coloured liquid. Yield: 75% (reported yield: 76%)[17]

A.4.4. Synthesis of diisopropyl naphthobipyrrole[18]

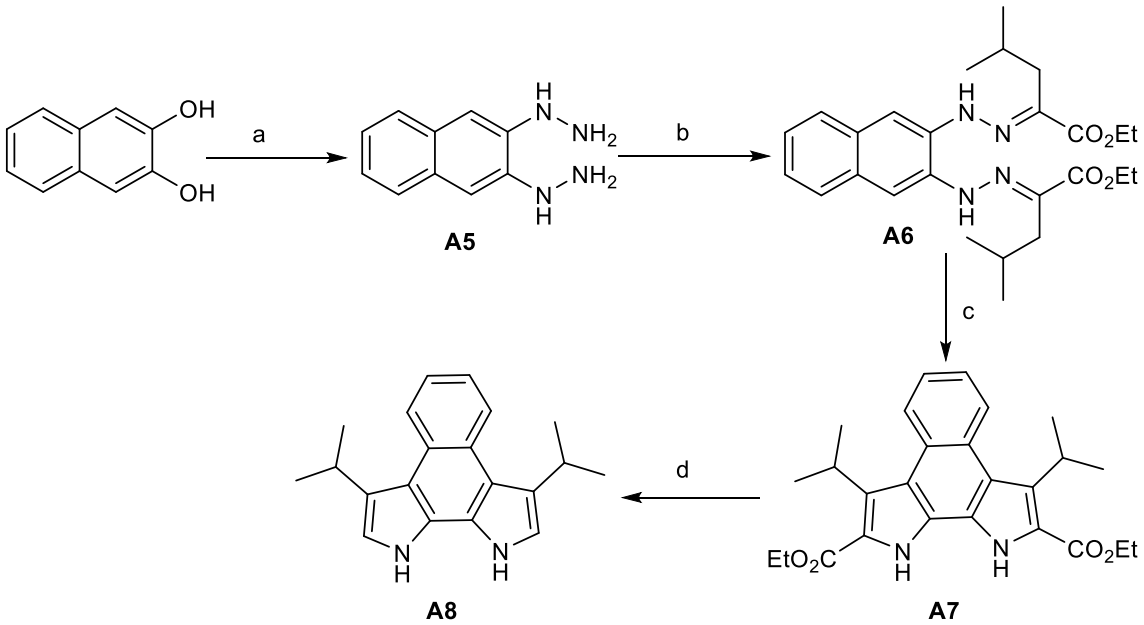

Scheme A4: Synthesis of diisopropyl naphthobipyrrole: a) Hydrazine sulphate, hydrazine hydrate, ethanol; b) **A4**, ethanol; c) *p*-TSA, ethanol; d) NaOH, ethylene glycol.

A.4.4.1. Synthesis of A5

Dihydroxynaphthalene (10 g) and hydrazine sulphate (5. 6 g) were finely mixed in a mortar-pestle. Then the powder was transferred to a 2-necked RB and absolute ethanol (7 mL) was added to it under N_2 atmosphere. Then hydrazine hydrate (14 mL) was added to it and reaction mixture was stirred under reflux for 8 h. Then reaction mixture was cooled and precipitate formed. It was filtered and washed with cold ethanol.

Yield obtained: 65 %

A.4.4.2. Synthesis of A6

To a suspension of **A5** (5 g) in ethanol (185 mL), **A4** (14.5 g) was added and stirred continuously under N_2 atmosphere at room temperature for 24 h. Then it was dried under reduced pressure. Excess of **A4** was distilled out under vacuum. All the isomers formed were collected from silicagel column chromatography. Then it was used for next step reaction without further purification.

A.4.4.3. Synthesis of A7

p-TSA (36 g) was dried properly under vacuum till it becomes powdery. Then it was dissolved with ethanol (200 mL) under N_2 atmosphere. Then to this **A6** (10 g) was added and stirred at reflux condition for 24 h. Then it was cooled to room temperature and poured to ice bath. Then the mixture was washed with EtOAc and dried under reduced pressure. Crude mixture was purified in silica gel column chromatography to get pure off white colored solid product.

Two-step yield obtained: 26%(reported yield: 26%)[18]

A.4.4.4. Synthesis of diisopropyl naphthobipyrrole, A8

Diisopropyl napthobipyrrole diester (1.5 g) was taken in a two necked RB and ethylene glycol (15 mL) was added to it. Then it was kept under reduced pressure for some time. Subsequently, NaOH pellets (0.79 g) were added to it. It was stirred under reflux for 3 h. Then it was cooled to room temperature and then ice was poured to it. Product was precipitated out and was filtered.

Yield obtained: 90% (reported yield: 97%)[18]

A.4.5. Synthesis of naphthobipyrrole derived BODIPY[19]

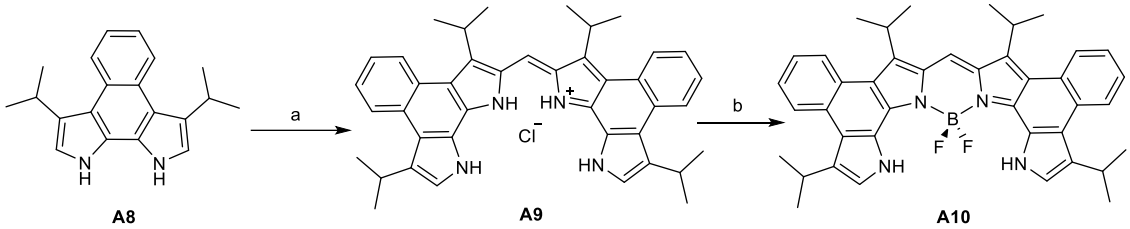

Scheme A5: Synthesis of naphthobipyrrole derived BODIPY. a) $POCl_3$, triethylorthoformate, DCM; b) NEt_3, $BF_3.OEt_2$, DCM.

A.4.5.1. Synthesis of bis-naphthobipyrrolylmethene hydrochloride, A9

Diisopropylnaphthobipyrrole (200 mg) was dissolved in DCM (20 mL) under N_2 atmosphere. To this, triethylorthoformate (0.12 mL) was added followed by addition of freshly distilled $POCl_3$ (32 µL). Then it was stirred at room temperature for overnight. After that reaction mixture was washed with water and organic layer was passed over Na_2SO_4. Crude mixture was dried under reduced pressure. Then it was purified by silica gel column chromatography to obtain pure green coloured solid.

Yield obtained: 70% (reported yield: 78%)[19]

A.4.5.2. Synthesis of bis-naphthobipyrrolylmethene-BF_2 complex, A10

A9 (150 mg) was dissolved in DCM (16 mL) under N_2 atmosphere and to this NEt_3 (1.08 mL) was added. After stirring for 10 min, reaction mixture was cooled under ice bath. To this, $BF_3.OEt_2$ (1.35 mL) was added and stirred for overnight at room temperature. Reaction mixture was diluted with DCM and washed with 1M HCl. Organic layer was dried over anhyd. Na_2SO_4 and evaporated under reduced pressure. Crude mixture was purified with silica gel column chromatography.

Yield obtained: 75% (reported yield: 81%)[19]

A.4.6. Synthesis of Acetoxy pyrrole ester[20-22]

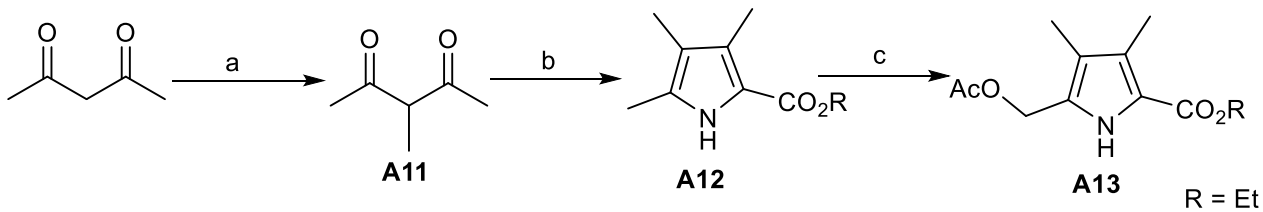

Scheme 2.6: Synthesis of acetoxy pyrrole ester. a) K_2CO_3, CH_3I, pentane-2,3-dione, acetone; b) CH_3COOH, $NaNO_2$, acetyl acetonate, Zn; c) Acetic acid, acetic anhydride, $Pb(OAc)_2$.

A.4.6.1. Synthesis of 3-methylpentane-2,4-dione, A11[20]

Mixture of anhyd. K_2CO_3 (38.6 g) and acetone (57 mL) were taken in a 2-necked RB. Pentanedione (30.7 mL) and methyl iodide (22.5 mL) were added to it. The mixture was refluxed for 20 h. It was cooled to room temperature and insoluble materials are filtered out. Filtrate was concentrated under reduced pressure and then purified by distillation.

Yield obtained: 59% (reported yield: 77%)[20]

A.4.6.2. Synthesis of ethyl 3,4,5-trimethyl-1H-pyrrole-2-carboxylate, A12[21]

Acetic acid (46 mL) and ethyl acetoacetate (11.2 mL) were taken in a three necked RB fitted with $CaCl_2$ guard tube, dropping funnel and thermometer. It was stirred for 10 minutes and kept in ice bath. Subsequently, aq. $NaNO_2$ (7.26 g in 23 mL) solution was added dropwise maintaining the reaction temperature below 10 °C. After addition got over, it was kept for stirring in ice bath for 4-5 h. Then ice bath was removed and was stirred at room temperature for further 18 h. To this Zn dust (12 g) and **A11** (10 g) were added slowly and simultaneously with temperature below 55 °C. After that mixture was heated at 60 °C for 2 h. In hot condition only, mixture was poured into normal water. Precipitate formed was filtered and washed with water. It was dried under vacuum.

Yield obtained: 70% (reported yield: 73%)[21]

A.4.6.3. Synthesis of ethyl 5-(acetoxymethyl)-3,4-dimethyl-1H-pyrrole-2-carboxylate, A13[22]

Pyrrole ester, **2.12** (5 g) and acetic anhydride (6.5 mL) were taken with glacial acetic acid (50 mL) in a RB fitted with a guard tube. Then $Pb(OAc)_4$ (12.97 g) was added portion wise within 15-20 min. Then reaction mixture was stirred for 4-5 h under reflux. After that it was poured into water. Precipitate formed was filtered and washed with water.

Yield obtained: 65 % (reported yield: 82%)[22]

A.5. Summary

A brief account of various solvents and chemicals used in the synthesis and different techniques and other physical and computational methods employed for characterization in our investigation, is given in this chapter. All reported compounds are synthesized and characterized by following reported procedure, which are employed as starting materials for the thesis work, were also described here.

A.6. References

1) Perrin, D. D.; Avmigno, W. L. F., *3rd* Eds. *Purification of Laboratory Chemicals*: Pergamon Press, **1988**. (b) Armarego, W. L. F.; Chai, C. In *Purification of laboratory chemicals*; sixth edition, Elsevier, Burlington**, 2003**.

2) SAINT, version 6.45 /8/6/03 and version 8.34A, Bruker AXS, **2003**, 2014.
3) Sheldrick, G. M. SADABS and SADABS 2014/5, Program for Empirical Absorption Correction of Area Detector Data, University of Göttingen, Germany, **1997**, 2014.
4) SHELXL -Version 2014/7; Program for the Solution and Refinement of Crystal Structures, University of Göttingen, Germany, 1993-2014;
5) Sheldrick, G. M. A short history of SHELX. *Acta Cryst.* **2008**, *A64*, 112.
6) Spek, A. L. PLATON, A Multipurpose Crystallographic Tool, Utrecht University, Utrecht, the Netherlands, **2002**.
7) Spek, A. L. Single-crystal structure validation with the program PLATON. *J. Appl. Cryst.,* **2003**, *36*, 7.
8) CrysAlisPRO, Oxford Diffraction /Agilent Technologies UK Ltd, Yarnton, England.
9) Gaussian 09, (Revision C.01), M. J. Frisch et al. Gaussian, Inc., Wallingford CT, **2010**.
10) Schleyer, P. von R.; Maerker, C.; Dransfeld, A.; Jiao, H.; Hommes, N. J. R. V. E. *J. Am. Chem. Soc.,* **1996**, *118*, 6317.
11) Krygowski, T. M.; Cryański, M. *Tetrahedron*, **1996**, *52*, 1713.
12) Krygowski, T. M.; Cryański, M. *Tetrahedron*, **1996**, *52*, 10255.
13) Krygowski, T. M.; Cryański, M. *Chem. Rev.,* **2001**, *101*, 1385.
14) Dohi, T.; Morimoto, K.; Maruyama, A.; Kita, Y. *Org. Lett.,* **2006**, *8*, 2007.
15) Ostapko, J.; Nawara, K.; Kijak, M.; Buczynska, J.; Lesniewska, B.; Pietrzak, M.; Orzanowska, G.; Waluk, J. *Chem. Eur. J.,* **2016**, *22*, 17311.
16) Stilts, C. E.; Nelen, M. I.; Hilmey, D. G.; Davies, S. R.; Gollnick, S. O.; Oseroff, A. R.; Gibson, S. L.; Hilf, R.; Detty, M. R. *J. Med. Chem.,* **2000**, *43*, 2403.
17) Bueno, J. M.; Carda, M.; Crespo, B.; Cunat, A. C.; de Cozar, C.; Leon, M. L.; Marco, J. A.; Roda, N.; Sanz-Cervera, J. F. *Bioorg. Med. Chem. Lett.,* **2016**, *26*, 3938
18) Sarma, T.; Panda, P. K.; Anusha, P.T.; Rao, S. V. *Org. Lett.,* **2011,** 13, 188.
19) Sarma, T.; Panda, P. K.; Setsune, J. -I. *Chem. Commun.,* **2013**, 49, 9806.
20) Johnson, A. W.; Markham, E.; Price, R. *Org. Synth*., **1962**, *42*, 75
21) Cho, D. H.; Lee, J. H.; Kim B. H. *J. Org. Chem.,* **1999**, *64*, 8048.
22) Zhu, B.-K.; Wei, X.-Z.; Xu, Y.-Y.; Xu, Z.-K. *Gaodeng Xuexiao Huaxue Xuebao*, ***2003***, *24*, 1945.

Publications from Thesis:

1. Monothia [22]pentaphyrin(2.0.1.1.0): a core-modified isomer of sapphyrin. Sahoo, S. S.; Sahoo, S.; Panda, P. K. *Dalton Trans.*, **2022**, *51*, 6526.
2. Functionalization of Napthobipyrrole Derived BODIPY. Sahoo, S. S.; Panda, P. K. (Manuscript under preparation)
3. Bis(napthobipyrrolyl)methene derived helical BODIPY. Sahoo, S. S.; Panda, P. K. (Manuscript under preparation)

Other Publications:

1. β-Octaalkoxyporphyrins: Versatile fluorometric sensors towards nitrated explosives. Rana, A.; Sahoo, S. S.; Panda, P. K. *J. Porphyrins Phthalocyanines* **2019**, *23*, 287.
2. Unsymmetrical bipyrrole derived highly soluble and emissive β-dialkylporphycenes with good singlet oxygen generation ability. Pati, N. N.; Kumar, B. S.; Sivadasan, D.; Sahoo, S. S.; Panda, P. K. *J. Porphyrins Phthalocyanines*, **2019**, *23*, 1.
3. Chromatographically separable ruffled non-planar isomeric octaalkylporphycenes: consequences of unsymmetrical substitution upon structure and photophysical properties. Pati, N. N.; Sahoo, S.; Sahoo, S. S.; Banerjee, D.; Rao, S. V.; Panda, P. K. *New J. Chem.*, **2020**, *44*, 9616.
4. 3,6,13,16-Tetraalkylporphycenes: Synthesis and Exploration of Effect of Alkyl Groups on Structure, Photophysical Properties, and Basicity. Jodukathula, N.; Dutta, A.; Sahoo, S. S.; Sahoo S.; Panda, P. K. *New J. Chem.*, **2022**, DOI: **10.1039/D2NJ01550A**

Conferences:

1. "Recent Advances in bis and tetra-Pyrrolic Molecular Materials" virtual meeting held from 24-26th August, 2020 held at Central University of Kerala, Kerala.
2. National Seminar on "RECENT ADVANCES IN MATERIALS CHEMISTRY" virtual meeting held from 8-9th March, 2021 held at Utkal University, Bhubaneswar, Odisha.
3. Chemfest-2021 (Chemistry beyond challenges), an annual in-house symposium organized by the School of Chemistry from 19-20th February, 2021 at University of Hyderabad, India.
4. ICPP 11 (International Conference on Porphyrins and Phthalocyanines), virtual meeting held from 28th June-3rd July 2021.

Exploration of Novel Sapphyrin Isomer through Design, its Coordination Chemistry and Naphthobipyrrole-Derived BODIPYs as NIR Emitting Dyes

by Sipra Sucharita Sahoo

Exploration of Novel Sapphyrin Isomer through Design, its Coordination Chemistry and Naphthobipyrrole-Derived BODIPYs as NIR Emitting Dyes

ORIGINALITY REPORT

10%	2%	10%	1%
SIMILARITY INDEX	INTERNET SOURCES	PUBLICATIONS	STUDENT PAPERS

PRIMARY SOURCES

1	Sipra Sucharita Sahoo, Sameeta Sahoo, Pradeepta Panda. "Monothia [22]pentaphyrin(2.0.1.1.0): A core modified isomer of Sapphyrin", Dalton Transactions, 2022 Publication	3%
2	Sipra Sucharita Sahoo, Pradeepta Panda. "Monothia [22]pentaphyrin(2.0.1.1.0): A core modified isomer of Sapphyrin", American Chemical Society (ACS), 2022 Publication	1%
3	Tamal Chatterjee, A. Srinivasan, Mangalampalli Ravikanth, Tavarakere K. Chandrashekar. "Smaragdyrins and Sapphyrins Analogues", Chemical Reviews, 2016 Publication	1%
4	pubs.rsc.org Internet Source	1%

5	Harvey, J.D.. "Developments in the metal chemistry of N-confused porphyrin", Coordination Chemistry Reviews, 200312 Publication	<1 %
6	Sipra Sucharita Sahoo, Sameeta Sahoo, Pradeepta K. Panda. "Monothia [22]pentaphyrin(2.0.1.1.0): a core-modified isomer of sapphyrin", Dalton Transactions, 2022 Publication	<1 %
7	Yogita Pareek, M. Ravikanth, T. K. Chandrashekar. "Smaragdyrins: Emeralds of Expanded Porphyrin Family", Accounts of Chemical Research, 2012 Publication	<1 %
8	onlinelibrary.wiley.com Internet Source	<1 %
9	www.science.gov Internet Source	<1 %
10	Rima Sengupta, Mangalampalli Ravikanth, Tavarekere K. Chandrashekar. "Inverted and fused expanded heteroporphyrins", Chemical Society Reviews, 2021 Publication	<1 %
11	Marcin Stępień, Elżbieta Gońka, Marika Żyła, Natasza Sprutta. "Heterocyclic Nanographenes and Other Polycyclic	<1 %

Heteroaromatic Compounds: Synthetic Routes, Properties, and Applications", Chemical Reviews, 2016
Publication

---

12 Soji Shimizu, Ryuichiro Taniguchi, Atsuhiro Osuka. "meso-Aryl-Substituted [26]Hexaphyrin(1.1.0.1.1.0) and [38]Nonaphyrin(1.1.0.1.1.0.1.1.0) from Oxidative Coupling of a Tripyrrane", Angewandte Chemie International Edition, 2005
Publication

<1 %

---

13 www.nature.com
Internet Source

<1 %

---

14 Yuan, Lin, Weiying Lin, Kaibo Zheng, Longwei He, and Weimin Huang. "Far-red to near infrared analyte-responsive fluorescent probes based on organic fluorophore platforms for fluorescence imaging", Chemical Society Reviews, 2013.
Publication

<1 %

---

15 Kais Dhbaibi, Ludovic Favereau, Jeanne Crassous. "Enantioenriched Helicenes and Helicenoids Containing Main-Group Elements (B, Si, N, P)", Chemical Reviews, 2019
Publication

<1 %

---

16 Yong Ni, Jishan Wu. "Far-red and near infrared BODIPY dyes: synthesis and applications for

<1 %

fluorescent pH probes and bio-imaging", Organic & Biomolecular Chemistry, 2014
Publication

17	Dong‐Hao Li, Cynthia L. Schreiber, Bradley D. Smith. "Sterically Shielded Heptamethine Cyanine Dyes for Bioconjugation and High Performance Near‐Infrared Fluorescence Imaging", Angewandte Chemie International Edition, 2020 Publication	<1 %
18	Motoki Toganoh, Hiroyuki Furuta. "Creation from Confusion and Fusion in the Porphyrin World—The Last Three Decades of N-Confused Porphyrinoid Chemistry", Chemical Reviews, 2022 Publication	<1 %
19	Seenichamy Jeyaprakash Narayanan, Bashyam Sridevi, Tavarekere K. Chandrashekar, Ulrich Englich, Karin Ruhlandt-Senge. "Core-Modified Smaragdyrins: First Examples of Stable Meso-Substituted Expanded Corrole", Organic Letters, 1999 Publication	<1 %
20	Timothy D. Lash. "Carbaporphyrinoid Systems", Chemical Reviews, 2016 Publication	<1 %

21	Krystyna Rachlewicz, Natasza Sprutta, Lechosław Latos-Grażyński, Piotr J. Chmielewski, Ludmiła Szterenberg. "Protonation of 5,10,15,20-tetraphenylsapphyrin—identification of inverted and planar dicationic forms", Journal of the Chemical Society, Perkin Transactions 2, 1998 Publication	<1 %
22	Takayuki Tanaka, Atsuhiro Osuka. " Chemistry of -Aryl-Substituted Expanded Porphyrins: Aromaticity and Molecular Twist ", Chemical Reviews, 2016 Publication	<1 %
23	gyan.iitg.ac.in Internet Source	<1 %
24	Basheer, M.C.. "Design and synthesis of squaraine based near infrared fluorescent probes", Tetrahedron, 20070212 Publication	<1 %
25	S. K. Pushpan, T. K. Chandrashekar. "Aromatic core-modified expanded porphyrinoids with meso-aryl substitutents", Pure and Applied Chemistry, 2002 Publication	<1 %
26	Kristina Ilina, Maged Henary. "Cyanine Dyes Containing Quinoline Moieties: History,	<1 %

Synthesis, Optical Properties and Applications", Chemistry – A European Journal, 2020
Publication

27	Lim, Jong Min, Min-Chul Yoon, Kil Suk Kim, Jae-Yoon Shin, and Dongho Kim. "6 Photophysics and Photochemistry of Various Expanded Porphyrins", Handbook of Porphyrin Science, 2010. Publication	<1 %
28	Pawel M. Kozlowski. "The inner-hydrogen migration and ground-state structure of porphycene", The Journal of Chemical Physics, 1998 Publication	<1 %
29	Surya Prakash Singh, G. D. Sharma. "Near Infrared Organic Semiconducting Materials for Bulk Heterojunction and Dye-Sensitized Solar Cells", The Chemical Record, 2014 Publication	<1 %
30	patents.google.com Internet Source	<1 %
31	lirias.kuleuven.be Internet Source	<1 %
32	Submitted to Hong Kong University of Science and Technology Student Paper	<1 %

33	Submitted to Yonsei University Student Paper	<1 %
34	Dijo Prasannan, Mangalampalli Ravikanth. "Synthesis, properties and coordination chemistry of [14]triphyrins(2.1.1)", Coordination Chemistry Reviews, 2020 Publication	<1 %
35	Xiaojun Peng, Jianjun Du, Jiangli Fan, Jingyun Wang, Yunkou Wu, Jianzhang Zhao, Shiguo Sun, Tao Xu. " A Selective Fluorescent Sensor for Imaging Cd in Living Cells ", Journal of the American Chemical Society, 2007 Publication	<1 %
36	Zakerhamidi, M.S.. "Anisotropic and isotropic solvent effects on the dipole moment and photophysical properties of rhodamine dyes", Journal of Luminescence, 201204 Publication	<1 %
37	chemrxiv.org Internet Source	<1 %

Exclude quotes	On	Exclude matches	< 14 words
Exclude bibliography	On		